Thesis submitted for the degree of
Doctor of Philosophy

A quantitative forward modelling analysis of the controls on passive rift-margin stratigraphy

by

Peter Mark Burgess

Department of Earth Sciences
and
St. Cross College
Trinity Term 1994

Abstract

A quantitative forward modelling analysis of the controls on passive rift-margin stratigraphy

Peter Mark Burgess
St. Cross College

A quantitative forward model has been developed to investigate the controls on the deposition, erosion, and preservation of passive rift margin stratigraphy. The model includes thermal subsidence, variable absolute sealevel, flexural isostasy, subaerial and submarine deposition on fluvial and marine equilibrium profiles, and the facility to vary sediment supply through time. Results from the quantitative model can be used to reproduce elements of the sequence stratigraphic depositional model. Conducting sensitivity tests demonstrates that variables such as sediment supply and fluvial profile behaviour are likely to be of equal importance to thermal subsidence and eustasy in passive margin stratigraphy. Sensitivity tests with the quantitative model also demonstrate the problems associated with attempting to use a discretised stratigraphic model to investigate unforced cyclicty resulting from complex interactions in stratigraphic systems. Although the model appears capable of producing such unforced cyclical behaviour, this cyclicity is shown to be due to a numerical instability within the model which occurs with certain initial conditions and assumptions. The applicability of the model to observed stratigraphy is tested by comparing specific model output to patterns of stratigraphy from the North American Atlantic margin. The results from this test demonstrate that although the model is in many respects simplistic when compared to the complexities of natural systems, it is nevertheless capable of reproducing some of the basic elements of the observed stratigraphic patterns.

Thesis submitted for the degree of
Doctor of Philosophy
Trinity Term 1994

Contents

List of Figures

Extended Abstract

A quantitative forward modelling analysis of the controls on passive rift-margin stratigraphy

Peter Mark Burgess

St. Cross College

A quantitative forward model has been developed to investigate the controls on the deposition, erosion, and preservation of passive rift margin stratigraphy. Previous studies in this area have been dominated in recent years by the sequence stratigraphic methodology. In this methodology stratigraphy is subdivided into a hierarchy of units separated by significant surfaces which, it is assumed, can be used as the basis for regional correlation. The patterns of stratigraphy are controlled primarily by eustasy and thermal subsidence, with sediment supply assumed to play a modifying role. Other studies have questioned this, and there has been an increase in the use of quantitative models to examine controls on stratigraphy. These quantitative models have the advantage that they can be tested more rigorously than their qualitative equivalents, and hence problems with uniqueness which restrict the use of the qualitative models may be avoided.

The model developed in this thesis includes thermal subsidence, variable absolute sealevel, flexural isostasy, subaerial and submarine deposition on fluvial and marine profiles, and the facility to vary sediment supply through time. Thermal subsidence is calculated according to either a one-layer or a two-layer stretching model, and the stretching factors can be varied along the length of the model profile. A parameter giving the age since the onset of postrift thermal subsidence allows both young and old postrift margins to be modelled. Absolute sealevel in the model may be varied according to one or two sinusoidal curves with specified periods and amplitudes, or it can be defined outside the model using curves from the literature.

A flexural model is used to calculate the response of the model lithosphere to loading and unloading. The value for the elastic thickness can be held temporally and spatially constant, or it may be varied throughout the duration of the model run according to the three times the square root of age relationship. The value for the elastic thickness may also be varied along the length of the profile. Erosion and deposition are controlled by geometrically-defined fluvial and marine equilibrium profiles. For each time step these profiles are defined according to the position of the beach, the width of the coastal plain, and the available sediment supply. Portions of older chrons with elevations higher than these profiles are eroded, while deposition of available sediment area occurs on those parts of the profile where older chrons have lower elevations. This geometrical method is compared for the fluvial profile with a method based on diffusion, and the relative merits and failings of the two approaches are discussed.

Sediment supply can be held constant at a pre-defined value, or it can be varied through a model run. When it is variable, there are three options for calculating its magnitude. The area of sediment available for deposition may be calculated purely from erosion occurring on the fluvial and the marine profile. Alternatively, it can be varied according to a model-generated curve with, for example, a sinusoidal or a saw-tooth form. The third option for calculating sediment supply is to combine these two methods, with both an external input from a pre-defined curve, and with extra sediment provided by profile erosion.

Results from the quantitative model can be used to reproduce elements of the sequence stratigraphic depositional model. Key elements of the depositional model, such as type-1 and type-2 sequences, and the various significant surfaces, can be reproduced using the quantitative model. Conducting sensitivity tests demonstrates that variables such as sediment supply, and fluvial profile behaviour are likely to be of equal importance to thermal subsidence and eustasy in passive margin stratigraphy. These tests demonstrate the significance of the uniqueness problem to the sequence stratigraphic depositional model.

In the quantitative model, with the same absolute sealevel and subsidence parameters that are used to generate a type-1 sequence, but with a less-concave fluvial profile, it is possible to generate a pattern of stratigraphy very similar to that seen in a type-2 sequence. This illustrates the potential importance of the behaviour of the fluvial profile in stratigraphic systems. It also illustrates the problems with non-unique solutions in the sequence stratigraphic model. This can also be demonstrated in the quantitative model by keeping absolute sealevel constant, but varying sediment supply with a sawtooth curve. With these parameters, the model can reproduce some of the basic patterns seen in the standard sequence stratigraphic type-2 sequence, without the need for fluctuations in absolute sealevel. All the results presented demonstrate the potential problems inherent in trying to interpret the ancient record in order to derive details of eustatic sealevel.

Executing sensitivity tests with the quantitative model also demonstrates the existence within the model of a complex interaction between thermal subsidence, deposition, flexure and erosion which is capable of producing cyclical stratigraphy without the need for external periodic forcing. The effect occurs when thermal subsidence drives the shoreface landwards with a relative sealevel rise. Erosion on the shoreface provides a pulse of sediment which is deposited offshore. The erosion causes flexural uplift around the shoreface which then acts to prevent further landward movement of the beach. In subsequent time steps this uplift is eroded by the fluvial profile, which in turn leads to further flexural uplift, though of lesser magnitude. The cycle begins again when thermal subsidence outpaces the uplift, and the shoreface is driven landward once more by another relative sealevel rise.

The behaviour of this complex interaction is tested with a series of model runs that vary the values of the parameters critical to the effect. Several model runs are carried out, varying the magnitude of thermal subsidence, the initial thermal age of the model lithosphere, the geometry of the shoreface and the geometry of the fluvial profile.

Although the details of the stratigraphic pattern are affected by these changed parameters, the basic pattern due to the feedback effect remains. Two model runs using shorter time steps are also carried out to ascertain whether or not the periodicity of the cyclicity is independent of the length of the model time step used. These two tests show that in fact the period of the cyclicity is not independent of the time step. Further sensitivity tests demonstrate that reducing the time step to values approaching zero also reduces the period of the cyclicity to values approaching zero. Thus, the feedback effect is shown to be a numerical instability due to the discretised nature of the model.

In order to further investigate the nature of the numerical instability further sensitivity tests are run using a linear flexural response function. The results from these two sensitivity tests show that the inclusion of the linear flexural response complicates the behaviour of the feedback effect, but does not remove the dependence of the periodicity of the cyclicity upon the model time step. The numerical instability in the model producing the cyclicity means that the model cannot be used to draw any conclusions regarding the operation of such feedback effects within natural stratigraphic systems.

The applicability of the model to observed stratigraphy is tested by comparing specific model output to observed patterns of stratigraphy from the North American Atlantic margin. The initial conditions for the model are taken from previous work on the margin. Three different eustatic sealevel curves are used, two containing high-frequency high-amplitude oscillations, the other consisting of a low-frequency low-amplitude signal. The model runs using these curves show that the low-frequency low-amplitude curve produces the best match with the observed stratigraphy. Using this curve the model can reproduce some of the basic features of the observed stratigraphy, such as the distance of shoreline progradation.

The fit between the model results and the observed stratigraphy is improved when the model is run with the low-frequency eustatic curve, and variable sediment supply, and a

variable value for the sediment partitioning coefficient. The accuracy of the distance of progradation is improved slightly, and the observed changes in the rates of beach progradation are also more closely matched. The results from these model runs demonstrate that although the model is in many respects simplistic when compared to the complexities of natural systems, it is nevertheless capable of reproducing some of the basic elements of the observed stratigraphic patterns.

Acknowledgements

Where to begin? Well, firstly, I would like to thank my supervisors, Phil Allen and Tony Watts. Phil has been more like a friend than a supervisor, and despite the occasional outbreak of sarcasm, has never failed to be inspirational to me in terms of both science and general childish behaviour. I would like to thank Tony for demonstrating to me the importance of honesty, and a rigorous methodology, in science.

Next comes the thanks to all those people in the Oxford Earth Sciences department. Thanks must first go to all the postgraduate students in the department, both current and ex, for their support, advice, jokes, tolerance etc. etc., especially Graham "Emotionally Inarticulate" Robertson, Andy "McKnobhead" Curtis, Andy "Granny" Bingham, Catherine "Geordy" Marr, Sanjeev "Incised Vailey" Gupta, Jon "Fan of Flagstaff" Verlander, John "lock up your daughters" Kennedy, Malcolm "Ears" Dransfield, Halcyon "What a serve" Martin, Sarah "Kiwi" Vickery, Louis "Blind date" Moresi, Neils "Wholemeal" Hovius, Duncan "Jumper" Macilroy, John "Secret" Argent, Lena "rhymes with" Stranks, Roxby "Cool" Hartley, Pete "G.P.S." Clarke, Rob "Cave" Davies, Audrey "Mc" Willet, Miguel "Manuel" Mora, Pam "Twin Peaks" Sansom, Sarah "Pope" Crampton, Claire "Show me your thong" Mandeville, Helen "Cyclicity" Morgans and last, but possibly not least, Julian "V.C." Bessa. Thanks for informative chats to Tom Martel, Steve Hesselbo and Colin Stark. Thanks to Graham Robertson, and Andy Curtis for help with the occasional mathamatical question, and for treating me as cannon fodder on x-pilot. Thanks to Phil England for the curve fitting program. Thanks to all the staff, especially John O'Sullivan, Diane Relton, Steve "Saint" Usher, Martin Leese, Carol Coggins, Karen Crause and Richard Macavoy. Thanks also to many of the undergraduates for the field trips, the demonstrating, and the silence in the back of minibus during particularly tight corners, especially Ben Woodhouse, Pat Trimby, Mark Cooper, Barny Smith, Kathyrn Goodenough, Caroline Hill, Jacqui Booth, and Mike Goddard.

Onto college : Thanks to all at St Cross for providing a mostly-non-geological refuge, especially to Mark "The Wild One" Jones, Rebecca "What a tidy room!" Hunt, Christina "Bonk" Schams, Sharon "Fruit Shortcake" Newnham, Douglas "I like Clinton" Wigdor, Jim "Muscles" Huntly and to all the college staff, including the stars in the kitchen for the veggie meals.

Finally, I would like to say a big thankyou to my family. Thanks Mum and Dad for the support above and beyond the call of duty, and for buying me lego when I was a child; knowing that you are so proud makes me go all soppy. Thanks to my big brother Phil for teaching me to look after myself (it is useful at conferences), and thanks to Janette for being just so downright ace as my big sister.

Chapter 1

Chapter 1 - Introduction

"I need your clothes, your boots,

and your motorcycle."

(James Cameron, Terminator II)

1.1 The sequence stratigraphic model

The conceptual model of sequence stratigraphy introduced by Mitchum *et al.* (1977) has been the basis for ongoing research in passive rift-margin stratigraphy for the past decade (e.g. Greenlee et al., 1988; Poag and Valentine, 1988; Ross and Ross, 1988; Greenlee et al., 1992). The model is based upon the concept of the depositional sequence, defined by Mitchum *et al.* (1977) as a "stratigraphic unit composed of a relatively conformable succession of genetically related strata and bounded at its top and base by unconformities or their correlative conformities." Depositional sequences are themselves built up from a hierarchy of stratigraphic units, from laminae to parasequences and system tracts (Van Wagoner *et al.*, 1990). This hierarchy provides a framework for description of stratigraphy from a variety of data sources and at a variety of scales. Sequences are separated by unconformities or their correlative conformities, where an unconformity was defined by Van Wagoner *et al.* (1988) as "a surface separating younger from older strata, along which there is evidence of subaerial erosional truncation (and, in some areas, correlative submarine erosion) or subaerial exposure, with a significant hiatus indicated."

Sequences are made up of groups of systems tracts, which themselves are made up of parasequences. Parasequences are defined by Van Wagoner *et al.* (1990) as "a relatively conformable succession of genetically related beds or bedsets bounded by marine flooding surfaces or their correlative surfaces" where a marine flooding surface is defined as "a surface separating younger from older strata across which there is evidence of an abrupt increase in water depth." Parasequences are assumed by Van Wagoner *et al.* (1990) to

form in response to higher frequency relative sealevel oscillations than those responsible for the formation of sequences. Systems tracts (also referred to as parasequence sets) are groupings of parasequences which have particular stacking patterns, and form at particular positions on a relative sealevel curve. For example, the transgressive systems tract would be made up of a series of retrogradational parasequences that are deposited during a time of rising relative sealevel.

The chronostratigraphic significance of depositional sequences hinges on the assumption that sequences are globally synchronous due to the primary control of eustasy on their development (Vail *et al.* 1977b; Posamentier et al., 1988; Posamentier and Vail, 1988; Van Wagoner *et al.* 1990). Maintaining this assumption of synchronous eustatic control, it is possible to derive eustatic curves from the patterns of coastal onlap, defined by Mitchum (1977) as "the progressive landward onlap of the coastal (littoral or coastal non marine) deposits in a given stratigraphic unit" where onlap is defined as "a base-discordant relation in which initially horizontal strata terminate progressively against an inclined surface, or in which initially inclined strata terminate progressively up dip against a surface of greater initial inclination." Using coastal onlap curves to determine eustatic sealevel has led to the definition of eustatic sealevel curves for the Mesozoic and Cenozoic (Haq et al., 1987; Haq et al., 1988). Such eustatic curves are then used as the basis for global correlations of sequences between basins.

The sequence stratigraphic depositional models have become progressively more sophisticated since Mitchum *et al.* (1977). Posamentier *et al.* (1988) and Posamentier and Vail (1988) expanded on the original depositional models. This work was still based around the assumption of dominant eustatic control on sequence development, but it investigated the relationship between eustasy and tectonic subsidence in creating accommodation space. The model also used qualitative fluvial equilibrium profiles to make predictions regarding fluvial deposition and erosion in response to eustatic changes.

Van Wagoner *et al.* (1990) gave considerable detail on how the sequence stratigraphic depositional model can be applied to well logs, cores and outcrop data. It defines a hierarchy of stratigraphy, from laminae to megasequences, which can be used as a descriptive basis for the analysis of stratigraphy. The dominant controlling mechanism was once again stated to be eustasy, occurring in cycles from approximately 50,000 to 5Myr duration., though alternatives such as tectonics and autocyclical effects were discussed.

Posamentier (1992) took the depositional model a little further by differentiating between "forced regressions" caused by relative sealevel fall, when eustatic fall outpaces tectonic subsidence, and "normal" regressions caused by excess sediment flux relative to the accommodation space available on the shelf. Eustasy was not explicitly mentioned as the controlling factor in this aspect of the model. Posamentier and Allen (1993a) attempted to apply these depositional models to an active compressional tectonic setting rather than the normally considered passive margin. The main difference considered was in the pattern of tectonic subsidence across the basin, and this affects the predictions made by the depositional model. Posamentier and Allen (1993b) examined the influence of other factors, namely sediment flux and physiography, on sequence geometries, but still concluded that eustasy and tectonic subsidence and uplift are the primary controls on sequence timing. It also stated, however, that the stratal geometries are primarily controlled by sediment flux and physiography.

1.2 Problems with the sequence stratigraphic model

An assumption central to all the sequence stratigraphic models has been that eustasy is the primary control on sequence development (e.g. Van Wagoner *et al.* 1990), and that the effects of eustasy can be deduced from observation of stratigraphy (e.g. Posamentier *et al.* 1988). Much of the appeal of the sequence stratigraphic methodology comes from its supposed ability to correlate sequence boundaries across global distances. This is obviously dependent on eustasy as a mechanism to give global synchronicity to sequence

boundaries. However, little real consideration has been given to the validity of this assumption by sequence stratigraphic workers, and alternatives such as tectonic controls and variations in sediment supply are not seriously investigated (e.g. Posamentier and Allen, 1993a).

This problem can be considered as one of uniqueness. Although the qualitative sequence stratigraphic models can explain in simple terms why a certain stratigraphic unit has certain features, there may well be several other possible explanations. It is always implicitly assumed in the sequence stratigraphic model that if its predictions match with observations, then it must be correct (e.g. Greenlee *et al.*, 1988). This is not necessarily the case. Other models may be equally capable of reproducing observed features. Sequence stratigraphic models have been widely applied in a variety of temporal and spatial settings, (e.g. Mesozoic-Cenozoic passive margin off East Coast, US; Greenlee *et al.*, 1992 and Baum and Vail, 1988; Carboniferous and Permian cratonic shelves; Ross and Ross, 1988). In most cases such application of the model reveals little, except that a particular piece of stratigraphy has characteristics that can be fitted to the model predictions. Since other possible models are rarely tested against the same stratigraphy, the uniqueness problem is not investigated, and no firm conclusions regarding the controls on the observed stratigraphy should be made.

Given the increasingly apparent problems with eustasy acting alone as the single control on stratigraphy, various workers have been raising the possibility of other factors such as tectonics (Hubbard et al, 1985, Underhill, 1991; Jordan and Flemings, 1991; Sloss, 1991, McGinnis *et al.* 1993) and sediment supply variations (Galloway, 1989; Thorne and Swift, 1991) playing a larger part than previously recognised in controlling sequence development, but it is difficult to isolate examples that can prove the case either way. The particular problem is the recognition from the preserved rock record of the role of different components such as eustasy, tectonics and sediment supply. Accurately assessing their relative contributions with only qualitative models and the rocks themselves is often

difficult, and as a result attempts have been made to overcome the problem with quantitative modelling.

Problems with correlation based on the eustatic curves have been described by Miall (1991) and Miall (1992) which argued that third order cycles defined on such curves cannot be supported because their precision is greater than that of the best chronostratigraphic methods, and that many correlations are simply statistical noise. Even the primary mechanism of ice volume changes used to account for third order eustatic changes has been called into question. Rowley and Markwick (1992) compared the oxygen isotopic composition of planktonic foraminifera with values calculated for the removal of a given water volume inferred by the Haq curve. It found that there was no correspondence, which casts doubt on glacio-eustasy as a mechanism.

Galloway (1989) showed an alternative approach to the definition of sequence boundaries and emphasised the importance of sediment supply and subsidence on sequence development, suggesting that any of the three controls may dominate, and the results would be indistinguishable. Pitman and Golovchenko (1988) suggested small amplitude sealevel changes may produce shelf wide erosional surfaces by a process of regrading, without the need for subaerial exposure of the whole shelf. This idea is particularly interesting since it is central to the model of Posamentier and Vail (1988) that such surfaces must be the result of subariel exposure due to rapid and large magnitude eustatic fall. Miall (1991) questioned the geomorphological accuracy of the depositional models of Posamentier and Vail (1988). This criticism highlights the fact that the sequence stratigraphic models are entirely qualitative, and as such have never been rigorously tested. Even a very simple quantitative analysis of the model would have demonstrated many of the weaknesses highlighted by Mial (1991). Christie-Blick (1991) questioned the timing of sequence boundaries in relation to relative sealevel changes. This has implications for the use of such surfaces in correlation, as previously discussed.

Another fundamental and yet unstated assumption in the sequence stratigraphy methodology, is that observed cyclical stratigraphy must be the result of a cyclically varying controlling mechanism or mechanisms (e.g. Posamentier *et al.* (1988) and Van Wagoner *et al.* (1990)). This is taken to be eustasy, occurring in cycles from approximately 5Myr duration to approximately 50,000 year duration. It is assumed that other controls such as tectonics cannot be responsible for such cyclical stratigraphy, since cyclicty in tectonic controls cannot be demonstrated. Therefore no consideration is given to the possibility of cyclical tectonic effects. Possible cyclical climatic variations are also ignored, as is the possibility of several non-cyclical interacting processes producing cyclical patterns. Both these possibilities are suitable for investigation by quantitative modelling methods.

1.3 Quantitative modelling methodology

Quantitative modelling has an important role to play in investigating the uniqueness problem described above, and in assessing the contribution of eustasy and other possible controls such as tectonics and sediment supply on the development of sequences. Cross and Harbaugh (1989) and Lerche (1989) outlined a methodology for the development and use of quantitative forward models. They defined forward models as models which simulate processes and responses operating on a system with some assumed initial condition and configuration. Figure 1.1 summarises the forward modelling methodology adopted in this work. Cross and Harbaugh (1989) also described a hierarchy of relationships which can be used to construct models. These range from fundamental laws, through first order approximations and empirical relationships, to gross empirical relationships.

Cross and Harbaugh (1989) suggested that the choice of relationships to use in the model is based on two main criteria; the amount of information available about the system being modelled, and the desired complexity and general applicability of the model. The amount

of information available about a system varies, but in general terms most geological systems are too poorly understood to be described with fundamental laws alone. It is necessary to compromise and combine fundamental laws such as the conservation of mass, with gross empirical relationships such as fluvial equilibrium profile geometry. Although some systems may be described more rigorously, this is often at the expense of general applicability, and may lead to overly complex models which become difficult to test.

Despite the potential pitfalls and inherent inaccuracies with quantitative modelling methodologies, used with careful consideration of these problems they do provide a very powerful method of expanding the understanding of the controls on stratigraphy. In particular, such models can provide insight into many of the problems which have been highlighted by the sequence stratigraphic methodology.

1.4 Applications of quantitative models

The development of qualitative sequence stratigraphic models has led to the formulation of a number of quantitative forward models to study controls on stratigraphy. Watts (1982) and Watts *et al.* (1982) showed that patterns of thermal subsidence and flexural isostatic response to sediment loads with an increase in flexural rigidity through time, for example, could produce patterns of coastal onlap which had been taken as indicative of eustatic effects (e.g. Vail et al., 1977b). This in turn led to the work of White and McKenzie (1988) which showed that such patterns of coastal onlap could also be produced without eustasy or flexure using a two layer stretching model. Jervey (1988) argued that a combination of eustasy and regional basin tilting could produce the patterns of onlap seen in basin margins, though the details of the model are sparse, and it appears extremely simplistic. For example, the model does not include erosion in any form.

Watts (1989) examined the patterns of onlap produced with a simple model of sediment progradation and flexural isostasy. The model results showed that with just a simple

geometrical model of progradation and time-variable elastic thickness it is possible to generate some complex patterns of onlap and offlap. Reynolds *et al.* (1991) included flexural isostasy and compaction in a stratigraphic model, alongside tectonic subsidence and eustasy, and used sensitivity tests to assess the effects of these processes on sequence development. It concluded that the inclusion of flexure and compaction could strongly affect the geometry of the resulting stratigraphy, including whether type-1 or type-2 unconformities were produced, and also the timing of sequence boundaries, since both flexure and compaction can create or destroy accommodation space.

McGinnis *et al.* (1993) used a simple model of lithospheric flexure to investigate the effects of marine erosional unloading on stratal geometries. The model results presented suggested that erosion of marine shelf and slope sediments by bottom currents could induce flexural uplift which would be capable of variously modifying stratal patterns on the shelf. The flexural uplift could, depending on the width of the shelf, and the values for lithospheric thickness, produce widespread relative sealevel fall on the shelf, which may prove difficult to distinguish from an eustatically induced fall. McGinnis *et al.* (1993) showed that on a narrow continental shelf, such flexurally driven relative sealevel fall could produce stratal geometries commonly interpreted as eustatically-driven type-1 sequence boundaries. This is another strong example of the way in which the uniqueness problem significantly weakens the sequence stratigraphic model.

Strobel *et al.* (1989), Kendall *et al.* (1991) and Kendall *et al.* (1992) used a stratigraphic model called SEDPAK to simulate basin stratigraphy. The model uses user-defined functions to determine absolute sealevel history, sediment supply and tectonic behaviour, and is made up of a series of gross-empirical algorithms with little or no basis in actual stratigraphic processes or geometries. The model has only been tested by direct comparison of its output with synthesised details of observed stratigraphy. No sensitivity tests have been carried out, and no consideration has been given to problems of uniqueness

in the model results. Given the demonstrable weakness of the model elements and the lack of rigorous testing, the model inspires little confidence.

Lawrence *et al.* (1990) used an essentially geometrical approach to simulate stratigraphy with the emphasis on fine scale lithology prediction. The model includes tectonic subsidence, with the subsidence at any point on the model profile either input directly, or calculated using the two-layer stretching model of Sclater and Christie (1980). Absolute sealevel is varied according to an externally input curve. Sediment supply is also defined externally, but sediment eroded on the non marine profile according to elevation and an erosion time constant, is added to the total available for deposition on the marine profile. Deposition on a marine profile is calculated according to an empirically derived exponential function. Though Lawrence *et al.* (1990) claimed to be able to use the model to evaluate the importance of different controls on stratigraphy, it does not do so, and the only testing criteria apparently applied to the model is whether its output matches in appearance with subsurface data.

Schroeder and Greenlee (1993) used a stratigraphic model, based on the principles of the Exxon depositional model, in an attempt to test the validity of several different eustatic sea-level curves. The modelling seems to suffer from the same problems already discussed; no real tests are applied to the output except to compare the output visually with the observed stratigraphy. One of the conclusions reached is that the eustatic curve from Watts and Steckler (1979) is incorrect because it contains no higher-order fluctuations needed in the model to explain the fine-scale patterns of onlap and facies distribution. However, no consideration is given to the possibility that such fine-scale patterns may be produced by a processes other than eustasy, which are not included in the model. Thus because of the weaknesses in the assumptions, this conclusion is of little value.

Cant (1991) defined a geometrical model to examine patterns of facies migration and erosion controlled by relative sea-level changes and sediment supply. The model suggests

that erosion surfaces can occur because of small changes in slope angles and general facies migration during relative sea-level changes. This could significantly complicate interpretations of stratigraphy. Heller *et al.* (1993) used a geometrical model in an attempt to illustrate how it may be possible to place quantitative limits on the potential combinations of sediment supply, subsidence, and absolute sealevel that could be responsible for any particular stratigraphic pattern. The method invoked stratigraphic solution sets, which consist of various variables such as subsidence and absolute sealevel plotted in multidimensional plots. Sub areas within the plots can then be defined, on the basis of field observations and measurements.

Several workers have used a diffusion based approach to model stratigraphy (Kenyon and Turcotte, 1985; Kaufman *et al.,* 1992; Rivenaes, 1992). Kenyon and Turcotte (1985) use the diffusion equation to model the progradation of a delta assuming sediment movement by bulk-transport processes. This approach was shown to produce a good match between the model predictions and the present bathymetry and the historical progradation of the Fraser and Mississippi river deltas, and the Rhine delta in Lake Constance.

Kaufman *et al.* (1992) used a solution of the diffusion equation that allowed the diffusion coefficient to decay exponentially with water depth to model the deposition of sediment on a shallow marine siliciclastic, carbonate, and mixed siliciclastic shelf. The exponential decay of the diffusion coefficient with depth was intended to represent the exponential decrease in wave power and hence bed shear stress with water depth. However, the values for the diffusion coefficient used in the model runs appear to be rather arbitrary in that the actual values used are not based upon any direct measurements or observations.

The application of the diffusion equation in Rivenaes (1992) used two lithologies, sand and shale, in the model and defined a separate transport-coefficient function for each lithology. Diffusivity varies with water depth, and compaction of sediment is included in the mass-balance of the model equations. Tectonic subsidence and eustasy and defined as

external functions. Flexural isostasy is also included. Rivenaes (1992) used the model to predict the patterns of stratigraphy obtained with a simple sinusoidal eustatic curve, and found that the model was capable of reproducing some observed features of passive margin stratigraphy, such as shoreline migration, stratal onlap and downlap, and the trapping of sand in the coastal plain area during times of transgression.

The Rivenaes (1992) model shares a similar problem to that of Kaufman *et al.* (1992) in that there is a lack of quantitative observational evidence to support the values of diffusion coefficients used for the sand and shale lithologies within the model. The value for sand ranges from approximately $10000m^2yr^{-1}$ at elevations of 10m and above, to $50m^2yr^{-1}$ at and below 20m below sealevel. The values for shale show the same trend but with a slightly higher value at positive elevation, and a higher value in the marine environment of approximately $2.5m^2yr^{-1}$. Although the magnitude of the curves is based on values given by other workers (e.g. Flemings and Jordan, 1989), the patterns of variation with elevation are based upon qualitative observation of the efficiency of transport of the grain size populations in different environments, and have been selected in advance to give features such as trapping of sand in the marine environment and bypassing of shale into deeper water. Such selection of diffusion coefficients, even if partly based on observational evidence, must limit the interpretation of the model results.

Thorne and Swift (1991) modelled erosion and deposition in a marine shelf setting using surfaces of dynamic equilibrium which were determined by a series of mutually interdependent variables, sediment input rate, sediment character, sediment transport rate, and the rate of relative sealevel change. Five different types of equilibrium surface are defined, of which the isostatic equilibrium profile is most useful in terms of its spatial and temporal scale, for investigating continental margin deposition. Results from the model, using another type of profile, which is dependent on the rate of relative sealevel change, simulate sequence stratigraphic systems tracts. Thorne and Swift (1991) concluded from this model work that the generation of type-1 versus type-2 sequences in the model is

dependent on the gradient of the shelf and the slope, and also the magnitude of the sediment supply. The model does not include any subaerial deposition or erosion which makes it difficult to compare the results directly with the sequence stratigraphic model.

Shaw (1987) and Slingerland (1989) raised the possibility of non-linear behaviour producing cyclicty in the stratigraphic record. Slingerland (1989) described some of the principles of chaos theory and suggested that if stratigraphic systems are chaotic, small changes in initial conditions in such a system may lead to gross differences in the final configuration of the stratigraphy. Shaw (1987) proposed that apparent periodicitys in the geological record, for example periodic mass extinctions, may not be due to simple periodic forcing mechanisms, but may instead be due to more complex non-linear feedbacks between more than one mechanism. Thus examples of periodic stratigraphic phenomenon such as Milankovitch cyclicity (e.g. Matthews and Frohlich, 1991; Imbrie, 1985) may not be caused by periodic mechanisms such as orbital forcing, but may instead be due to as yet unidentified couplings and feedbacks between various autocyclic processes.

Gaffin and Maasch (1991) and Gaffin (1992) illustrated this principle with a very simple model of sedimentary basin development which showed cyclicty produced by unforced free oscillations. The model consists of a simplified low-order implementation of a general time evolution continuity equation for a sedimentary surface. The equation includes an expression for subsidence, and an expression for the non-linear diffusive transport of sediment. Although the implementation is simple, the model shows clear unforced oscillatory behaviour. This results from a feedback effect; falling relative sealevel increases the magnitude of erosion, which increases progradation, which further increases erosion exponentially, until progradation becomes unstable and a transgression occurs. Thus an apparent cyclicity in the model output is due purely to a feedback between model elements, with no periodic external input. Such unforced cyclicity could be extremely

important with respect to stratigraphy generally, and the sequence stratigraphic model in particular.

1.5 Aims and objectives

The aim of this thesis is to build upon the modelling work described above using a quantitative stratigraphic forward model to investigate passive rift margin stratigraphy. Chapter two describes the formulation of the model and the assumptions that underlie it. The implementation of the various model components is described in detail, and a comparison is made between a dynamic diffusion approach and a geometrical approach to modelling the fluvial profile.

The model is then used to three main ends. Firstly, in chapter 3, it is used to investigate the various controls on sequence geometry. This is achieved by firstly using the model to reproduce the basic conceptual sequence geometry defined by Van Wagoner *et al.* (1988), Posamentier *et al.* (1988) and Posamentier and Vail (1988), considering the discrepancies between the two, and then conducting a series of sensitivity tests in order to determine rigorously the importance of the different parameters in the model. From this it is possible to draw conclusions regarding the possible importance of various controls on the stratigraphy in actual stratigraphic systems.

Secondly, the model is used to investigate the possibility of cyclical patterns of stratigraphy produced not by an external periodic forcing mechanism, but by the complex feedback interaction between several different model elements. Chapter 4 describes such a feedback within the model, and shows a series of sensitivity tests used to investigate the feedback. The sensitivity tests demonstrate that the feedback effect is produced by a numerical instability inherent within the model. This demonstrates that discretised geometrical models are not suitable for investigating such feedback effects.

Thirdly, in chapter 5, the stratigraphic model is used to investigate aspects of the Tertiary stratigraphy of the North American Atlantic passive margin. However, rather than simply using the model to reproduce basic aspects of the observed stratigraphy, and assuming that a good match proves the validity of the model, it is used instead to examine the envelope of possible causes for the observed stratigraphy. This is achieved by conducting sensitivity tests to determine which controls may be important, and which may not. In particular, the model is used to test three different eustatic curves, and to examine the possible effects of variable sediment supply.

The conclusions drawn from the model results presented in chapters 3, chapter 4 and chapter 5, are summarised and discussed in chapter 6. A list of the parameters used in the model is given in appendix 1, and a full listing of the source code is included in appendix. 2.

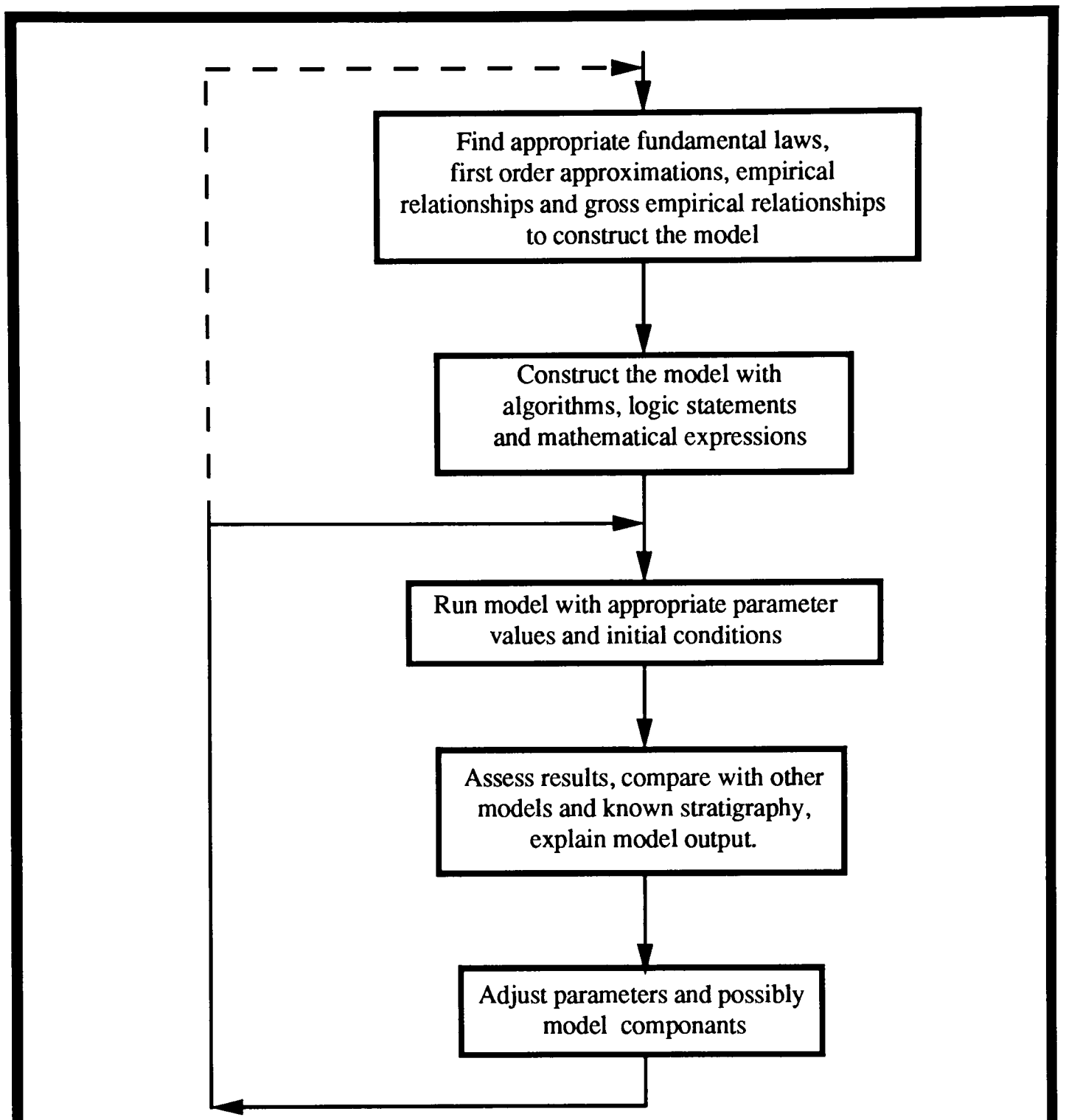

Figure 1.1. A modelling methodology flowchart

Chapter 2

Chapter 2 - Methodology and Assumptions

"Travelling through hyperspace ain't like dusting crops
boy! Without the precise calculations we'd fly right
through a star or bounce too close to a supernova, and
that would end your trip real quick wouldn't it?"

(George Lucas, Star Wars)

2.1 Introduction

This chapter describes the equations, algorithms, and parameters which together comprise a forward model of passive rift-margin stratigraphy. Also described are the assumptions which underlie the various elements of the model and the values for the model parameters. A full appreciation of the details of the model formulation, the assumptions which underlie the equations and algorithms chosen, and the values chosen for model parameters is essential in order to correctly interpret the model results. Comprehensive descriptions of the hardware, the operating systems and the programming languages used in constructing the model are given, along with a full listing of the source code, in appendix 2. The description of the methodology given below, and the source code listing in appendix 2 should together allow the model results given in subsequent chapters to be reproduced.

2.2 The formulation of the model

The model can be summarised in a simplified form as one equation which defines the contribution to the elevation of a chron in two-dimensions as a function of time and distance thus

$$H(x, t + \Delta t) = H(x, t) - S(x, t) + \Delta H(x) + F(x) \qquad (1)$$

where H is the elevation of a chron surface, S is the magnitude of thermal subsidence, ΔH is the magnitude of deposition or erosion, and F is the magnitude of the flexural subsidence or uplift due to deposition or erosion. All these individual model elements, the model assumptions, and the details of the model coordinate system, are described in detail in the following sections.

2.3 Basic model assumptions

2.3.1 Two versus three dimensions

A fundamental assumption behind the model coordinate system is that passive rift-margin stratigraphy can be modelled as a two-dimensional section to a sufficient degree of accuracy as to make the model results useful in investigating stratigraphic patterns. In reality such stratigraphy is the result of processes operating in three dimensions, so it is important to attempt to assess the degree to which the accuracy of the model results is reduced by the assumption of two-dimensionality.

The principal fundamental law in the model is the conservation of mass, implemented as the conservation of area along the two-dimensional model profile. In natural systems the principle of the conservation of mass operates in three dimensions. Hence because the model is two-dimensional, its accuracy must be reduced, but the different model components are affected to different degrees depending predominantly upon the degree of symmetry or asymmetry inherent in the process or system being modelled. Assessing the exact effects of this weakness is difficult, but it should be considered carefully when interpreting the model output.

2.3.2 Discretised representation of continuous processes

Another fundamental problem with all quantitative models on digital computers is the need to represent continuous natural systems in a discretised format. This problem manifests itself in this model coordinate system in two ways; the horizontal spacing of data points on the model profile, and the length of the model time step.

The length of the horizontal step on the model profile controls the precision of the area calculations used to ensure the conservation of area, and also the precision of the marking of environments of deposition. The magnitude of this spacing is a trade off between accuracy, the total profile length, and the computer time required for calculations. Increasing the spacing of points on the profile allows faster model runs and longer profiles, but reduces the accuracy of the area fitting, and hence leads to small amounts of area being lost or gained. This loss of accuracy is an important constraint on the model, since larger point spacing would introduce unacceptable errors in the area calculations.

2.3.3 The length of the model time step

The length of the time step between generation of chrons is also very important to the validity and accuracy of the model. All geological processes that act to form stratigraphy are continuous in nature. Thus with a digital computer model various assumptions have to be made to approximate such continuous processes in a discretised form. In this model it is implicitly assumed that all the modelled processes, but particularly deposition and erosion, and flexure, occur instantaneously for a particular time step, after which there is a period of absolute quiescence prior to the next time step. This has some very important implications for the model results depending on the length of the time step used, and should always be considered when interpreting the model results. This problem is demonstrated with a particular example in chapter 4.

2.4 Description of the coordinate system and the data structures

The model is constructed around a three-dimensional coordinate system used to represent stratigraphy. The first two dimensions represent horizontal distance in kilometres and elevation in metres respectively. Together they define the two-dimensional model sections. The third dimension is elapsed model time (E.M.T.), measured in millions of years, or mega years (Myr). Figure 2.1 summarises this coordinate system.

The primary data structure in the model is used to represent the chronostratigraphic surfaces ("chrons" for short). The data structure consists of a two-dimensional array where the array subscripts represent E.M.T. and horizontal distance respectively, and the array contains elevation values. Figure 2.2 shows this data structure in diagrammatic form. The structure can store up to 200 chrons with 4906 elevation values along each chron. Thus if the total profile length is 1024km, the separation in kilometres between points is 0.25km.

The horizontal position, in kilometres, of each point on each chron may be calculated by dividing the profile length in kilometres by the total number of points to give the point separation, also in kilometres. Multiplying this value by the subscript value for that point gives the distance in kilometres of that point from the profile origin. All aspects of the model, such as for example, the definition of the position of the beach, and the elevation of the sealevel datum, are based around the same coordinate system described above and shown in figure 2.1.

The E.M.T. is the third dimension in this primary data structure. One chron is generated at each time step, and stored in a temporary working array, but the interval at which chrons are actually stored in the data structure can be greater than this time step. This allows a model run with time steps of, for example, 0.01Myr to run for longer than 2.0Myrs. The age of any chron is calculated by taking the array subscript values and multiplying this by the duration of each chron which is specified as a model input parameter (see appendix 1).

A second separate data structure is utilised to record the distribution of depositional environments. These environments, calculated on the basis of water depth, are represented by codes at each point on each chron (Table 2.1). The codes along the initial chron are set to the integer value of 250 to represent initial non-deposition. As each subsequent chron is generated, the depositional environments along its length are recorded. When points on the new chron are erosional, the value of points at the same horizontal position on older chrons being eroded, are reset to indicate this erosion. The algorithms controlling erosion of chrons are described in more detail in section 2.6.5.

Numeric Code	Depositional Environment
1	Fluvial
2	Beach and shoreface
3	Offshore shelf
4	Shelf slope
6	Fluvial erosion
7	Marine erosion
250	Non-deposition/non-erosion

Table 2.1

The final major data structure in the model is used to store values for several time-dependent model elements. These are absolute sealevel elevation, areas of sediment deposition and erosion, relative sealevel at a given point, cumulative thermal subsidence at a given point, and elevation of the point of stratal onlap. The structure consists of another two-dimensional array. The first subscript gives the number of the time step (which can be converted directly to E.M.T. as described above), and the second gives a code for the type of data contained in that array element. Table 2.2 shows these codes and the associated data types.

Subscript value	Data type
0	Elapsed model time (Myr)
1	Absolute sealevel elevation (m)
2	Area of fluvial deposition (m^2)
3	Area of fluvial erosion (m^2)
4	Area of marine deposition (m^2)
5	Area of marine erosion (m^2)
6	External sediment input (m^2)
7	Relative sealevel at a point (m)
8	Thermal subsidence at a point (m)
9	Elevation of stratal onlap (m)

Table 2.2

The absolute sealevel element differs from the other data types in that rather than recording the values of the variables as they are generated during the model run, these values are defined during model initialisation and then used as a reference to update the value of the absolute sealevel datum as the model runs. Details of the generation of the absolute sealevel curve are given in section 2.6.1.

The other elements in this data structure are used to store the relevant values calculated during the model run. Separate values for fluvial erosion, fluvial deposition, marine erosion and marine deposition are stored in the data structure. For each chron the sum of the area of fluvial deposition and the area of marine deposition should equal the sum of the area of fluvial erosion and marine erosion, since no out-of-plane sediment transport is included in the model. This is not the case, however, when the option for external sediment input is selected. In this case, the sum of the area of fluvial and marine deposition together equals just the area of external sediment input in the case of constant sediment supply, or

the sum of the external input and the fluvial and marine erosion. The initialisation of the external sediment input curve is described in section 2.6.1.

The values of cumulative thermal subsidence and relative sealevel are calculated at a point on the profile given as a model input parameter. Relative sealevel at any point is given by calculating the elevation difference between the initial model chron, which is used as the reference surface, and the current absolute sealevel datum. This is not the same as water depth, since the initial chron may have been buried by deposition on subsequent chrons. Negative values for relative sealevel indicate elevations of the point above its initial elevation. Stratal onlap is calculated at the end of the model by taking the height of those points where the fluvial portion of a chron terminates against an older chron below.

2.5 Model parameters

The model has thirty eight parameters, not including the values used to calculate the lithospheric stretching factor profiles and the initial topography. Several of these parameters control various options in the model e.g. what type of flexure calculations are to be used, what type of sediment supply model is to be used. The remaining parameters contain values for variables used directly in the model e.g. the model time step (Myrs), and the gradient of the offshore shelf profile (mkm^{-1}). The purpose and the range of values for all these variables are given in appendix 1.

2.6 The sequence of the algorithms

Once the model parameters have been set the model must be initialised. The initialisation routines are executed once before each model run. They are described in section 2.6.1. The input parameters may also be adjusted whilst the model is running. Figure 2.3 shows a flowchart outlining the sequence of algorithms to generate each chron in the model. This indicates the order in which the equations described in the following sections should be

applied to reproduce the model output. The first step for each chron is to increment the E.M.T. by the model time step, adjust the elevation of the absolute sealevel datum according to the pre-defined absolute sealevel curve, and, if appropriate, to calculate the area of sediment to be applied to the top of the fluvial profile as the external sediment budget. The next step is to calculate the magnitude of the thermal subsidence at each point along the profile (section 2.6.3). Once this has been done, the position of the chron-sealevel datum intersection (for the sake of brevity this will be referred to more loosely as "the beach") on the profile can be found (section 2.6.4). This position is then used in the generation of first the fluvial, and then the marine equilibrium profiles. These profiles, described fully in sections 2.6.5, control erosion and deposition of stratigraphy, and can thus be used to determine the magnitude and distribution of sediment loading and unloading across the profile. The final step for each chron is to use this magnitude and distribution of loading across the profile to calculate the lithospheric flexural response (section 2.6.6).

2.6.1 Model initialisation

The first step in each model run is to initialise the model parameters, execution variables, and the model data structures. The values of the input parameters are read from input windows, and the value of key model variables (e.g. the number of chrons generated, the E.M.T.) are set to their starting values. The absolute sealevel curves are defined using sinusoidal curves or straight lines of a given gradient. The sinusoidal curves are calculated using the equation

$$d(t) = \left(\frac{y_1 - y_2}{2}\right) + \left(\frac{y_1 - y_2}{f} \sin\left(\frac{2\pi}{f\,t}\right)\right) \qquad (2)$$

where y_1 and y_2 are the maximum and minimum sealevel datum elevations respectively, f is the period of the curve in mega years, and t is E.M.T. These are all given as model parameters. Two sinusoidal curves of different periods may be used. Thus a short-term

curve of period 0.1 to 1.0Myrs may be superimposed upon a longer-term curve of period 1.0 to 100.0Myrs. The longer term curve may also be defined as a simple linear increase of decrease in absolute sealevel elevation thus

$$d(t) = d(t - t_{inc}) + \left(\frac{y_1 - y_2}{f}\right) \qquad (3)$$

where t_{inc} is the length of the model time step in Myrs. The curves controlling the area of external sediment supply (i.e. the area supplied to the top of the model fluvial profile independent of erosion on the profile) are defined using similar equations where maximum and minimum datum elevations are replaced by maximum and minimum areas of sediment. Both sinusoidal and linear curves may be defined, and also saw-tooth curves where sediment supply increases or decreases linearly for a specified period and then reverts to the original minimum or maximum value. External sediment supply can also be held at a constant given value.

Finally in the initialisation procedure the initial topography and the stretching factors required for the thermal subsidence calculations (see section 2.6.3) across the profile are set. The initial topography is defined in a data file consisting of coordinate pairs, the first value being a position on the model profile in kilometres, and the second being the elevation in metres at that point. These coordinate pairs are read two at a time, and the elevation values at each point on the profile between the specified positions are calculated using simple linear interpolation. The values for the stretching factors across the profile are defined using the same method.

2.6.2 Updating the model variables

Several model variables are updated at this point. The E.M.T. is incremented by the value of the time step parameter, and the total number of time steps completed is incremented by one. The elevation of the absolute sealevel datum is adjusted according to the pre-defined

absolute sealevel curve. If appropriate, the area of external sediment supply is also adjusted according to the pre-defined external sediment supply curve.

2.6.3 Thermal subsidence

Thermal subsidence is the fundamental tectonic mechanism by which accommodation space is created in passive margin basins. It is modelled here using either the one-layer uniform stretching model of McKenzie (1978) or the two-layer non-uniform stretching model of Hellinger and Sclater (1983).

The one-layer uniform stretching equations from McKenzie (1978) allow the lithospheric stretching factor to be varied laterally across the profile, although this is not actually used in McKenzie (1978). Values for the stretching factor are specified at a small number of points on the profile. Linear interpolation is then used to calculate the stretching value at each point on the profile. The magnitude of subsidence at each point is given by :

$$S_t = e(0) - e(t) \qquad (4)$$

where e is the subsidence in metres at a given time t in seconds, and is given by :

$$e(t) = \frac{a\rho_m \alpha T_m}{\rho_m - \rho_w}\left\{\frac{4}{\pi^2}\sum_{n=0}^{\infty}\frac{1}{(2n+1)^2}\left[\frac{\beta}{(2n+1)\pi}\sin\left(\frac{(2n+1)\pi}{\beta}\right)\right]\exp\left(-(2n+1)^2\frac{t}{\tau}\right)\right\} \qquad (5)$$

Table 2.3 lists and defines the parameters used in the equations. The value for the magnitude of subsidence at each point is used to adjust the elevation of previous chrons.

Parameter	Definition	Values
a	initial thickness of lithosphere	125 km
t_c	initial thickness of continental crust	35 km
ρ_m	density of mantle at 0°C	3330 kg m^{-3}
ρ_c	density of crust at 0°C	2800 kg m^{-3}
ρ_w	density of water	1030 kg m^{-3}
ß	lithospheric stretching factor	input parameter
$ß_c$	crustal stretching factor	input parameter
$ß_{sc}$	subcrustal stretching factor	input parameter
$ß_L$	ratio of t_c to stretched crustal thickness	dimensionless
α	thermal expansion coefficient.	3.28E10^{-5}°C^{-1}
T_m	temperature at lithosphere base	1333°C
τ	$a^2 / \pi^2\kappa$ lithospheric time constant	62.8 Myr

Table 2.3

The non-uniform stretching model works on very similar principles, except that two stretching factors are utilised, one for the crust ($ß_c$) and a second for the lithospheric mantle ($ß_{sc}$). Values for both stretching factors are given as initial model parameters, and the values of subsidence used to adjust previous chron elevations. The equations used in this model are taken from Hellinger and Sclater (1983). There is no facility in the model to check for space problems between the crust and the mantle caused by differential stretching. This is assumed to be done when defining the stretching value profiles.

The value for subsidence S(t), where t is time in seconds, is given by:

$$S(t) = e(0) - e(t) \qquad (6)$$

where e(t) is given by :

$$e(t) \approx \frac{2a\alpha\rho_m T_m}{(\rho_m - \rho_w)\pi} \sum_{k=0}^{\infty} \frac{C_{2k+1}}{2k+1} \exp\left[\frac{-(2k+1)^2 t}{\tau}\right] \qquad (7)$$

where

$$C_n = \frac{2(-1)^{n+1}}{n^2\pi^2}\left[(\beta_c - \beta_{sc}) \sin\left(\frac{n\pi t_c}{a\beta_c}\right) + \beta_{sc} \sin\left(\frac{n\pi}{\beta_L}\right)\right] \qquad (8)$$

and

$$\frac{a}{\beta_L} = \frac{t_c}{\beta_c} + \frac{a - t_c}{\beta_{sc}}. \qquad (9)$$

Parameters used in these equations are defined in Table 2.3.

Neither of the models used here include the effects of lateral heat flow (e.g. Steckler and Watts, 1981). Though these effects may be important during rifting and for up to 20Myr after rifting (Jarvis and McKenzie, 1980; Cochran, 1983), and in narrow basins where lateral temperature gradients are high (Pitman and Andrews, 1985), they are less important on older thermally subsiding passive margins.

2.6.4 Finding the Beach

Once the effects of thermal subsidence have been calculated and applied to all previous chrons, the position of the intersection between the last chron and the absolute sealevel datum can be found. The algorithm to find this beach position starts with the first point at the landward end of the profile and checks each point in turn to determine if it is below sealevel, i.e. its elevation is less than the elevation of the absolute sealevel datum. The first point to meet this criterion defines the position of the beach. Once the beach position is known, it can be used in the definition of the fluvial and the marine equilibrium profiles.

2.6.5 Depositional and erosional profiles

A crucial central element in a stratigraphic model is the method used to determine the distribution of deposition and erosion of stratigraphy in time and space in the model. The following section compares and contrasts two alternative approaches to the problem, namely a geometrical approach using equilibrium profile curves with a specified geometry, and a diffusional approach using a solution of the standard diffusion equation in which the rate of change of topographic elevation is proportional to the rate of change of topographic slope.

2.6.5.1 The concept of geometrically defined equilibrium curves

The concept of the fluvial equilibrium profile

Using this approach deposition and erosion of stratigraphy in both the subaerial and the submarine portions of the basin is modelled using the concept of geometrically defined equilibrium profiles. Much previous work has been done in an attempt to define equilibrium with respect to fluvial systems. Davis (1899; 1902) assumed that over a geologically significant period of time the downstream portions of rivers attain a "graded" profile in equilibrium with the prevailing conditions "by a process of cutting and filling, until an equable slope is developed along which the transport of its load is most effectively accomplished." Mackin (1948) defined a graded stream as "one in which, over a period of years, slope is delicately adjusted to provide, with available discharge and with prevailing channel characteristics, just the velocity required for the transportation of the load supplied by the drainage basin. The graded stream is a system in equilibrium; its diagnostic character is that any change in any of the controlling factors will cause a displacement of the equilibrium in a direction that will tend to absorb the effect of the change." Leopold and Bull (1979) expanded on this by suggesting that the adjustment to a "graded

(equilibrium) stream is one in which, over a period of years, slope, velocity, depth, width, roughness, pattern and channel morphology delicately and mutually adjust to provide the power and efficiency necessary to transport the load supplied from the drainage basin without aggradation or degradation of the channel."

All these definitions assume that a stream undergoes some perturbation away from its original equilibrium profile, and then regains equilibrium by adjusting one or several of the variables such as slope, channel morphology and channel width. This is referred to as static equilibrium. A second type of equilibrium, referred to as dynamic equilibrium was described (Hack, 1960; Bull, 1991) in which a stream maintains a delicate balance of variables to maintain its profile in response to constantly changing conditions. An example of this would be a steam flowing over an area of tectonic uplift. If the stream had sufficient power, it would erode downwards at a rate equivalent to the rate of tectonic uplift, and hence maintain its profile shape. This was referred to by Bull (1991) as type 1 dynamic equilibrium. Type 2 dynamic equilibrium occurs when a stream is responding to changes in conditions, such as for example, tectonic uplift, but cannot maintain a particular profile shape.

Although the concept of dynamic equilibrium may more accurately represent the behaviour of streams responding to continuous changes in conditions, the concept of static equilibrium more accurately represents the operation of an equilibrium profile in a stratigraphic model with discrete time steps with a magnitude of thousands of years. The assumption then is that such profiles can respond to changes in base-level, changes in beach position, and surface uplift and subsidence on the profile, within the duration of a model time step. This assumption raises the question of fluvial response times. Howard (1982) calculated that the Yampa and the Little Snake rivers in North America would adjust to base-level changes in three to five kiloyears, while the much larger Mississippi river would take 50 to 80Kyrs. Thus it seems reasonable to assume that with a model time

step of 100Kyrs the fluvial profile has sufficient time to adjust to changes in base-level and profile shape.

Another question regarding the nature of stream response to changes in system variables such as base-level was highlighted by Schumm (1993), which argued that streams can respond to a slow fall in base-level by changing their channel pattern without the need for aggradation or downcutting. While this may well be the case on shorter time scales, it seems unlikely that this will apply for longer time scales when events such as avulsions force the stream to create new channel courses in a new position on the flood plain, and hence allow the fluvial system to aggrade or degrade while re-establishing a channel pattern. This question does highlight the lack of data regarding the response of fluvial systems to base-level changes over a period of a kilo year and longer. Such data would be invaluable to stratigraphic modelling.

Geometrical curve fitting

It is possible to fit mathematically generated curves to modern river profiles. Snow and Slingerland (1987) showed that such curves can provide a fit with only a small error to a profile modelled from first principles using sediment transport equations. Figures 2.4 and 2.5 show four topographic profiles from rivers on the North American and African Atlantic margins. Plotted against each topographic profile for comparison are best-fit complementary error function curves, calculated using the Levenberg-Marquardt method (Press et al., 1986; England, pers. comm. 1993). The complementary error function curve has the form

$$\mathrm{erfc}(\eta) \equiv 1 - \left(\frac{2}{\sqrt{\pi}} \int_0^{\eta} e^{-\eta'^2} d\eta' \right) \qquad (10)$$

where η is the dimensionless error function parameter, and η' is a dummy variable of integration.

Such fits are significant in the context of diffusional profiles and are discussed further in section 2.6.5.3, but if the complementary error function is treated as a purely geometrical entity, the fits are also significant, since they demonstrate that the curve has the correct geometrical form to approximate river profile geometry at a given time. This is supported by the conclusions of Snow and Slingerland (1987).

2.6.5.2 The implementation of the geometrical fluvial profile

Taking the geometrical approach to fluvial profile modelling, the fluvial profile is represented by an exponential curve or a complementary error function curve treated as a geometrical entity. The curve is scaled and fitted between the beach and a point landward of the beach which is taken to be analogous to the upstream edge of the coastal plain on a passive margin. Thus the fluvial profile in the model does not represent the whole length of a fluvial profile from the beach to the drainage divide, but rather just the lower portion of the profile where preservation potential for deposited stratigraphy is highest. The position of the landward limit of the fluvial profile can either be held fixed throughout the model run, or it can be moved landward at a rate given as a model parameter. This allows for a situation in which the width of the coastal plain increases with time with respect to the initial position of the beach.

The exponential curve has the form

$$y(x) = e^{n(x - x_1)} + d(t) - 1 \qquad (11)$$

where

$$n = \frac{\ln (y_2 - d(t) + 1)}{(x_2 - x_1)}. \qquad (12)$$

The variables x_1 and x_2 are the horizontal start and end points of the profile respectively, the start point being the edge of the coastal plain, the end point being the beach (see figure 2.6). The variable d(t) is the elevation of the absolute sealevel datum, and y_2 is the elevation above the zero datum of the topography at the landward limit of the profile.

The complementary error function curve has the form

$$y(x) = \frac{\operatorname{erfc}((x - x_1)\cdot \omega - \theta)}{\Phi} + d(t) \qquad (13)$$

where

$$\omega = \frac{\theta}{(x_1 - x_2)} \qquad (14)$$

and

$$\Phi = \frac{1 - \theta}{y_1 - d(t)}. \qquad (15)$$

Figure 2.6 explains the variables x_1, x_2 and y_1 in diagrammatic form. The equations are essentially scaling functions for the output from the complementary error function. The variable θ controls the section of the complementary error function used to define the profile such that the error function parameter values range from 1.0 to θ. It can be seen from the plot of the function in figure 2.7 that the steepness of the curve decreases with increasing values of x along the horizontal axis of the plot. Thus the value of θ used determines the section of the curve used, and hence the concavity of the geometrical fluvial profile. Higher values of θ increase the concavity of the profile, and vice versa.

The geometrical curves are used to control deposition and erosion by comparing at each relevant point on the model profile, the elevation of the fluvial profile generated for the

current time step, and the elevation of previous chrons. This is summarised in quantitative form as

$$\Delta H(x) = y(x) - H(x, t - \Delta t) \qquad (16)$$

where y is the elevation of the new profile, as defined in equations 11 and 13, and $H(t - \Delta t)$ is the elevation of the chron from the previous time step. Thus positive values of ΔH leads to deposition, since the area between the new profile and the previous chron is treated as subaerial accommodation space and filled with available sediment. Negative values of ΔH lead to erosion as the elevation of the old chron is reduced to the elevation of the new profile. This process of deposition and erosion in the model is illustrated in figures 2.8 to 2.11.

The area deposited or eroded is subtracted from, or, depending on the model options specified, added to the total sediment budget available for deposition. Conservation of mass is maintained, so that when appropriate according to the sediment supply options chosen, the area of sediment deposited is always equal to the area of sediment eroded, plus any external input. Areas of erosion and deposition are calculated using simple trigonometry. Adjacent points on two chrons form a trapezium shape, the area of which can be calculated by splitting the shape into its component rectangles and triangles (figure 2.12). The elevation difference between the older chrons and the new profile is the magnitude of sediment loading and unloading used to calculate the flexural response, as explained in section 2.6.6.

Fixed and free geometrical profiles

When using a geometrically defined equilibrium profile to model the fluvial profile there are two alternative methods regarding the positioning of the beach and hence the geometry and the pattern of deposition and erosion on the profile. In the case of the fixed profile, the

beach is maintained at the position determined by the algorithm described in section 2.6.4. The profile is fixed in the sense that the profile is allowed to subside due to thermal subsidence without causing fluvial aggradation. However, any part of the profile uplifted above the original curve, for example as a result of flexural uplift, is removed. This is shown in diagrammatic form in figure 2.8. The fixed profile is thus analogous to a river system with very low sediment supply, unable to initiate significant deposition, but with sufficient power to erode uplifted parts of the profile. This algorithm is only valid for relative or absolute sealevel rise.

The second method is to allow the fluvial profile the freedom to determine the position of the beach by means of a sediment partitioning coefficient. The sediment partitioning coefficient determines the relative areas of external sediment supply that are deposited in the fluvial and the marine portions of the profile. For example, a partitioning coefficient value of 0.3 means that if there is $1.0km^2$ of external sediment input, $0.3km^2$ will be deposited as fluvial sediment and the remaining area, plus any sediment produced by fluvial and marine erosion, will be deposited as marine stratigraphy. Thus the position of the beach is determined by iteratively adjusting the beach position until the closest match is obtained between the area of fluvial stratigraphy deposited, and the required area specified by the partitioning coefficient (figure 2.13).

The partitioning coefficient is difficult to constrain as a model parameter. It can be constrained to a limited extent by examining the planform areas and thicknesses of terrestrial and marine deposition for modern systems, and using the ratio between these two volumes as the partitioning coefficient. However, such data on marine and fluvial depositional volumes are not easily available. A second and less accurate method is to use the subaerial and submarine areas of a delta to calculate the ratio. For example, the Delaware river delta has a total depositional area of $13660m^2$, of which $2160m^2$ is subaerial (Pers. comm. Hovius, 1993). This gives a fluvial-marine partitioning coefficient of 0.16. Obviously such calculations are limited by the accuracy and extent of the data

available, and provide no information on how the partitioning coefficient should be varied through time. However, they do provide limited constraint on the values used.

Response of the free fluvial profile to absolute sealevel change

This section explains how the geometrical fluvial profile responds to absolute sealevel change, and also how the profile is used to control the distribution of deposition and erosion. Figure 2.9 shows the profile response to falling sealevel. At time 2 absolute sealevel has fallen and the elevation of the new fluvial profile is less than that of the previous profile along much of its length. Hence erosion occurs on these parts of the new profile. Beyond the position of the beach from time 1, however, the elevation of the profile is greater than the elevation of the previous chron, and hence some deposition occurs. The horizontal and vertical extent of this deposition depends upon the magnitude of the sealevel fall, the magnitude of the sediment supply, and the value of the partitioning coefficient.

The geometry of the fluvial profile during rising absolute sealevel is also dependent not only on the magnitude of the sealevel rise, but also upon the magnitude of sediment supply and the partitioning coefficient. Figure 2.10 shows the profile geometry and the distribution of deposition and erosion in response to rising absolute sealevel when either the rate of sealevel rise is slow, sediment supply is high, or the partitioning coefficient is high. In this case there is no erosion on the profile, only aggradation and progradation. Figure 2.11 contrasts this with an example of the geometry produced when sealevel rise is rapid, sediment supply is low, or the partitioning coefficient is low. In this case, there is some erosion on the upper part of the profile, accompanied by aggradation on the lower portion of the profile.

The realism of this profile behaviour will be discussed and compared with the behaviour of the diffusional profile below in section 2.6.5.4.

2.6.5.3 The concept of the diffusional profile

Diffusion describes the transport of matter in physical systems from one part of the system to another as a result of random molecular motions (Crank, 1975). The rate of transport of the matter in such cases is proportional to the concentration gradient, and this relationship leads to the classical diffusion equation

$$\frac{\partial C}{\partial t} = \kappa \frac{\partial^2 C}{\partial x^2} \qquad (17)$$

where C is the concentration of the diffusing substance, t is time, x is the space coordinate measured normal to the section, and κ is the diffusion coefficient which has the units length^2 time^{-1}. This diffusion equation can be used to describe, for example, the transfer of heat by conduction in a solid, or the transfer of material across some boundary between material types. It can also be used to describe the erosion, transport, and deposition of sediment by assuming that topographic height h is analogous to concentration C in equation 17, thus giving

$$\frac{\partial h}{\partial t} = \kappa \frac{\partial^2 h}{\partial x^2} \qquad (18)$$

This is derived by combining the one-dimensional sediment continuity equation for bedload transport which conserves mass

$$\frac{\partial h}{\partial t} = -\frac{1}{\rho_s(1-\lambda)} \frac{\partial Q}{\partial x} \qquad (19)$$

where ρ_s is the density of sediment grains, λ is the porosity of the deposited sediment, and Q is the rate of sediment transport, with the simple diffusional relationship

$$Q = -K\frac{\partial h}{\partial x} \qquad (20)$$

where K is a sediment transport coefficient with the units length^2 time^{-1}. Substitution of (20) in (19) gives the diffusion equation in (18) where $\kappa = K/\rho_s(1-\lambda)$. The value of κ for a solid volume of sediment of unit width (18) is simply K, with units of length^2 time^{-1}.

It is important to note that one of the fundamental assumptions that underlies the derivation of the diffusion equation as given above is that there is no change in the suspended sediment concentration in the stream flow across its bed, i.e. that the deposited sediment contains no contribution from suspended load. This is obviously unrealistic since sediment grades such as fine sand, silt and clay comprise a substantial portion of alluvial stratigraphy. Attempting to include extra terms in the diffusion equation to account for this leads to the problem that the rate of transport of non-bedload sediment may bear no relationship with flow power or slope (Leeder, 1992). Consequently, predictions made by diffusional models should be treated with caution on the basis of these difficulties.

Two methods are used in this modelling study to solve equation 18 and thus provide an alternative method in the model to describe the evolution of fluvial profiles with time.

Diffusion from a semi-infinite half-space

In order to solve the diffusion equation analytically it is necessary to define simple geometries, linear boundary conditions, and to maintain a constant value for the diffusion coefficient. One such example is to use the condition of surface evaporation from a semi-infinite medium, or half space (Crank, 1975). In this case the boundary condition for the solution describes, for example, a flow of dry air over a surface with some moisture concentration. Moisture is then lost from the surface by evaporation. The rate of flux of the

moisture depends on the relative moisture concentration on the surface, and the moisture concentration of the air. The concentration C in the air after time t is given by

$$\frac{C - C_1}{C_0 - C_1} = \text{erfc}\frac{x}{2\sqrt{(\kappa t)}} \qquad (21)$$

where C_0 is the constant concentration at the surface of medium, C_1 is the initial moisture concentration in the air, κ is the diffusion coefficient, and C is the concentration at distance x.

Putting these boundary conditions into the context of erosion, transport and deposition of sediment, the concentration of moisture at the surface of the semi-infinite medium C_0 is analogous to the elevation of a drainage divide in a continental interior, such that there is assumed to be an infinite supply of sediment available for transport from the half space which is the continental area behind the drainage divide. The concentration of moisture in the air, C_1, is analogous to sealevel. Thus replacing the symbol C with h to represent topographic elevation and rearranging equation 21 to solve for h gives

$$h = (h_0 - h_1)\,\text{erfc}\frac{x}{2\sqrt{(\kappa t)}} + h_1 \qquad (22)$$

The parameter $\sqrt{(\kappa t)}$, termed the diffusion distance, is of significance since it has the units of length and can be calculated for modern river profiles by fitting curves generated by equation 22 to such profiles as described in section 2.6.5.2. Figures 2.4 and 2.5 show topographic profiles and best-fit complementary error function curves for two rivers from the North American and African Atlantic passive margins respectively. The North American profiles are generated from the DBDB5 global D.E.M., and the interpolated profiles are constructed by linear interpolation between valley bottoms on the profile. The African profiles are taken from 1:500,000 tactical pilotage charts, and linear interpolation is used to complete the profile between the data points. Table 2.4 shows the values of $\sqrt{(\kappa t)}$ for the rivers in figures 2.4 and 2.5.

River Name	Diffusion distance $\sqrt{(\kappa t)}$ in km
Savannah, U.S.A.	107
James, U.S.A.	82
Giraul, Angola	65
Rio Catumbela, Angola	105

Table 2.4

Thus this solution of the diffusion equation is suitable to be used as an initial condition for an iterative finite difference solution, and can be given parameters that are taken from observation of real-world examples. It should be noted, however, that this method cannot allow values of κ alone to be measured, unless t, which represents the time taken for the development of the profile, is known.

Finite difference method

In order to provide a more generally applicable solution to the diffusion equation it is necessary to resort to the use of numerical methods, rather than the more limited analytical solution, an example of which was described above. One such numerical solution utilises the explicit finite difference method. Using this method the variable space under consideration is broken down into a grid of a specified resolution, and a series of equations defined and solved to give the value of the variable at each intersection point on the grid, relative to some initial conditions, and a set of pre-defined boundary conditions.

Smith (1985) shows how this method can be applied to the diffusion equation, giving

$$h(x, t + \Delta t) = h(x, t) + \kappa\frac{\Delta t}{\Delta x^2}[h(x + \Delta x, t) - 2h(x, t) + h(x - \Delta x, t)] \qquad (23)$$

where Δt is the model time step, and Δx is the horizontal grid spacing. A common problem with such finite difference solutions is the stability of the solution. Smith (1985) shows that the solution in equation 23 is valid only for

$$0 < \frac{\kappa \Delta t}{\Delta x^2} < 0.5$$

Values of 0.5 or greater lead to the formation of unstable oscillation which magnify with increasing t. As a result of this stability constraint it is necessary to reduce the size of Δt or increase the size of Δx in line with increasing values of κ.

This numerical solution to the diffusion equation makes no explicit reference to sealevel. However, it is possible to implement a variable sealevel datum elevation quite simply by employing an algorithm for finding the beach position as described in section 2.6.4. The examples of diffusional profile shown in section 2.6.5.4 use this method, and set the profile below sealevel to a fixed gradient slope. This is an obvious simplification of the behaviour of the marine system, but seems justifiable here since the essential purpose is to investigate the behaviour of the fluvial profile, and hence it is desirable to keep the treatment of the marine profile as simple as possible.

2.6.5.4. A comparison of the geometrical and the diffusional methods

The following section compares and contrasts the response of the geometrical profile and the diffusional profiles to sealevel changes.

Sealevel rise

The first examples illustrate the response of the geometrical and the diffusional profiles to a 20m sealevel rise. Figure 2.14 shows the diffusional profile example. This is calculated using an initial complementary error function profile with a value for $\sqrt{\kappa t}$ of 50km. This

was chosen to approximate the initial length of the geometrical profile of 200km. The profile was then calculated for a model duration of 1.0Myrs, with a diffusion coefficient κ of $1000m^2yr^{-1}$, using the finite difference method described in section 2.6.5.3. Figure 2.14 shows that the sealevel rise causes landward movement of the beach, and fluvial aggradation along the whole length of the fluvial profile. The magnitude of the aggradation decreases landward along the profile, and is greatest where the rate of change of topographic slope is greatest. Thus more aggradation occurs on the lower portions of the profile where it is more concave. Aggradation behind the beach is also influenced slightly by the break in slope from the bottom of the fluvial profile onto the marine profile.

Comparing this with the geometrical approach shown in figure 2.15 shows that the main difference between the behaviour of the two profiles is in the presence of small amounts of erosion on the upper portion of the geometrical profile. Figure 2.15 was generated over the same time and with the same 20m magnitude sealevel rise as the diffusional example. A complementary error function curve with a parameter of 2.0, an external sediment budget of $1.0km^2$, and a partitioning coefficient of 0.5 were used as model parameter values. The beach moves landwards in response to the sealevel rise, as it does in the diffusional example, producing aggradation in the lower fluvial profile. However, in the geometrical case, the landward movement of the beach causes shortening of the profile, which leads to small amounts of erosion on the upper portions of the fluvial profile.

Thus the most significant difference between the response of the geometrical and the diffusional models to base level rise is the presence or absence of erosion or aggradation on the upper portion of the profile. Determining which of these is the most accurate representation of actual coastal plain depositional patterns is problematic. Leopold and Bull (1979) studied via repeated surveys, the response of a number of small rivers to artificial sealevel rise induced by the construction of dams, In one case a dam approximately 0.6m high was constructed across the course of an ephemeral tributary stream in New Mexico. The presence of the dam initiated aggradation in the reaches

immediately upstream, producing a wedge of sediment approximately 30m in length, which reduced the gradient of the stream bed behind the dam site. The 200m of fluvial profile between the top of the aggradational wedge and the drainage divide appeared unaffected by the sealevel rise. The other rivers studied in the same way showed similar behaviour.

Obviously Leopold and Bull's study has the disadvantage of being conducted only on a small scale, but with a lack of data regarding the behaviour of larger systems, it seems reasonable to extrapolate similar behaviour to larger scale systems. Since aggradation does not appear to occur along the whole length of the profile after a sealevel rise, the diffusional model is inaccurate. The geometrical approach has the advantage that it predicts a wedge of aggradational deposition in response to the sealevel rise, that tapers out upstream. However, depending on the sediment supply, the partitioning coefficient and the error function parameter used, this erosion can be minimised. Consequently it seems reasonable to conclude that it is reasonable to use the geometrical approach in this case.

Sealevel fall

The next two examples show the response of the diffusional and the geometrical profiles to a 20m sealevel fall. All other parameters in both cases are the same as those used in the sealevel rise example. In the diffusional example in figure 2.16 the sealevel fall creates a pattern of continuous aggradation on most of the profile, with only a small amount of spatially limited erosion in the lower 50km of the profile. In contrast, the geometrical approach shown in figure 2.17 produces more widespread and vertically significant erosion on the lower 150km of the profile, with limited amounts of aggradation on the upper profile produced by the lengthening of the profile.

Begin *et al.* (1981) studied the effects of base level fall in a flume tank. It concluded that the effect of the sealevel fall was to initiate stream incision at the head of the stream, which

then migrated upstream towards the top of the flume tank. Wood *et al.* (1993) found similar results using a flume tank and fluctuating sealevel. Sealevel fall was found to cause incision which progresses upstream. However, Wood *et al.* (1993) also noted that the rate of the sealevel change relative to the response time of the stream, was crucial to determining the stream response, and that this response are complex in that individual episodes of deposition and erosion by the stream may have little direct link with an external forcing such as base level. For example, sediment may be stored by aggradation in the upper portions of a channel while incision is occurring downstream.

Comparing the response of the geometrical profile with that of the diffusional profile, it seems that the geometrical profile may have the advantage in that the incision in response to the sealevel fall is more clearly delineated and extends further up the profile. However, in both cases the prolonged aggradation on the upper profile seems unrealistic, though in the case of the geometrical profile such aggradation has very low preservation potential since it is very unlikely to survive reworking by profile shortening during a subsequent sealevel rise.

Sinusoidal sealevel variation - low sediment supply

Since many of the model runs through the rest of this thesis use sinusoidal absolute sealevel curves, two examples are included here to show the response of the geometrical and the diffusional profiles to the same 20m amplitude, 2.0Myrs period sinusoidal absolute sealevel oscillation. Figure 2.18 shows the diffusional example, with a transport coefficient value of $1000m^2yr^{-1}$, an initial $\sqrt{\kappa t}$ value of 50km, and an elapsed model time of 2.5Myrs. The movement of the beach in response to the sealevel changes is clearly visible. The beach initially moves landward slightly in response to the initial sealevel rise, and then moves rapidly seaward as sealevel falls. It reaches its most seaward position at an E.M.T. of 1.5Myrs, after which it undergoes rapid transgression which slows as the rate of sealevel rise decreases.

The beach movement can be compared directly with the absolute sealevel curve in figure 2.19. The spatial extent of deposition, non-deposition, and erosion on the fluvial profile can be seen on the chronostratigraphic diagram in figure 2.19. Aggradation on the upper portions of the fluvial profile is continuous throughout the model run, and occurs on the lower portion of the profile from chrons 1 to 10 (E.M.T. of 0.0 to 1.0Myrs) and from chrons 19 to 24 (E.M.T. 1.9 to 2.4Myrs). The fluvial profile is responsible for small amounts of erosion on the lower profile during the sealevel fall and the initial rise. This 100km wide area of non-deposition and erosion is shown on the chronostratigraphic profile from chron 11 to chron 18 (E.M.T. of 1.1 to 1.8Myrs), and correspond to the time of transition from the lower portion of the falling limb of the sealevel curve to the inflexion point on the rising limb.

These patterns can be compared directly with those produced by the geometrical profile for the same sealevel variation. The model was run with a complementary error function parameter value of 2.0, a constant external sediment supply of $0.1km^2$, and a partitioning coefficient of 0.5. The profile section in figure 2.20 shows the pattern of beach movement produced by the sinusoidal sealevel variation. The initial sealevel rise produces a landward migration of the beach of approximately 70km. The following sealevel fall causes a seaward translation of approximately 50km, and the final rise produces another landward movement of approximately 100km. Fluvial stratigraphy is only preserved from aggradation on the lower profile during the final sealevel rise. Previous deposition has subsequently been eroded by the sealevel fall, and on the upper profile, by the final sealevel rise. Only the addition of subsidence would ensure preservation beyond the duration of a single sealevel cycle.

The pattern of deposition and erosion is more clearly visible on the chronostratigraphic diagram in figure 2.21. Deposition occurred on the lower part of the profile during the initial sealevel rise, and on the upper part of the profile during the sealevel fall. All the

fluvial stratigraphy prior to chron 16 has been eroded, either by downcutting of the profile during the sealevel fall from chrons 5 to 15 (E.M.T. 0.5 to 1.5Myrs) or by erosion on the upper profile due to profile shortening forced by the initial sealevel rise from chron 15 to 18 (E.M.T. 1.5 to 1.8Myrs). A period of non-deposition and erosion produced by fluvial downcutting during the sealevel fall, and approximately 100km in width, produces a similar pattern to that seen in the diffusional example.

Thus a comparison of the results from the geometrical and the diffusional profiles shows that:

- Aggradation occurs on the upper portion of the diffusional fluvial profile throughout the sealevel cycle.
- Vertically limited but horizontally extensive non-deposition and erosion occurs on the lower part of the diffusional profile during the period between the inflexion points on the lowest portion of the absolute sealevel curve.
- Aggradation occurs on the upper portion of the geometrical fluvial profile only during time of sealevel fall. This is due to profile lengthening forced by the seaward movement of the beach. During sealevel rise the upper portion of the geometrical fluvial profile is erosional.
- Vertically more significant and horizontally extensive non-deposition and erosion occurs on the lower half of the geometrical profile throughout the duration of the falling limb of the absolute sealevel curve.

Sinusoidal sealevel variation - higher sediment supply

Since the response of the geometrical profile to sealevel change is sensitive to the sediment supply, this second example using the sinusoidal sealevel variation uses a higher value of external sediment supply of $0.5km^2$ for the geometrical profile, and a higher value for the diffusion coefficient of $5000m^2yr^{-1}$. All the other model parameters are the same as those described in the low sediment supply example.

The higher value for the diffusion coefficient has the effect of reducing the landward movement of the beach during the sealevel rises, and increasing the thickness of fluvial aggradation, and decreasing the vertical and horizontal extent of the erosion and non-deposition produced by the sealevel fall (figure 2.22). The distance of seaward movement of the beach during the sealevel fall is not significantly affected. The reduced width of the zone of non-deposition and erosion is shown more clearly in the chronostratigraphic diagram in figure 2.23. This reduction in the width of the zone is due to the increased aggradation produced by the increased diffusion coefficient.

Increasing the external sediment supply on the geometrical profile has the effect of reducing the distance of the transgression of the beach during sealevel rise, increasing the distance of seaward movement of the beach during sealevel fall, and reducing the erosion on the upper fluvial profile during sealevel rise (figure 2.24). This change in the pattern can be seen on the chronostratigraphic diagram in figure 2.25. Deposition on chrons 1 to 7 during the initial sealevel rise is now preserved. The horizontal extent of this deposition has been increased by the higher sediment supply.

Thus a comparison of the results from the geometrical and the diffusional profiles shows that:

- Aggradation occurs on the upper portion of the diffusional fluvial profile throughout the sealevel cycle.
- Vertically and horizontally limited non-deposition and erosion occurs on the lower part of the diffusional profile during the three time steps before and during the low point on the absolute sealevel curve.
- Aggradation occurs on the upper portion of the geometrical fluvial profile only during time of sealevel fall. This is due to profile lengthening forced by the seaward movement of the beach. During sealevel rise the upper portion of the geometrical

fluvial profile is erosional, but the extent of this erosion is reduced because of the higher sediment supply acting against profile shortening.

- Vertically more significant and horizontally extensive non-deposition and erosion occurs on the lower half of the geometrical profile throughout the duration of the falling limb of the absolute sealevel curve.

A comparison of sediment flux magnitudes

Another important comparison to make between the geometrical and the diffusional approach to fluvial profile generation is in regard to the magnitudes of the sediment flux for the two approaches. Figure 2.26 shows three plots of sediment flux with distance along the profile for both the geometrical and the diffusional approaches. Both examples were generated with a 1.0Myr model run, constant sealevel and an initial profile length of approximately 200km, generated in the case of the diffusional profile with a value for $\sqrt{(\kappa t)}$ of 50km. The geometrical model has a partitioning coefficient value of 0.5. The three curves for each plot were generated with different values of external sediment supply in the geometrical case, and diffusion coefficient in the diffusional case. The diffusion coefficient values are based on the range of values from Flemings and Jordan (1989) and Jordan and Flemings (1991). The methods for calculating the flux differ in the two approaches. In the geometrical case the flux is calculated by subtracting the area of stratigraphy deposited at distance x from the total external sediment supply, and then dividing by the length of the time step to give a flux in m^2yr^{-1}. In the diffusional case the flux is calculated using equation 20, and K and κ are assumed to have the same value.

Comparison of the two plots in figure 2.26 shows that with varying values for the external sediment supply and the diffusion coefficient shows that :

- The magnitudes of the fluxes are similar. For example, with a diffusion coefficient value of $10000m^2yr^{-1}$ the diffusional flux curve has a magnitude ranging from approximately $10m^2yr^{-1}$ to $2m^2yr^{-1}$, and with an external sediment supply of $1.0km^2$

per 0.1Myr ($10m^2yr^{-1}$) the geometrical flux curve has a magnitude ranging from approximately $10m^2yr^{-1}$ to $7m^2yr^{-1}$.

- Both cases show reducing magnitude of flux with increasing distance from the landward end of the fluvial profile.
- The gradients on the curves also show similar trends, increasing and then decreasing with distance down the length of the profiles.

The most significant difference between the curves for the different methods is the final values of flux at the 300km point on the profile. In the diffusional case these values are controlled by the slopes at this point, which are low because of the concave shape of the profile. Thus this suggests that the sediment flux at the mouth of the river should be low. This does not agree with observation which shows that because of increased discharge downstream produced by the contribution from tributary streams, the flux actually increases in most rivers. The value of the sediment flux at 300km in the geometrical case is controlled by the external sediment supply and the value of the partitioning coefficient, not by the slope. Thus the values for the flux decrease downstream as sediment is deposited as fluvial stratigraphy in the coastal plain, but some of the available external sediment supply is bypassed into the marine portion of the profile, as determined by the partitioning coefficient. Consequently the values for the flux at the seaward end of the profile are consistently higher than in the diffusional examples, and as stated above are more in line with observations of flux in real rivers.

Conclusions from the comparison

The previous section has shown that the geometrical and diffusional approaches each have advantages and disadvantages. In general however, the geometrical approach seems most suited to use in this modelling study, since it is capable of producing patterns of erosion and deposition which are reasonably acceptable in the context of a numerical experimental approach intended to investigate aspects of the sequence stratigraphic depositional model.

For example, the diffusional profile does not produce any patterns of stratal onlap, whereas the geometrical approach does. Although the geometrical approach is probably unrealistic in some respects, such as minor erosion on the upper profile during a sealevel rise, and small amounts of aggradation on the upper profile during a sealevel fall, such inaccuracies are less severe than some of the inaccuracies produced by the diffusional profile, and they can be readily accounted for in the interpretation of the model results.

2.6.5.5 The concept of the marine equilibrium profile

The concept of a marine equilibrium profile has been described by a number of workers. Thorne and Swift (1991) gives a review of the development of the concept. Curray (1965) suggested that fine-grained nearshore sediment might over time be redeposited out on the present continental shelf, and re-establish an equilibrium profile that had been destroyed by the Holocene transgression. Swift (1970) reviewed this work, and suggested that over geological time, storm sedimentation which is capable of affecting the whole shelf, is the norm. Pitman (1978) used the concept of an equilibrium shelf profile to explain occurrences of shelf-wide unconformities in the geological record. Most recently, Swift and Thorne (1991) and Thorne and Swift (1991) discussed the equilibrium model for shelf sedimentation in terms of a regime model, which is similar to the concept of dynamic equilibrium applied to river profiles. The regime model uses surfaces of dynamic equilibrium that are determined by a series of mutually interdependent variables, namely sediment input rate, sediment character, sediment transport rate, and the rate of relative sealevel change.

Unfortunately, many of these ideas regarding marine equilibrium profiles are poorly quantified. Although Thorne and Swift (1991) presented a mathematical model for shelf and slope profiles, this model does not appear to include the shoreface. Although shoreface geometry has been shown diagrammatically by many workers (e.g. Swift and Thorne, 1991; Everts, 1987) it has never been quantified in a simple way consistent with the level

of detail required in this model. Turcotte and Kenyon (1985) used a diffusional approach to model slope transport processes on a prograding delta front, but this did not reproduce shoreface erosion. Diffusion has also been used to model marine shelf and slope deposition (e.g. Kaufman *et al.*, 1992; Rivenaes, 1992) but suffers from the problem that the rate of transport may not be proportional to slope in the marine shelf environment, and rates of transport on the shelf are difficult to constrain.

As a result of these difficulties, and to maintain consistency with the geometrical approach adopted for the fluvial profile, the marine equilibrium profile will be represented very simplistically by a geometrically defined exponential shoreface passing laterally into a shelf of fixed gradient. This is a gross approximation of the real processes and resulting geometries, but should prove sufficient for the purposes of this modelling work.

The implementation of the marine profile

As previously discussed, the marine equilibrium profile is composed of two parts. An exponential curve is used to define the shoreface, the width and the depth input as initial model parameters. The equation for this curve has the following form :

$$y(x) = e^{k(x - x_1 - \Omega)} + y_1 - \alpha \qquad (25)$$

where

$$k = \frac{\ln(\alpha)}{-\Omega} \qquad (26)$$

The variables α and Ω represent the height in metres and the width in kilometres respectively of the shoreface. The profile then passes seaward into a straight line of a given gradient, which represents the offshore graded shelf. This is given by :

$$y(x) = d(t) - \alpha - mx \qquad (27)$$

where m is the shelf gradient and d(t) is the absolute sealevel datum. Figures 2.27 and 2.28 show diagrammatic examples of the proximal and distal marine equilibrium profile geometry respectively. The profile controls deposition and erosion in the same way as the fluvial profile previously described in section 2.6.5.2.

The distal end of the marine equilibrium profile consists of the marine break-of-slope where the profile passes from the shelf to the slope. The position of the marine break-of-slope is determined by sediment supply. Sediment from the fluvial profile, and sediment from erosion on the shoreface is fed onto the shelf (figure 2.28). Since the depositional model is purely 2-D, no allowance is made for effects such as submarine canyon erosion, delta lobe switching and sediment bypassing the shelf directly onto the slope and into the deep marine environment. No out-of-plane sediment transport is included either, for two reasons. Firstly, any out-of-plane removal of sediment would quite possibly be balanced by an equal out of plane addition of sediment, both due to processes of longshore drift. Secondly, the proportion of sediment area added or removed would have to be a largely arbitrarily imposed variable, given that there is little data regarding such transport on the shelves. The shelf-slope break is thus positioned to use up all the available area of sediment transported onto the shelf.

The algorithm which positions the marine break-of-slope consists of an iterative routine which searches for the position of the shelf-slope break that uses an area of sediment most closely matching the area of sediment available for deposition. The areas are calculated using the trapezium method shown in figure 2.12. The accuracy of this area fitting routine is significantly decreased when it is attempting to find the shelf-slope break position for progradation into deep water. This reduced accuracy is a function of the horizontal resolution of the model. With a point spacing on the horizontal profile of 250m, and a water depth of 500m, the difference in sediment area deposited between two points would

be 0.125km^2, which for sediment supplies in the order of 1km^2 is not insignificant. This inaccuracy affects the precision of the area of sediment deposition, but it does not significantly affect the resulting stratigraphic patterns.

A special condition can arise in which all the positions for the marine break-of-slope seaward of the beach position, result in too much sediment being deposited. When this occurs, the position of the beach must be moved landward, and the fluvial profile recalculated, until the total area of sediment deposited is as close as possible (see previous discussion of the affects of model resolution on the accuracy of area fitting) to the total available (figure 2.29). Recalculating the fluvial profile for the new beach position means that the partitioning coefficient has to be ignored, because in this situation the beach position is no longer free to move landward or seaward to balance the amount of fluvial sediment used. More marine sediment is deposited than has been specified by the sediment partitioning coefficient, since the beach has been moved landwards, reducing the area of fluvial sediment deposited. Thus, when the beach has to be moved landward in the way described, sediment is effectively bypassing the fluvial profile, and being deposited on the marine slope.

2.6.6 Flexural Isostasy

The flexural response of the lithosphere to sediment loading and unloading is calculated using a thin elastic plate model which assumes that the deflections are small compared to the plate thickness. The flexural response of the lithosphere to distributed loads is calculated using the fourth order differential flexure equation applied to the specific case of an infinite lithospheric plate of flexural rigidity D, underlain by fluid-like mantle material :

$$D\frac{d^4z}{dx^4} + (\rho_m - \rho_{infill})gz = \Delta H(x) \qquad (28)$$

where z is the plate deflection due to the vertically applied load $\Delta H(x)$, assuming no applied torques or in-plane loads, ρ_m is the density of the mantle, ρ_{infill} is the density of the infilling material, g is acceleration due to gravity, and the expression $(\rho_m - \rho_{infill})gz$ gives the restoring force. Two methods of solving this equation to calculate the deflection of the lithosphere for a given load are used in the model.

The first method uses the response function technique. Solving equation 28 for a periodic load gives

$$z(x) = \frac{(\rho_{infill} - \rho_w)\, h\, g \cos(kx)}{((\rho_m - \rho_{infill})\, g + Dk^4)} \qquad (29)$$

where h is the maximum height of the load, g is the average gravity, and k is the wave number of the load. If the lithosphere is considered as a filter when responding to loading, then a response function can be defined;

$$\phi_c = \left[\frac{Dk^4}{(\rho_m - \rho_{infill})\, g} + 1\right]^{-1}. \qquad (30)$$

This can be used to calculate the flexural response using a delta function $\delta(x)$ to approximate the load function (replacing the h cos.(kx) term in equation 29) where $\delta(x) = 0$ when $x \neq 0$ and

$$\delta(x)\partial x = 1,\ x = 0.$$

Taking $\Delta H(k)$ and z(k) as the discrete Fourier transforms of L(x) and z(x) respectively, then equation 29 can be reduced to

$$z(k) = \phi_c(k)\, \Delta H(k) \frac{(\rho_{infill} - \rho_w)}{(\rho_m - \rho_{infill})}. \qquad (31)$$

Hence, to calculate the flexure z(x), the periodic load L(x) is transformed into the frequency domain, equation 31 is applied, and the result is inversely transformed back into the spatial domain.

The second method uses a numerical finite difference technique described by Bodine (1981). The advantage that this method has over the Fourier transform method is that it allows for lateral changes in the restoring force and also in the elastic thickness of the lithosphere via the boundary conditions used in the formulation of the finite difference solution. The changes in the restoring force are caused in this case by changes in the density of the material, either air or water, that is displaced by flexural uplift. The restoring force along the profile is calculated simply by recording which points are above and which points are below sealevel before the load is applied. For those points above sealevel, the restoring force is calculated assuming that air will be displaced. For those points below sealevel, the restoring force is calculated assuming that water will be displaced. This method introduces a small inaccuracy since flexural subsidence in the region of the beach will flood parts of the profile where the restoring force has been calculated assuming that air will be displaced. However, this inaccuracy can be shown to be negligible by comparing a flexural profile for the same load calculated first assuming water displacement across the profile, and then assuming air displacement.

The elastic thickness of the lithosphere (T_e) in the model can have a variety of values. It can be held constant, both spatially and temporally, at values of 5km or 30km. Alternatively, T_e can be varied through model time. In this case, values are calculated using the 3 times the square root of time relationship (Bodine *et al.*, 1981). The value of T_e can also be varied spatially along the length of the model profile, but only when the finite difference technique is used to solve the flexural equations.

2.6.6.1. Flexural response times

The flexural isostatic response time of the asthenosphere and the lithosphere to surface loading and unloading is a crucial factor in this modelling work, and yet it appears to be a poorly understood parameter. Flexural response time, as it is used here, refers to the length of time required for the lithosphere and the asthenosphere to adjust, via flexure, to surface loading or unloading. The separate responses of the asthenosphere and the lithosphere, caused by their different rheological properties, together account for the flexural response to loading and unloading observed at the earth's surface. Studies of post-glacial rebound (e.g. Peltier, 1986) suggest that response times for the asthenosphere are in the order of 10kyr. Walcott (1970a) suggested a lithospheric response time to loading in the order of 10 to 20Kyrs. The response time of the lithosphere is more controversial, due to the more complex rheologies involved, and an often complex thermal and loading history. Bodine *et al.* (1981) suggested that an applied load causes stress relaxation from the initial seismic thickness of the lithosphere to the final elastic thickness, which is essentially complete within one million years or less.

Thus, due to the lack of detailed understanding, choosing and then constraining a method of implementing a finite flexural response time in the model is difficult. There is currently no consensus regarding flexural response times, and the lithosphere on passive rift margins is likely to have a complex rheology, having experienced a potentially complex thermal history. For this reason, and because the flexural response is a potentially important control on stratigraphy, the model has three simple alternative methods to implement finite response times.

The first and simplest is the instantaneous response option in which the full magnitude of the flexural subsidence and uplift generated by the present load is applied to all the present chrons at the end of the time step for which the load was generated. This is essentially assuming that either the flexural response is instantaneous, or that the response is complete

within one time step which can range from 10Kyrs to 1Myr, but is generally set to be 100Kyrs. Thus the significance of the response time to the stratigraphy cannot be investigated with this method.

The second method of dealing with flexural response times in the model calculates the total magnitude of flexure due to a given load, but then does not apply it to all the chrons immediately. Instead, the flexural response time parameter is used to calculate what proportion of the uplift and subsidence should be applied for each time step. Thus if the time step is 0.1 Myrs and the flexural response time parameter is set at 0.5 Myrs, for each time step 20% of the uplift and subsidence due to the load will be applied. The algorithm can be described by treating F, the flexure to be applied at a particular time step, as a function of the total flexure z for a given load so that

$$F(x,t) = \sum_{n=t-T_f}^{t} z(x, n) \times \frac{t_{inc}}{T_f} \qquad (32)$$

where t is the E.M.T., T_f is the flexural response time, and t_{inc} is the length of the model time step, all measured in millions of years.

The algorithm is implemented using a stack structure which is used to store the flexural profiles generated for each load applied at each time step. This can then be scanned for a number of previous time steps dependent on the size of t_{inc} and T_f, and the appropriate proportion of the total magnitude of the flexure applied to the chrons. The model currently uses a linear method to calculate the magnitude of flexure applied at each time step, but non-linear functions such as a power function or an exponential could easily be applied. Although this method is also very simplistic, it at least has the advantage of allowing a flexural response time greater than the model time step. This then allows the significance of the response time to be investigated.

The third method treats the flexural response as an exponential decay function. This is implemented very simply by halving the applied flexural amplitude due to the applied load, for each subsequent time step. Thus the flexural response takes the form of an exponential decay. The disadvantage with this method is that the response time is again dependent on the length of the time step. Hence, if a time step of 100Kyrs is chosen, the time for the flexural effects due to any given load to be 96.9% complete would be 500Kyrs. Alternatively, if a time step of 1Myrs was chosen, it would take 5Myrs for 96.9% of the flexure due to any load to be completed.

2.7 The Model Output

Once a model run has been completed, the contents of the various data structures are displayed graphically. The output can be split into two groups. The first consists of sections through the stratigraphy, either the whole length of the model profile, or smaller sections of the profile which are then magnified. The second group consists of a Wheeler chronostratigraphic diagram on which horizontal distance is plotted alongside E.M.T., and a series of curves showing values of model variables through model time. Examples of this output can be seen throughout chapters three, four and five.

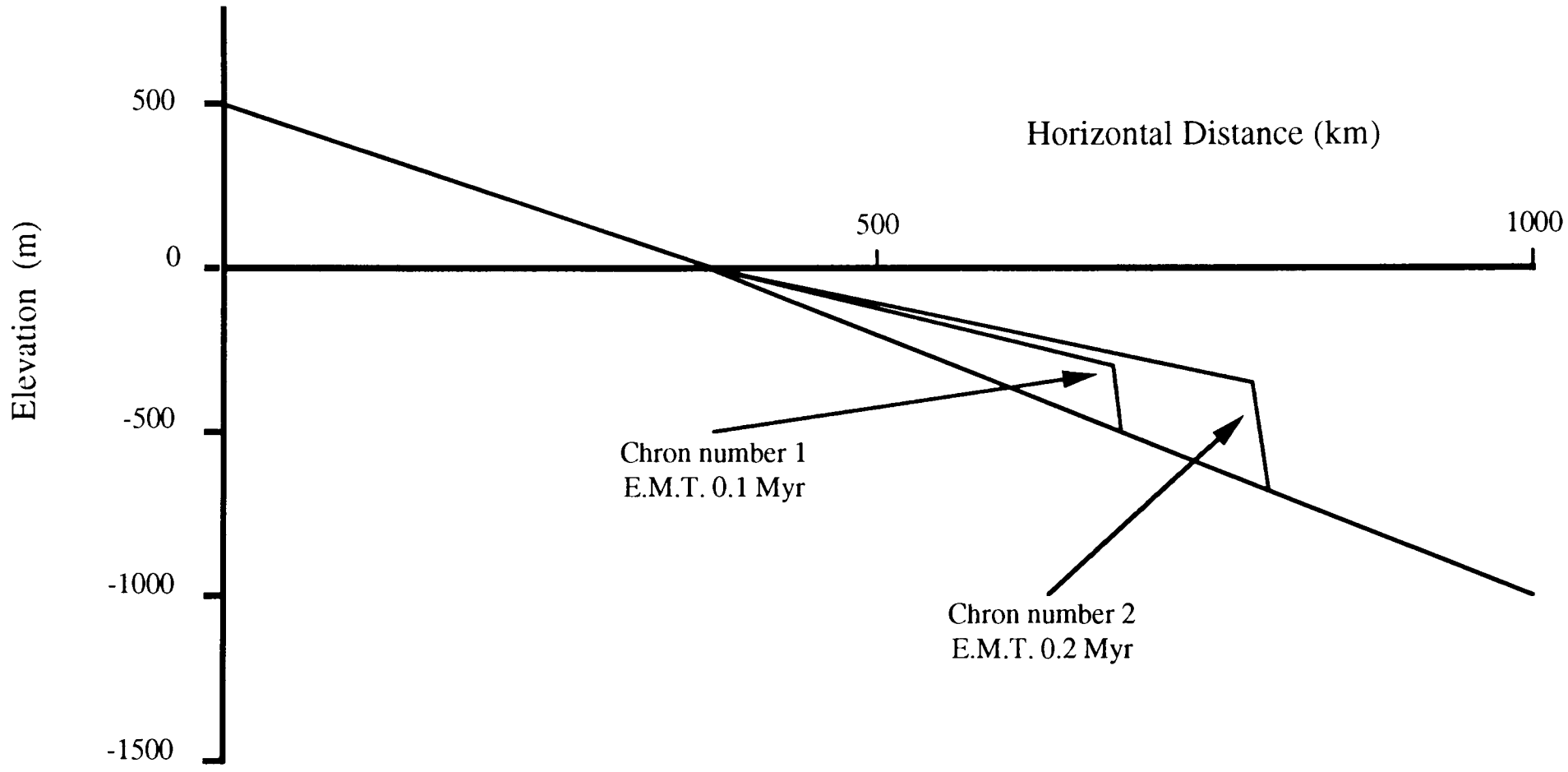

Figure 2.1 The model coordinate system

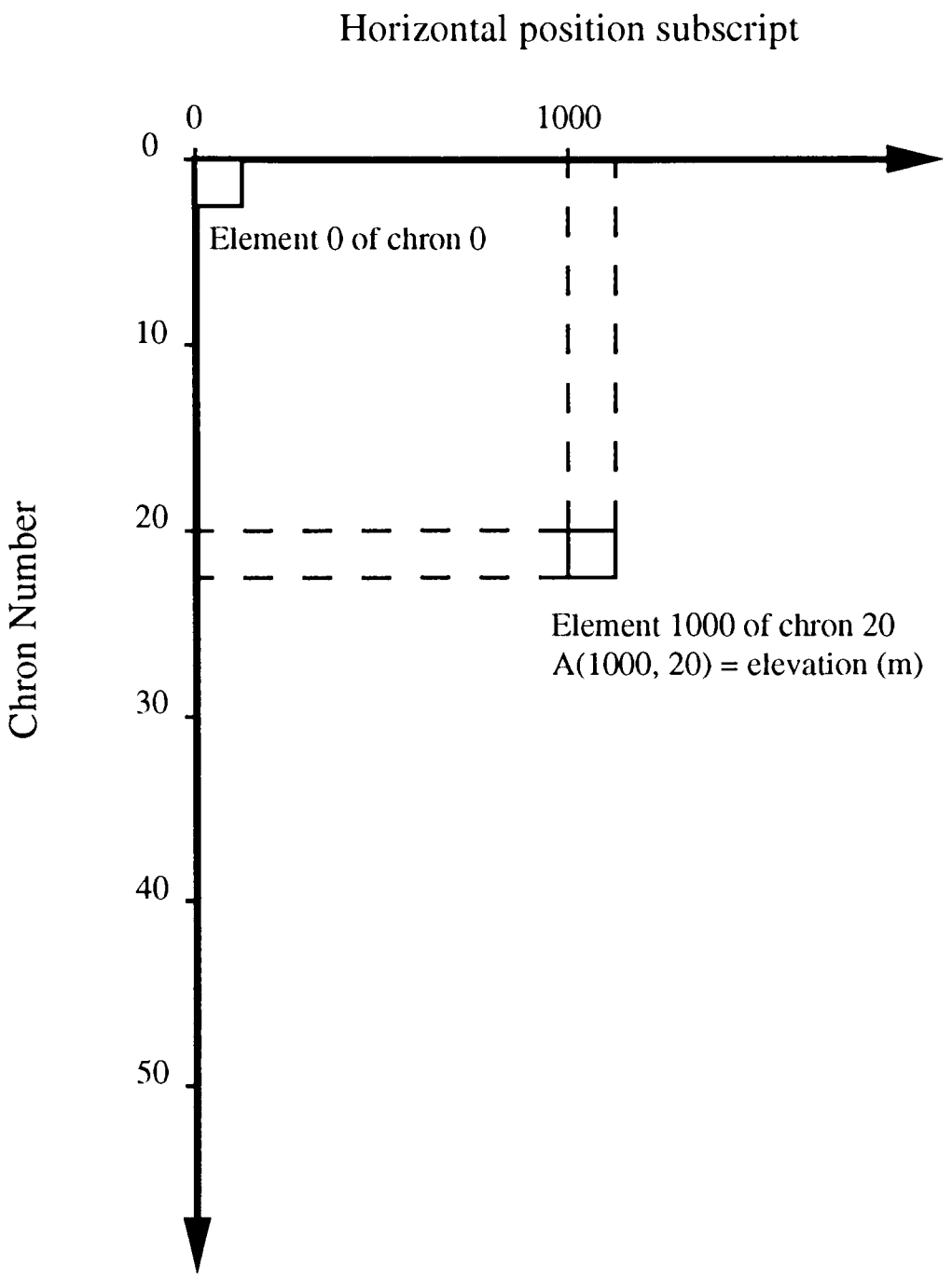

Figure 2.2 A diagrammatic description of the model data structure

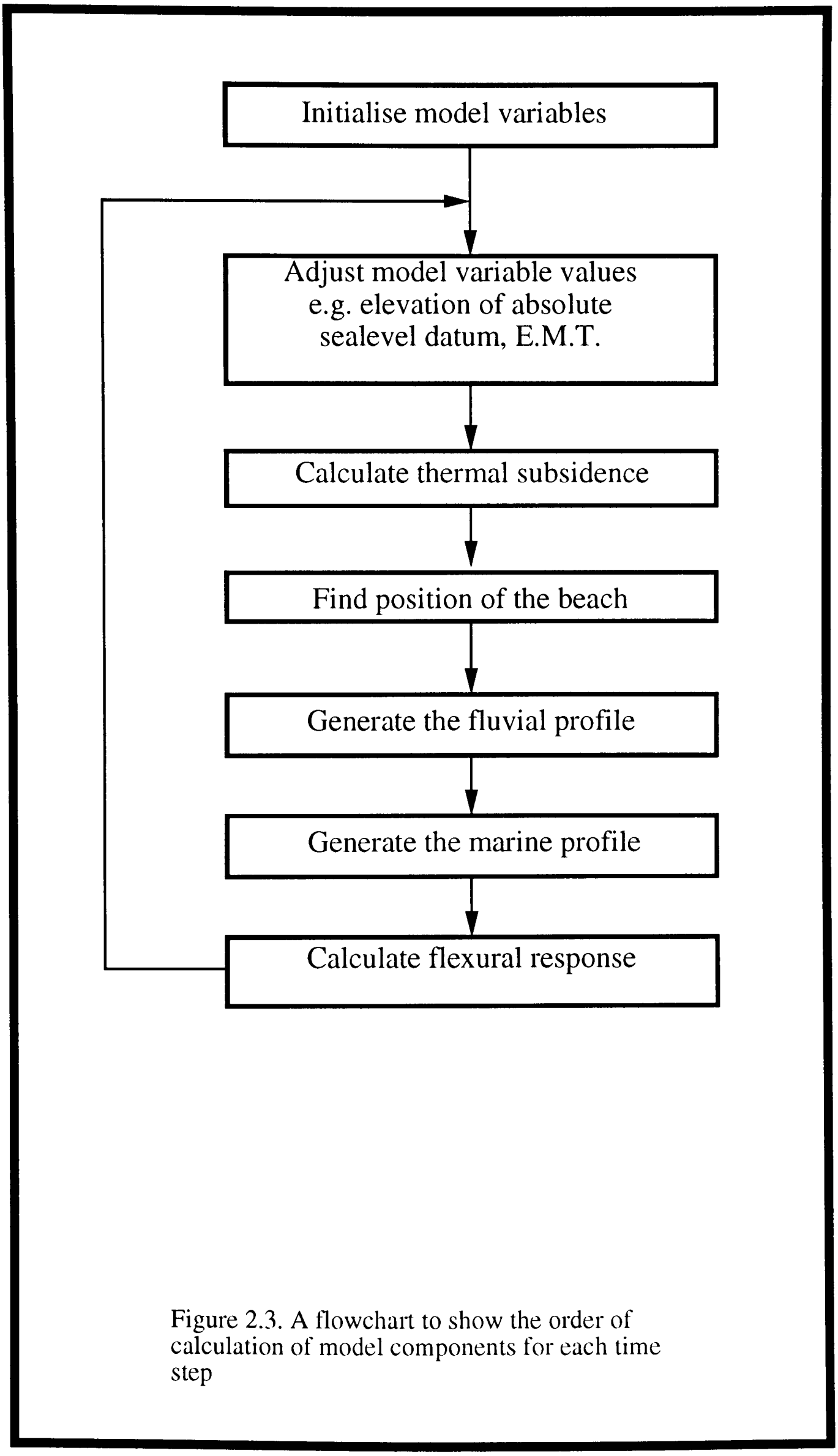

Figure 2.3. A flowchart to show the order of calculation of model components for each time step

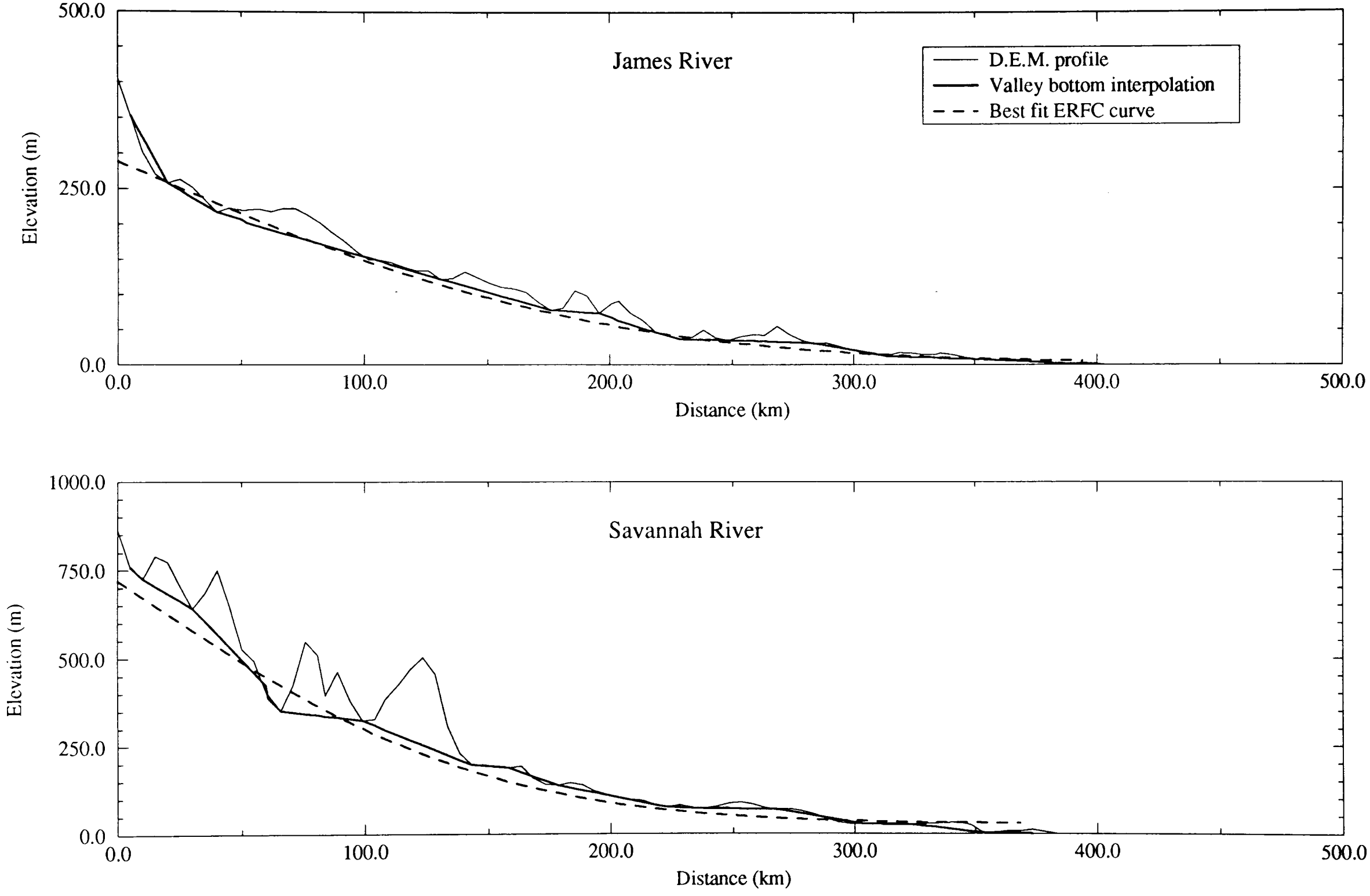

Figure 2.4. Two topographic profiles from the North American Atlantic margin, with interpolated valley bottom profile and best fit complementary error function curve.

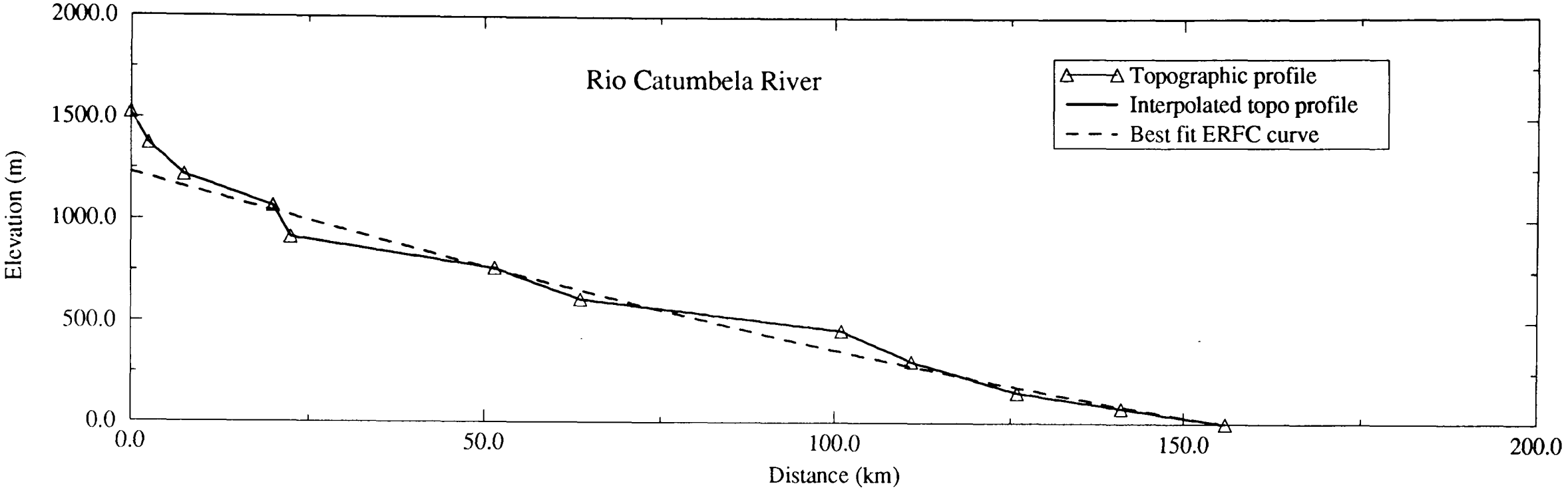

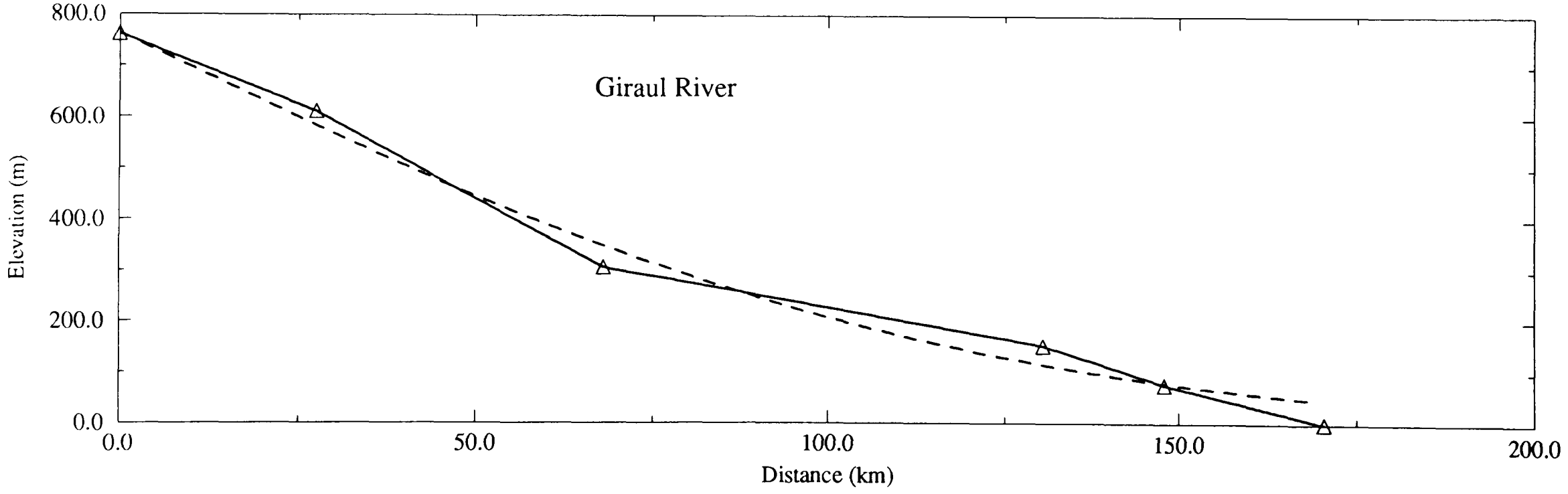

Figure 2.5. Two topographic profiles from the African Atlantic margin, produced by linear interpolation between the profile data points, and the best fit complementary error function curves.

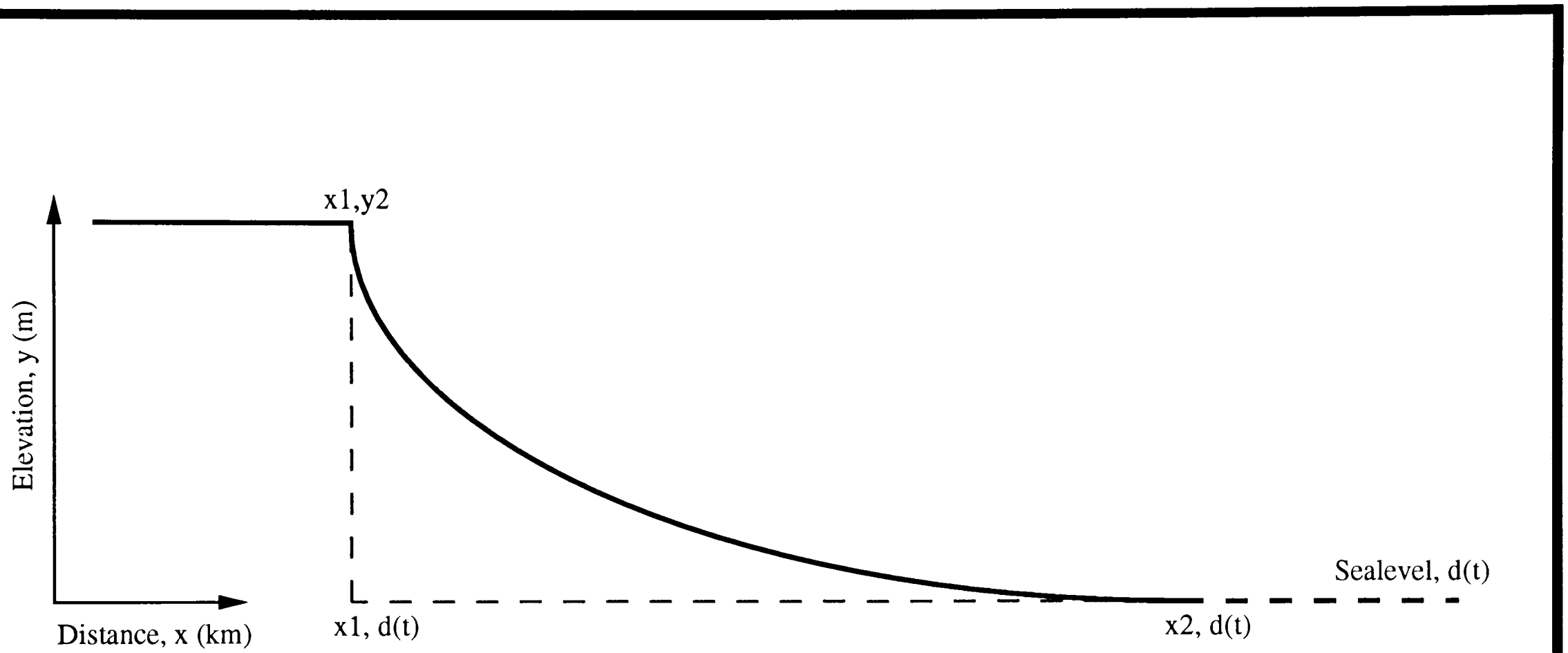

Figure 2.6 A digram to show the coordinate terms used in the definition of the fluvial profile.

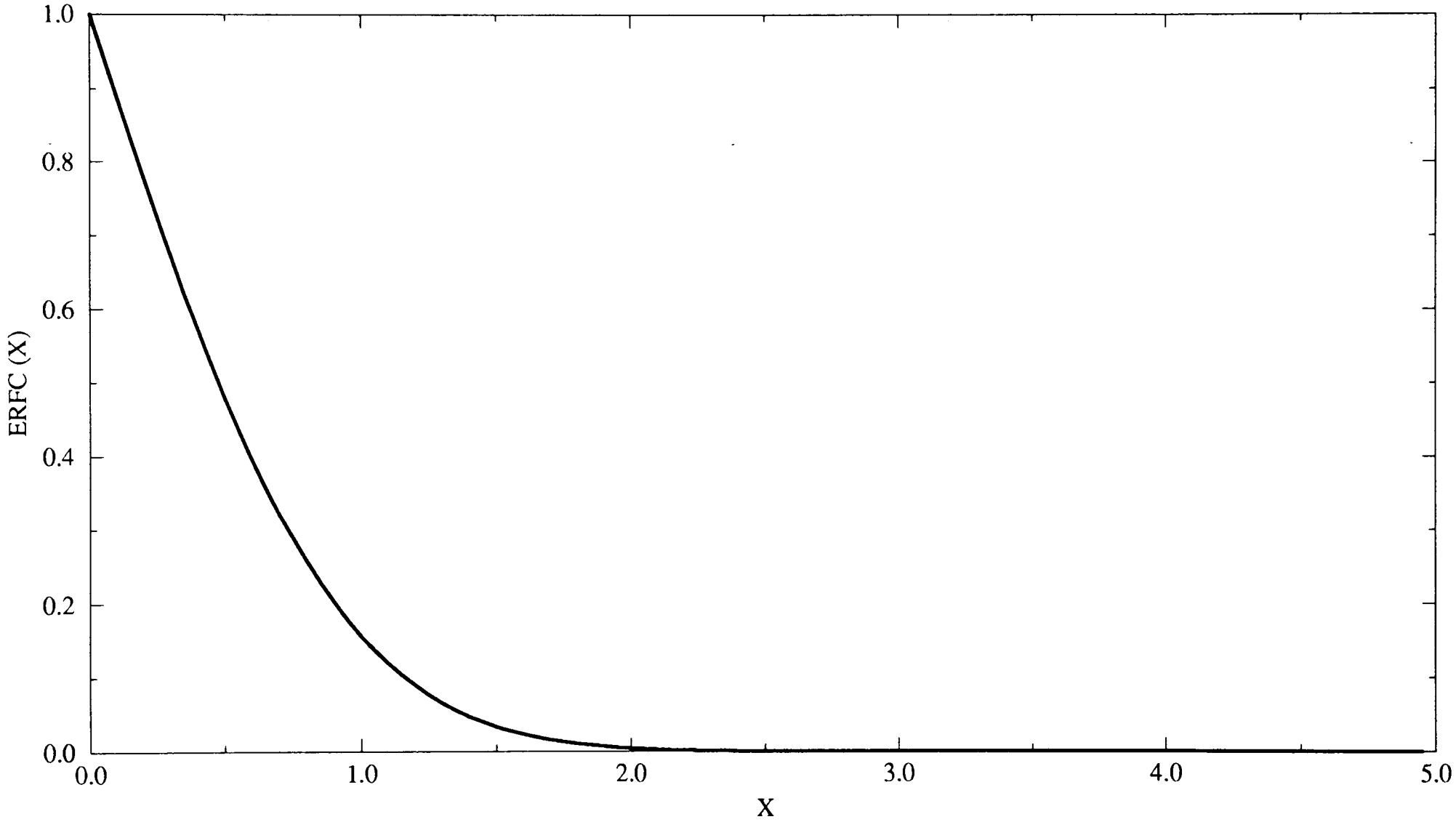

Figure 2.7. A plot to show the form of the complementary error function curve.

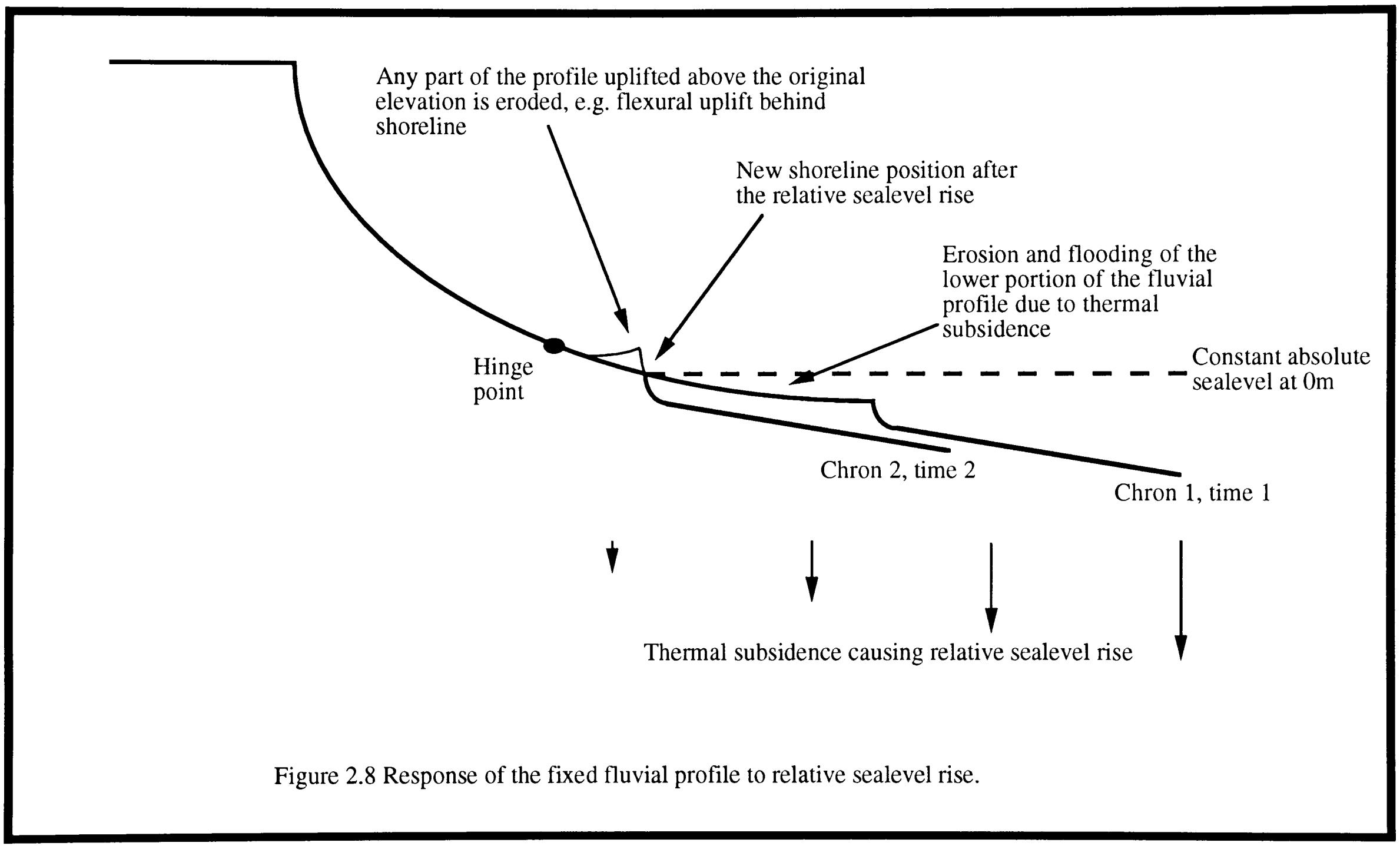

Figure 2.8 Response of the fixed fluvial profile to relative sealevel rise.

Falling relative sealevel : Fluvial degradation. Possible fluvial progradation. - Progradation dependent on sediment supply and magnitude of relative sealevel fall.

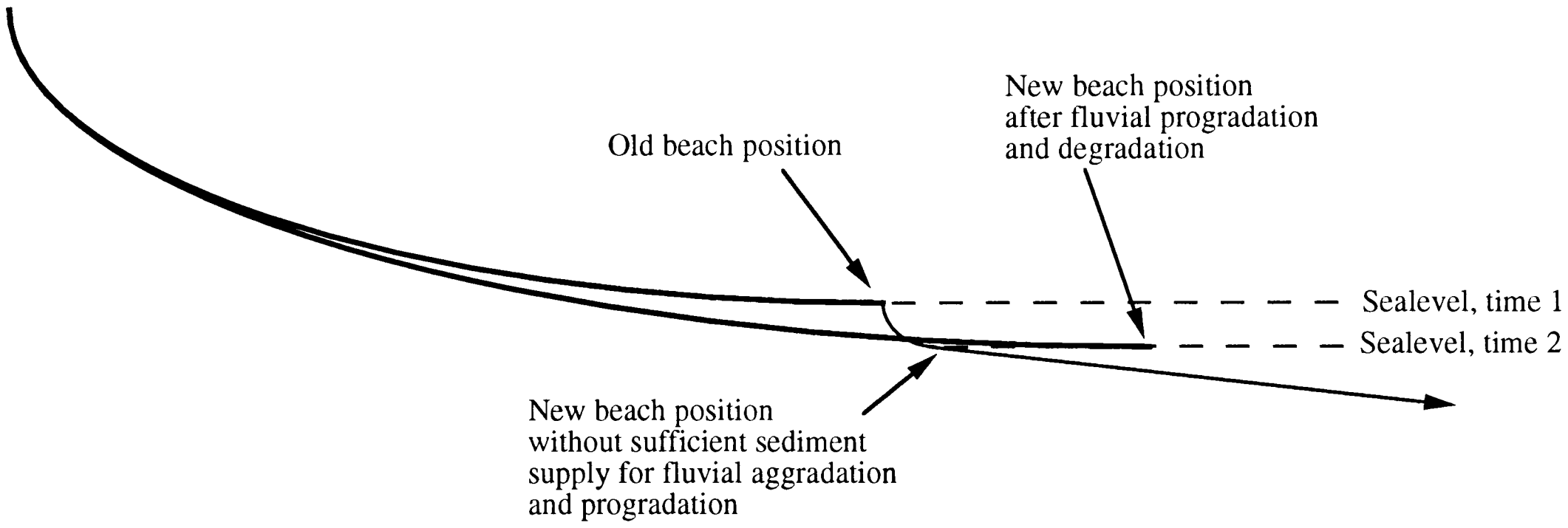

Figure 2.9 The response of the geomtrical fluvial profile to falling absolute sealevel.

Rising relative sealevel : Fluvial aggradation. - Both dependent upon
Fluvial progradation sediment supply as well as
rate of relative sealevel rise

Slow relative sealevel rise, high sediment supply, or high fluvial-marine partitioning coefficient

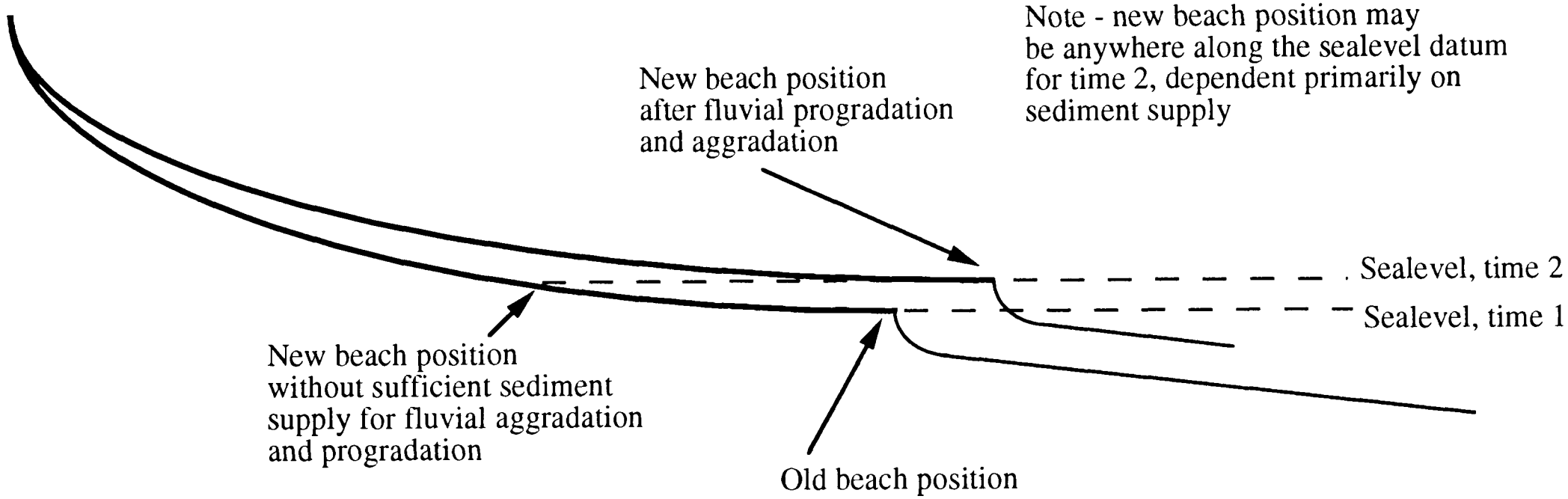

Figure 2.10 The response of the fluvial profile to rising absolute sealevel for either a slow rise, a high value of sediment supply, or a high value for the fluvial-marine partitioning coefficient.

Rising relative sealevel : Fluvial aggradation. Fluvial progradation - Both dependent upon sediment supply as well as rate of relative sealevel rise

Fast relative sealevel rise, low sediment supply, or a low value for the fluvial marine partitiong coefficient

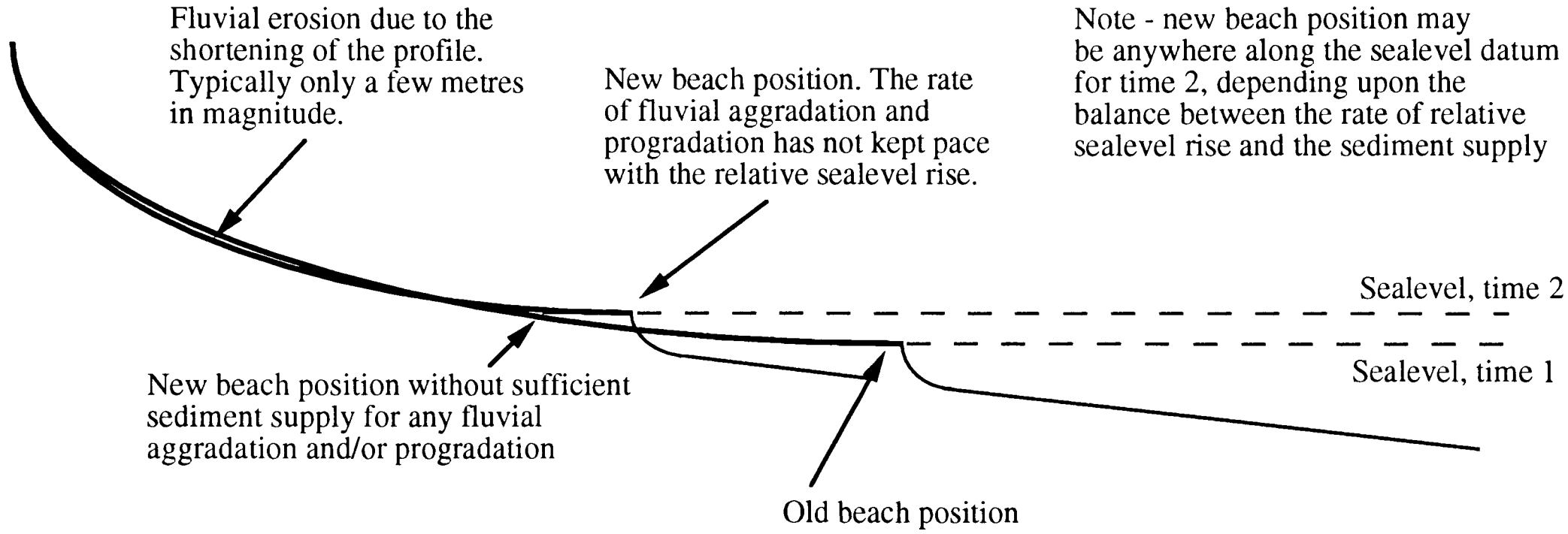

Figure 2.11 The response of the geometrical profile to an absolute sealevel rise for either a fast rise, a low value of sediment supply, or a low value for the fluvial marine partitioning coefficient

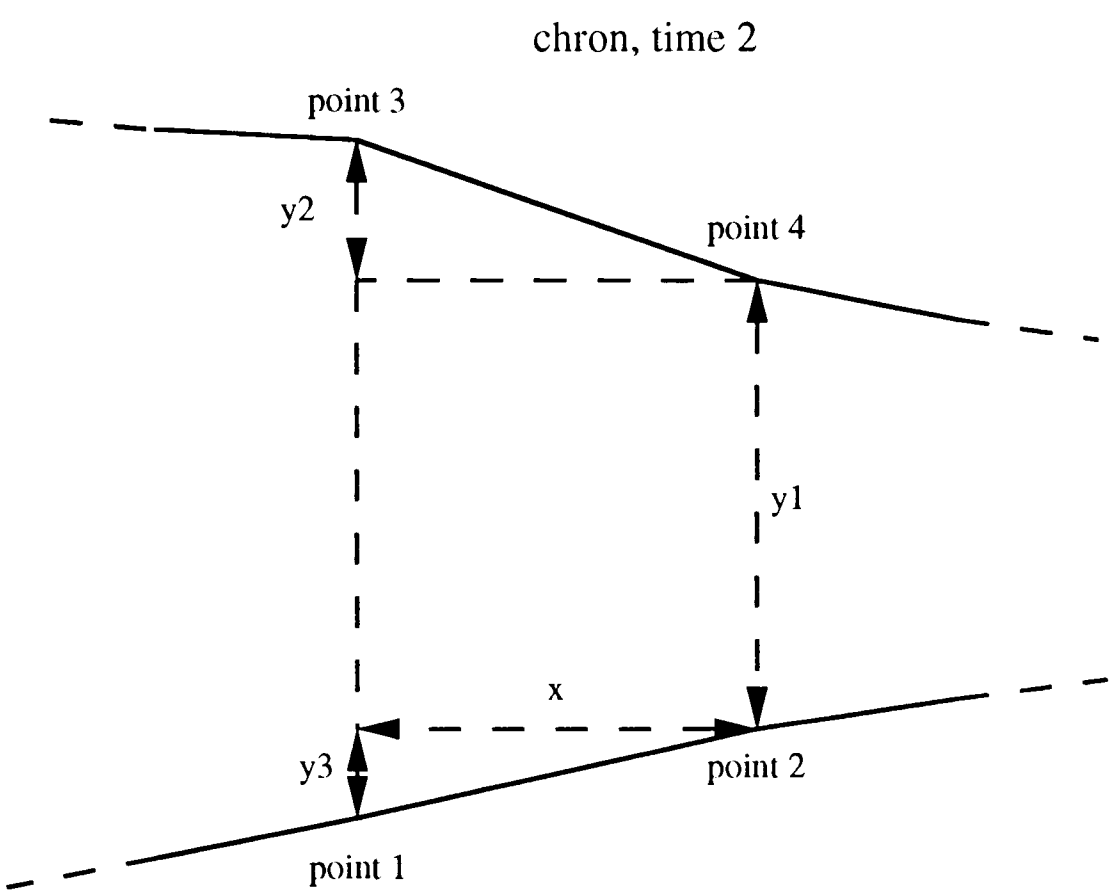

Total area between chrons for interval between point1 and point2
= area of trapezium defined by four points
= (x * y1) + (0.5x * y2) + (0.5x * y3)

Figure 2.12 The geometry of the trapezium shape used to calculate areas of deposition and erosion

1. Find the initial beach position - chron-sea intersection
2. Generate a fluvial profile
3. Has sufficient fluvial sediment been deposited?
4. If not, move the position of the beach seaward.

E.G. In the example below, the external sediment input is 1.0sq.km, and the sediment partitioning coefficient is 0.5.

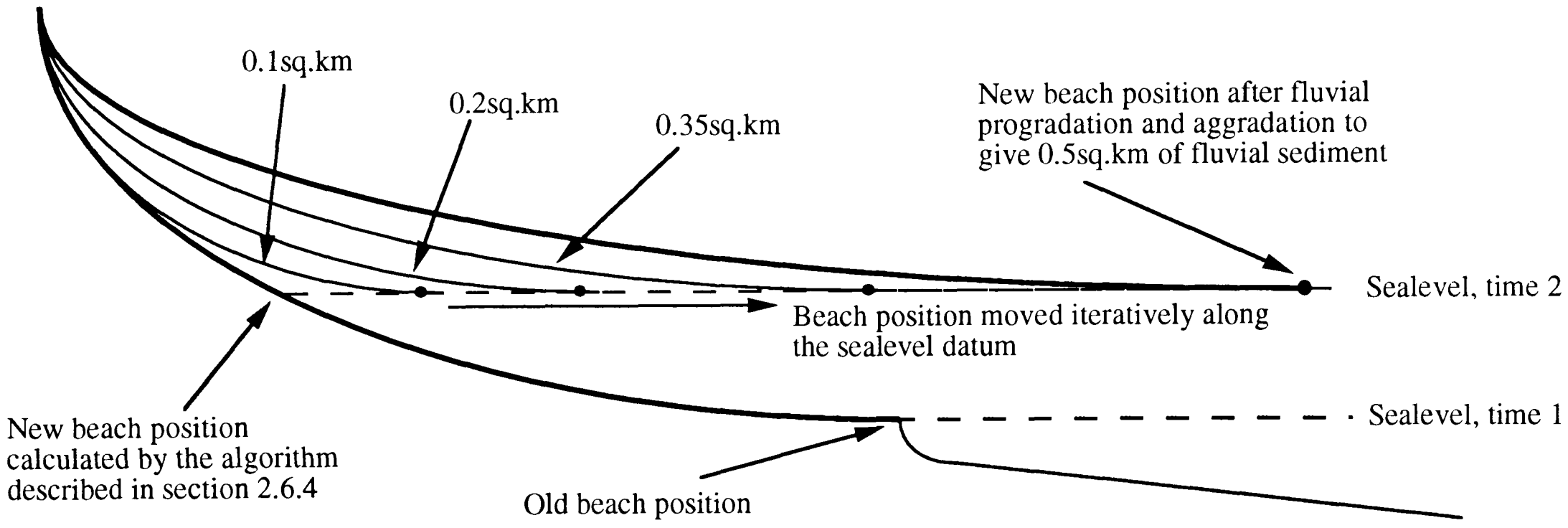

Figure 2.13. A diagrammatical explanation of the iterative routine used to deterimine the beach position and the geometry of the fluvial profile with a specified partitioning coefficient.

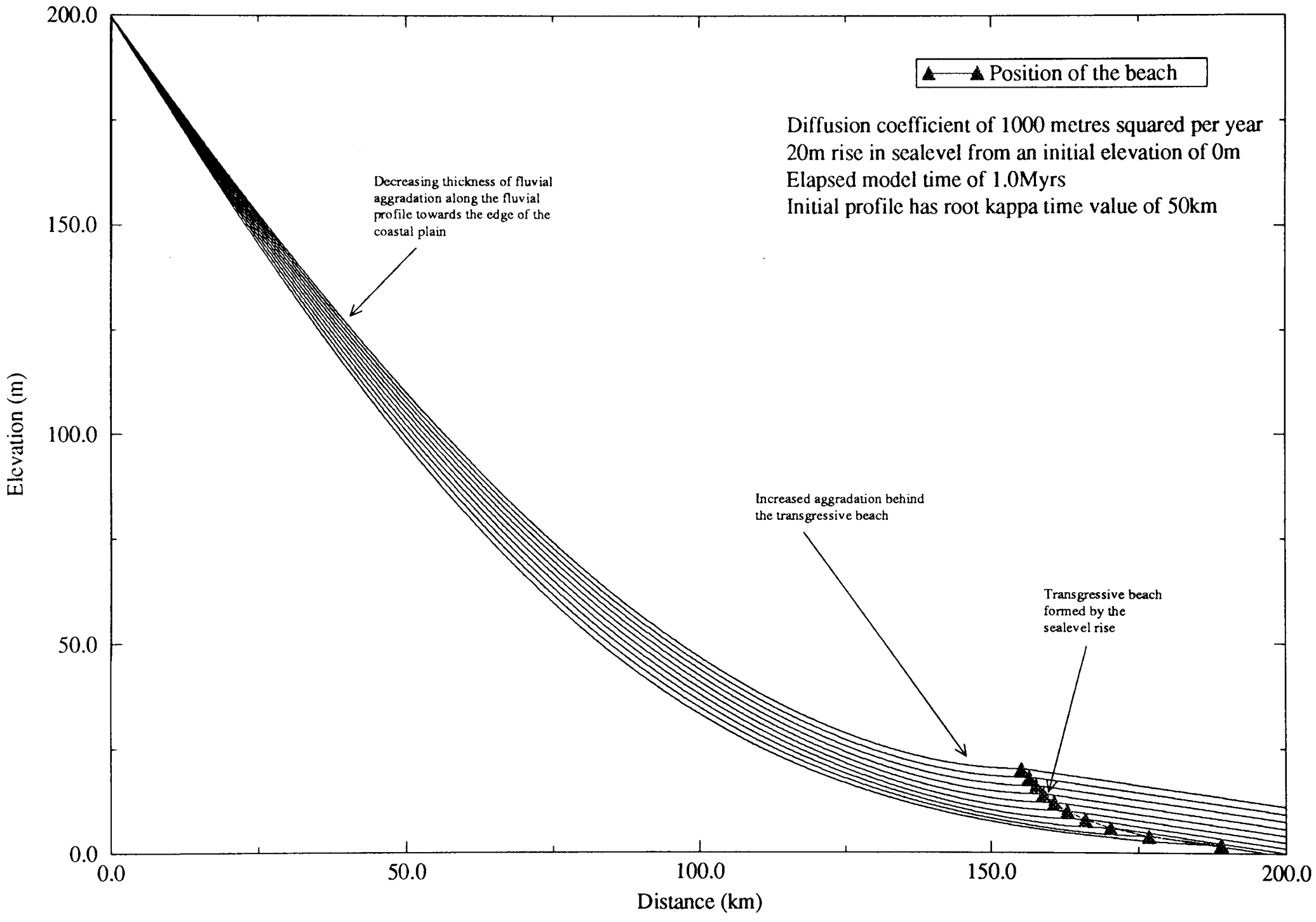

Figure 2.14. The response of the diffusional fluvial profile to a 20m sealevel rise.

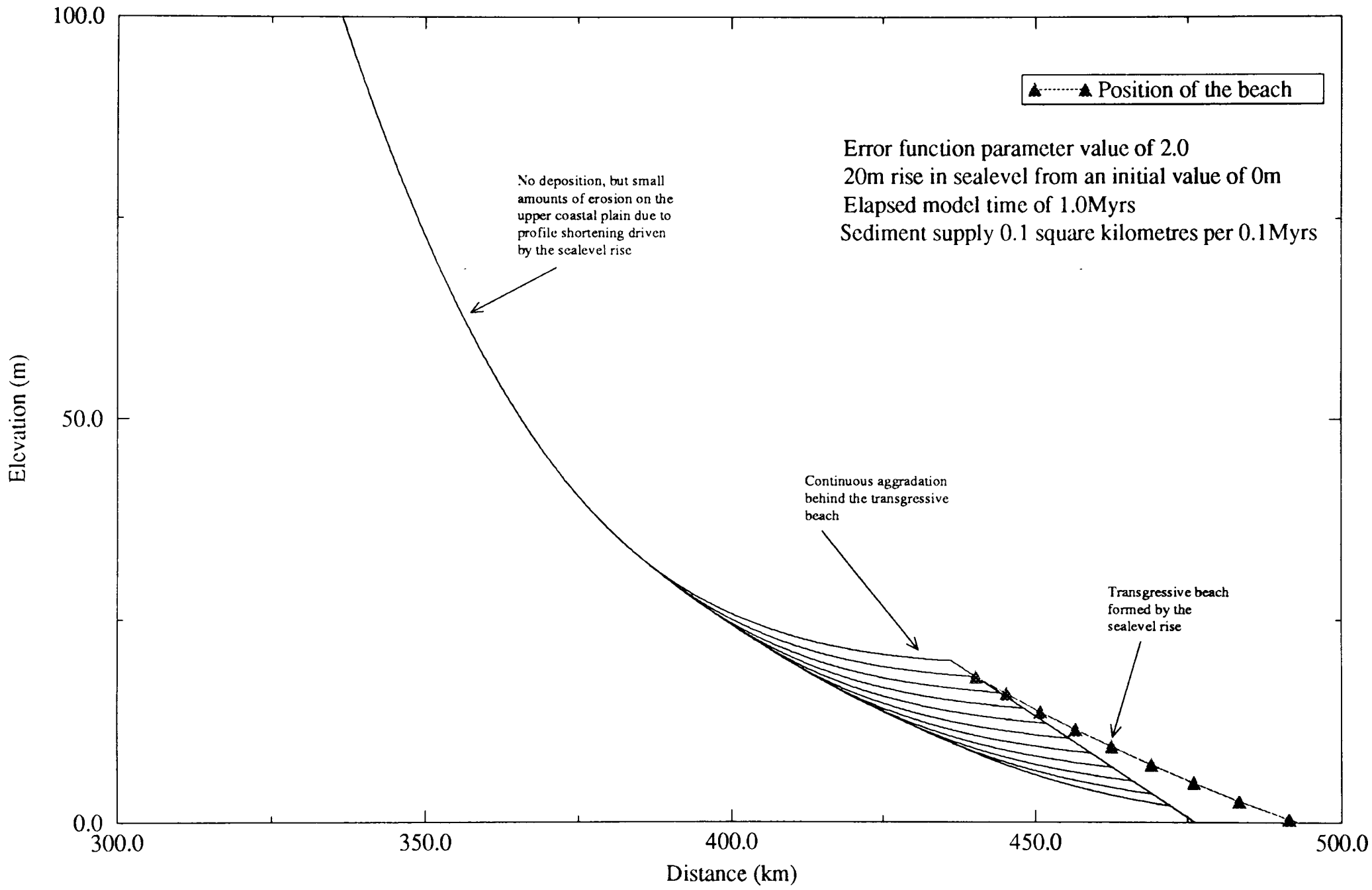

Figure 2.15. The response of the geometrical profile to a 20m sealevel rise.

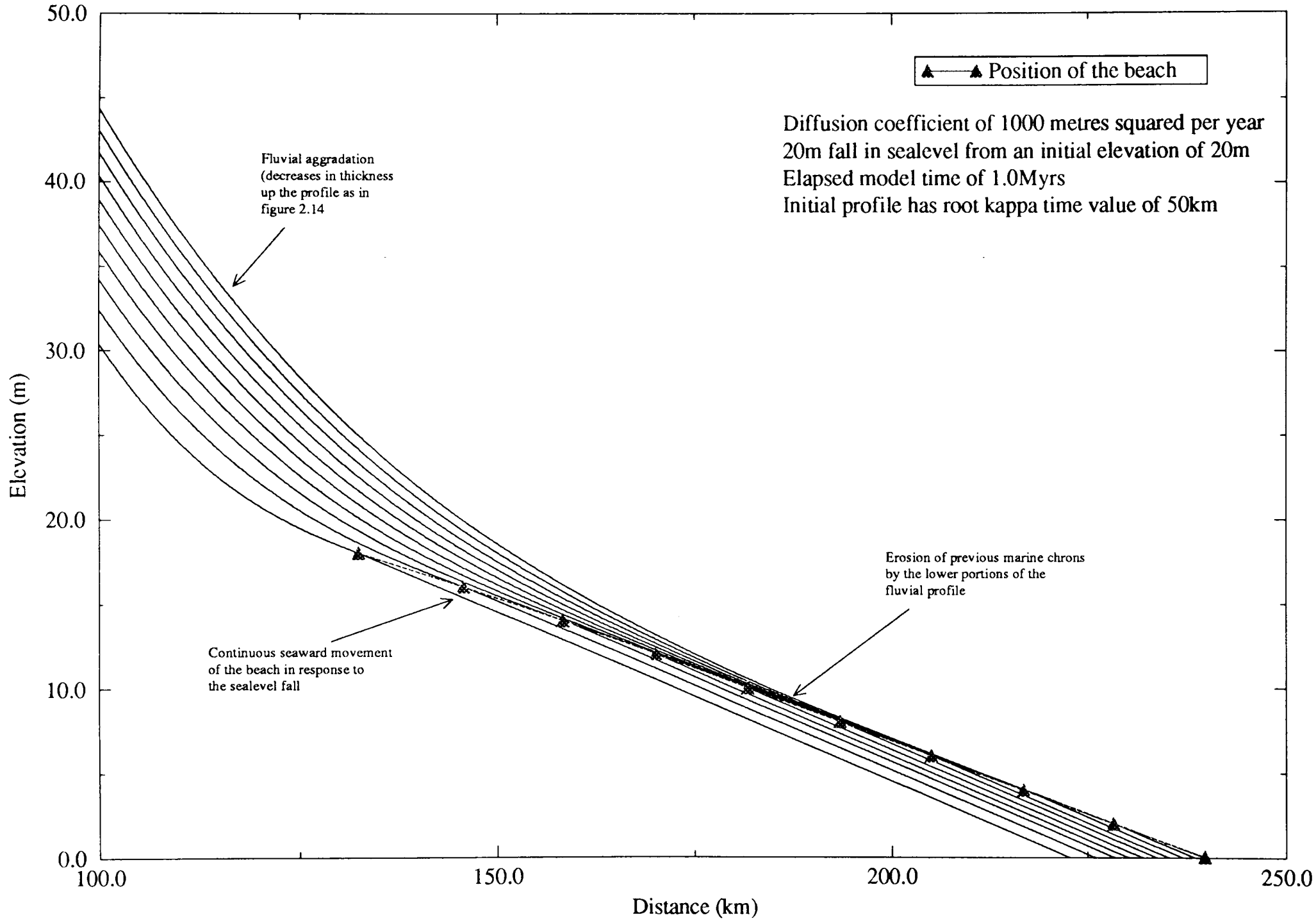

Figure 2.16. The response of the diffusional fluvial profile to a 20m sealevel fall.

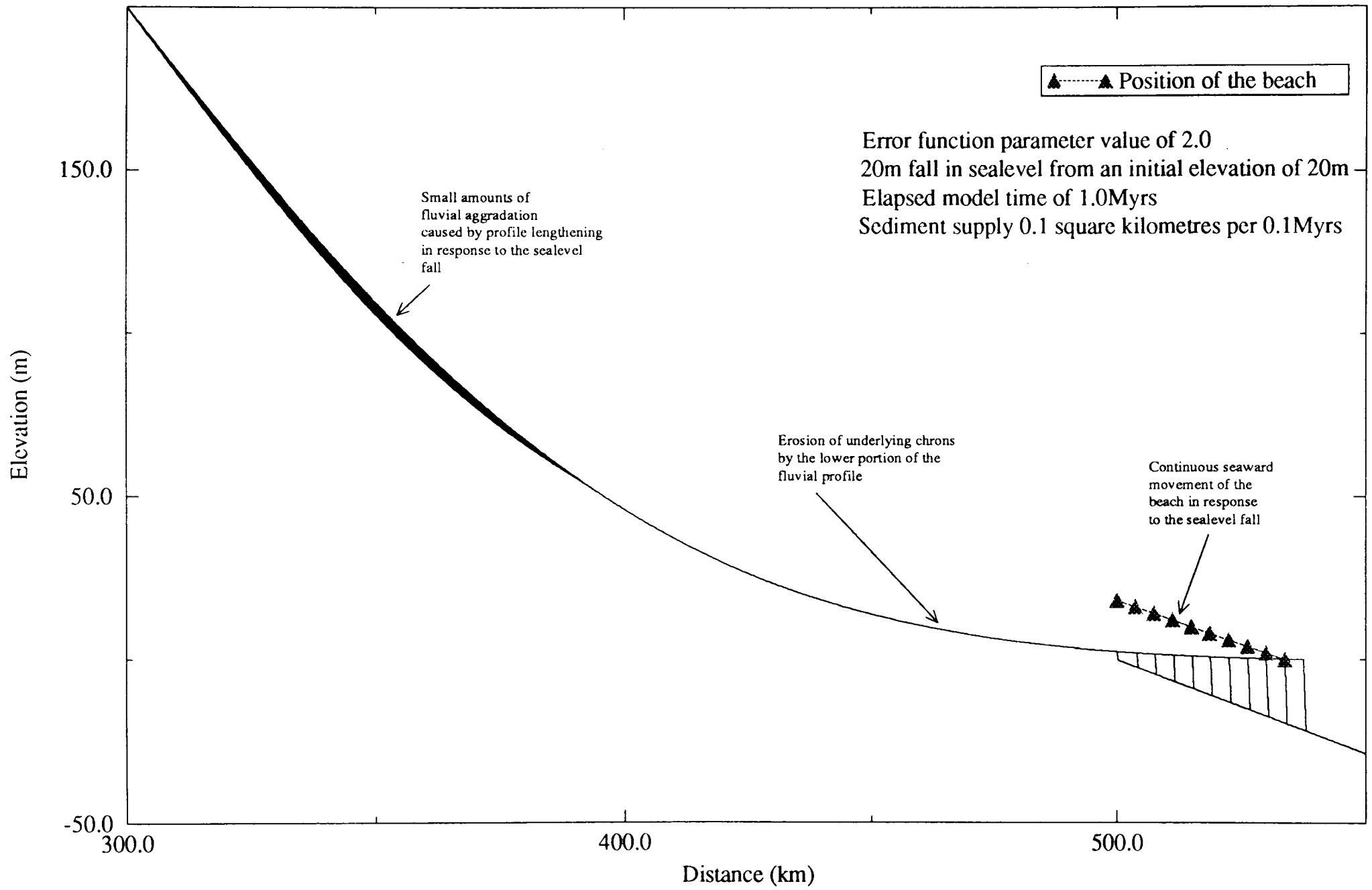

Figure 2.17. The response of the geometrical profile to a 20m sealevel fall.

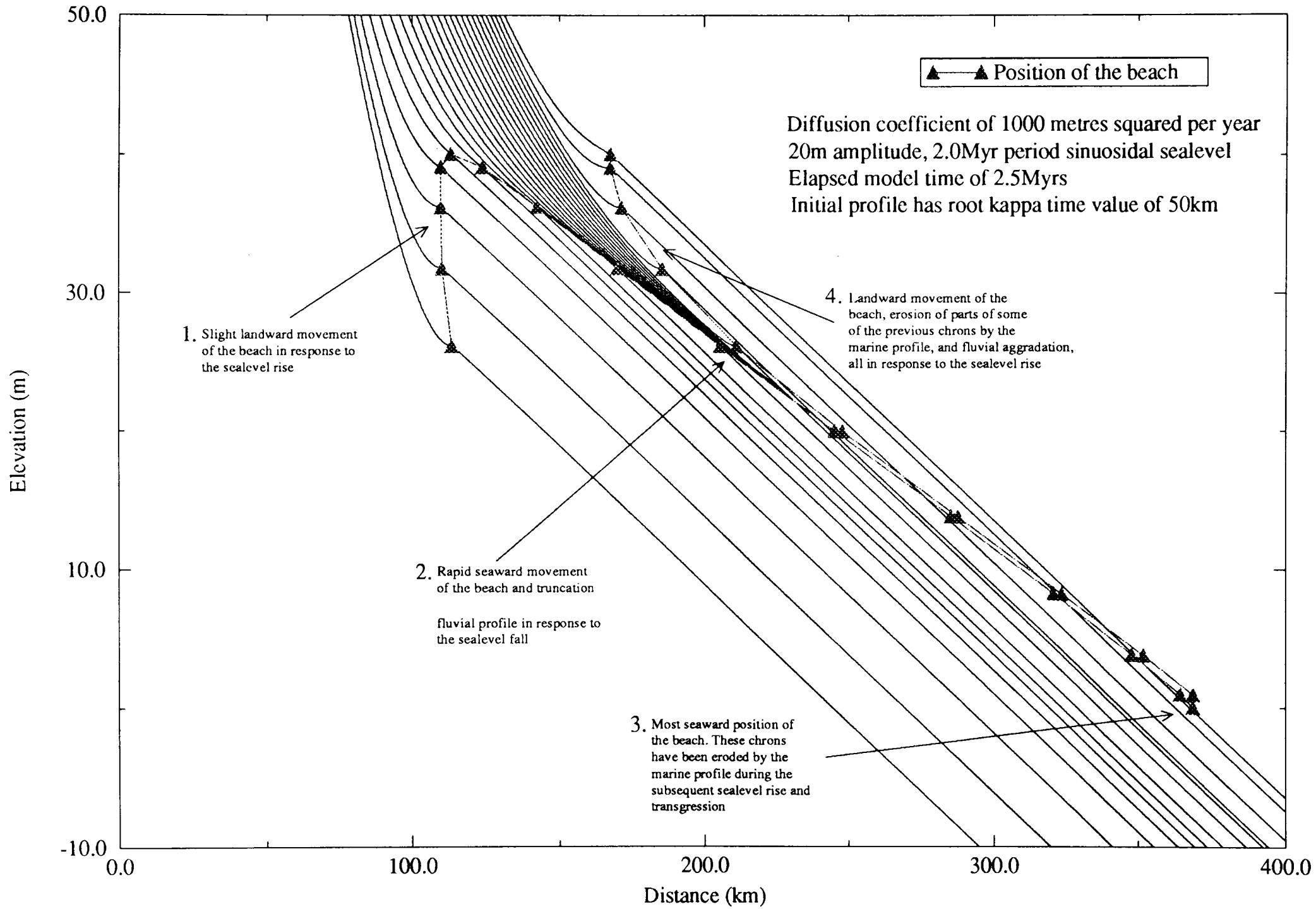

Figure 2.18. The response of the diffusional fluvial profile to a 20m amplitude sinusoidal sealevel curve with a diffusion coefficient of 1000 metres squared per year.

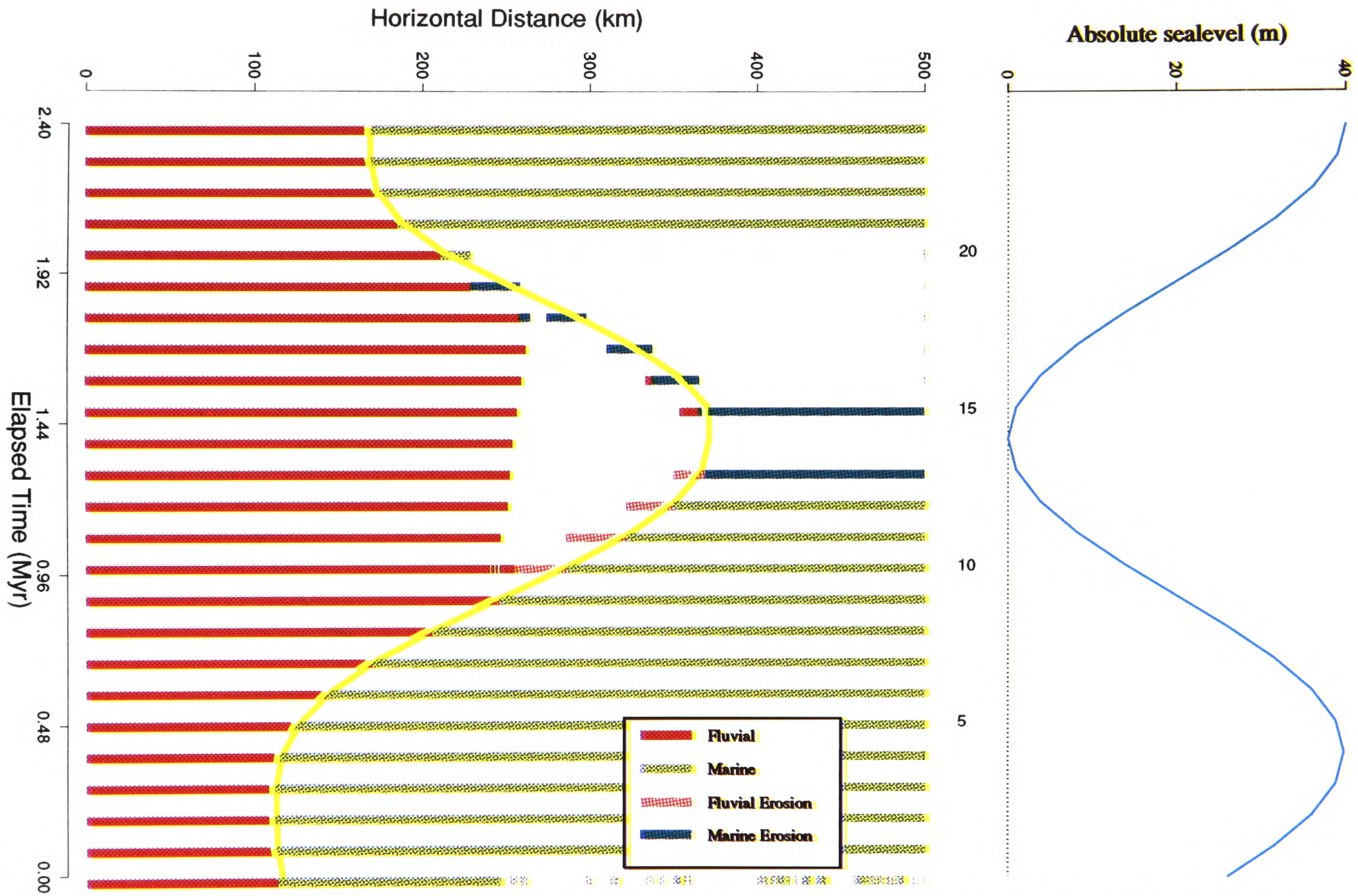

Figure 2.19. A chronostratigraphic diagram and an absolute sealevel curve from the diffusional profile model shown in figure 2.18. The model was run with the sinusoidal absolute sealevel curve shown and a diffusion coefficient value of 1000 metres squared per year. Note the region of fluvial erosion and bypass in chrons 11 to 17 caused by the absolute sealevel fall.

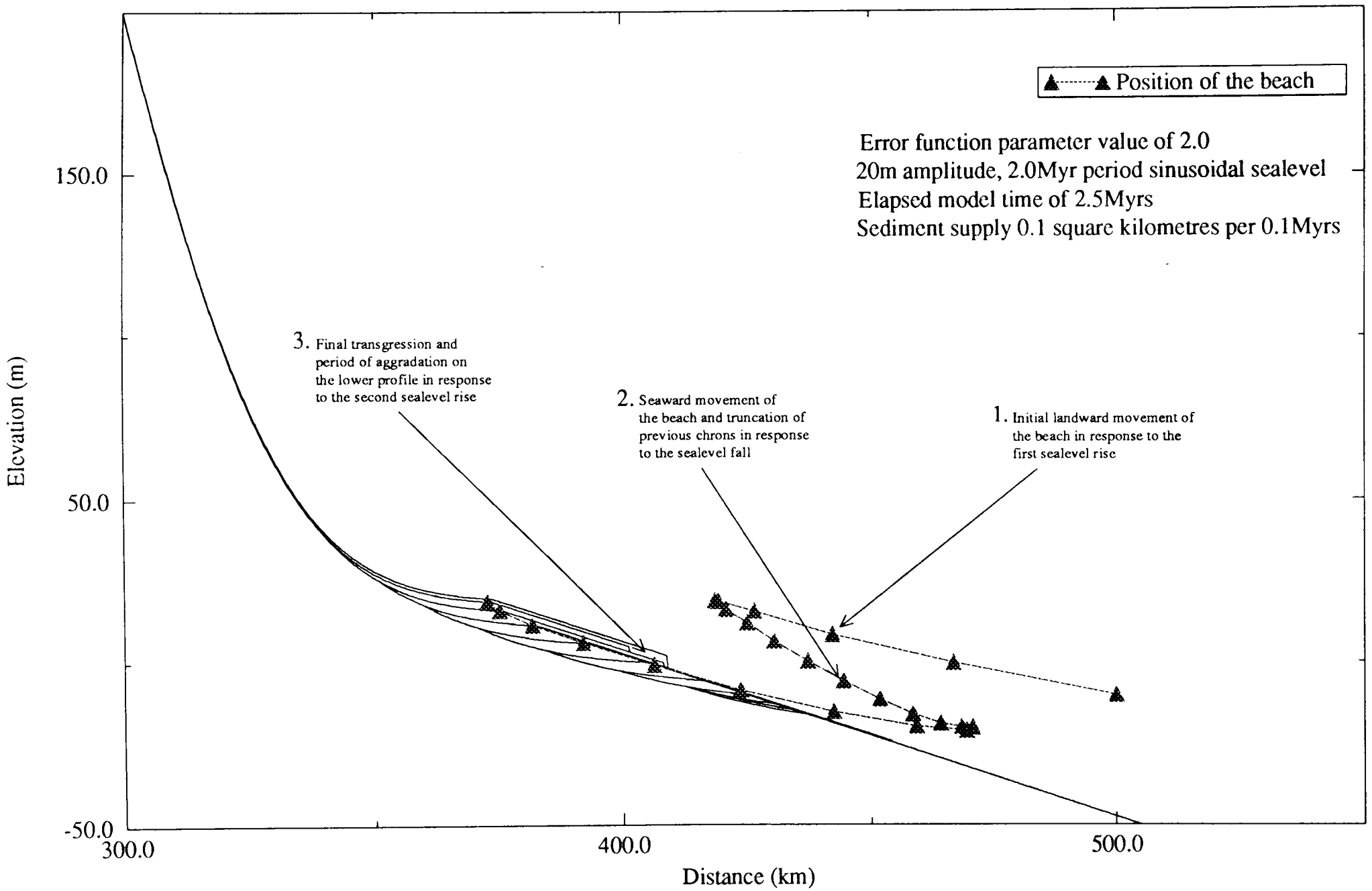

Figure 2.20. The response of the geometrical profile to a 20m amplitude sinusoidal sealevel curve with a sediment supply of 0.1km squared per 0.1Myr timestep.

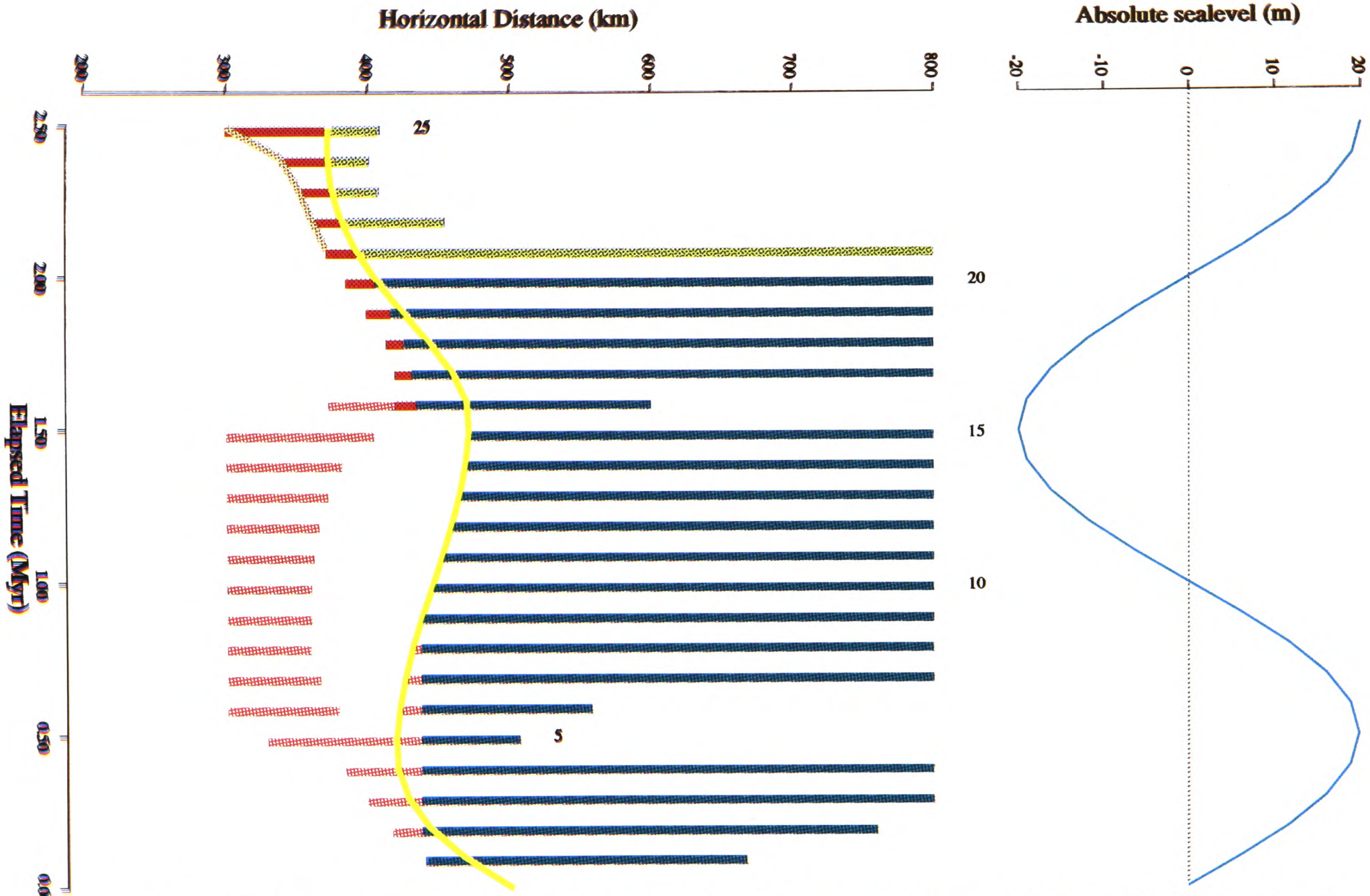

Figure 2.21. A chronostratigraphic diagram and an absolute sealevel curve from the model run shown in figure 2.20. The model used a geometric profile with an error function parameter value of 2.0 and a sediment supply of 0.1 square kilometres per year.

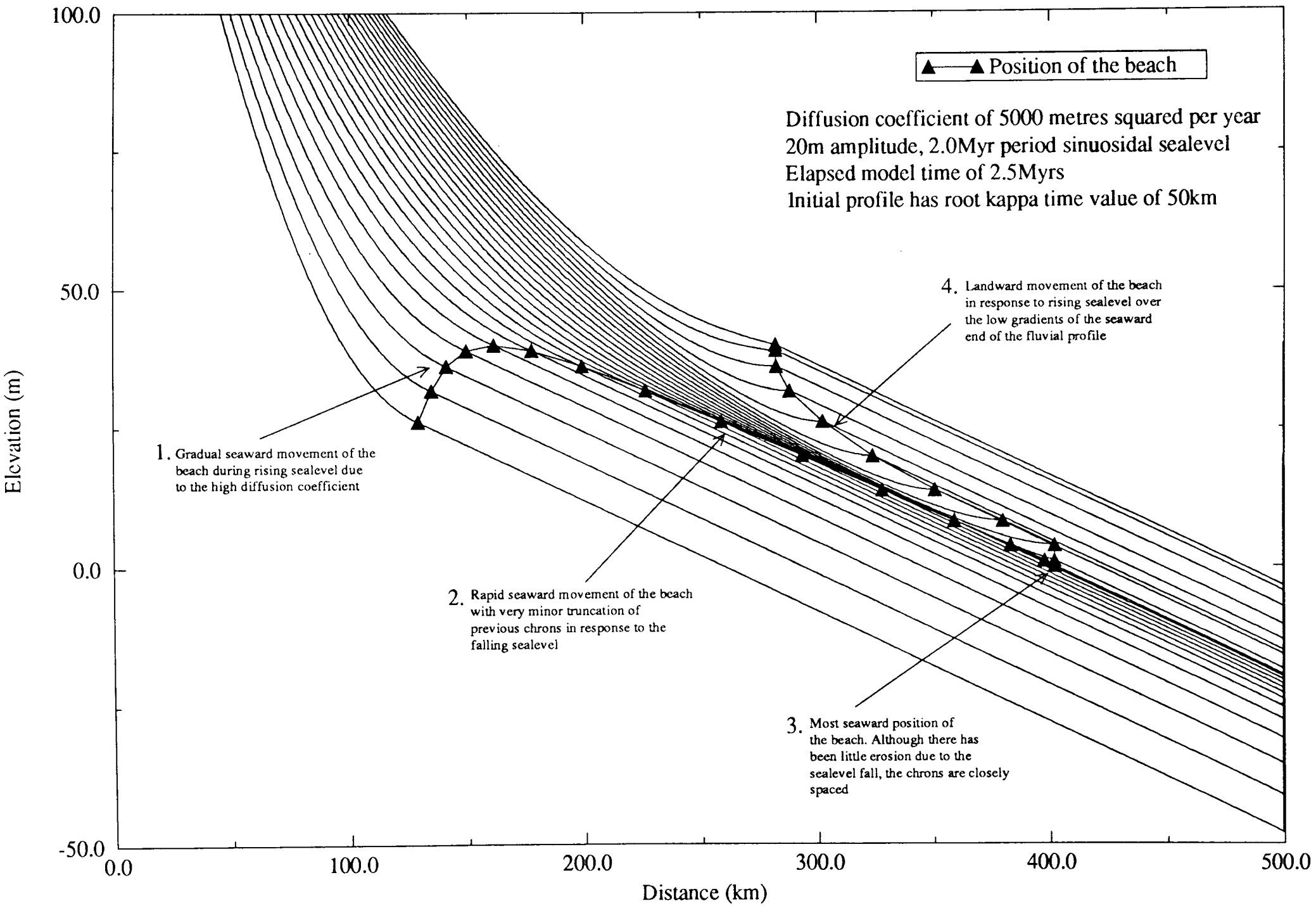

Figure 2.22. The response of the diffusional fluvial profile to a 20m amplitude sinusoidal sealevel curve with a diffusion coefficient of 5000 metres squared per year.

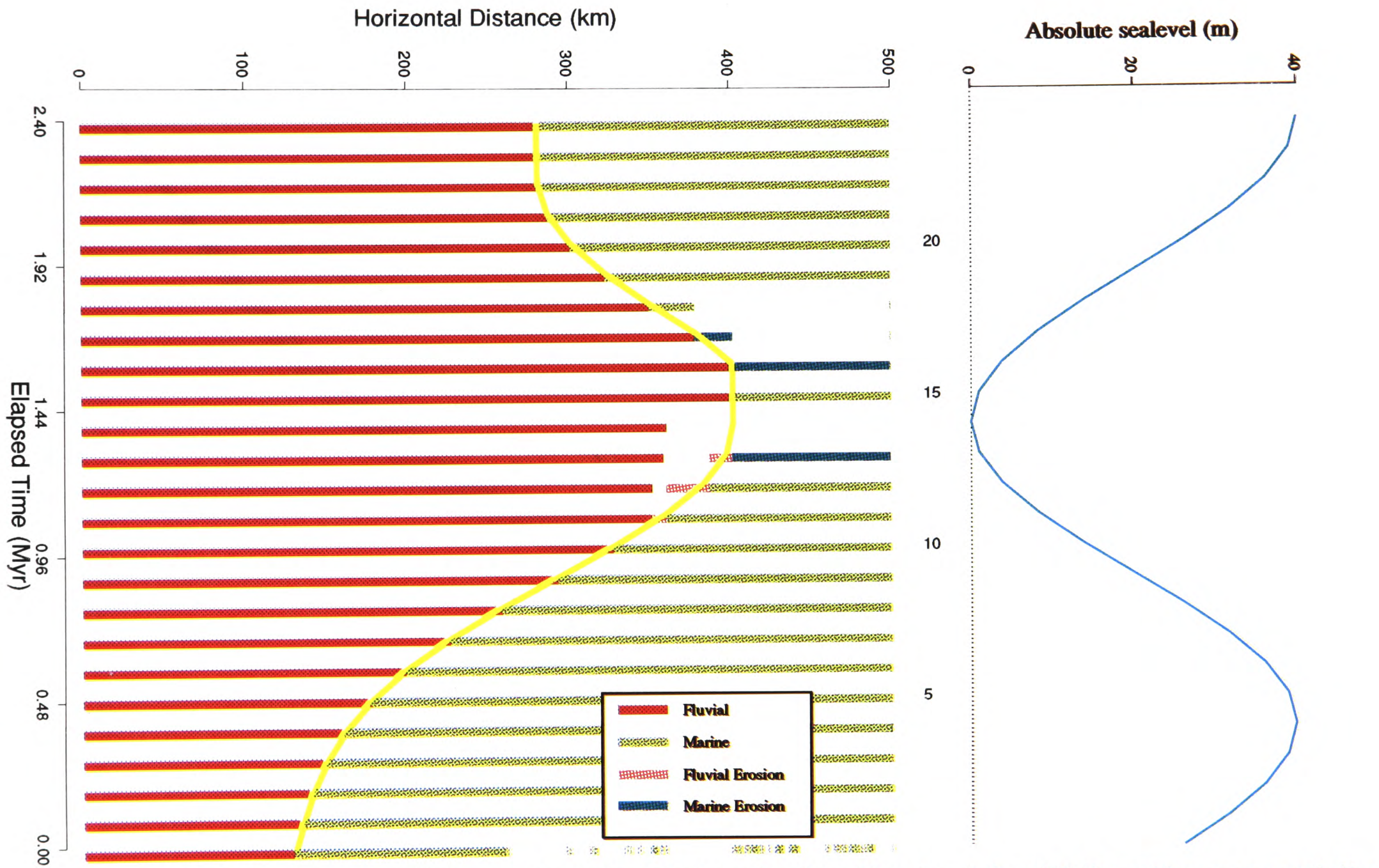

Figure 2.23. A chronostratigraphic diagram and an absolute sealevel curve from the model run shown in figure 2.22. The model run was generated with a diffusional profile with a diffusion coefficient of 5000 metres squared per year and the absolute sealevel curve shown.
Note how the increased sediment supply has reduced the width and duration of the region of fluvial erosion and non-deposition.

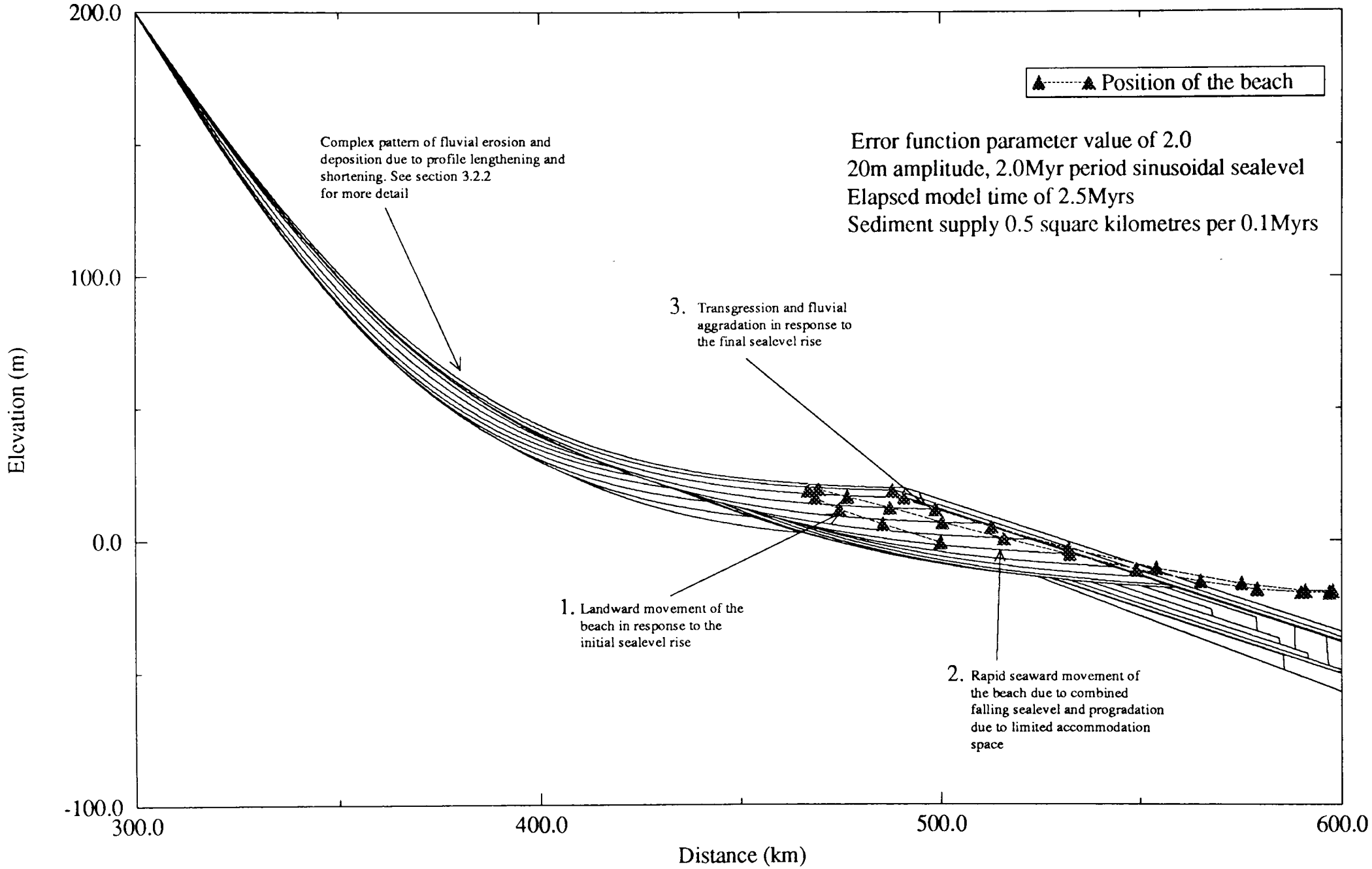

Figure 2.24. The response of the geometrical profile to a 20m amplitude sinusoidal sealevel curve with a sediment supply of 0.5 square kilometres per 0.1Myr timestep.

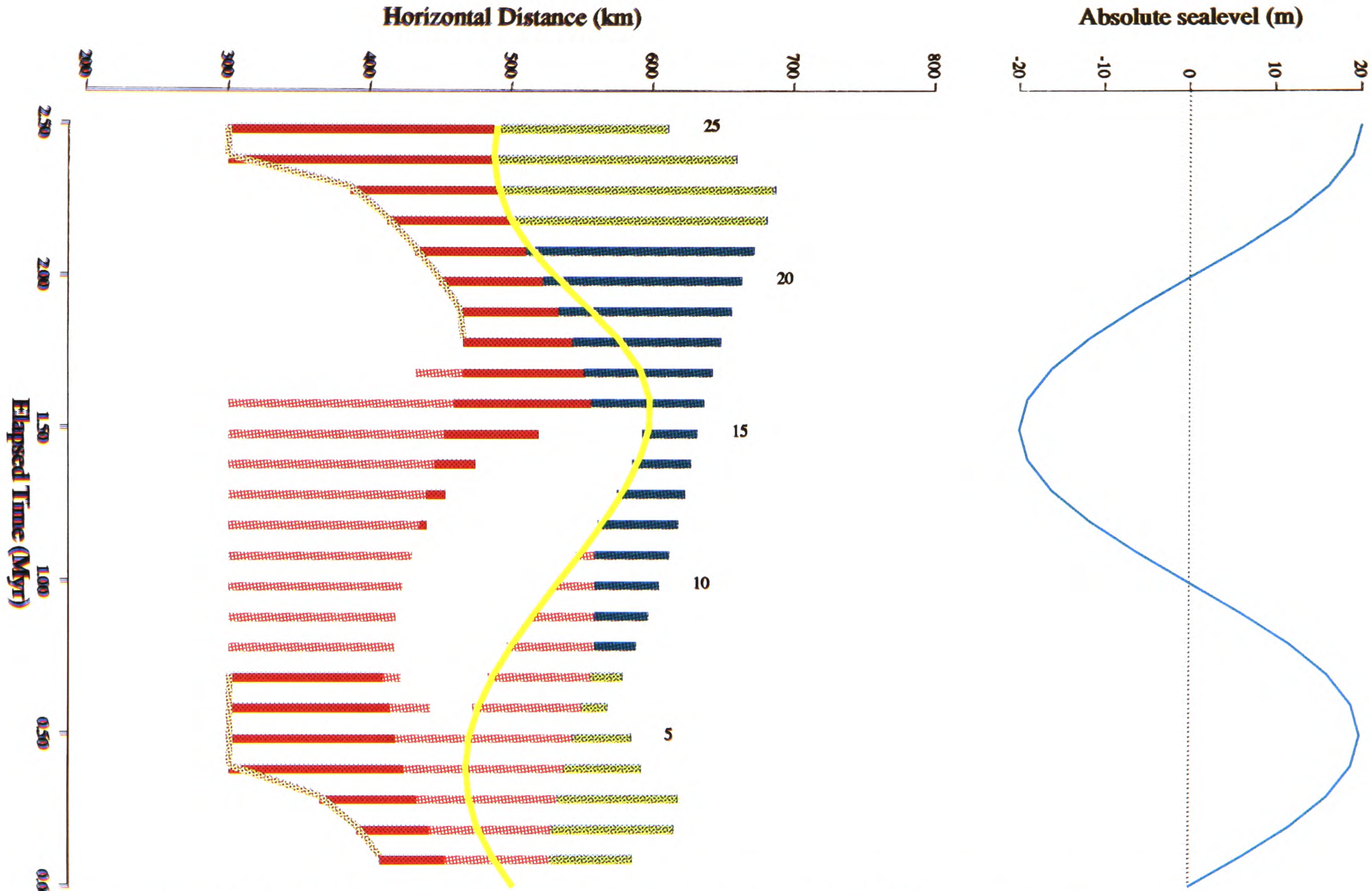

Figure 2.25. A chronostratigraphic diagram and an absolute sealevel curve from the geometric profile model run with an error function parameter value of 2.0 and a sediment supply of 0.5 square kilometres per year. Note the pattern of deposition and erosion on the profile. This is discussed in section 2.6.5.4

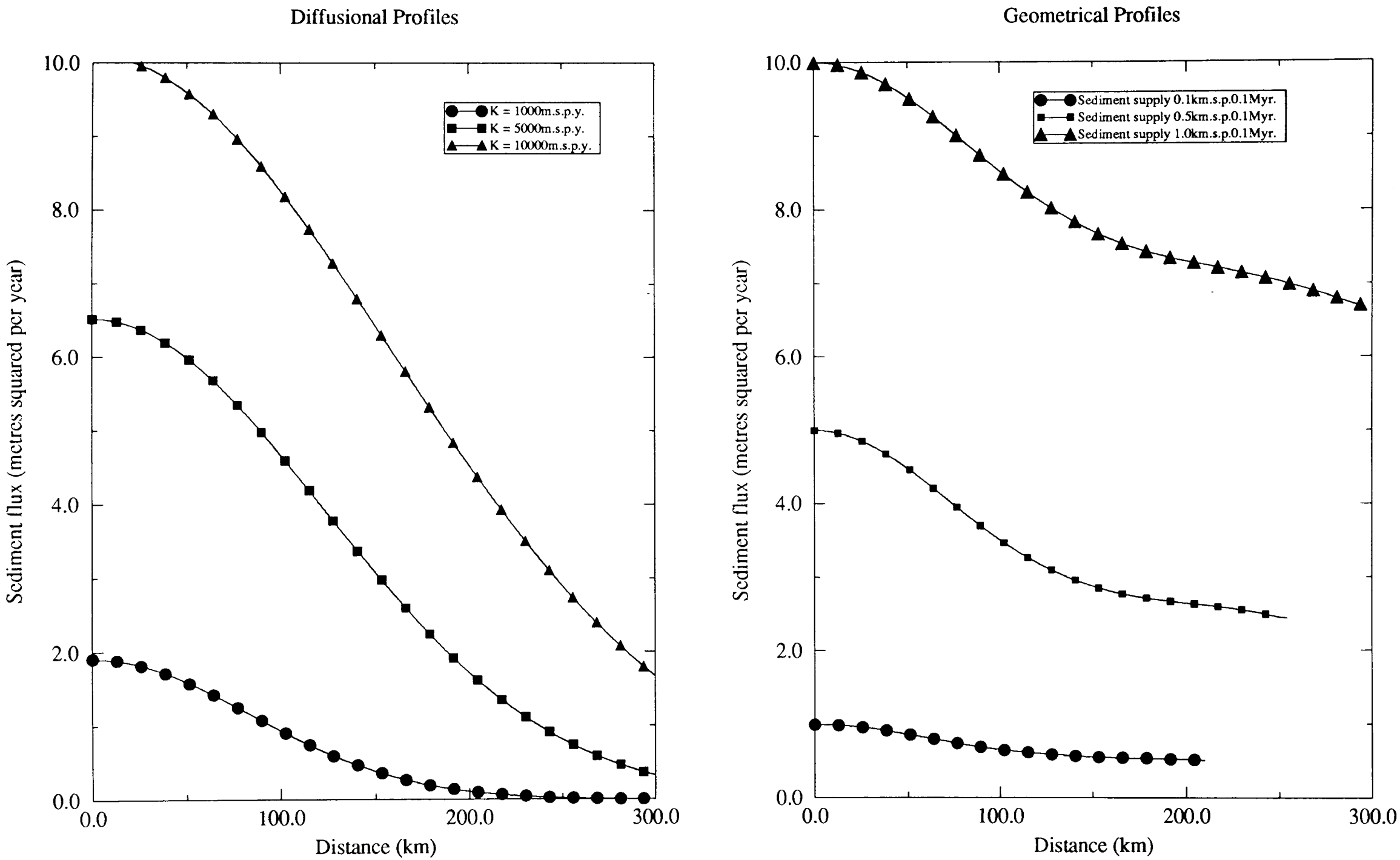

Figure 2.26. The magnitude of sediment flux with distance along the geometrical and the diffusional fluvial profiles. Three examples for each approach are shown, with varying values for the diffusion coefficient and for the external sediment supply. See text for a full discussion of the model parameters and the methods used to calculate the sediment flux.

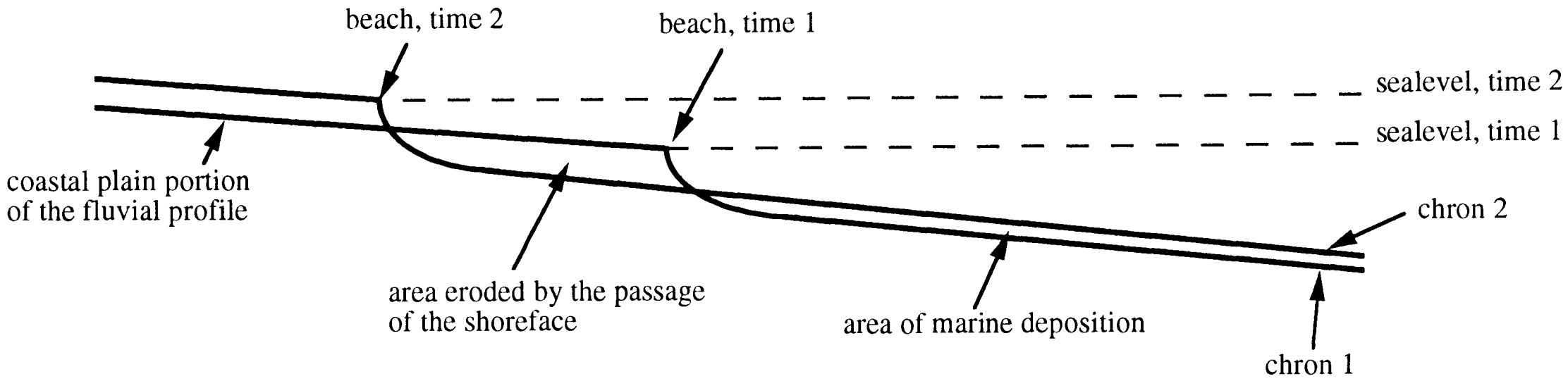

Figure 2.27 The marine equilibrium profile response to relative sealevel rise.

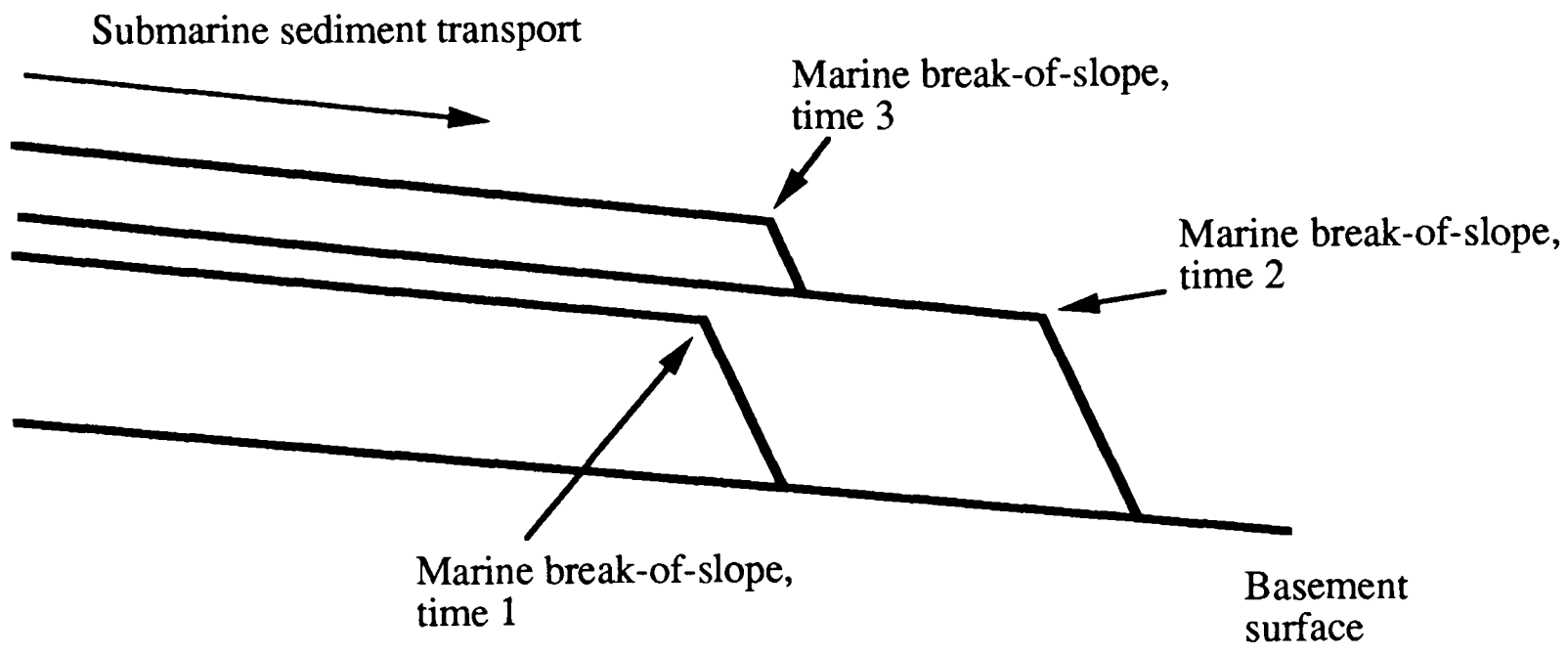

Figure 2.28 The changing position of the shelf-slope break for different chrons

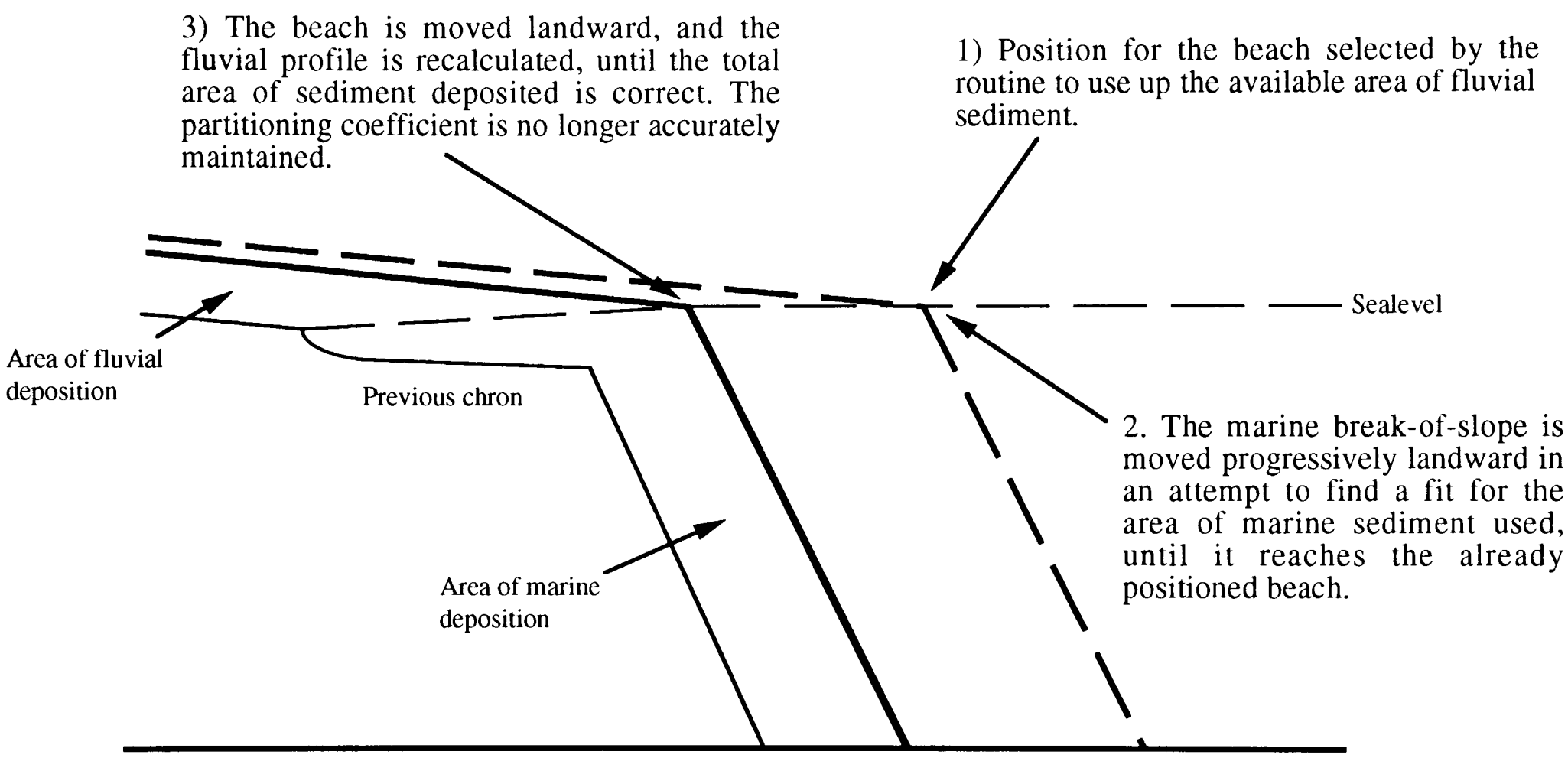

Figure 2.29 Details of the calculation of the position of the shelf-slope break.

Chapter 3

Chapter 3 - Controls on Sequence Geometry

"'tis a tale told by an idiot,

full of sound and fury,

yet signifying nothing."

(Shakespeare, Macbeth)

3.1 Introduction

This chapter shows how results from a quantitative forward model of passive rift-margin stratigraphy compare with the conceptual qualitative models describing the development of siliclastic depositional sequence geometries, presented by various authors such as Posamentier *et al.* (1988), Posamentier and Vail (1988) and more recently Van Wagoner *et al.* (1990) and Vail *et al.* (1991). It is shown that the quantitative model can reproduce some of the basic features of the sequence stratigraphic models such as systems tracts (with a variety of stacking patterns), sequence bounding unconformities, and stratal onlap patterns. Using the quantitative model to perform a series of sensitivity tests, it is possible to investigate the significance of a variety of controls on these features of depositional sequences. The controls include changing absolute sealevel, thermal subsidence, flexural isostasy, variable sediment supply, and fluvial profile geometry. The results can then be used to assess the validity of the current sequence stratigraphic model, and to determine what controls may prove to be important that are not currently adequately represented in such models.

3.2 Reproducing the basic elements of depositional sequences

The qualitative sequence stratigraphic depositional models consist of three main controlling processes which can be related directly to the elements of this quantitative forward model. These processes are tectonic subsidence, eustasy, and erosion and

deposition on equilibrium surfaces. Selecting appropriate initial conditions and model parameters allows the basic features of the sequence stratigraphic depositional model to be reproduced with the quantitative model. Similarities and discrepancies between the two models can then be used to investigate some of the assumptions behind the sequence stratigraphic model.

3.2.1 Initial conditions and parameter values

In order to generate a type-1 sequence (see section 1.1) of duration 2.0Myr E.M.T. (i.e. a third order cycle using the terminology of Vail *et al.* (1977b)) with twenty chrons each of duration 100Kyrs, the following initial conditions and parameter values are used. Tectonic subsidence is calculated using one-layer thermal subsidence (McKenzie, 1978) with an initial lithospheric thermal age of 10Myrs, and stretching values ranging from 1.0 at 400km from the origin, to 1.01 at 500km from the origin, and 2.0 at 1024km from the origin. No lithospheric flexure is included in the calculations for these model runs. An absolute sealevel curve with a 2.0Myr period and a 20m amplitude is used. The period is chosen to produce a third-order cycle (Vail *et al.* 1977b). The amplitude is lower than many of the third-order cycles shown by Haq *et al.* (1988) to demonstrate that high-amplitude changes are not necessary to create sequence geometries. External sediment supply is held constant at an arbitrary value of 1.0km^2, and the area of sediment eroded on both the marine and fluvial profiles is not added to the total sediment available for deposition on each chron so that sediment supply remains constant throughout the model run.

The fluvial profile has an initial length of 200km, based on the width of the coastal plain on the North American passive margin, and the landward end of the profile is held in a fixed horizontal and vertical position. The profile is defined using a complementary error function curve with an arbitrary error function parameter value of 2.0. Fluvial progradation is included, with the fluvial partitioning coefficient set to an arbitrary value of 0.5. The

initial topography has 200m elevation from the origin to 500km right of the origin, and then a constant slope from 0m at 500km to -500m at 1024km right of the origin. The marine profile has a shoreface 10m high and 2km wide, a shelf with a gradient of 0.5mkm^{-1} and a slope with a gradient of 43.66mkm^{-1}. These values for the topography are based on general passive margin topography. Uncompacted sediment density is 1.8kgm^{-3}. These initial conditions and parameters are summarised in figure 3.1.

3.2.2 Description of the type-1 sequence

Both Van Wagoner *et al.* (1988) and Van Wagoner *et al.* (1990) show cross sections of stylised type-1 sequences (figure 3.2). The essential characteristics of a type-1 sequence are a basal unconformity due to subaerial exposure and erosion, associated with a basinward shift of facies, a downward shift in coastal onlap, and onlap of the overlying strata (Van Wagoner *et al.* 1988). This is stated to be caused by the rate of eustatic fall exceeding the rate of basin subsidence, hence dropping the beach over the edge of the shelf-slope break. In the example diagram (figure 3.2) both Van Wagoner *et al.* (1988) and Van Wagoner *et al.* (1990) show a highstand systems tract with a progradational trend to the parasequences overlain by a type-1 sequence boundary which is caused by a fall in relative sealevel, which in turn is caused by a fall in eustatic sealevel. The sequence boundary is overlain by the lowstand systems tract with a lowstand wedge and an incised valley fill. This is then overlain by the transgressive system tract composed of parasequences with a retrogradational trend. This passes vertically into the highstand system tract, with parasequences showing an aggradational to progradational trend. A second sequence boundary, either type-1 or type-2, overlies the highstand systems tract.

Figure 3.3 is a section from the quantitative model showing twenty five chrons generated over an E.M.T. of 2.5Myrs. This section is analogous at a basic level to the type-1 sequence examples described above. The sequence boundary in figure 3.3 is placed on chron 15, at an E.M.T. of 1.5Myrs, at the lowest point on the absolute sealevel curve. It is

defined on the basis of the resumption of fluvial deposition and hence the end of fluvial erosion in the lower portion of the fluvial profile, and the continuation of the surface basinward as a correlative conformity. The sequence boundary as it is defined here, is more difficult to fit into the standard sequence stratigraphic model for a type-1 sequence, because the pattern of fluvial down-cutting, erosion and sediment bypass in this model is more complex, and highly diachronous. The significance of this and other discrepancies are discussed fully in section 3.3.

Groupings of chrons within the model run shown in figure 3.3 are analogous in terms of geometry and positioning to the systems tracts described in the sequence stratigraphic model. Although the use of systems tracts in describing actual stratigraphy can be criticised because of the necessary assumption of the dominant control of relative sealevel change, their use here is justifiable, since in a conceptual model, either qualitative or quantitative, the influence of relative sealevel is always known. Chrons one to five represent the highstand systems tract which has been eroded and truncated by the subsequent subaerial erosion on the fluvial profile as relative sealevel dropped. Chrons 6 to 15 are analogous in some ways to the lowstand systems tract, in that fluvial deposition is minimal, the fluvial profile is eroding the old shelf surface, and the largest area of deposition is on the deep marine slope. However, the diachronous nature of the sequence boundary complicates this, since chrons 6 to 15 both underlie and overlie the sequence boundary, unlike in the sequence stratigraphic depositional model in which the lowstand systems tract overlies the sequence boundary (see figure 3.2). Chrons 16 to 25 are analogous to transgressive and highstand systems tracts in terms of their position on the eustatic sealevel curve, their stacking patterns, and their onlap patterns.

Figure 3.4 shows the corresponding chronostratigraphic diagram, absolute sealevel curve, and the stratal onlap curve. The chronostratigraphic diagram shows clearly the distribution of different environments of deposition in response to changing absolute sealevel. The beach can be seen moving basinward as absolute sealevel falls, and moving back

landwards when it starts to rise. Onlap on the fluvial profile is preserved in chrons 19 to 25. The positioning of the sequence boundary, the pattern of fluvial deposition and erosion, and the pattern of downlap do not fit well with the standard sequence stratigraphic model. The significance of these differences is discussed in section 3.3.

It is important to understand at this point how the fluvial stratigraphy shown in the type-1 standard reference model develops through time in response to changing relative and absolute sealevel. Figures 3.5 to 3.9 illustrate this development. Each figure represents an E.M.T. of 0.5Myrs, and shows an enlarged view of the fluvial profile and early proximal marine portion of the model profile. Figure 3.5 shows the first five chrons in the model run. The fluvial profile shows aggradation along its whole length, developed in response to a 20m rise in sealevel (figure 3.4). As the rate of absolute sealevel rise decreases, the beach changes from retrogradation to progradation.

As absolute sealevel begins to fall, an erosion surface starts to develop on the lower two thirds of the fluvial profile, while aggradation continues on the upper profile (figure 3.6). This occurs as a result of profile lengthening forced by the seaward movement of the beach in response to falling absolute sealevel. The continuing development of the surface of erosion and non-deposition (see figure 3.4), and a reduction in aggradation on the upper profile are shown in figure 3.7. At this stage the absolute sealevel curve is at its low point. When absolute sealevel starts to rise again aggradation commences on the lower third of the fluvial profile, while small amounts of erosion (less than 5m in vertical extent) form on the upper profile (figure 3.8). Aggradation occurs progressively further landward on the profile as the rate of absolute sealevel rise slows (figure 3.9) producing the pattern of stratal onlap seen in figure 3.4.

These examples show that the profile response to absolute sealevel change has both useful features such as aggradation and stratal onlap in response to absolute sealevel rise, and development of a laterally extensive surface of erosion and bypass in response to sealevel

fall. However, the profile also shows unrealistic behaviour in the form of erosion of limited vertical extent on the upper profile in response to absolute sealevel rise, and aggradation on the upper profile in response to absolute sealevel fall. These latter features should not be considered as predictive model results.

3.2.3 Description of the type-2 sequence

The essential difference between a type-1 and a type-2 sequence as described by Van Wagoner *et al.* (1988) and Van Wagoner *et al.* (1990) and shown in figure 3.10, is the lack of subaerial erosion and basinward shift in facies in a type-2 sequence (compare with the type-1 example in figure 3.2). Other factors such as coastal onlap patterns are common to both types of sequence. A type-2 sequence does not have a lowstand systems tract developed, but instead has a shelf margin system tract. This is composed of aggradational to slightly progradational parasequences which overlie the previous highstand systems tract and the sequence boundary (figure 3.10).

A section analogous to a type-2 sequence can be produced with the quantitative model by increasing the rate of tectonic subsidence, using stretching factors ranging from 1.0 at 400km to 8.0 at 1024km, and decreasing the amplitude of eustasy from 20m to 10m.. Figure 3.11 shows the section from the model run with these parameters. The fluvial erosion and truncation of chrons visible in the type-1 sequence is absent from the type-2 example. However, the patterns of progradation, aggradation and retrogradation are very similar to those in the type-1 example. The shelf margin systems tract as described by Van Wagoner *et al.* (1988) is not developed since both the position of the beach and, when developed, the marine break-of-slope, remain progradational throughout the model run. No aggradational stacking pattern characteristic of shelf margin system tracts in type-2 sequences is developed. The lack of subaerial erosion and the reduced mobility of the beach with respect to a type-1 sequence are shown in the chronostratigraphic diagrams in figure 3.12.

3.2.4 Predictions of reservoir and seal distribution

Although detailed predictions made with the model should be treated with extreme caution, the examples of type-1 and type-2 sequences shown in figures 3.3 and 3.11 do allow general predictions regarding the distribution of possible reservoirs and seals in a sequence stratigraphic framework. Figure 3.13 shows two examples of possible reservoir and seal geometries. In the type-1 sequence example, shoreface stratigraphy that is liable to be sand-rich, is preserved beneath a type-1 sequence boundary unconformity, and hence surrounded by probably impermeable shelf and coastal plain muds. The type-2 example shows extensive shoreface stratigraphy preserved beneath a type-2 sequence boundary, and sealed laterally and vertically by probably muddy coastal plain and shelf stratigraphy.

3.3 Underlying assumptions of the sequence stratigraphic model

Quantitative modelling of stratigraphy is a powerful method for highlighting the assumptions behind the sequence stratigraphic model, and for investigating the controls on stratigraphy. Since the sequence stratigraphic model is predominantly qualitative, it is difficult to rigorously test, except by direct comparison of model predictions against stratigraphic data, and adopting this approach alone leads to important uniqueness problems. The quantitative model has the advantage that the contribution of different conditions and parameters can be more carefully examined, and thus the assumptions behind the model, and behind the qualitative sequence stratigraphic models, may be investigated.

The previous section showed how the quantitative model can reproduce aspects of the sequence stratigraphic model, namely the gross geometry of type-1 and type-2 sequences. However, there are several discrepancies. The following sections use the quantitative model to investigate these discrepancies, to highlight some of the often unstated

assumptions behind the sequence stratigraphic model and to propose some alternatives to the controls on stratigraphy described by various workers such as Vail *et al.* (1977b); Posamentier *et al.* (1988); Posamentier and Vail (1988); Van Wagoner *et al.* (1990); Vail *et al.* (1991).

3.3.1 Definition of Coastal Onlap

Vail *et al.* (1977a) and Posamentier *et al.* (1988) described how patterns of coastal onlap develop in response to eustatic change. Vail *et al.* (1977a) defined coastal onlap as "the progressive landward onlap of littoral and/or non marine coastal deposits" while Posamentier *et al.* (1988) defined coastal onlap as "the landward limit on the shelf or upper slope of sediment distribution - marine or non marine." Controls on coastal onlap patterns will be discussed below, but it is important first to examine the methods by which coastal onlap is measured from preserved stratigraphy.

Vail *et al.* (1977a) showed several theoretical examples of coastal onlap patterns. Both a vertical component, termed coastal aggradation, and a horizontal component termed coastal encroachment can be measured from the termination of strata against an initial depositional surface as described by Vail *et al.* (1977a) (figure 3.14). These patterns of stratal termination occur and can be measured in the quantitative model results presented here. Such onlap will be referred to as stratal onlap rather than coastal onlap, since in this model the onlap occurs entirely within fluvial stratigraphy, and at elevations of up to several hundred metres. The vertical components are measured and shown as stratal onlap curves (e.g. figure 3.4).

3.3.2 Magnitude of coastal onlap and derivation of relative sealevel curves

Vail *et al.* (1977a) assumed that measurements of coastal onlap could be used as a direct quantification of relative sealevel change. It did however, point out complications with

such measurements arising from variations in sediment supply which can lead to an absence of a coastal plain, and so affect onlap measurement, and also with topography on the coastal plain which can introduce an error to the relative sealevel determination. Posamentier *et al.* (1988) show theoretical coastal onlap curves calculated using essentially the same method as given in Vail *et al.* (1977a).

The importance of topography on the coastal plain has been underestimated in Vail *et al.* (1977a). Fluvial processes may create accommodation space for fluvial deposition tens, or even hundreds of metres above sealevel. Thus landward onlapping stratal terminations in fluvial stratigraphy may occur at significant elevations above sealevel. The resulting amplitude of stratal onlap is likely to be more strongly controlled by the dynamics of the fluvial system than by the amplitude of the eustatic sea level change.

To illustrate this point, albeit in a relatively simplistic way, figure 3.4 shows the stratal onlap pattern measured from the type-1 sequence example model stratigraphy, generated with an absolute sealevel curve of 20m amplitude and a 2.0Myr period. The amplitude of the vertical component of the stratal onlap for chrons 19 to 25 is almost 200m. If this aspect of the fluvial profile behaviour is realistic, and fluvial stratigraphy can be deposited and preserved at such altitudes on a fluvial profile, the whole concept of coastal onlap patterns derived from seismic sections and used to determine amplitude of eustatic change, is fundamentally flawed. In order to derive relative sealevel change from a stratal onlap pattern such as that shown in figure 3.4, it would be necessary to know details of the behaviour of the fluvial profile upon which the strata was deposited. Deducing such details from preserved fluvial stratigraphy may well prove impossible.

3.3.3 Definition of the tectonic hinge point, the equilibrium point, and the bayline

Many of the assumptions behind the depositional sequence stratigraphic model were not clearly stated by Vail *et al.* (1977a) or Posamentier *et al.* (1988) but are implicit in the

results that they described. The basic assumption that was clearly stated is that coastal onlap is controlled by an interaction of eustasy and tectonic subsidence, with sediment supply possibly acting as a modifying influence. This assumption lead to the definition of three key points on a depositional profile (Posamentier et al., 1988). These are the tectonic hinge point, the equilibrium point, and the bayline.

The hinge point was not strictly defined in the model, but appears to be the point on the model profile separating a tectonically subsiding profile surface from a tectonically uplifting profile surface. This assumed a simplistic tilting beam model for tectonic subsidence. The equilibrium point is defined as that point on the profile where the rate of eustatic change is equal to the rate of tectonic subsidence. The bayline is defined as the boundary on the model profile between fluvial sediments deposited above sealevel and deltaic and coastal plain sediments deposited at sealevel. These points are shown diagrammatically in figure 16 of Posamentier *et al.* (1988), summarised here in figure 3.15.

The movement of the points on the model profile through time in response to eustatic change, is assumed in the sequence stratigraphic model, to control the pattern of deposition of stratigraphy. For example, figure 18 in Posamentier *et al.* (1988) showed how onset of fluvial deposition should occur when the bayline and the equilibrium point were at the same position on the depositional profile.

3.3.4 Quantitative implementation of the tectonic hinge point, the equilibrium point, and the bayline

Attempting to implement the definition of the key points on the profile such as the equilibrium point and the bayline in the quantitative model is problematical. Tectonic subsidence in the model is calculated using a one or two-layer stretching model with the magnitude of subsidence dependent on the stretching factor, ß. Thus there is no direct

equivalent of the hinge point where subsidence passes laterally into uplift. This leads to problems quantifying the equilibrium point, since there is no persistent tectonic uplift in the model, so the equilibrium point cannot be landward of the hinge point during a eustatic rise. Although flexure produces uplift due to deposition and erosion, this uplift is not persistent, since its distribution and magnitude changes with each time step. Flexural effects do not produce a simple transition from subsidence to uplift across a hinge zone, and hence flexure cannot be used to define an equilibrium point in the way described by Posamentier *et al.* (1988).

There is also a problem with the respective rates of eustasy and tectonic subsidence. At the equilibrium point the rate of eustatic change is said to equal the rate of tectonic uplift or subsidence. However, a third order eustatic cycle typical of those shown by Haq *et al.* (1988) has an amplitude of, for example, 50m and occurs over a period of, for example, 1.0Myrs. This gives a rate of 5m/100Kyr model time step. With a stretching factor of 1.5, at 20Myrs since the onset of thermal subsidence, the rate of thermal subsidence is 1.54m/100Kyr. Increasing the stretching factor to 4.0 gives a rate of 3.43m/100Kyr. After 50Myrs, the rate of subsidence is reduced to 0.95m/100Kyr with a stretching factor of 1.5, and 2.08m/100Kyr with a stretching factor of 4.0. Thus using the McKenzie model of thermal subsidence (McKenzie, 1978) very high stretching factors are needed to maintain equilibrium with falling sealevel throughout a cycle of sealevel fall. Therefore, the conceptual sequence stratigraphic model is unrealistic in assuming that rates of tectonic subsidence can match rates of eustatic fall throughout a third order type cycle, especially on an old (20Myrs or longer since the end of the synrift phase) passive margin.

The concept of the bayline has been criticised by Miall (1991) which pointed out that the bayline concept implied that there was no slope on the delta top, which is obviously erroneous since streams on the delta top still need a gradient in order to flow seawards. Even if the gradients are small, they still exist. Thus, since it appears to be a flawed

concept, the bayline is ignored in the quantitative model. The fluvial equilibrium profile is graded to the sealevel datum at the shoreline.

These problems with quantifying elements of the depositional model described by Posamentier *et al.* (1988) which are stated to control onlap patterns stem from the non-quantitative nature of the model. Many aspects of the model appear only to have been formulated in diagrammatic form, and thus problems such as relative rates of eustasy and tectonic subsidence have not been adequately considered.

3.3.5 Controls on stratal onlap patterns

Figure 3.16 is a chronostratigraphic diagram showing stratigraphy generated over two cycles of absolute sealevel, which is equivalent to figure 3.17, taken from figure 18 of Posamentier *et al.* (1988). Comparing the two diagrams it is possible to reach some interesting conclusions regarding controls on stratal onlap. The main differences between the two diagrams are due to the shape of the fluvial profile and erosion of older chrons by the fluvial profile.

Timing of fluvial deposition

The most obvious discrepancy between the two depositional patterns (figures 3.16 and 3.17) is that in the sequence stratigraphic model, fluvial deposition is limited to the period between the highstand on the eustatic curve, and the inflexion point on the falling limb. During this time the equilibrium point and the bayline are in superposition, and it is this superposition that is assumed to cause fluvial deposition. In the quantitative model fluvial deposition is more complex, occurring on different parts of the fluvial profile, depending on the position on the absolute sealevel curve. During periods of rising absolute sealevel, when the beach is transgressive, or nearly stationary, deposition occurs along the length of the fluvial profile. During periods of falling absolute sealevel, when the beach is

regressive, deposition is restricted to the upper landward portion of the profile, and there is an area of non-deposition on the basinward section of the profile.

Although elements of the profile behaviour are unrealistic (see discussion in section 3.2.2), this result highlights the importance of the assumption in the sequence stratigraphic model that fluvial deposition only occurs on the lower portion of the profile, and only in response to falling eustatic sealevel which is controlling the addition of accommodation space. What is not considered is that more complex behaviour of the fluvial system may also create accommodation space for fluvial sediments. Such behaviour has to be understood before predictions of the type made by Posamentier and Vail (1988) can be shown to have true predictive power,

The importance of fluvial erosion

The second factor which the qualitative sequence stratigraphic model does not account for is the modifying effect of fluvial erosion on the pattern of stratigraphy. For example, the chronostratigraphic diagram in figure 3.16 shows that on the lower portion of the fluvial profile deposition of fluvial stratigraphy from chrons 10 to 19 is subsequently eroded by downcutting of the fluvial profile during the falling limb of the absolute sealevel curve. The section from the same model run in figure 3.18 shows that truncation of fluvial chrons by this process is very important in the pattern of stratal termination in the fluvial stratigraphy.

3.3.6 Timing of significant surfaces

In the type-1 sequence example in figure 3.4 the sequence boundary is defined at chron 15, at an E.M.T. of 1.5Myrs, since this is when subaerial erosion on the fluvial profile stops. Identifying other characteristics of a type-1 sequence boundary is difficult. There is no instant basinward shift of stratal onlap, only a gradual offlap from an E.M.T. of 1.0Myrs to

an E.M.T. of 2.0, which has subsequently been modified by fluvial and marine erosion. Stratal onlap commences at 1.9Myrs and continues until the end of the model run at 2.5Myrs.

This result is very significant to the sequence stratigraphic model for two reasons. The first is that it is assumed in that model in the way that the sequence boundary is defined, that fluvial erosion of the subaerially exposed shelf ceases before the onset of deposition of the lowstand systems tract. The sequence boundary is implied to be a single chronostratigraphic surface. This is not the case in the quantitative model. Fluvial erosion continues as long as absolute sealevel and hence base level continues to fall. Thus the sequence boundary as it is defined in the model is highly diachronous in the sense that it truncates stratigraphy of varying age and forms over several time steps. For example, in figure 3.4, the sequence boundary cuts chrons 1 to 13 (0.1 to 1.3Myrs E.M.T.) and forms over a period of 0.9Myrs. Hence accurate correlation between sequence boundaries, if they formed in this way, would be very difficult, since they actually represent quite prolonged periods of time in their formation.

This leads to the second point which is that it is the lowest point of absolute sealevel on the sealevel curve, not the inflexion point, which is significant in this model. Thus, the rate of absolute sealevel change is not the crucial control, but the lowest point on the sealevel curve. This point is demonstrated in figure 3.4. Fluvial erosion creating a subaerial unconformity, with sediment bypassing, continues until chron 15, at the low point on the absolute sealevel curve. Hence the timing of the sequence boundary is controlled by the low point on the absolute sealevel curve, not the inflexion point. This same point applies to the maximum flooding surface, which is shown to occur at the inflexion point in Posamentier *et al.* (1988) (figure 3.17). The time of maximum flooding in the quantitative model occurs at some time between the inflexion point and the highest point on the absolute sealevel curve (e.g. chron 23 in figure 3.4), depending upon the magnitude of

sediment supply. This complicates the interpretation and hence correlation of maximum flooding surfaces.

The digital nature of the quantitative model and the weaknesses with the geometrical profile approach makes it difficult to assess the significance of these results regarding the timing of the formation of surfaces. The sequence stratigraphic depositional model notes the importance of the balance between different processes with regard to the creation and filling of accommodation space, but since it is entirely qualitative, it is not possible to fully assess the significance of this balance with that model. Using a quantitative model to test this concept is also difficult, since the results may well be influenced by the length of the time step chosen. However, it seems safe to conclude that the assumption within the sequence stratigraphic depositional model as described by Posamentier *et al.* (1988) and Posamentier and Vail (1988) of the timing of sequence boundaries and maximum flooding surfaces at inflexion points in an absolute sealevel curve, should be treated with extreme caution until it can be tested further.

3.4. Sensitivity Tests - Alternative controls on sequence geometry

The following sections show results from the model run with the initial conditions described in section 3.2.1 plus the addition of an extra factor such as flexure, variable sediment supply, or a different fluvial profile geometry. The purpose of these model runs is to establish the degree of relative control that absolute sealevel variations, sediment supply, flexure and fluvial profile geometry exert over the model stratigraphy.

3.4.1 Flexure

The standard model parameter set described in section 3.2.1 has an infinitely rigid lithosphere which does not respond to sediment loading or unloading due to erosion. In order to test the importance of flexure on the standard results shown in figure 3.3, and 3.4,

the model was run with a constant value for Te of 10km. The value of Te is also constant along the length of the model profile, so potential changes in strength of the lithosphere across the hinge zone are ignored. All the other parameters and initial conditions where the same as those for the standard model run.

Figure 3.19 shows the section from the model run with flexure included. The pattern of stratigraphy is basically similar to that of the standard model run. There are two noticeable differences.

- More of the seaward end of the fluvial profile is preserved with the addition of flexure (i.e. chrons 10 to 15). This is due to flexural subsidence creating a few metres more accommodation space and thus keeping the stratigraphy below falling absolute sealevel so that it cannot be eroded by the fluvial profile.
- The beach moves further landward during the transgression when absolute sealevel is rising. This is also due to flexural subsidence depressing the lower portion of the fluvial profile and thus allowing the shoreface to move further landward.

Both of these differences in the stratigraphic pattern are also clearly visible in figure 3.20 which is the chronostratigraphic plot, absolute sealevel curve and stratal onlap curve from the model run with flexure included. Although the timing of the sequence boundary (positioned on the basis of the resumption of fluvial deposition on the lower fluvial plain) is different in figure 3.20, occurring at chron 16 rather than chron 15 in the standard model run, the difference is not particularly significant, since it is caused by very small changes in elevation caused by flexural uplift and subsidence.

Despite the small differences described, the overall pattern of model stratigraphy is very similar. The influence of absolute sealevel change is still clearly visible on the stratigraphic pattern. For example, the period of stratal onlap from 1.9Myrs E.M.T. to 2.5Myrs E.M.T. is very similar in both runs. Thus it can be concluded that in the model flexure is of secondary importance when compared to changes in absolute sealevel.

3.4.2 The geometry of the fluvial profile

The geometry of the fluvial profile has not previously been considered a major control on sequence geometry in the sequence stratigraphic model. Although Posamentier *et al.* (1988) and Posamentier and Vail (1988) consider fluvial response to base level change using the concept of fluvial equilibrium profiles, they do not attempt to quantify such profiles, which is a necessary step in order to understand their significance to, and control upon stratigraphy. Even though the geometrically defined profile used here produces some unrealistic features, it still represents an advance over the purely qualitative profile geometries used by Posamentier *et al.* (1988).

In the standard model run described in section 3.2.1. the complementary error function parameter used to model the fluvial profile is 2.0 (see section 2.6.5.2). The effects of decreasing the value of this length scale to 1.2 can be seen in figure 3.21 and 3.22. The model section in figure 3.21 demonstrates how a less concave profile creates more accommodation space for fluvial sediment (see figure 3.23) and hence prevents much fluvial erosion, even during the 40m drop in absolute sealevel from 0.5Myrs to 1.5Myrs E.M.T. The stratigraphic pattern produced is actually more like a type-2 sequence than the type-1 example shown in figures 3.3 and 3.4.

Figures 3.24 and 3.25 show the standard model run modified to include a more concave fluvial profile with a length scale of 2.8. This, like the less concave profile, appears to be a first order control on the model stratigraphy. In the model section in figure 3.24 the thickness of the preserved fluvial stratigraphy is slightly less than that in the standard model, and the beach has moved further landward during the transgression from 1.7 to 2.5Myrs E.M.T. This movement of the beach and the altered pattern of fluvial erosion and deposition can also be seen on the chronostratigraphic diagram in figure 3.25. The stratigraphic gap below the sequence boundary, produced by increased erosion and

reduced deposition on the more concave profile as absolute sealevel has dropped, is wider and more prolonged. Once again, as with the flexural example, the timing of the sequence boundary has been slightly altered, this time as a result of the more concave profile continuing to erode for one time step longer than in the standard model.

These results demonstrate that the geometry of the fluvial profile is a first order control on stratigraphy in the model, along with thermal subsidence and changes in absolute sealevel. The degree to which this is true in actual natural systems is difficult to determine. The main weakness in the assumption of the fluvial profile geometry is the lack of a direct link to observable fluvial processes, and the unrealistic nature of some of the profile behaviour. However, despite these important weaknesses, it still seems reasonable to conclude from these results that the quantitative model demonstrates the importance of the fluvial profile behaviour to the resulting stratigraphic patterns, and hence to the use of the sequence stratigraphic depositional model as a predictive tool.

3.4.3 The sediment partitioning coefficient

In the standard model run the sediment partitioning coefficient (see section 2.5.7) was set to 0.5, so that 50% of the available sediment was deposited on the fluvial portion of the model profile, and the second 50% was deposited on the marine portion of the profile, which is made up of the shoreface, the shelf and the marine slope. Since this parameter controls both the distance of fluvial progradation and the magnitude of sediment supplied to the marine portion of the model profile, it will act as an important control on model stratigraphy.

To test this possibility, the model was run with the parameters and initial conditions as described in section 3.2.1, except that the partitioning coefficient was reduced from 0.5 to 0.2. The results from this model run can be seen in figures 3.26 and 3.27. The section in figure 3.26 shows the much wider shelf deposits developed because of the increased

sediment supply to the sea, and the much reduced fluvial deposits caused by the increased bypassing of sediment through the fluvial system. The chronostratigraphic diagrams in figure 3.27 also shows the differences in marine and fluvial deposition and erosion. In particular, more of the previously deposited fluvial stratigraphy has been eroded than in the standard model (e.g. a wider band of erosion in chrons 1 to 6), because of the different fluvial profile geometry caused by reduced fluvial progradation. This has lead to increased erosion on the upper profile during a relative sealevel rise, which is probably unrealistic, and should be noted when interpreting this model result.

To contrast with the low partitioning coefficient, figures 3.28 and 3.29 show results from the model run with a higher value of 0.8. The effect on the stratigraphy is to increase fluvial progradation so that little or no shoreface and shelf are produced. The pattern of fluvial stratigraphy shown in the chronostratigraphic diagram is very similar to that in the standard model, except that stratal onlap is less well developed. This is due to the increased fluvial deposition competing with the absolute sealevel rise and reducing the distance of transgression, and hence the production of stratal onlap on the fluvial profile.

These results suggest that the degree of sediment partitioning between fluvial and marine portions of a basin is an important control on stratigraphy in the model. Very different patterns of erosion and deposition are produced depending on the value of the partitioning coefficient chosen. It seems likely that the same could be true of a real system. A lack of sediment being deposited on the shelf is taken in the sequence stratigraphic model to be indicative of a time of transgression. However, it may be possible that other things, independent of eustasy, such as climatic variations affecting drainage basin development, could control partitioning. If more sediment were being trapped in the drainage basin and the coastal plain, due to a decrease in the transport capability of the drainage basin, possibly due to a change, for example, to a more arid climate, the partitioning coefficient would change. This possibility could lead to phenomenon such as condensed sections being misinterpreted within a eustatic framework.

3.4.4 Variable sediment supply

In the standard model run the sediment supply is kept constant at 1.0km^2 per time step. In order to investigate the significance of variations in sediment supply, the model has been run with a number of different sediment supply configurations.

Figure 3.30 and figure 3.31 were produced by the model running with the standard parameters and initial conditions, except that sediment supply was reduced to 0.5km^2, and held constant at that value. The reduced sediment supply increases the incidence of fluvial erosion so that little fluvial stratigraphy is preserved from before 1.5Myrs E.M.T., and causes the beach to move approximately 70km further landward during the transgression from 1.5 to 2.5Myrs E.M.T. This movement of the beach produces a marine ravinement surface which is clearly visible on the section in figure 3.30, and on the chronostratigraphic diagram in figure 3.31. The enhanced landward movement of the beach and the production of the ravinement surface are both due to the shift in balance from fluvial progradation to landward shoreface retreat, due in turn to the reduced sediment supply.

Increasing the sediment supply to 1.5km^2 per time step has the opposite effect, shifting the balance to fluvial progradation. The impact of this on the stratigraphy is to increase the distance of basinward progradation of the sediment wedge. This is shown in figures 3.32 and 3.33. Despite this increase in the distance of progradation, the overall pattern of erosion, deposition, and the movement of the shoreline is very similar to the standard model.

It can be concluded from these two model runs that reducing sediment supply has a more pronounced effect on the pattern of stratigraphy in the model than increasing sediment supply. If this is true in real systems, the implications are important. Sediment supply could be reduced independently of eustatic sealevel rise by, for example, climatic effects

such as a reduction in rainfall. Reduced sediment supply during an absolute sealevel rise might accentuate features such as transgressive ravinement surfaces and condensed sequences. Such effects could easily be misinterpreted as due to eustatic effects within a sequence stratigraphic framework of interpretation.

The previous two model runs held sediment supply constant throughout the duration of the run. The sequence stratigraphic depositional models (Posamentier *et al.* 1988; Posamentier and Vail, 1988; Van Wagoner et al., 1990) all assume constant sediment supply, but state that when studying any particular example of stratigraphy, the effects of variable sediment supply should be accounted for before the models are applied. No indication is given as to how this can be achieved. One possibility is to begin by studying the effects of variable sediment supply in a stratigraphic forward model.

The following three model runs all have variable sediment supply. The sediment supply curves have either a saw-tooth or a sinusoidal geometry and areas eroded on the fluvial and marine profiles were not added to the total available for deposition. The saw-tooth and sinusoidal curves could be considered to represent changes in sediment supply due to factors such as drainage basin morphology, point-source switching, climatic change or tectonic effects, or combinations of all three. The saw-tooth curves particularly may be analogous to sudden changes in sediment supply due to point-source switching.

Figures 3.34 and 3.35 show model output with sediment supply varying in a saw tooth pattern. The curve (figure 3.31) has a period of 1.6Myrs; sediment supply starts at $0.1km^2$ per time step, and increases to $1.0km^2$ at 1.6Myrs E.M.T. before returning to $0.1km^2$ at 1.7Myrs E.M.T. The solid red and green lines show the area of fluvial and marine stratigraphy deposited respectively, and the blue line is the combined total of the two. The dotted lines represent the areas eroded on the fluvial and marine profiles and can be ignored.

The effect of the sudden reduction in sediment supply at 1.7Myrs E.M.T. is quite striking (figures 3.34 and 3.35). The shoreline immediately begins to retreat landward, reversing the previous progradational trend. This is partly due to the rise in absolute sealevel from 1.5 to 2.5Myrs E.M.T., but the movement is exacerbated by the sudden reduction in sediment supply. Most of the fluvial stratigraphy prior to chron 16 is eroded by the sudden jump in the shape of the fluvial profile, and by a marine ravinement surface produced by the transgression, though the fluvial erosion should be disregarded since it is probably an unrealistic fluvial response to absolute sealevel rise.

Figures 3.36 and 3.37 show the effects of using a saw-tooth sediment supply curve also with a period of 1.5Myrs, but with supply decreasing from 1.0km^2 to 0.1km^2 per time step during each period. This is thus a rapid rise-slow fall type of curve. The impact of the change in sediment supply at 1.5Myrs E.M.T. is much less noticeable. Two effects are visible, particularly on the chronostratigraphic diagram in figure 3.37.

- A decrease in the distance of progradation in chrons 10 to 15 due to decreasing sediment supply.
- An increase in the spatial distribution of fluvial and marine erosion of stratigraphy in chrons 1 to 10. This is caused in part by profile shortening when the beach jumps landward at chron 16 (and thus should be disregarded as unrealistic), and by an increase in fluvial erosion on the lower fluvial profile during the period of low absolute sealevel due to the reduced fluvial progradation.

Overall, however, the differences between this model run and the standard model run are much less striking than the previous example. This is due mostly to the timing of the change in sediment supply. Low sediment supply during the rising limb of the absolute sealevel curve has a far more pronounced effect on the stratigraphy than low sediment supply during the falling limb. Conversely, high sediment supply during the transgression reduces the effect of the transgression by providing sediment for fluvial progradation, and maintains more closely the pattern of stratigraphy seen in the standard model.

The third model run with varying sediment supply uses a sinusoidal curve with a period of 2Myrs and an amplitude of $1km^2$. Figures 3.38 and 3.39 show the model output for this run. Most of the differences in the stratigraphic pattern, such as the lack of fluvial deposition in chrons 10 to 15, from 1.0 to 1.5Myrs E.M.T., slightly more landward movement of the shoreline from 0.0 to 0.5Myrs and 1.5Myrs to 2.5Myrs, and a different stratal onlap pattern in chrons 19 to 25, from 1.9 to 2.5Myrs, can be attributed to the low sediment supplies at 0.1Myrs, 1.2Myrs and 2.5Myrs E.M.T.

3.4.5 Variable sediment supply and constant absolute sealevel

From figures 3.34 and 3.35, produced with the model using a saw-tooth sediment supply curve, it is apparent that a sudden reduction in sediment supply may be a major control on sequence development. In that example, significant portions of the stratigraphy were eroded during erosional shoreface retreat due to the sudden drop in sediment supply combined with rising absolute sealevel. Figures 3.40 and 3.41, therefore, show the effects of running the model with the same saw-tooth sediment supply curve, but with absolute sealevel constant at 0m, and with a higher magnitude of thermal subsidence (stretching values from 1.0 to 8.0) which can act to preserve more of the stratigraphy eroded in the previous example.

The pattern of stratigraphy is in some respects very similar to that shown in figures 3.11 and 3.12 from the model run which attempted to reproduce the salient elements of a type-2 depositional sequence. The sudden drop in sediment supply at 1.7Myrs E.M.T. causes the shoreline to move rapidly landwards as would be expected in a transgressive systems tract. This is followed by fluvial progradation analogous to that seen in highstand systems tracts. The important point is that there is no change in absolute sealevel during the model run, only a constant rate of rise in relative sealevel. Thus, within the model, variable sediment supply can produce patterns of stratigraphy similar to those created by variable absolute

sealevel. This is an unequivocal demonstration of the uniqueness problem as it applies to the sequence stratigraphic depositional model.

It should be noted, however, that in this model at least, a change in sediment supply cannot cause the vertical juxtaposition of fluvial stratigraphy over marine stratigraphy, separated by a surface of subaerial erosion. This is one of the prime features of a type-1 sequence, and it is very difficult to see how such a feature can occur without at least relative sealevel fall. So although the uniqueness problem is important with respect to controls on stratigraphy and the sequence stratigraphic depositional model, it should be noted that some patterns of stratigraphy are more tightly constrained in their possible causes than others.

3.4.6 Combined controls

The deposition and erosion of stratigraphy in a real sedimentary basin is probably controlled by a variety of complex, often interacting controls each with a varying degree of importance to the resulting stratigraphy. Most models, whether quantitative or qualitative, attempt to simplify this situation down to one or two controls which may or may not interact (e.g. tectonic subsidence and eustasy in the sequence stratigraphic depositional model described by Posamentier *et al.* (1988) and Van Wagoner *et al.* (1990); thermal subsidence and flexure, Watts (1982)). This is often necessary in order to keep the model simple enough to be useful, especially in qualitative models. This means that to a large extent, the effect of the interaction of several different controls on stratigraphic patterns has not been investigated. Such simplification, however, may lead to misconceptions regarding the apparent simplicity of stratigraphic systems, and the importance of the uniqueness problem when using models, both quantitative and qualitative.

Figure 3.42 is a section from the model run for 10Myrs E.M.T., generating 100 chrons. The absolute sealevel curve used in the model run is a combination of a 2Myr, 20m curve

superimposed on a 15Myr 100m amplitude curve. The sediment supply curve is a sinusoidal curve, with a 1.6Myrs period, and an amplitude of 0.5km^2. The partitioning coefficient is varied through time according to a curve with a period of 1.4Myrs and a range from 0.2 to 0.8. Flexure is included in this model run, with a laterally and temporally constant value of Te of 10km. Other parameters and initial conditions are the same as those for the standard model.

The section from this model run (figure 3.42) demonstrates the complexity of the stratigraphy produced. There are several sequences visible, and the pattern of stratal onlap, truncation, offlap and downlap can be seen to be complex. Some of this pattern is produced by absolute sealevel change. Other aspects are caused by variable sediment supply, and the stratigraphy is modified by flexure. Figure 3.43 shows the chronostratigraphic diagram, absolute sealevel curve and sediment supply curve for the model run. The influence of absolute sealevel changes on the stratigraphy are readily apparent, but only through reference to the sealevel curve and sediment supply curve together is it possible to fully explain particular stratigraphic patterns.

For example, the pronounced transgressive ravinement surface at chron 62 (6.2Myrs E.M.T.) and the shift in the stratal onlap and downlap pattern may easily be misinterpreted to be due to a absolute change in sealevel alone, whereas it is actually due to a combination of rising absolute sealevel and reduced sediment supply. Accurately interpreting such a feature observed in ancient stratigraphy would be considerably more difficult, especially if insufficient consideration was given to the contribution of sediment supply, leading to an over-emphasis on the role of absolute sealevel change.

Consequently, these model results suggest again that the uniqueness problem is very important when considering such stratigraphy influenced by various controls. While one may be able to explain a particular feature, as due, for example, to eustasy, it is important

always to consider that this is unlikely to be a unique solution. Other controls could be responsible, or at least important.

3.5 Summary

The sequence stratigraphic depositional model makes detailed predictions regarding the geometry of stratigraphy preserved in sedimentary basins, on the basis of a series of assumptions, foremost of which is that a combination of eustasy and tectonic subsidence are the primary controls on stratigraphy. The model is entirely qualitative, and many of the assumptions behind it have been insufficiently investigated and tested. The quantitative forward model presented here has been used to test some of these assumptions and to investigate some possible alternative controls on stratigraphy.

1. The quantitative forward model can reproduce the general geometry of type-1 and type-2 sequences, but cannot reproduce some details such as particular aggradational parasequence set stacking patterns which require very specific distributions of accommodation space.

2. Calculation of the amplitude of absolute sealevel changes from coastal onlap patterns may be greatly complicated by the geometry of the fluvial profile.

3. The concepts of the hinge point and the equilibrium point used in the sequence stratigraphic model are flawed.

4. Flexure is not a first order control on the model stratigraphy when absolute sealevel is varied.

5. The behaviour of the fluvial profile is a first order control on model stratigraphy. For example, a less concave profile produces a stratigraphic pattern very different from that

produced by a more concave profile. Despite the weaknesses of the geometrical implementation of profile evolution through time, the model results suggest that profile geometry will be very a significant control in natural systems.

6. The sediment partitioning coefficient is also a first order control in the model, and the effects of sediment partitioning in stratigraphic systems could conceivably be misinterpreted to be due to eustasy.

7. Variable sediment supply is a first order control on model stratigraphy, and has a particularly pronounced impact on the stratigraphic pattern when sediment supply is low during a time of rising absolute sealevel.

8. Variable sediment supply alone, without any contribution from variable absolute sealevel, is capable in the model of producing stratigraphic patterns in some ways similar to those seen in type-2 sequences. This suggests that stratigraphy influenced by variable sediment supply due to factors such as point source switching, climatic changes, drainage basin morphology, or combinations of these, could in limited circumstances be misinterpreted as being due to eustasy alone. However, it should be noted that the model cannot reproduce the vertical juxtaposition of fluvial and marine stratigraphy across a subaerial erosion surface without a relative sealevel fall.

9. Combined complex controls on stratigraphy should not be underestimated in terms of the potential difficulty in correctly interpreting the results in the ancient record. A model run with combined controls is difficult to interpret, even given the simplicity of the model, and the availability of the complete details of all the model parameters, such as the absolute sealevel curve, and the sediment supply curve.

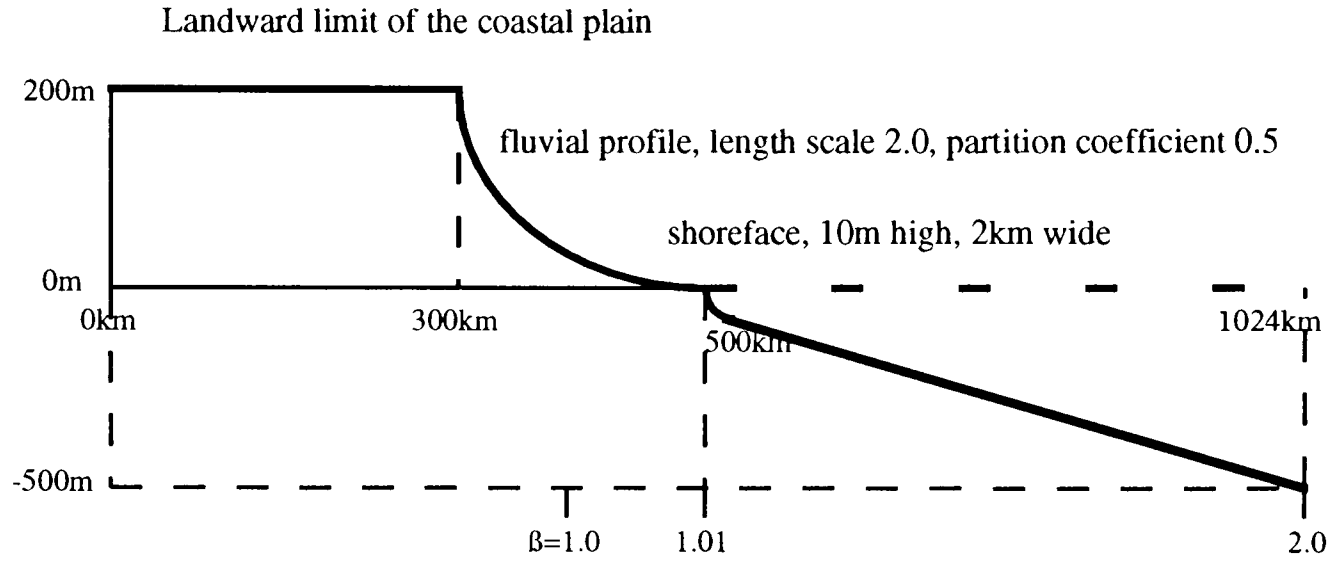

Sediment supply : Constand at 1.0sq.km

Absolute sealevel datum : Sinusoidal curve, 20m amplitude, 2Myr period

Figure 3.1 The initial conditions for the standard type-1 sequence model run

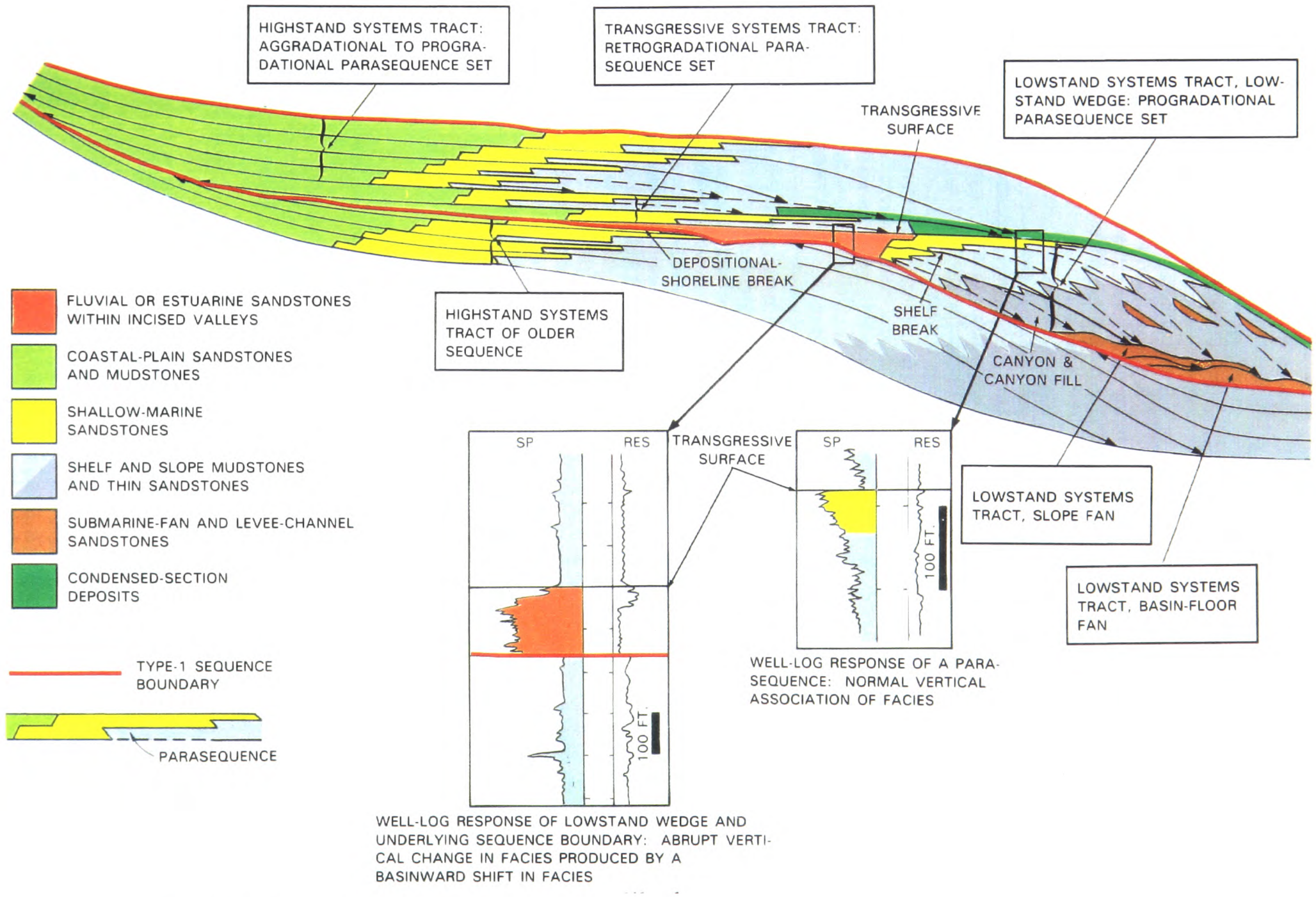

Figure 3.2 The depositional sequence stratigraphic model of a type-1 sequence, from Van Wagoner *et al.* (1990).

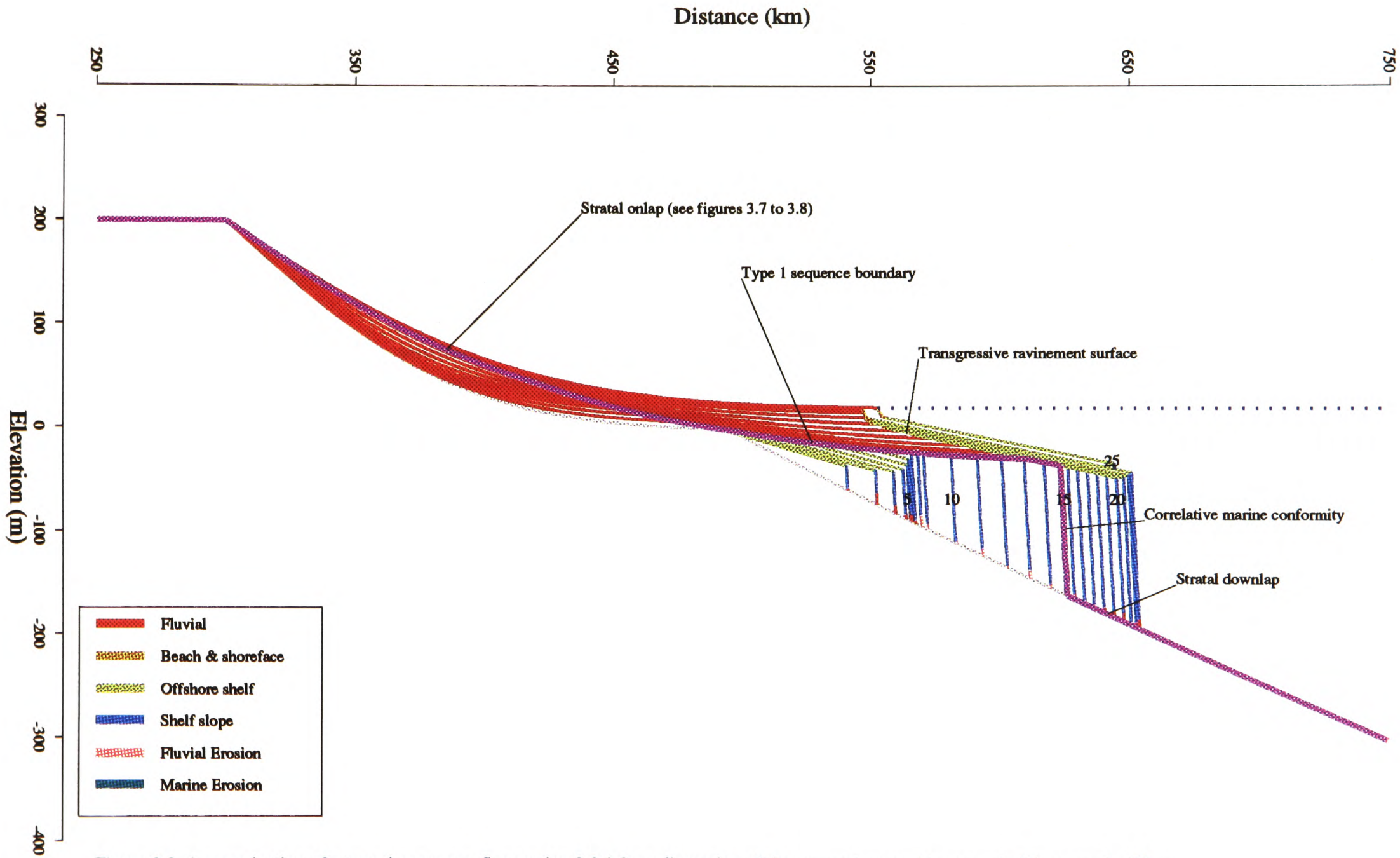

Figure 3.3. A reproduction of a type-1 sequence. See section 3.2.1 for a discussion of the parameters used to generate this example. Many of the features observable in this example are directly comparable with features of the depositional sequence stratighraphic model described, for example, by Van Wagoner et al. (1988). The thicker purple line marks the position of the type 1 sequence boundary. This model run forms the standard reference for the subsequent model runs throughout the rest of chapter 3.

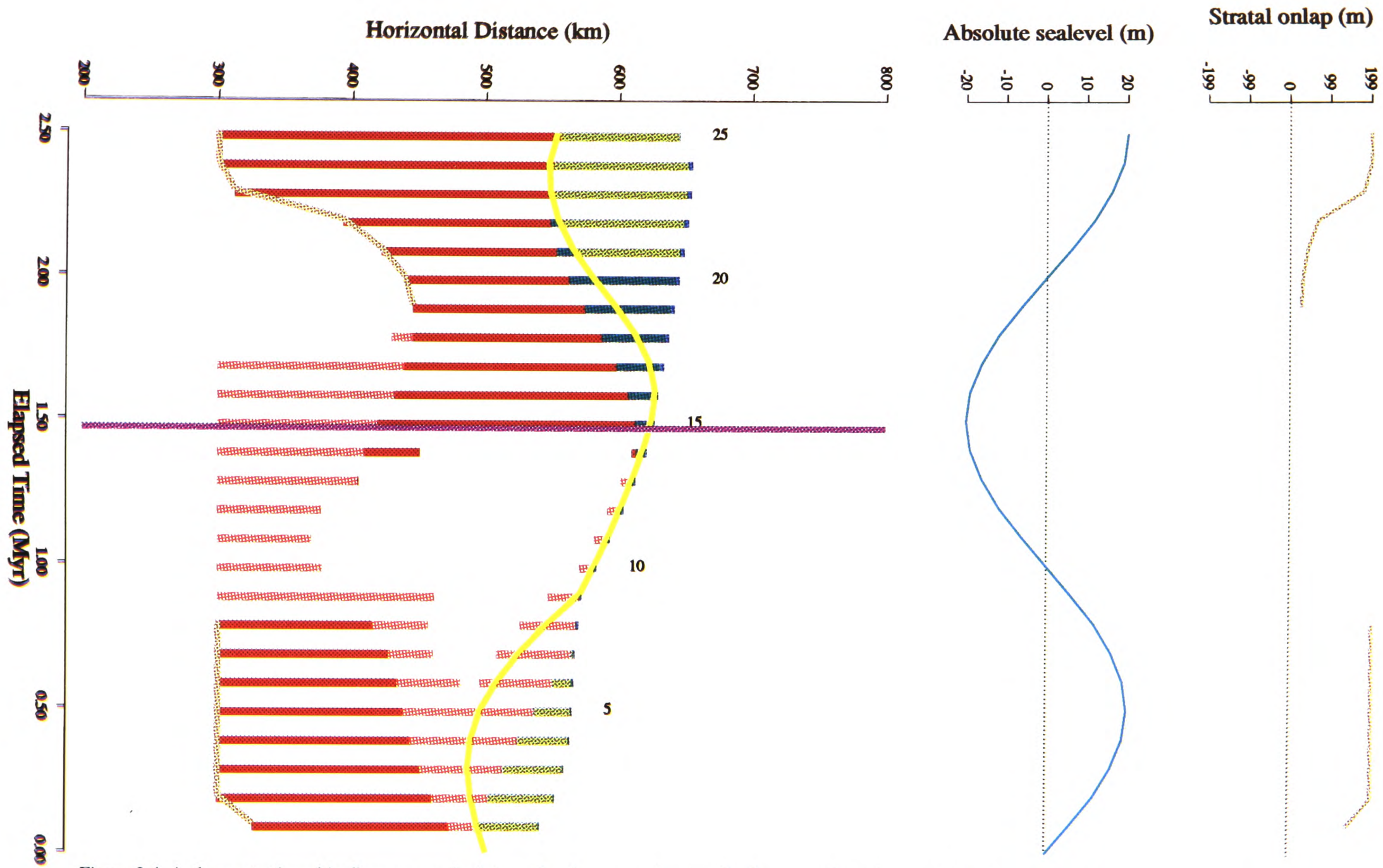

Figure 3.4. A chronostratigraphic diagram, an absolute sealevel curve, and a stratal onlap curve from the standard reference model run. The pattern of stratigraphy is analagous to the type-1 sequence described, for example, by Van Wagoner et al. (1988). The forcing of the stratigraphic pattern by changing absolute sealevel is clearly apparent. The choice of timing for the sequence boundary is described in section 3.3.6.

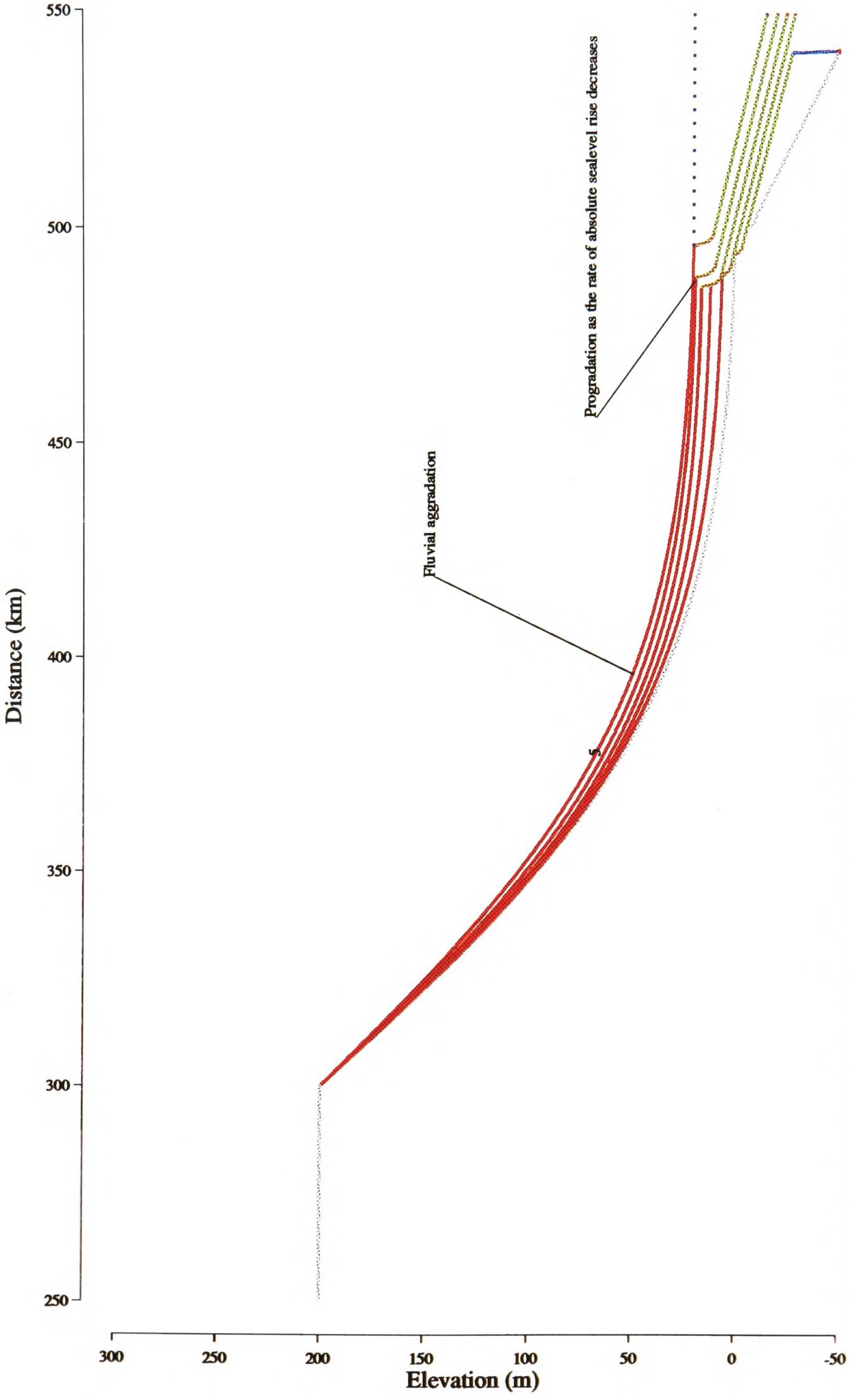

Figure 3.5. An enlargement of the area of fluvial deposition after the first 5 chrons (0.5Myrs E.M.T.) from the standard reference model run. The profile shows aggradation along most of its length in response to the rise in absolute sealevel. Note how progradation of the beach started at chron 4 in response to the decreasing rate of sealevel rise.

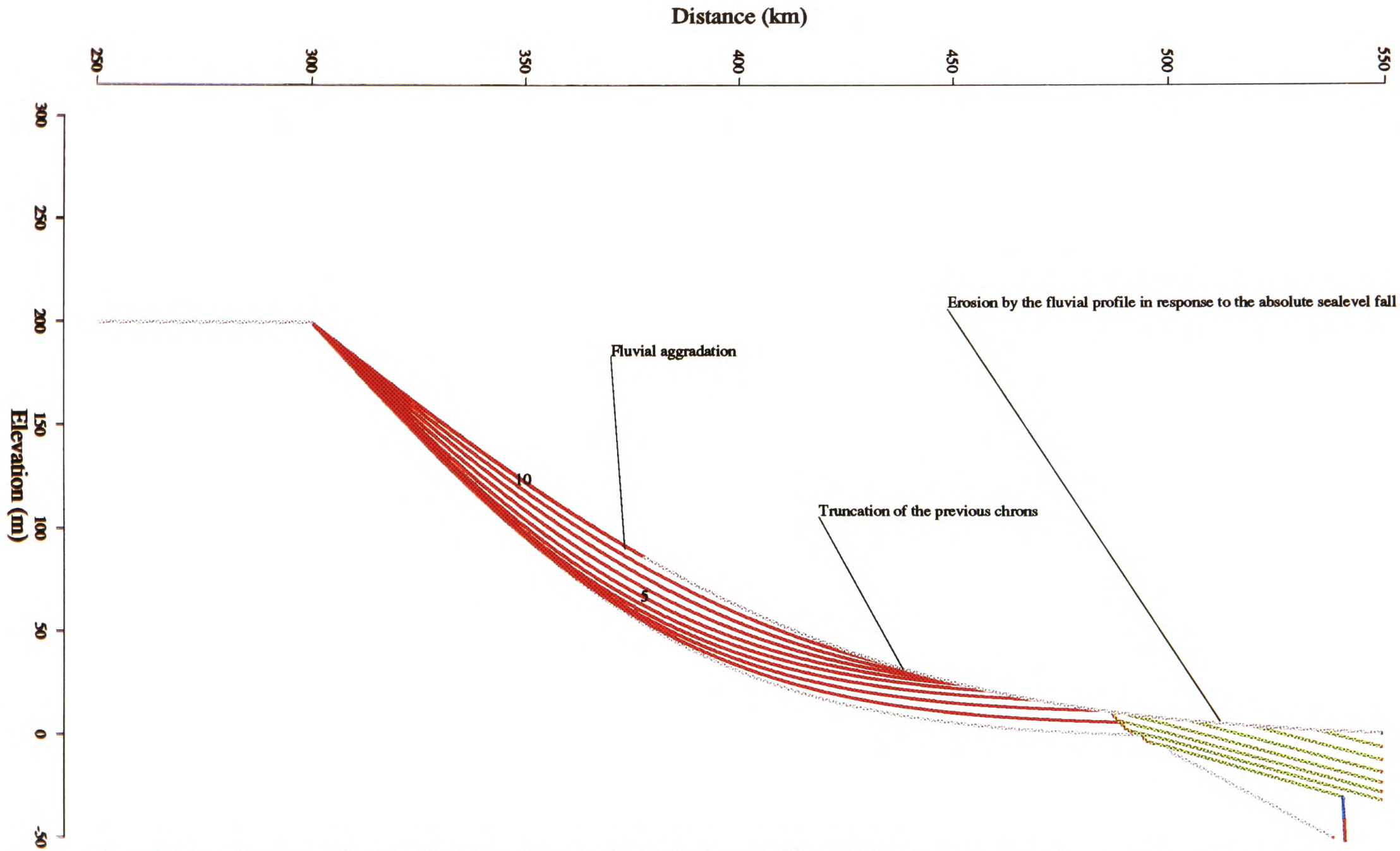

Figure 3.6. An enlargement of the area of fluvial deposition after the first 10 chrons (1.0Myrs E.M.T.) from the standard reference model run. The profile shows the formation of the erosion surface as the fluvial profile responds to the fall in absolute sealevel. Note the laterally limited aggradation on the upper part of the profile caused by profile lengthing in turn forced by falling absolute sealevel.

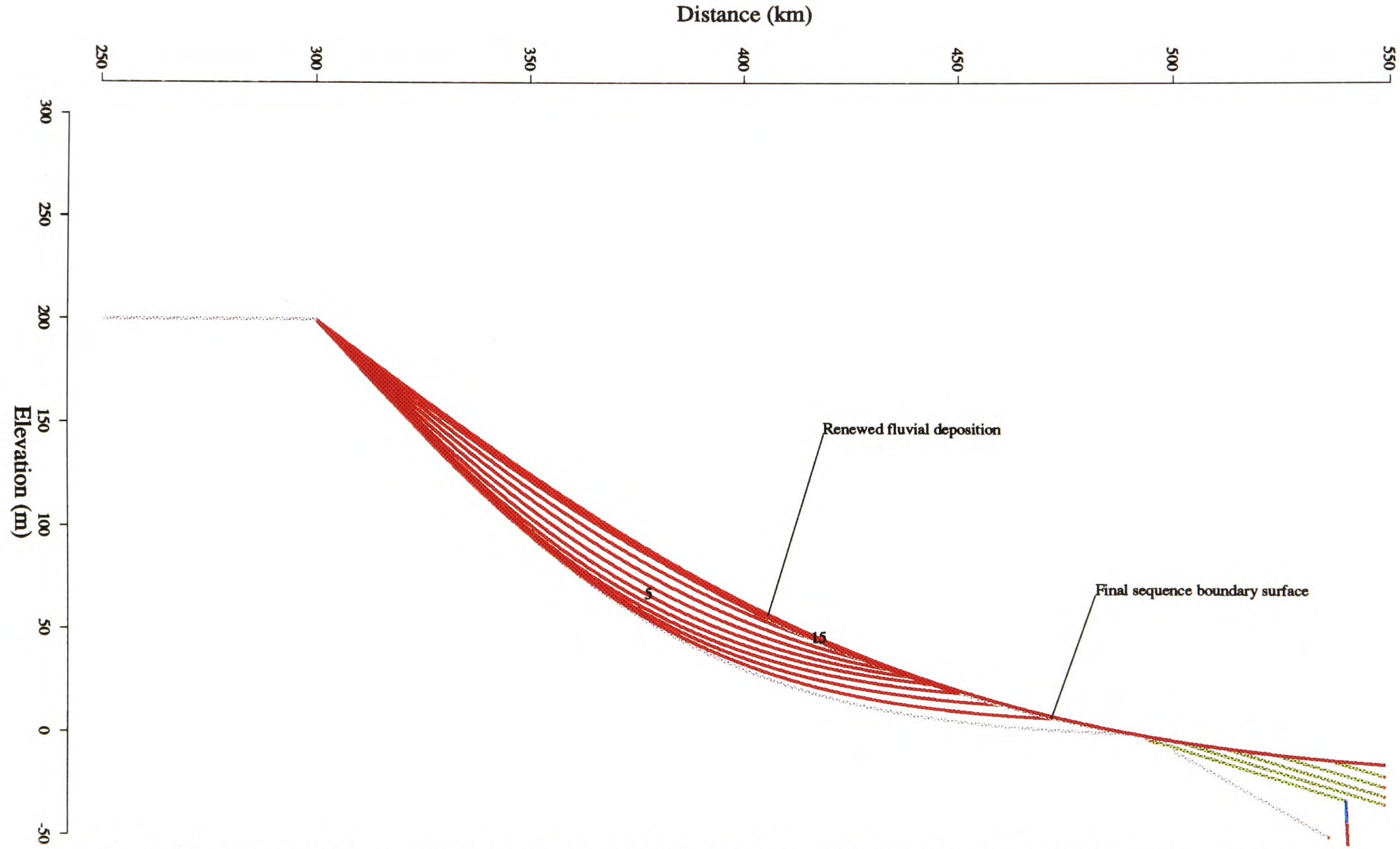

Figure 3.7. An enlargement of the area of fluvial deposition after the first 15 chrons (1.5Myrs E.M.T.) from the standard reference model run. The profile shows the final development of the erosion surface which forms the sequence boundary. By chron 15 deposition of fluvial sediment above this sequence boundary chron has commenced.

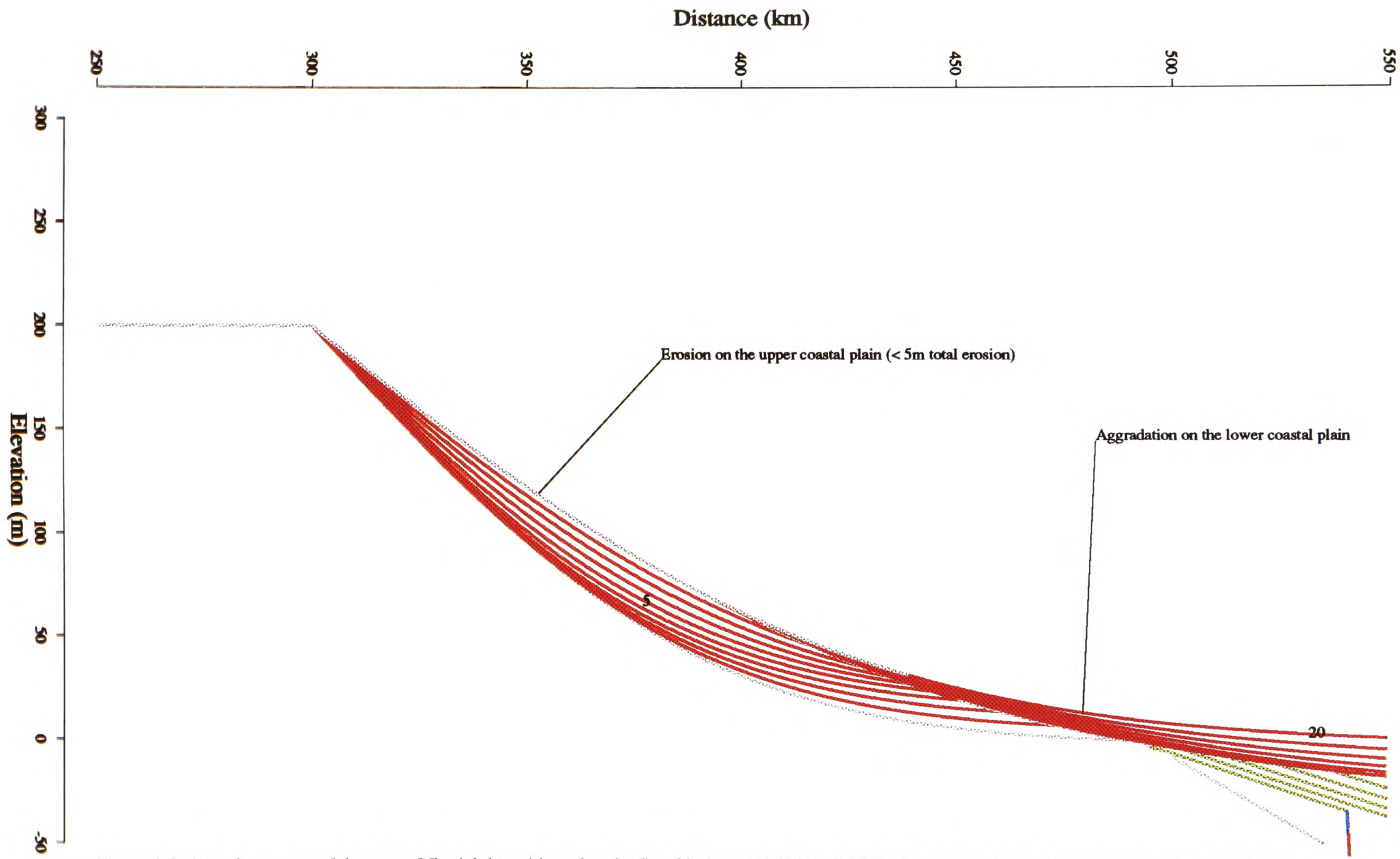

Figure 3.8. An enlargement of the area of fluvial deposition after the first 20 chrons (2.0Myrs E.M.T.) from the standard reference model run. The profile shows the aggradation on the lower profile due to rising absolute sealevel, and the erosion on the upper profile due to profile shortening also forced by the absolute sealevel rise. Note that this erosion only removes a few metres of fluvial stratigraphy.

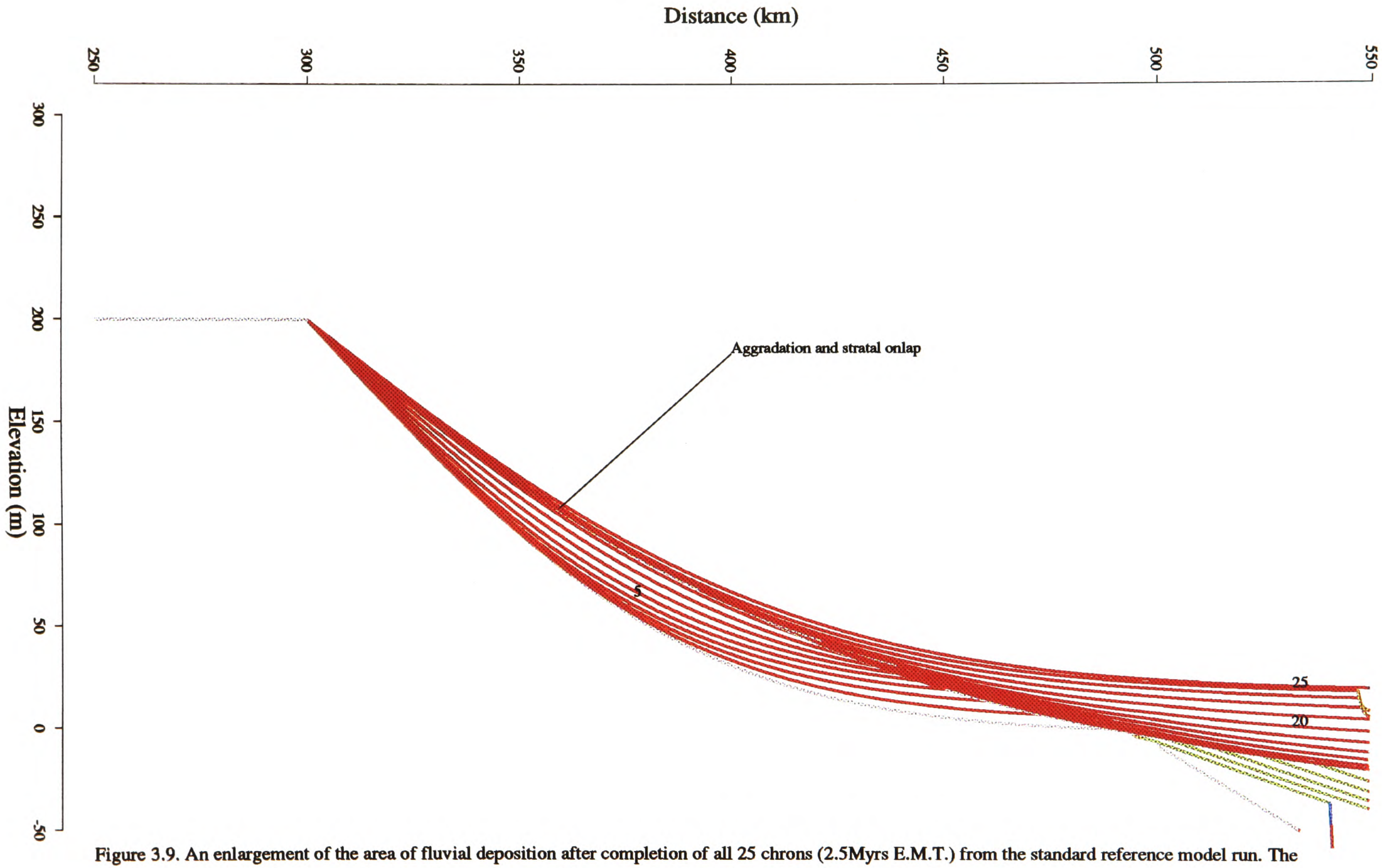

Figure 3.9. An enlargement of the area of fluvial deposition after completion of all 25 chrons (2.5Myrs E.M.T.) from the standard reference model run. The profile shows the stratal onlap produced on the upper part of the profile by the final absolute sealevel rise.

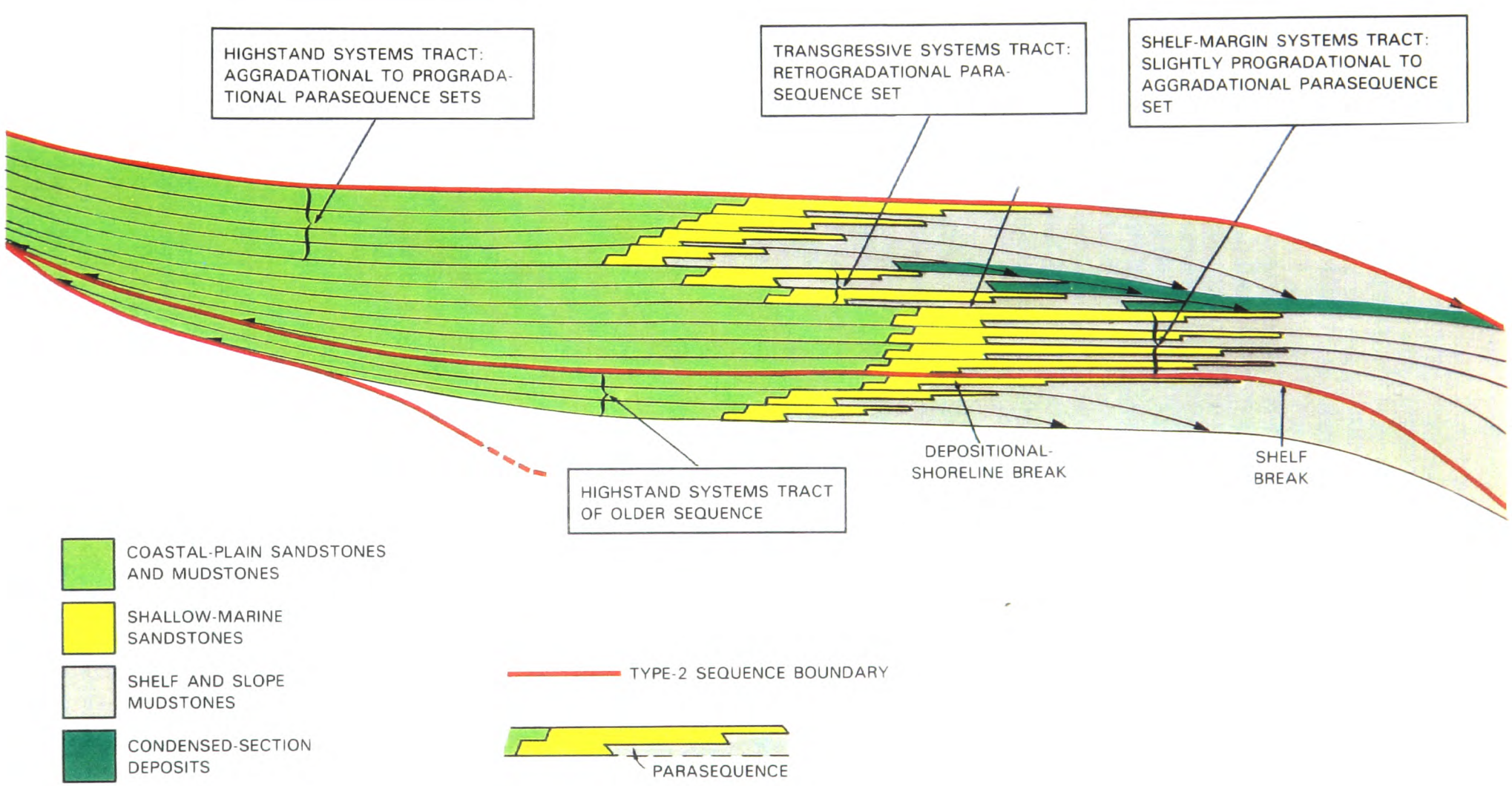

Figure 3.10 The depositional sequence stratigraphic model of a type-2 sequence, from Van Wagoner *et al.* (1990).

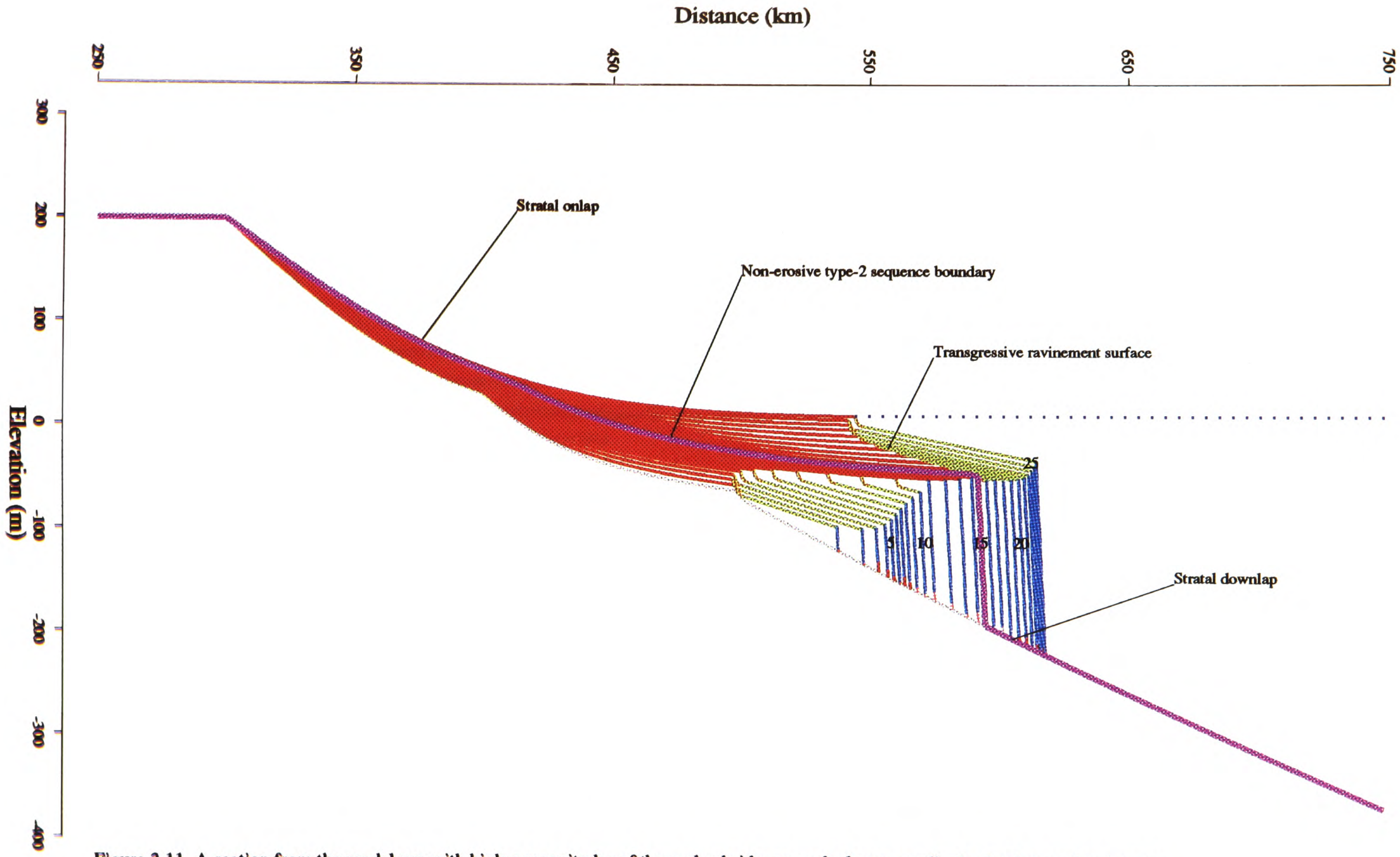

Figure 3.11. A section from the model run with higher magnitudes of thermal subsidence, and a lower amplitude absolute sealevel curve, both chosen to reproduce some of the features of a type-2 sequence. All the other parameters for this model run are the same as those for the standard reference model. Note that with the higher subsidence and reduced magnitude of absolute sealevel change the fluvial profile is no longer erosive during falling absolute sealevel.

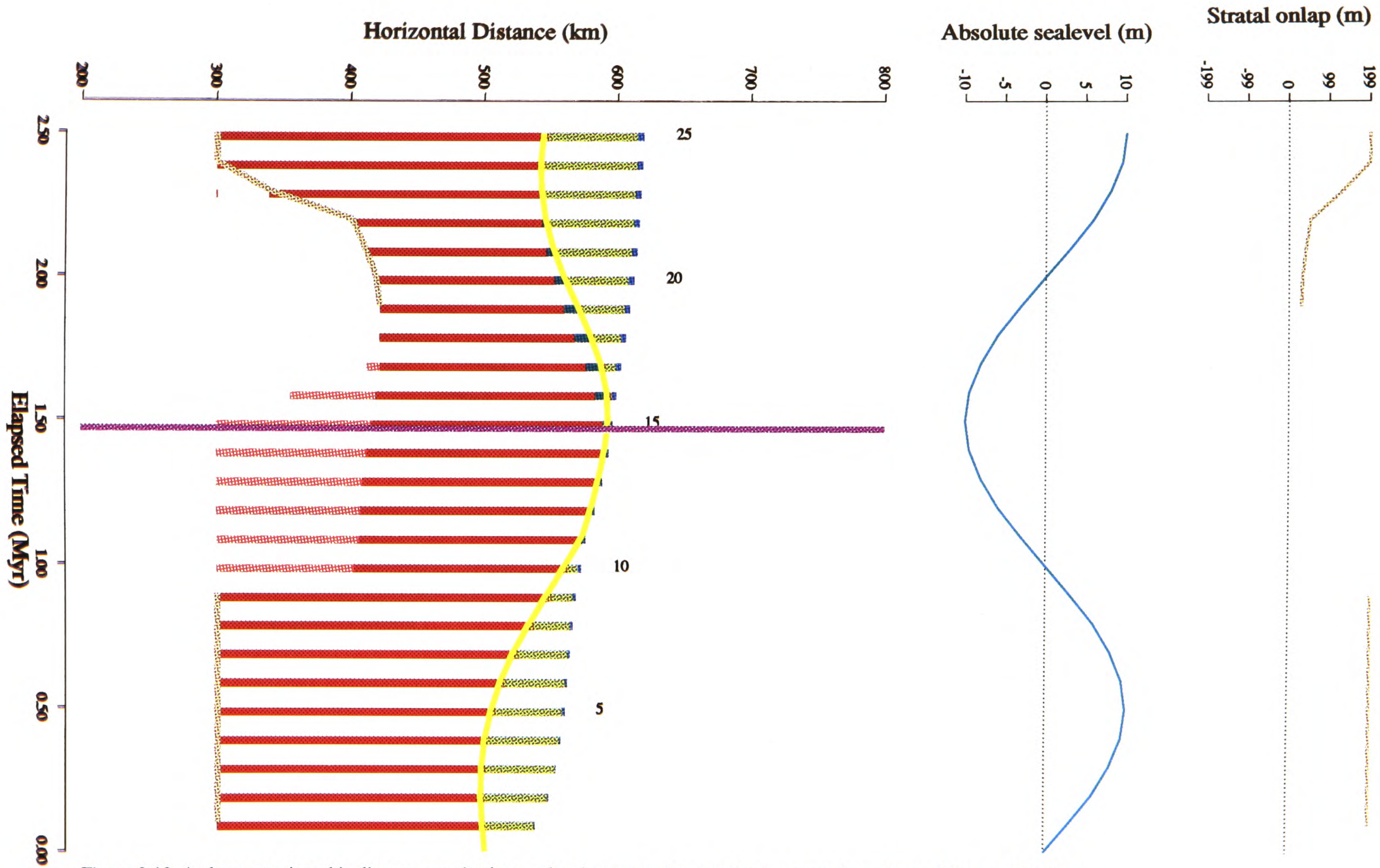

Figure 3.12. A chronostratigraphic diagram, an absolute sealevel curve, and a stratal onlap curve from the model run with higher magnitudes of thermal subsidence, and a lower amplitude of absolute sealevel change, both chosen to reproduce some of the features of a type-2 sequence. All the other parameters for this model run are the same as those for the standard reference model. With the increased subsidence and reduced magnitude fall in absolute sealevel, deposition on the lower portion of the fluvial profile is continuous. Note that the erosion on the upper fluvial profile during the sealevel rise represents only a few metres in thickness of lost stratigraphy.

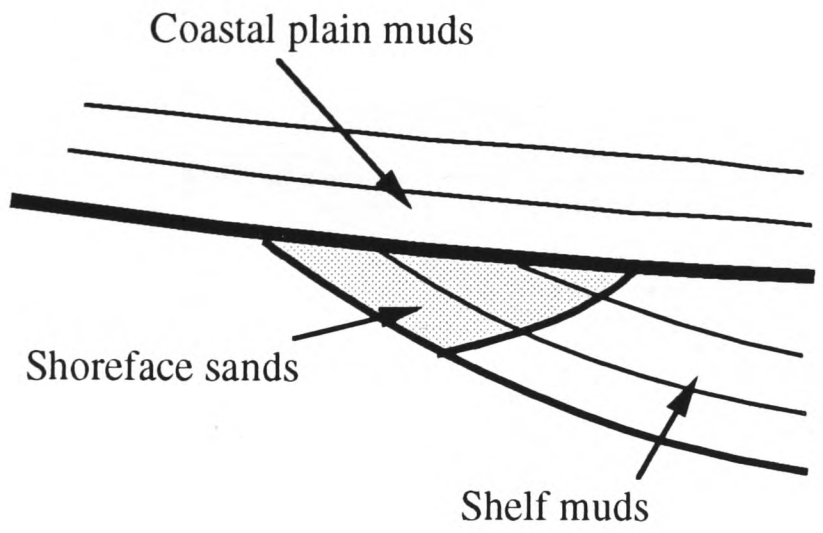

An example of a stratigraphic trap, as seen in figure 3.3. Shoreface sands are preserved beneath a type 1 sequence boundary unconformity, and are surrounded and sealed by shelf and coastal plain muds.

Type 1 unconformity

Example of a stratigraphic trap, as seen in figure 3.7 which shows a series of shoreface sands preserved beneath a type 2 sequence boundary and surrounded and sealed by coastal plain and shelf muds.

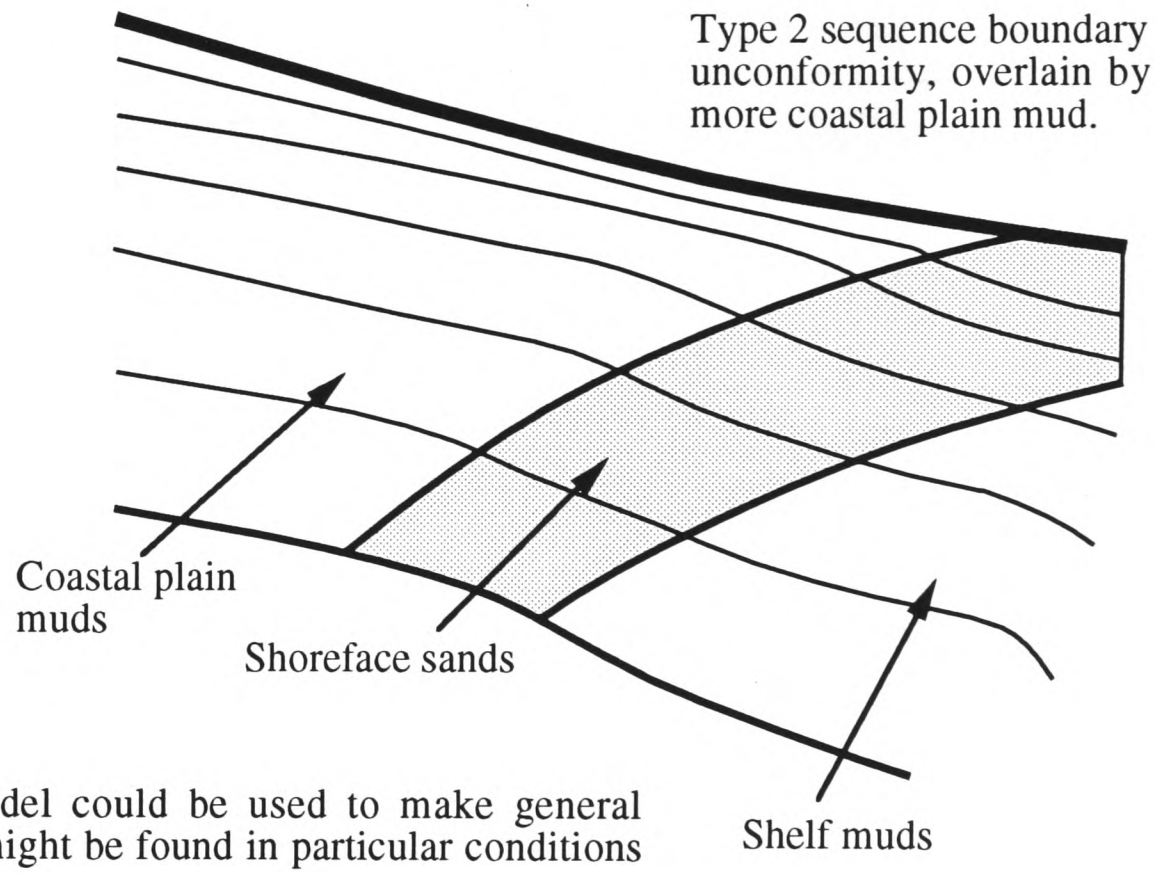

Figure 3.13. An example of how output from the model could be used to make general predictions regarding the type of stratigraphic traps that might be found in particular conditions of subsidence, absolute sealevel, and sediment supply

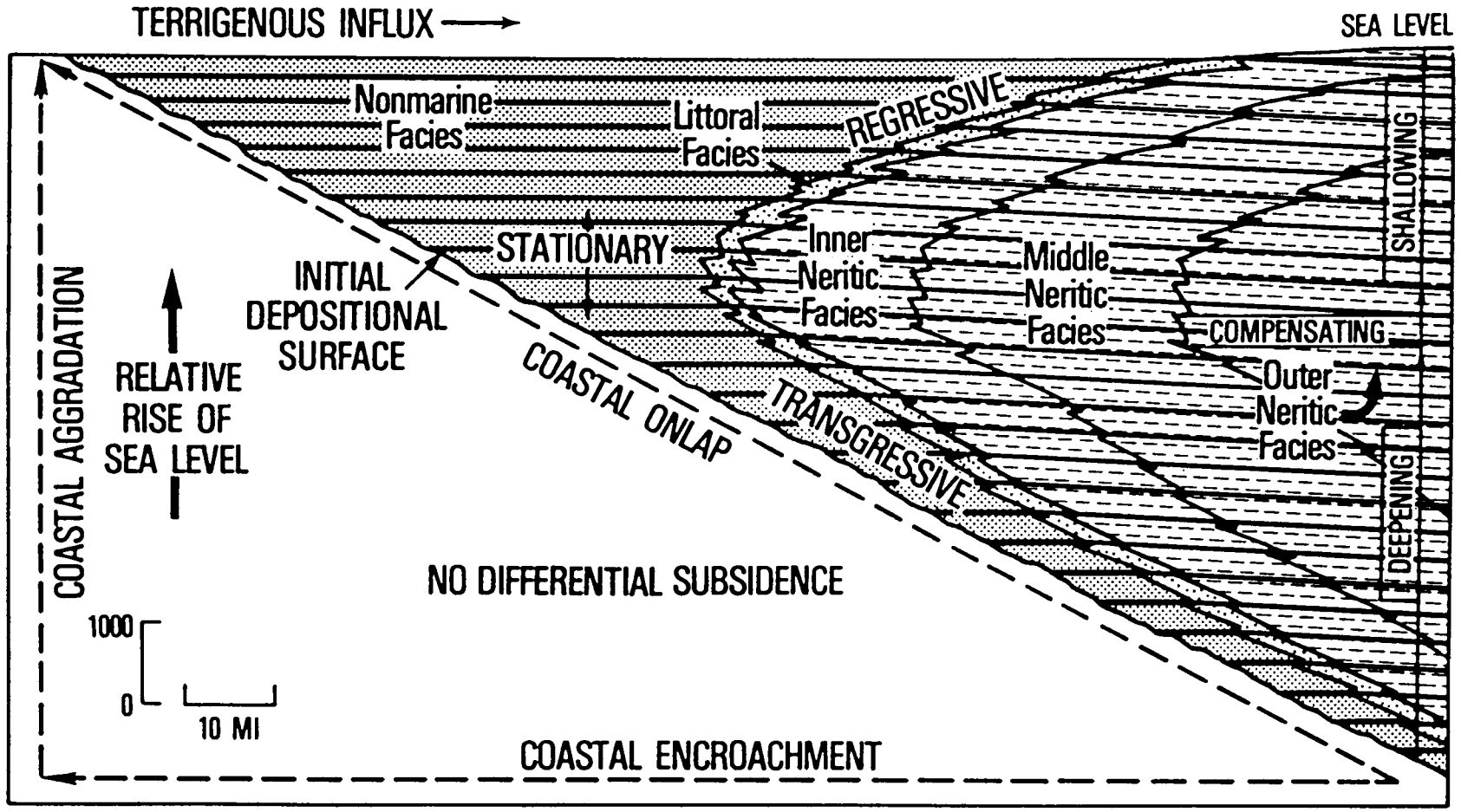

Figure 3.14 A diagram to illustrate the definition of coastal onlap in the sequence stratigraphic depositional model, from Vail *et al.* (1977a).

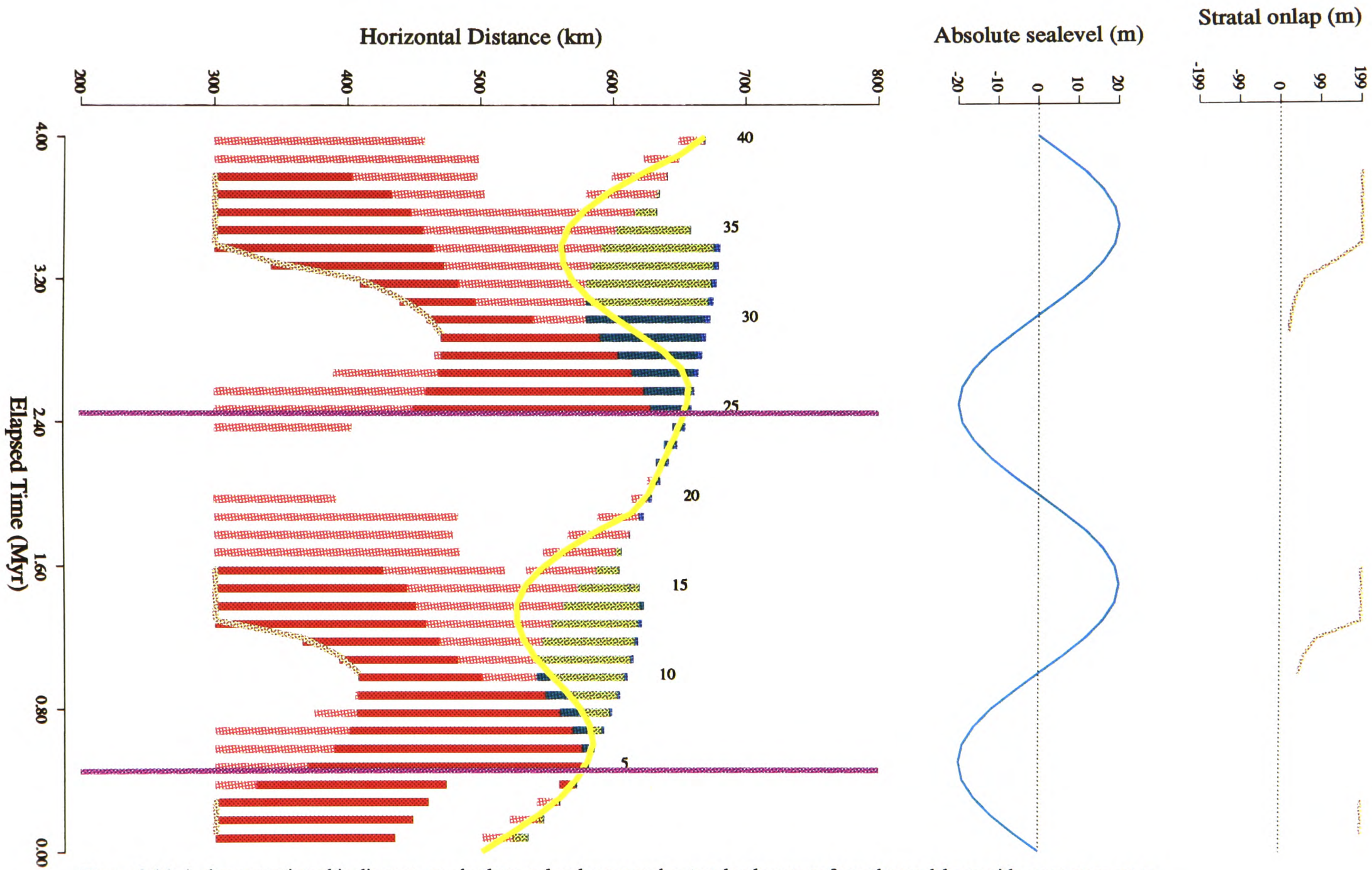

Figure 3.16. A chronostratigraphic diagram, an absolute sealevel curve and a stratal onlap curve from the model run with parameters set to reproduce the elements of the coastal onlap pattern shown in figure 18 of Posamentier et al. (1988) (figure 3.17). See the text for a full description of the model parameters. The pattern of deposition and erosion in this model is considerably more complex than that suggested by figure 3.17. In this case fluvial deposition is not controlled simply by movement of the bayline, but rather by a more complex interaction between subsidence, absolute sealevel change, and the response of the fluvial profile.

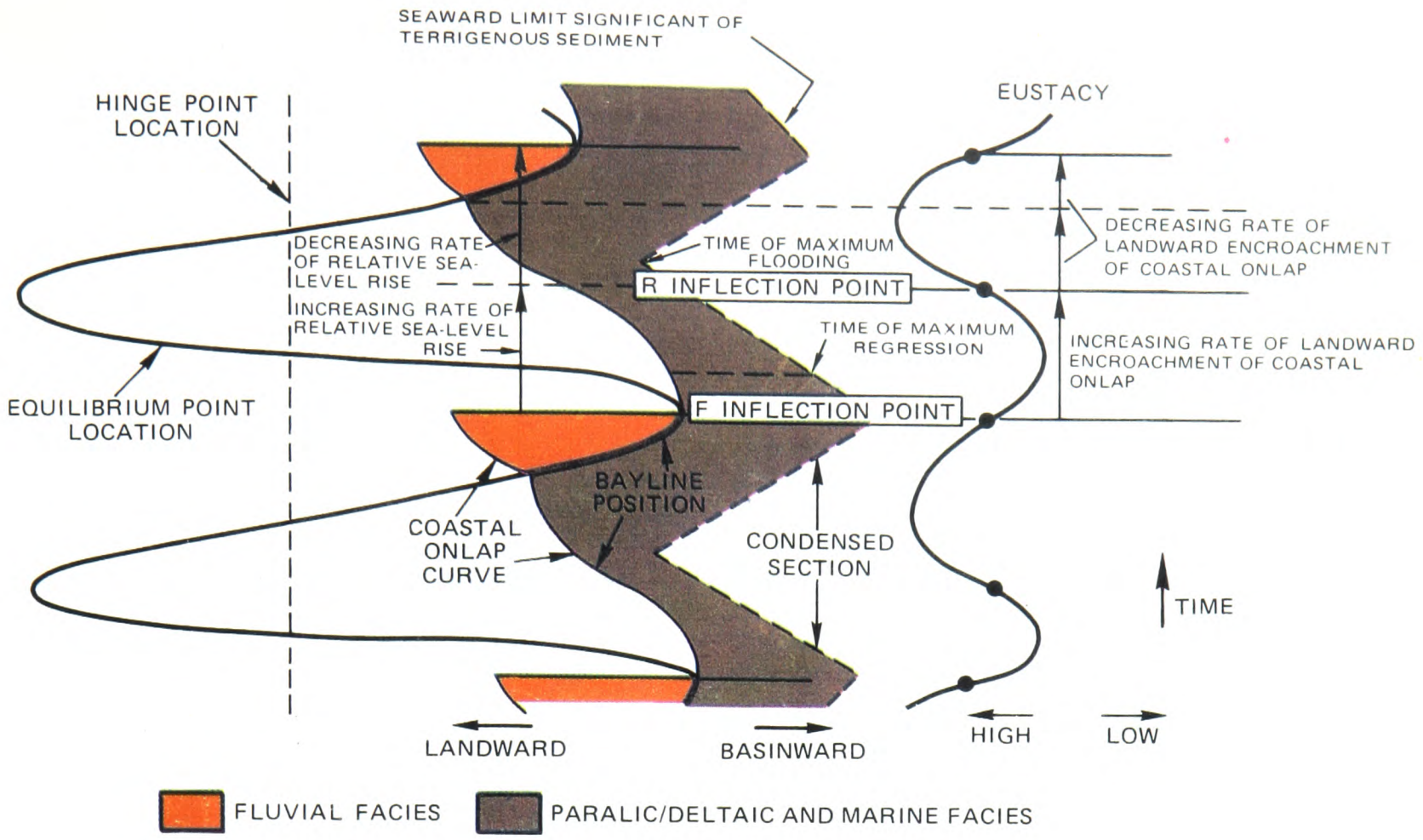

Figure 3.17 A diagram showing the elements of the coastal-onlap curve as defined in the depositional sequence stratigraphic model, from Posamentier *et al.* (1988).

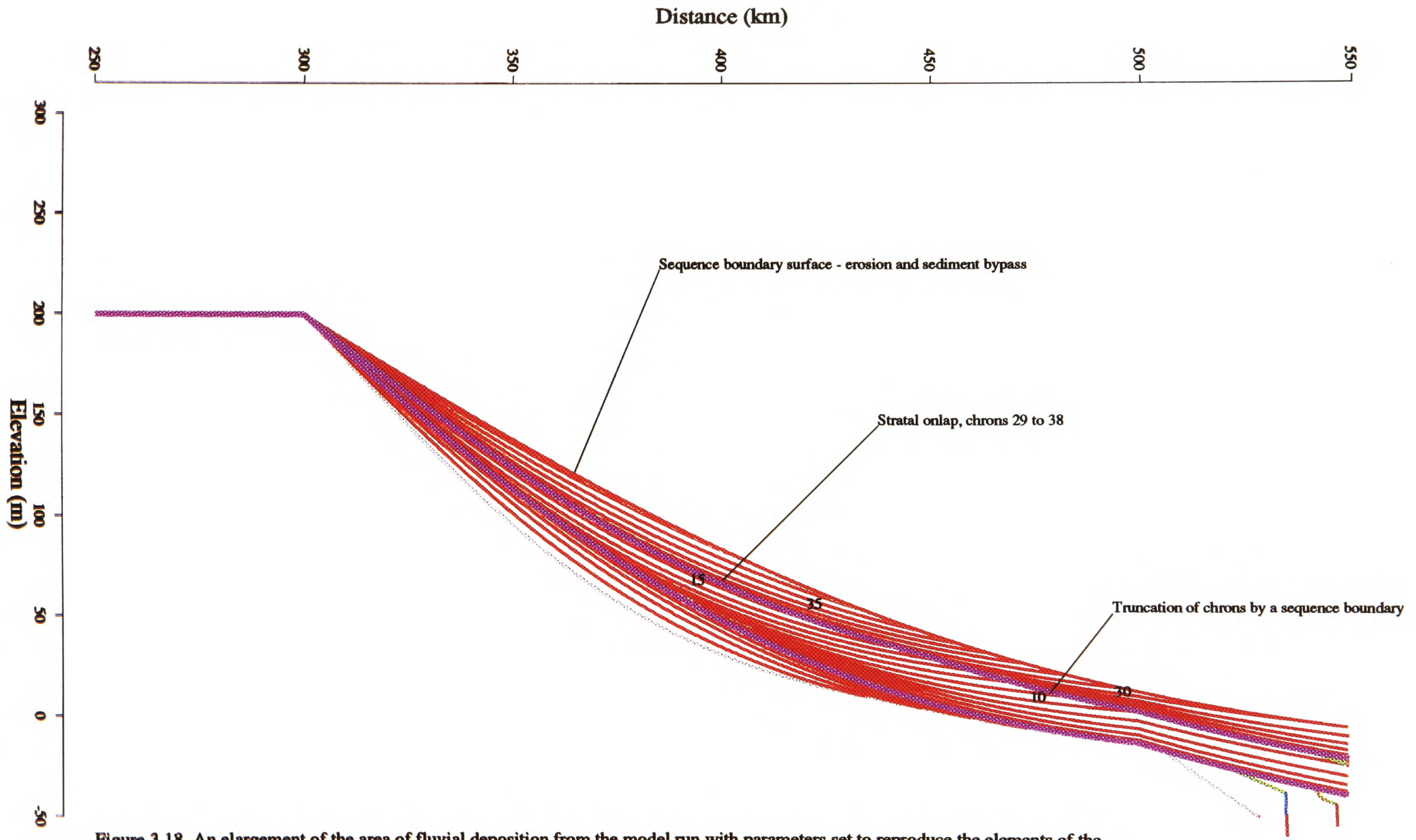

Figure 3.18. An elargement of the area of fluvial deposition from the model run with parameters set to reproduce the elements of the coastal onlap pattern shown in figure 18 of Posamentier et al. (1988) (figure 3.17). See the text for a full description of the model parameters. The plot illustrates the complex pattern of fluvial deposition, sediment bypass, and erosion that develops in response to the interplay between subsidence, absolute sealevel change and the fluvial profile geometry.

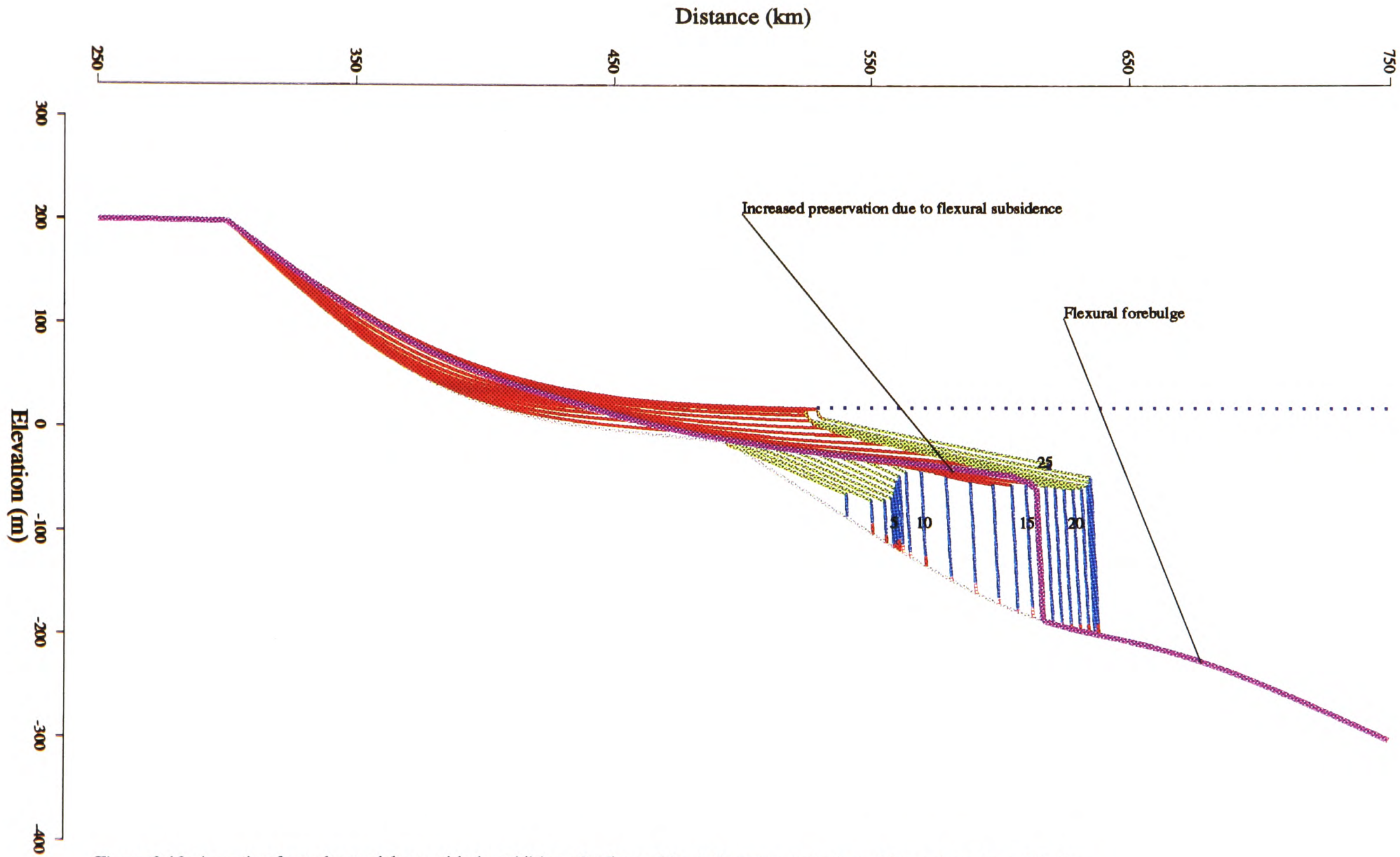

Figure 3.19. A section from the model run with the addition of a flexural isostatic response to deposition and erosion. All other parameters are the same as those for the standard reference model. The flexure is calculated using a value for elastic thickness of 10km. The impact on the pattern of the stratigraphy in the section is negligable, although the increased accommodation space does increase preservation and erosion on some chrons, but only by a few metres. The flexural forebulge produced in front of the prograding sediment wedge is clearly visible.

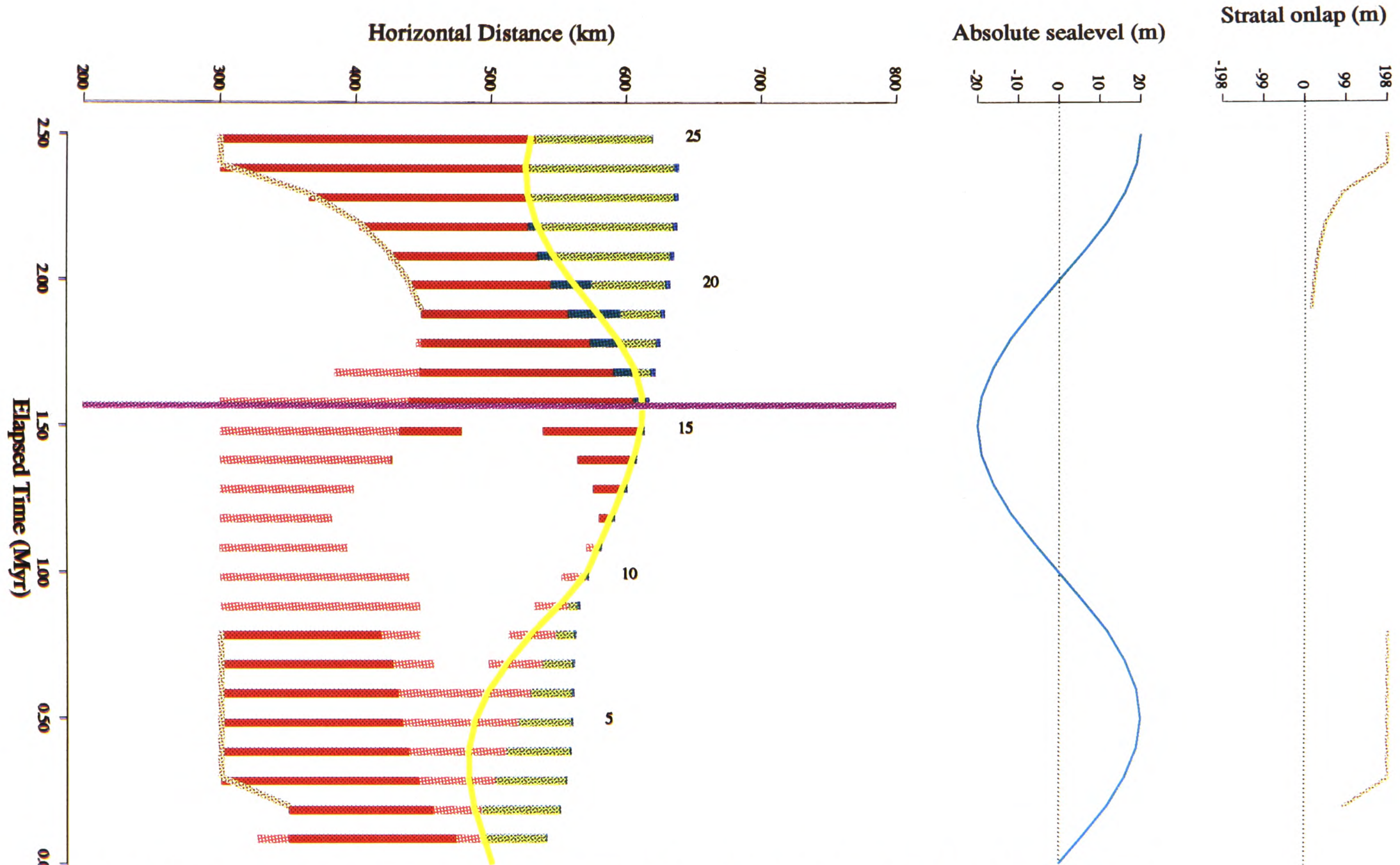

Figure 3.20. A chronostratigraphic diagram, absolute sealevel curve, and a stratal onlap curve from the model run with the addition of a flexural isostatic response to deposition and erosion. All other parameters are the same as those for the standard reference model. The flexure is calculated using a value for elastic thickness of 10km. The chronostratigraphic diagram shows that the basic pattern of deposition and erosion in response to the sealevel change is unaffected by the flexure. However, details such as the exact pattern of preservation on the lower fluvial profile during falling absolute sealevel are changed, and this changes the timing of the sequence boundary from chron 15 to chron 16 (1.6 Myrs E.M.T.).

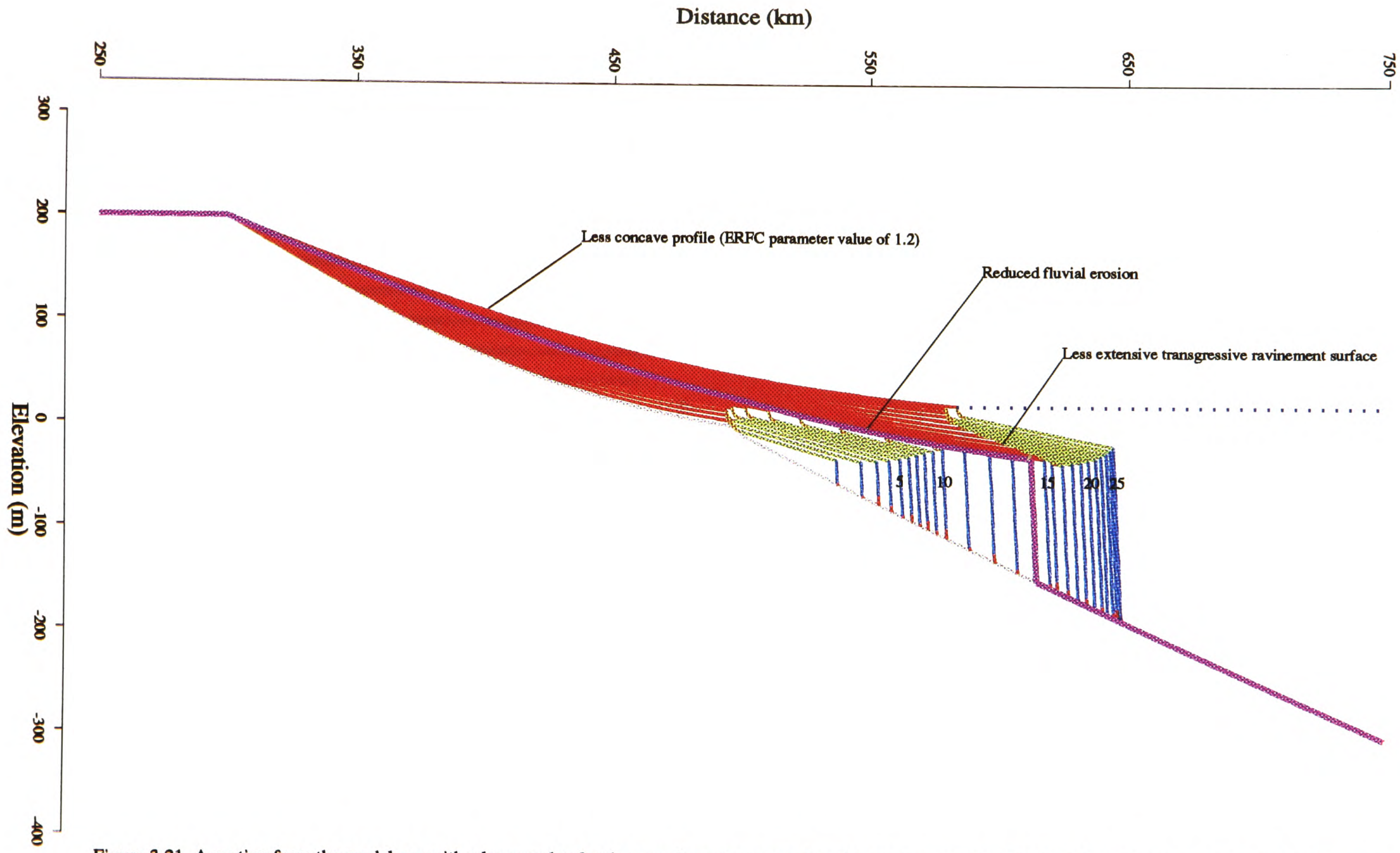

Figure 3.21. A section from the model run with a lower value for the complementary error function curve parameter of 1.2, giving a less concave fluvial profile geometry. All other parameters are the same as those for the standard reference model. The less concave fluvial profile has the effect of reducing the magnitude and lateral extent of fluvial erosion, producing a stratigraphic pattern similar to that seen for the type-2 sequence in figure 3.11, even though all the other model parameters such as the subsidence magnitude, and the absolute sealevel curve amplitude are the same as those for the type-1 sequence example in the standard reference model.

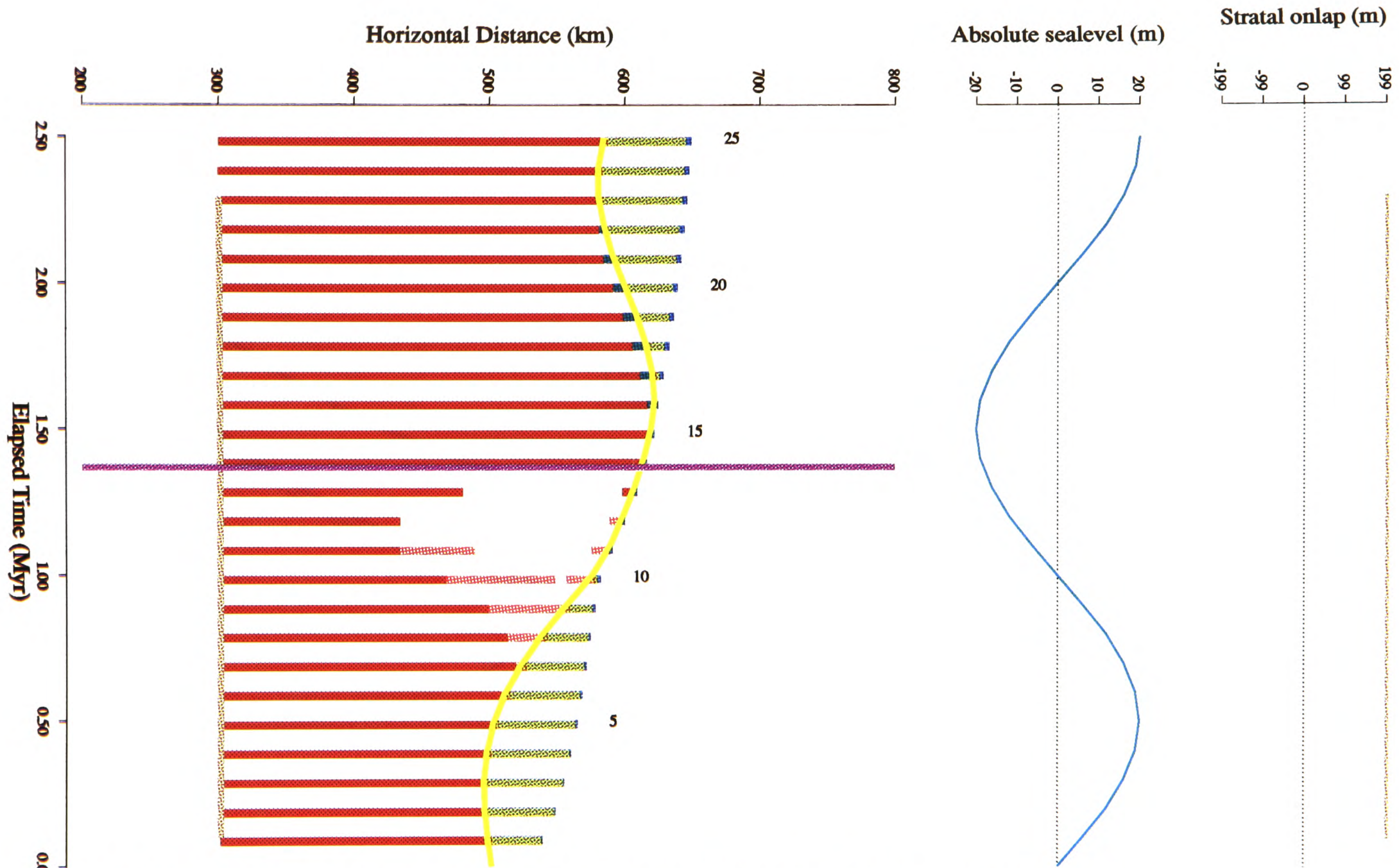

Figure 3.22. A chronostratigraphic diagram, an absolute sealevel curve, and a stratal onlap curve from the model run with an error function parameter value of 1.2. All other parameters are as described for the standard reference model. The chronostratigraphic diagram shows that the less concave fluvial profile has considerably reduced the lateral distribution of the erosion and non-deposition due to the absolute sealevel fall. The pattern is similar to that seen in the type-2 sequence example shown in figure 3.12.

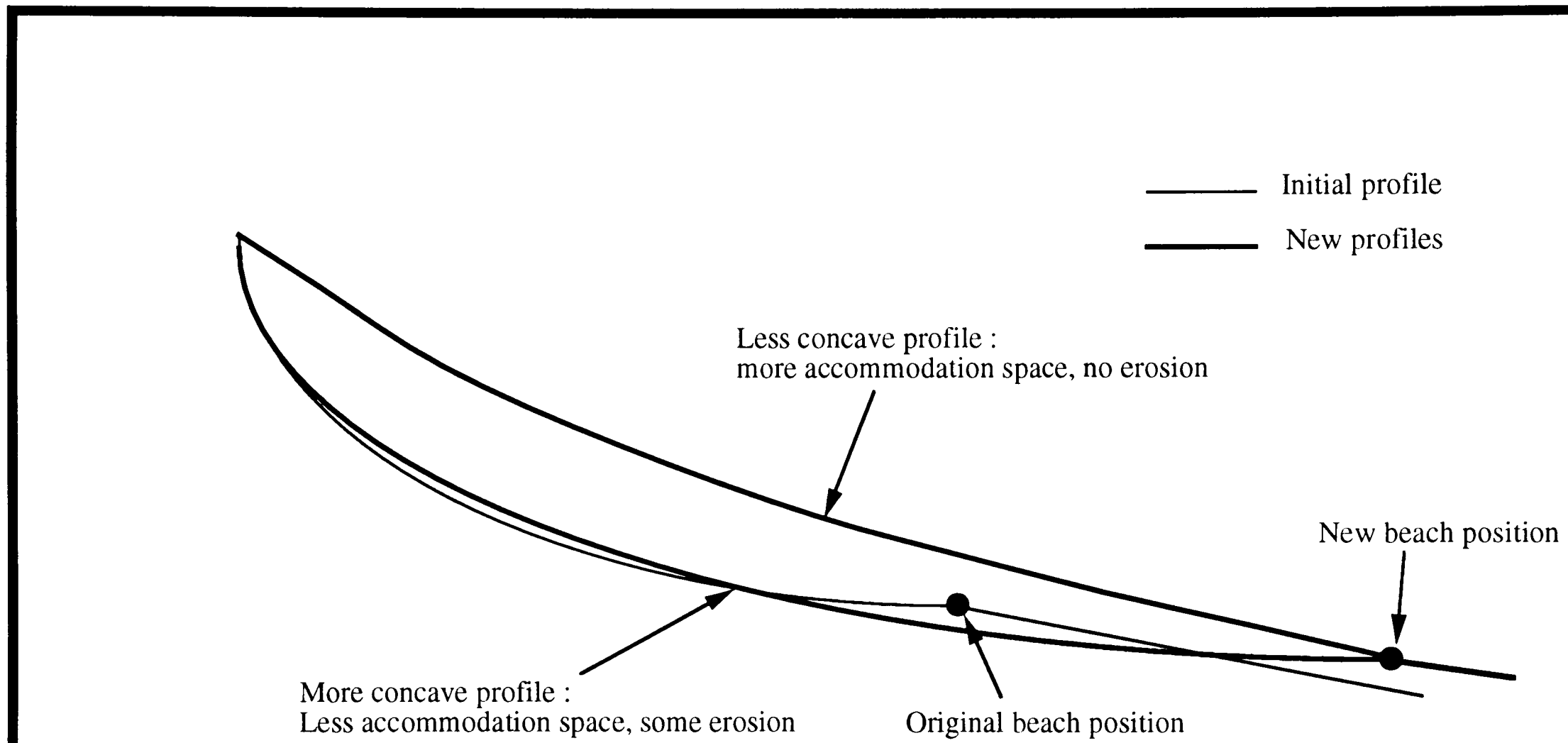

Figure 3.23. A diagram to show the effects on fluvial deposition and erosion of using a less concave and a more concave fluvial profile geometry.

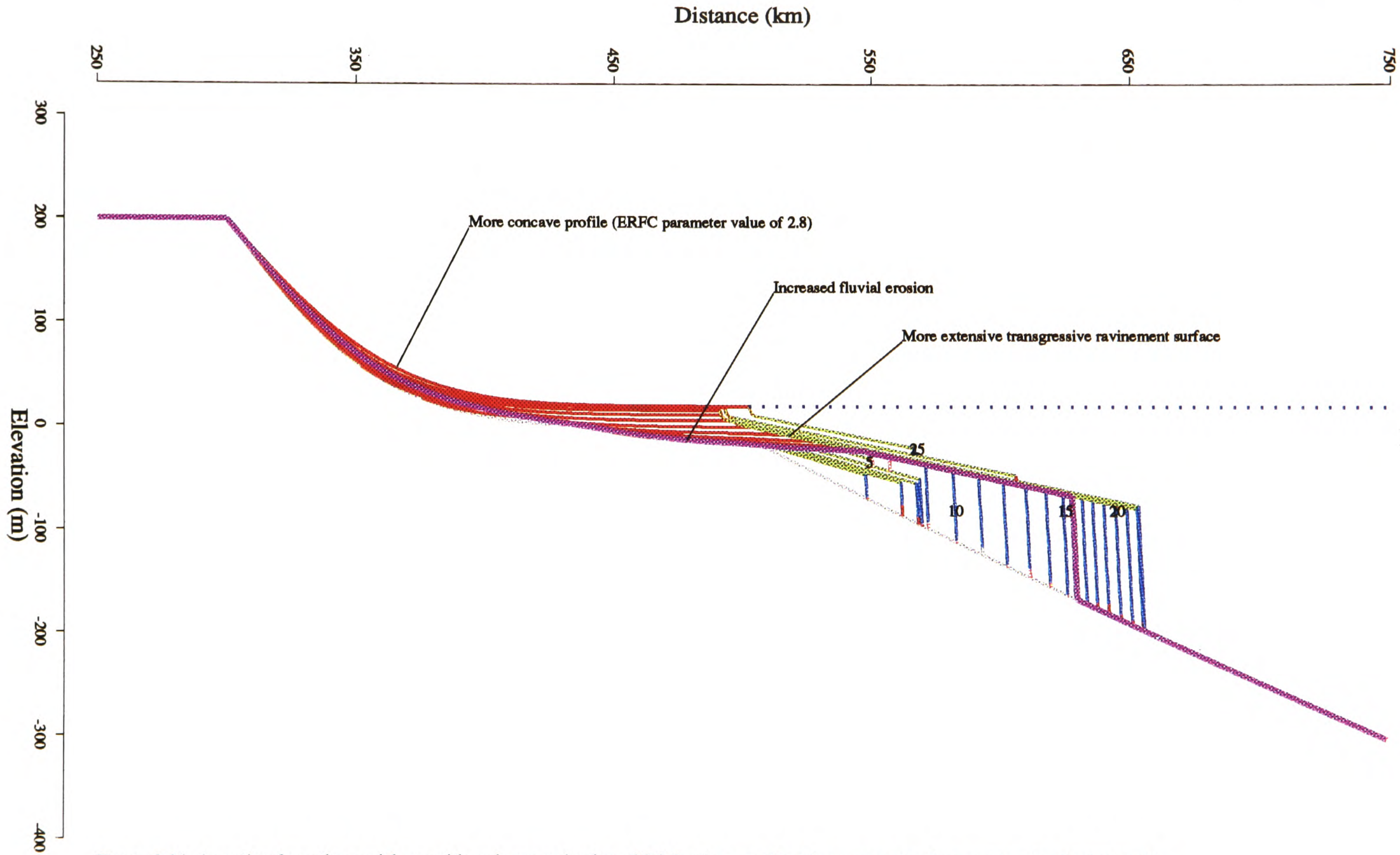

Figure 3.24. A section from the model run with an increased value of 2.8 for the error function parameter, thus making the fluvial profile more concave. All other paramters are the same as those used in the standard reference model. The more concave fluvial profile has the effect of increasing the lateral extent and the magnitude of erosion, both on the lower profile during the relative sealevel fall, and on the upper profile during the relative sealevel rise.

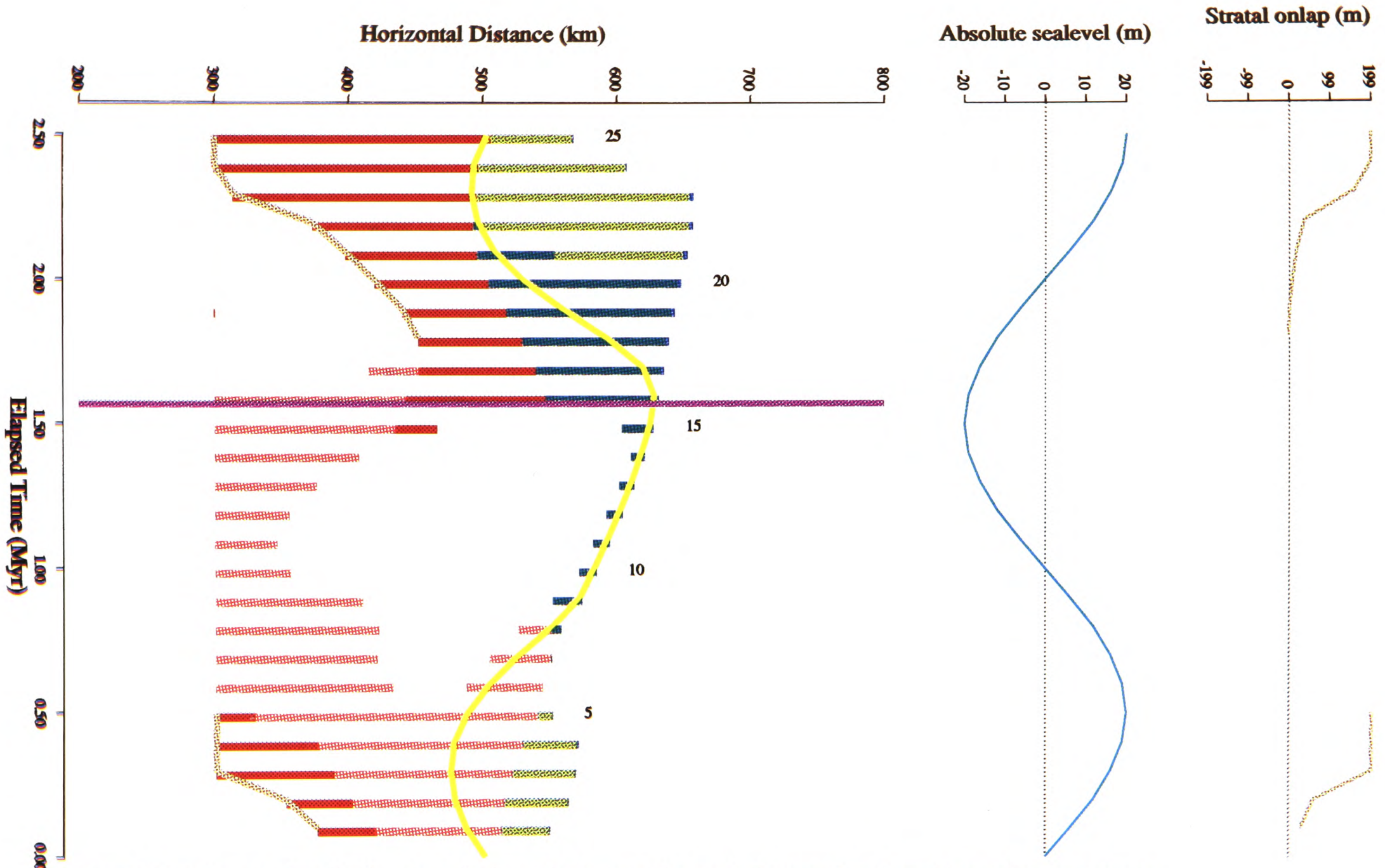

Figure 3.25. A chronostratigraphic diagram, an absolute sealevel curve and a stratal onlap curve from the model run with a more concave fluvial profile produced using an error function parameter value of 2.8. All other model parameters are the same as those given for the standard reference model. The more concave profile has lead to more erosion, on the lower profile during relative sealevel fall, and on the upper profile during relative sealevel rise. As a result the thickness and extent of fluvial stratigraphy preserved has been reduced. Also, the lower slopes on the seaward portion of the fluvial profile have accentuated the development of the transgressive ravinement surface.

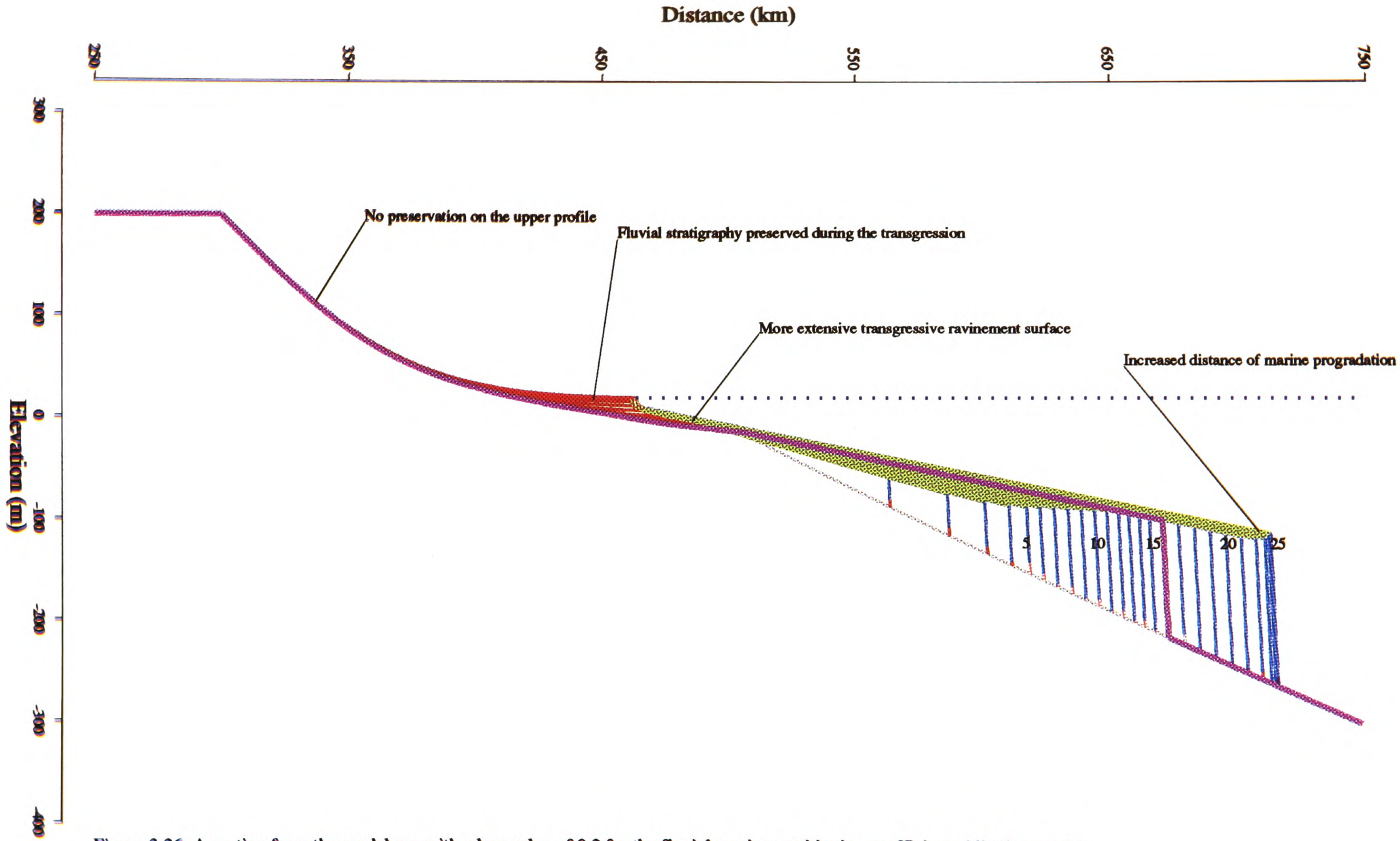

Figure 3.26. A section from the model run with a low value of 0.2 for the fluvial-marine partitioning coefficient. All other model parameters are the same as those used in the standard reference model. The lower partitioning coefficient reduces the area of deposition in the fluvial profile, increases deposition on the marine profile, and allows the beach to transgress further landward during an absolute sealevel rise, thus accentuating the development of the transgressive ravinement surface, and the erosion on the upper portion of the fluvial profile due to profile shortening.

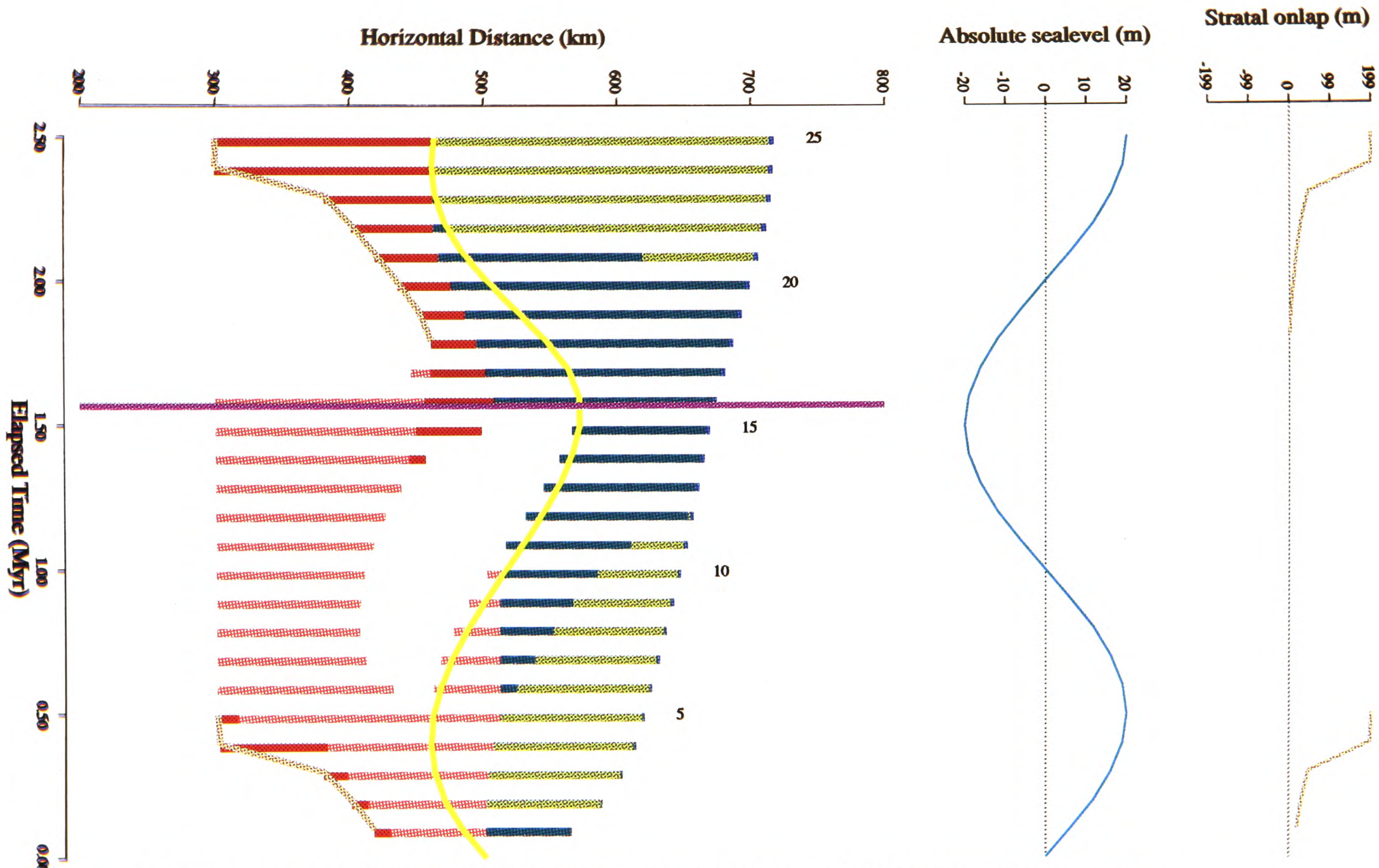

Figure 3.27. A chronostratigraphic diagram, an absolute sealevel curve, and a stratal onlap curve from the model run with a low value of 0.2 for the fluvial-marine partitioning coefficient. All other model parameters are the same as those used in the standard reference model. The lower value for the partitioning coefficient has reduced the initial deposition and subsequent preservation of fluvial stratigraphy, as well as significantly increasing the lateral extent of the marine erosion produced by the passage of the transgressive ravinement surface.

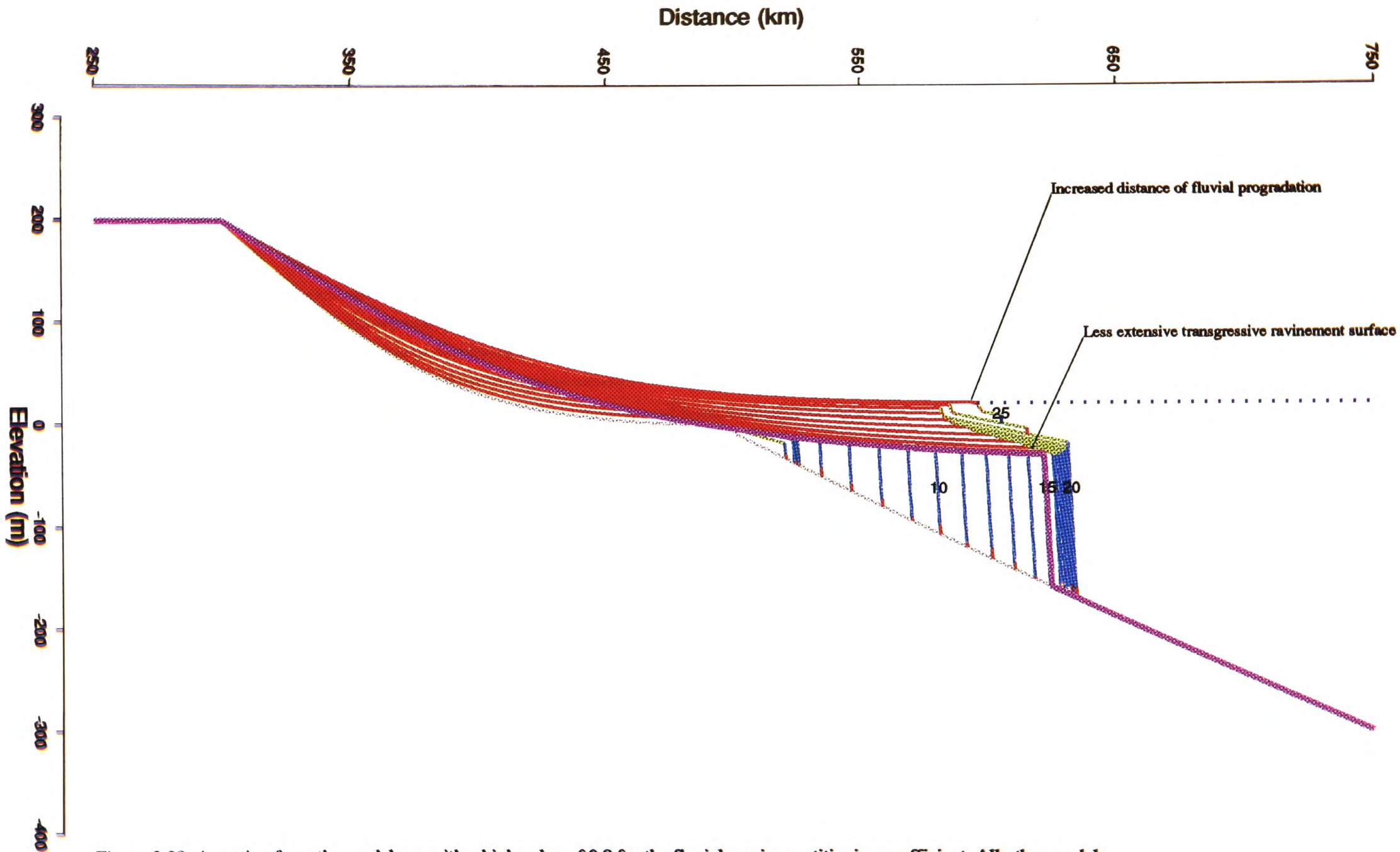

Figure 3.28. A section from the model run with a high value of 0.8 for the fluvial-marine partitioning coefficient. All other model parameters are the same as those used in the standard model. The higher value for the partitioning coefficient has increased the deposition on the fluvial profile, and the degree of fluvial progradation. The shelf is less well developed than in previous examples. The landward distance of the transgression and hence the development of the transgressive ravinement surface has been reduced by the increased fluvial progradation.

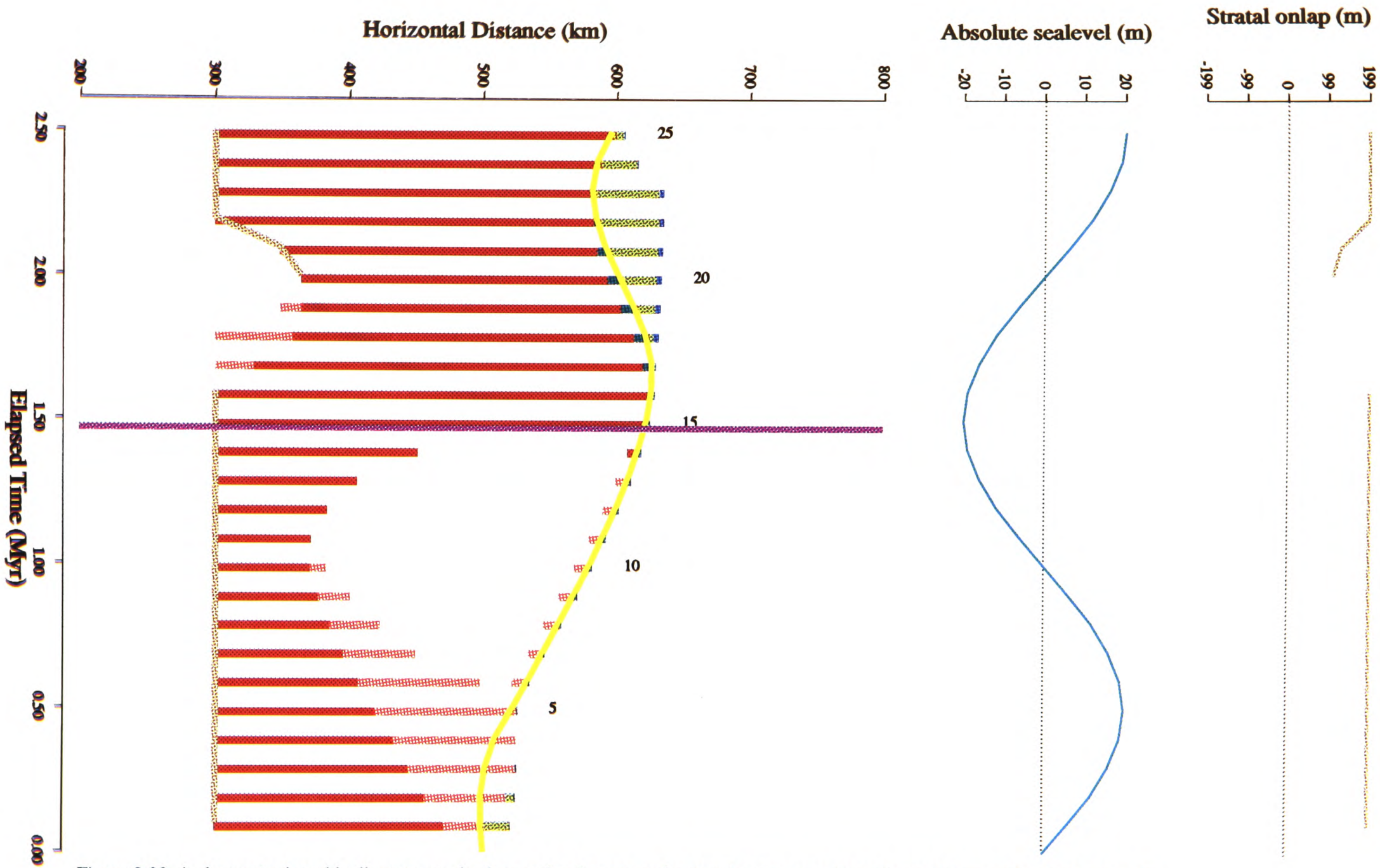

Figure 3.29. A chronostratigraphic diagram, an absolute sealevel curve, and a stratal onlap curve from the model run with a high value of 0.8 for the fluvial-marine partitioning coefficient. All other model parameters are the same as those used in the standard model. The higher value for the partitioning coefficient has increased the deposition on the fluvial profile, and the distance of fluvial progradation. In this example minimal erosion occurs on the upper profile during the transgression, and the marine erosion is reduced in both lateral and vertical extent.

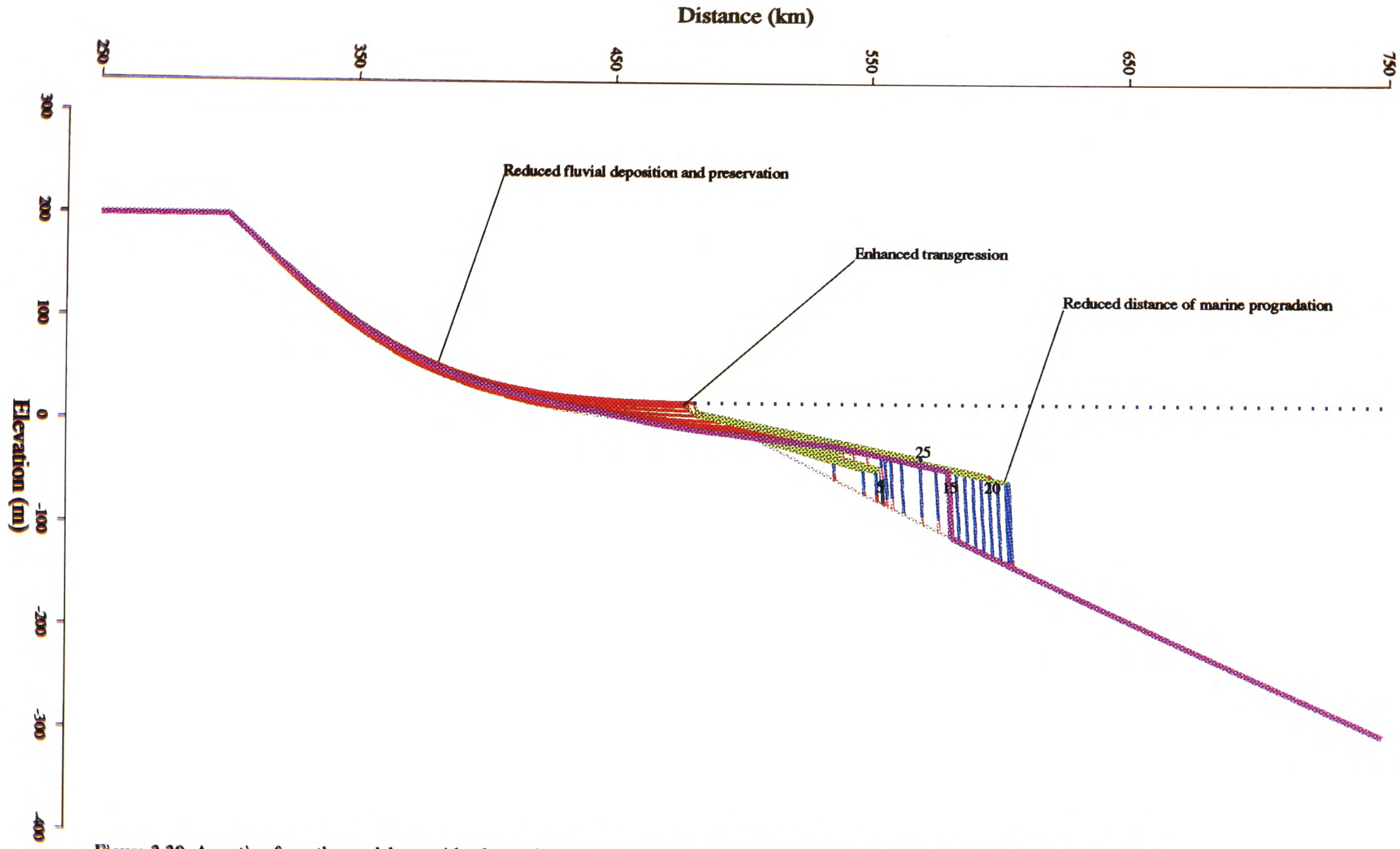

Figure 3.30. A section from the model run with a low value for external sediment supply of 0.5 square kilometres per timestep. All other model parameters are the same as those used in the standard reference model. The lower sediment supply has a similar effect to lowering the partitioning coefficient in that it has increased the influence of the absolute sealevel changes. For example, the transgression during the absolute sealevel rise is accentuated. Both fluvial and marine deposition are reduced as a direct result of the lower sediment supply.

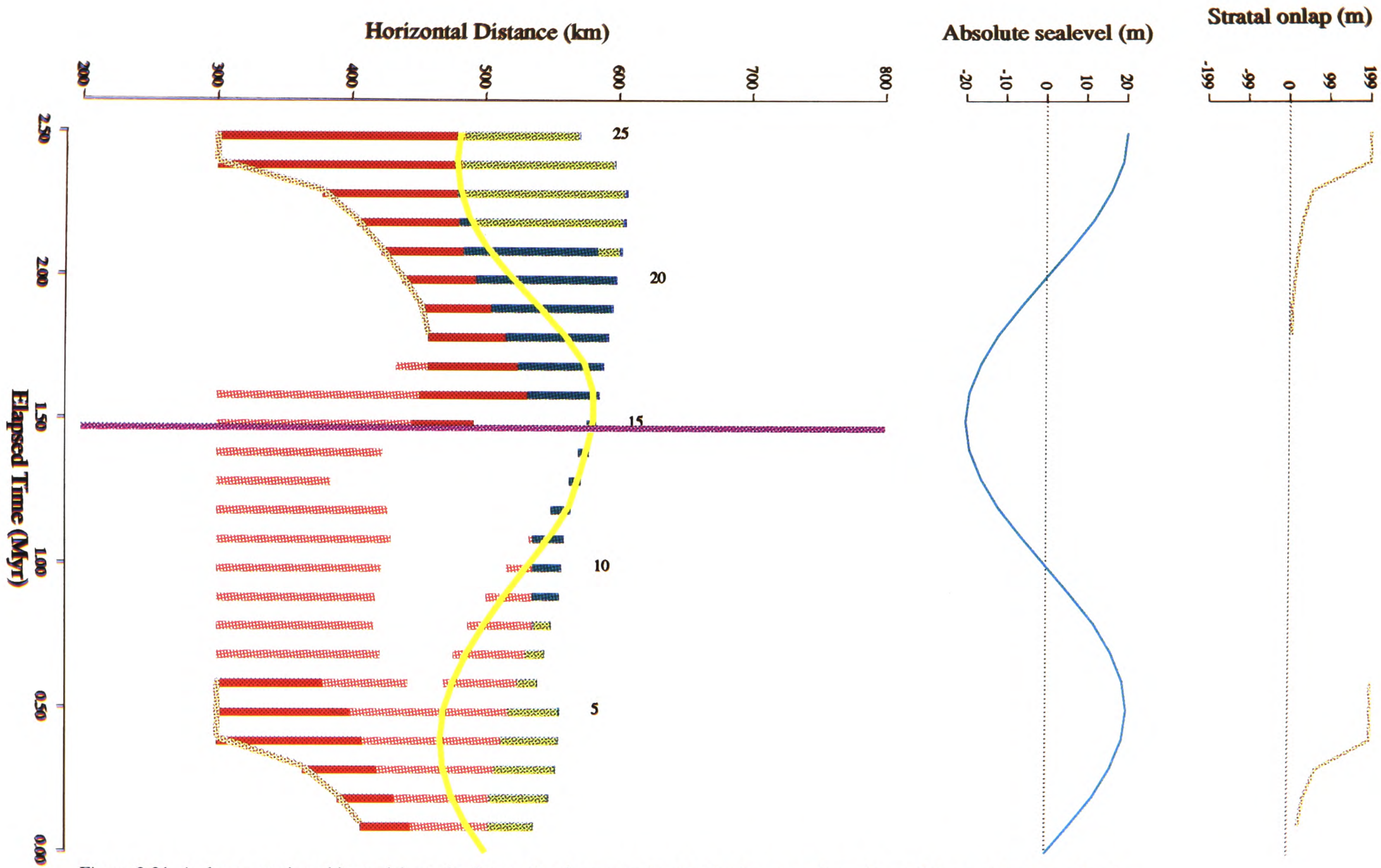

Figure 3.31. A chronostratigraphic model, an absolute sealevel curve and a stratal onlap curve from the model run with a low value for external sediment supply of 0.5 square kilometres per timestep. All other model parameters are the same as those used in the standard reference model. The lower sediment supply has a similar effect to lowering the partitioning coefficient in that it has increased the influence of the absolute sealevel changes. For example, the transgression has driven the beach further landward, shortening the fluvial profile, and leading to the erosion of all the stratigraphy previously deposited on the upper fluvial profile.

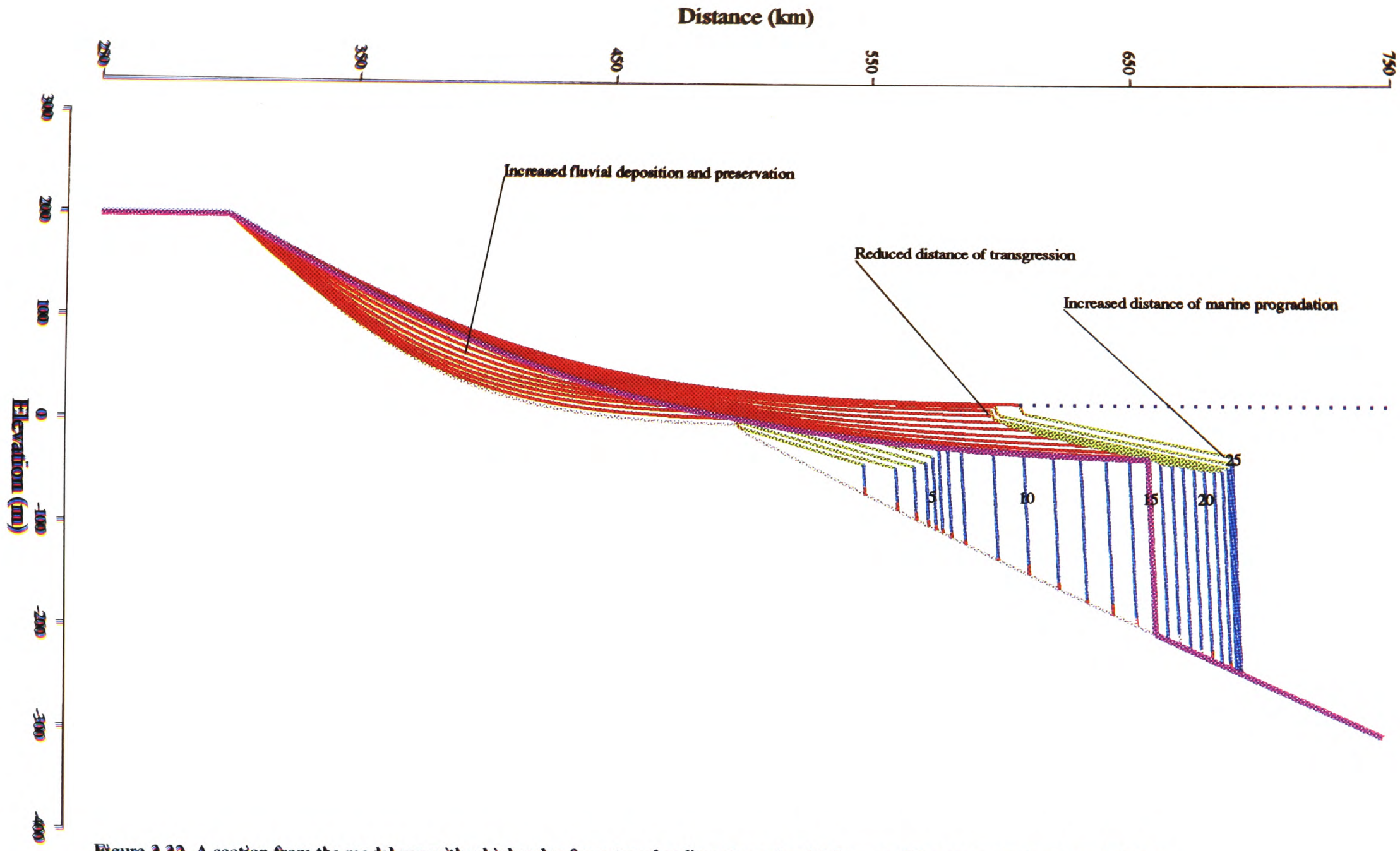

Figure 3.32. A section from the model run with a high value for external sediment supply of 1.5 square kilometres per timestep. All other model parameters are the same as those used in the standard reference model. The higher sediment supply has the effect of reducing the influence of the absolute sealevel change by increasing the distance of fluvial and marine progradation. This leads to increased thickness of fluvial and marine deposition, and increased preservation of the fluvial stratigraphy, particularly on the upper fluvial profile.

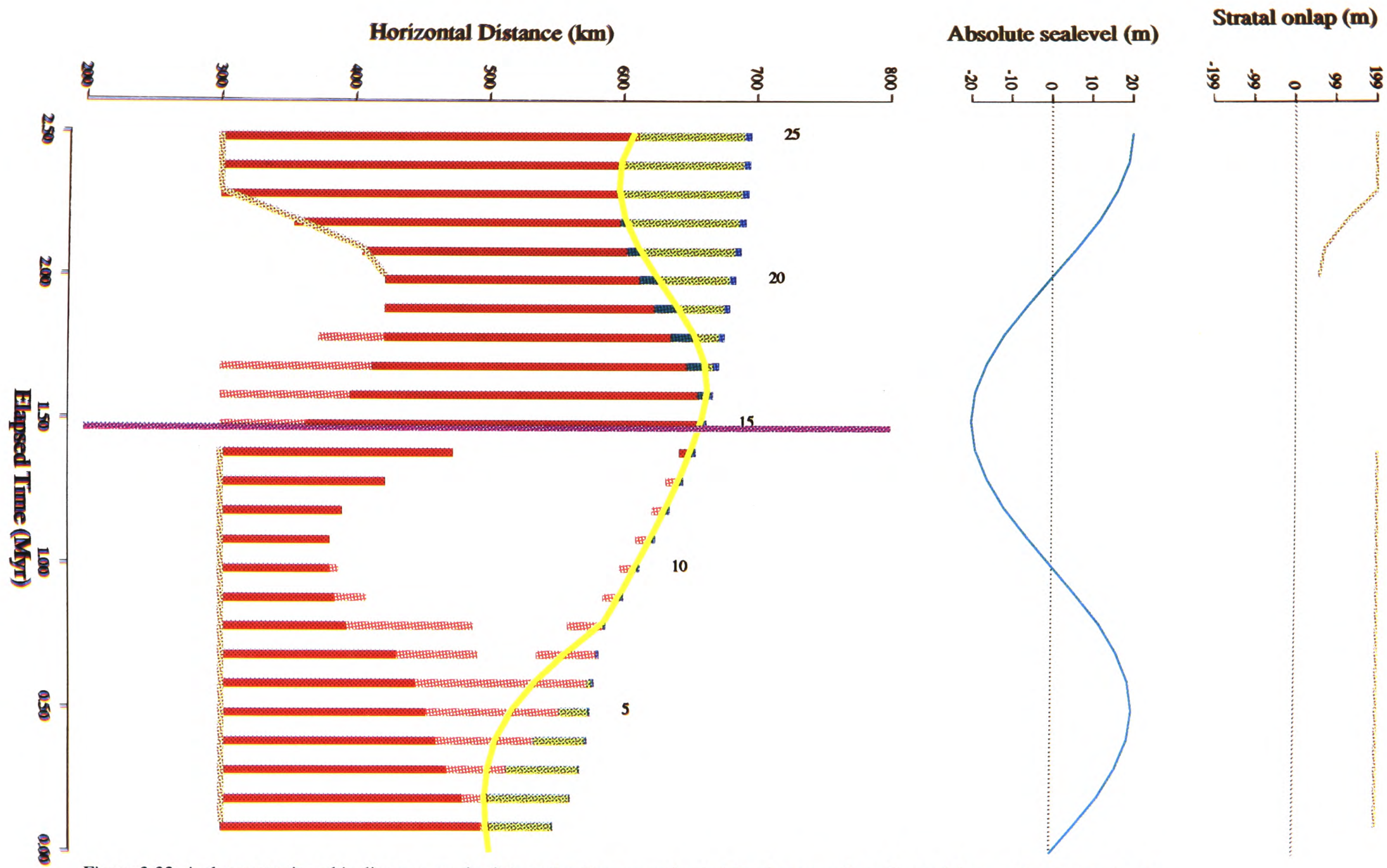

Figure 3.33. A chronostratigraphic diagram, an absolute sealevel curve, and a stratal onlap curve from the model run with a high value for external sediment supply of 1.5 square kilometres per timestep. All other model parameters are the same as those used in the standard reference model. The higher sediment supply has the effect of reducing the influence of the absolute sealevel change. This is shown by the decreased lateral extent of the transgression, and the increase in fluvial deposition and preservation.

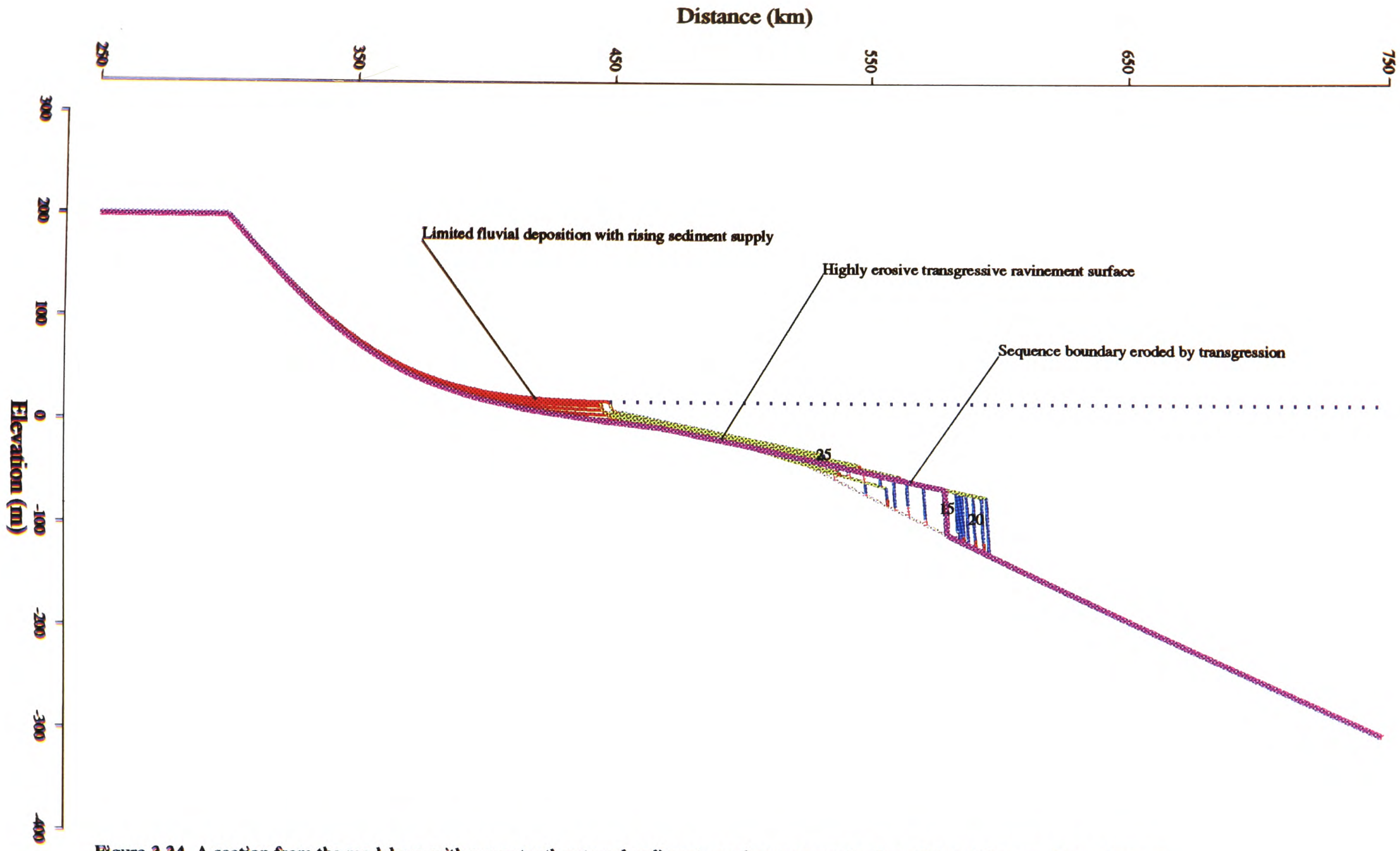

Figure 3.34. A section from the model run with a saw-tooth external sediment supply curve ranging from 0.1 to 1.0 square kilometres per timestep with a period of 1.6Myrs. Sediment supply increases steadily until chron 17 when it drops sharply. All other model parameters are the same as those used in the standard reference mdoel. The section is dominated by the results of the drop in sediment supply, which occurring as it does during a time of rising absolute sealevel, precipitates a major transgression, eroding much of the previous stratigraphy.

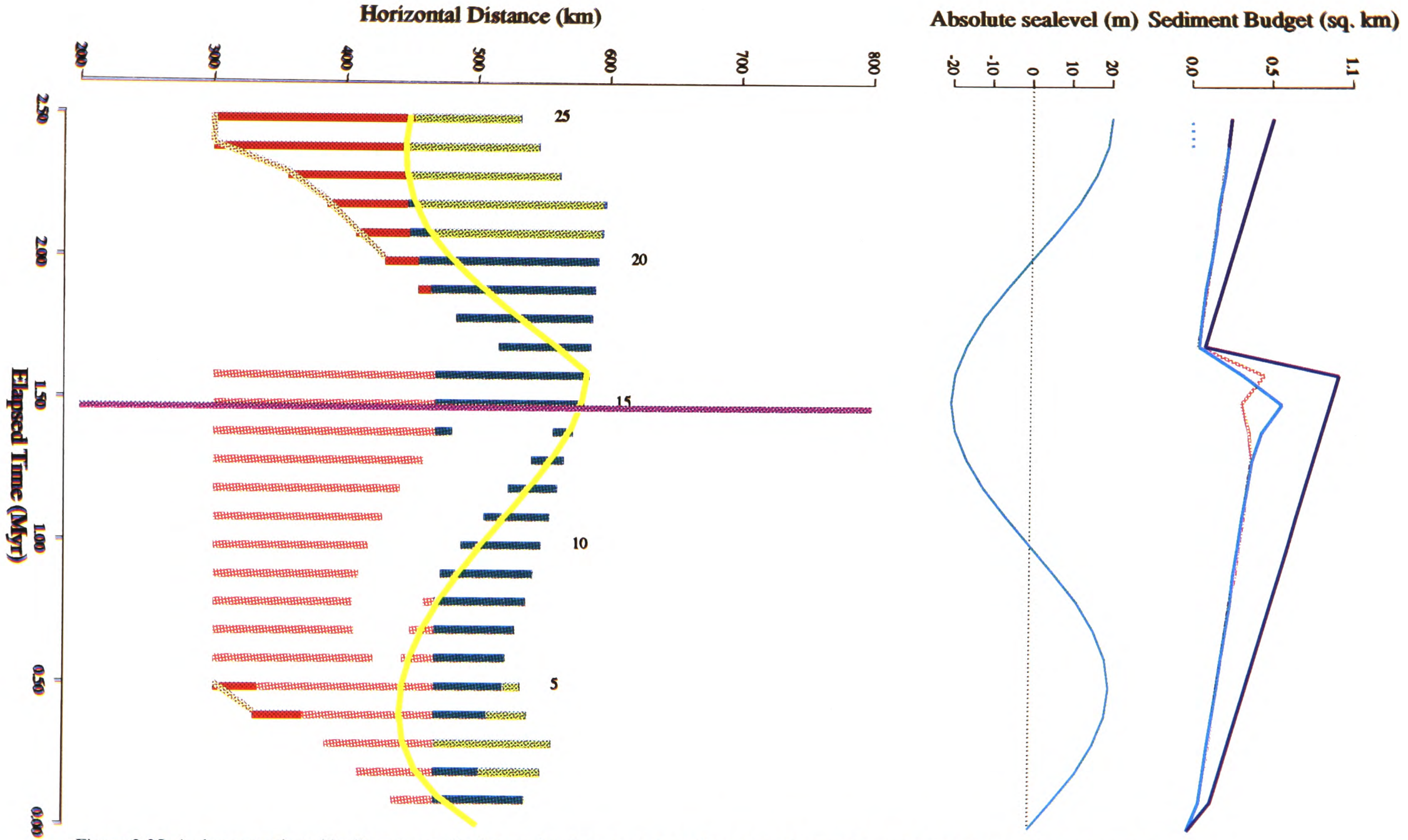

Figure 3.35. A chronostratigraphic diagram, an absolute sealevel curve, and a sediment supply curve from the model run with a saw-tooth external sediment supply curve ranging from 0.1 to 1.0 square kilometres per timestep with a period of 1.6Myrs. Sediment supply increases steadily until chron 17 when it drops sharply. All other model parameters are the same as those used in the standard reference model. The stratigraphy is dominated by the effects of the drop in sediment supply, which occurring as it does during a time of rising absolute sealevel, precipitates a major transgression, eroding much of the previous stratigraphy on a laterally more extensive transgressive ravinement surface.

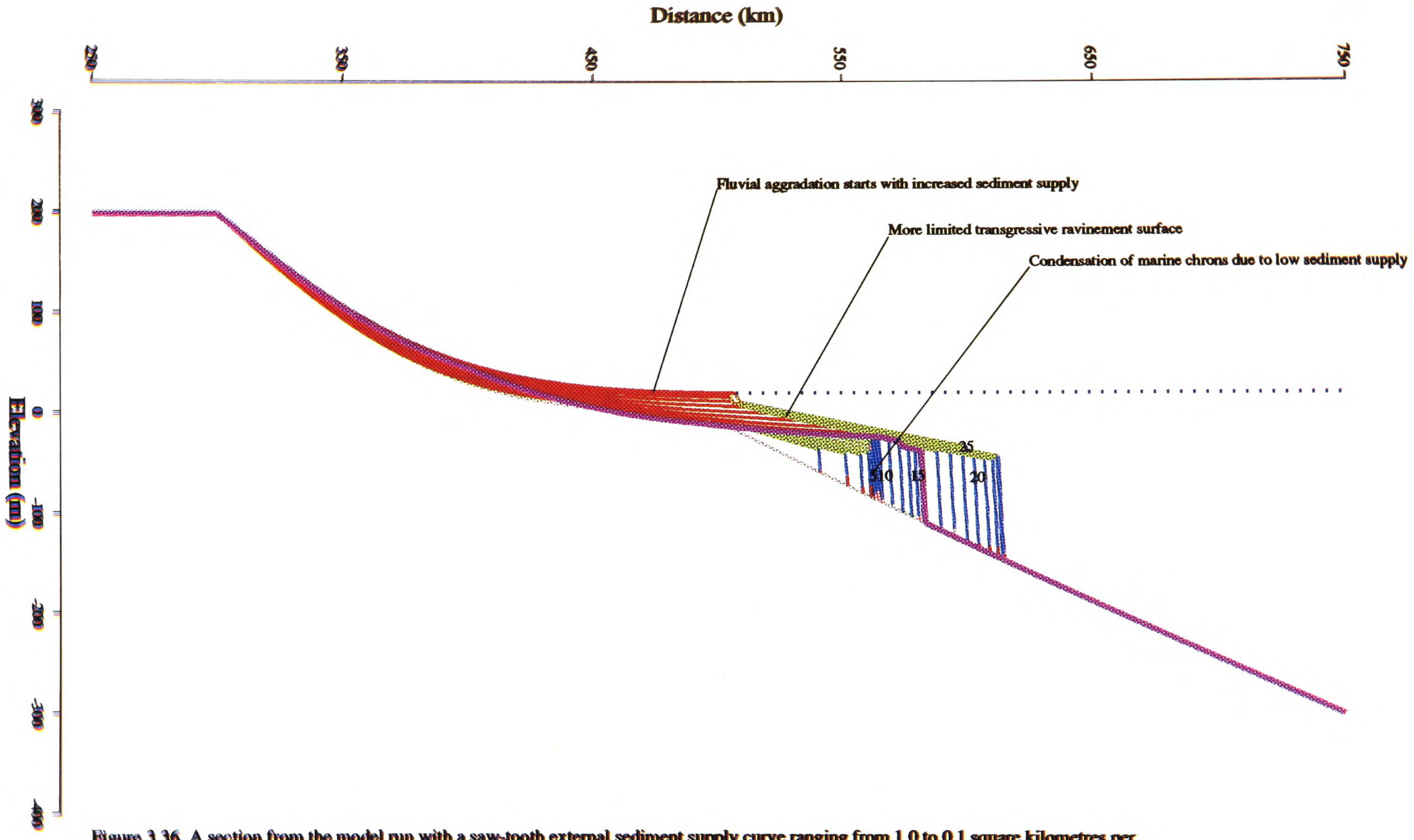

Figure 3.36. A section from the model run with a saw-tooth external sediment supply curve ranging from 1.0 to 0.1 square kilometres per timestep with a period of 1.6Myrs. Sediment supply decreases steadily until chron 17 when it rises sharply. All other model parameters are the same as those used in the standard reference model. In this example the effects of the saw tooth sediment supply curve are less pronounced, only really being visible on the section as a condensation on the marine slope for chrons 5 to 15. The increased sediment supply during the absolute sealevel rise prevents the formation of the extensive transgressive ravinement surface seen in figure 3.34.

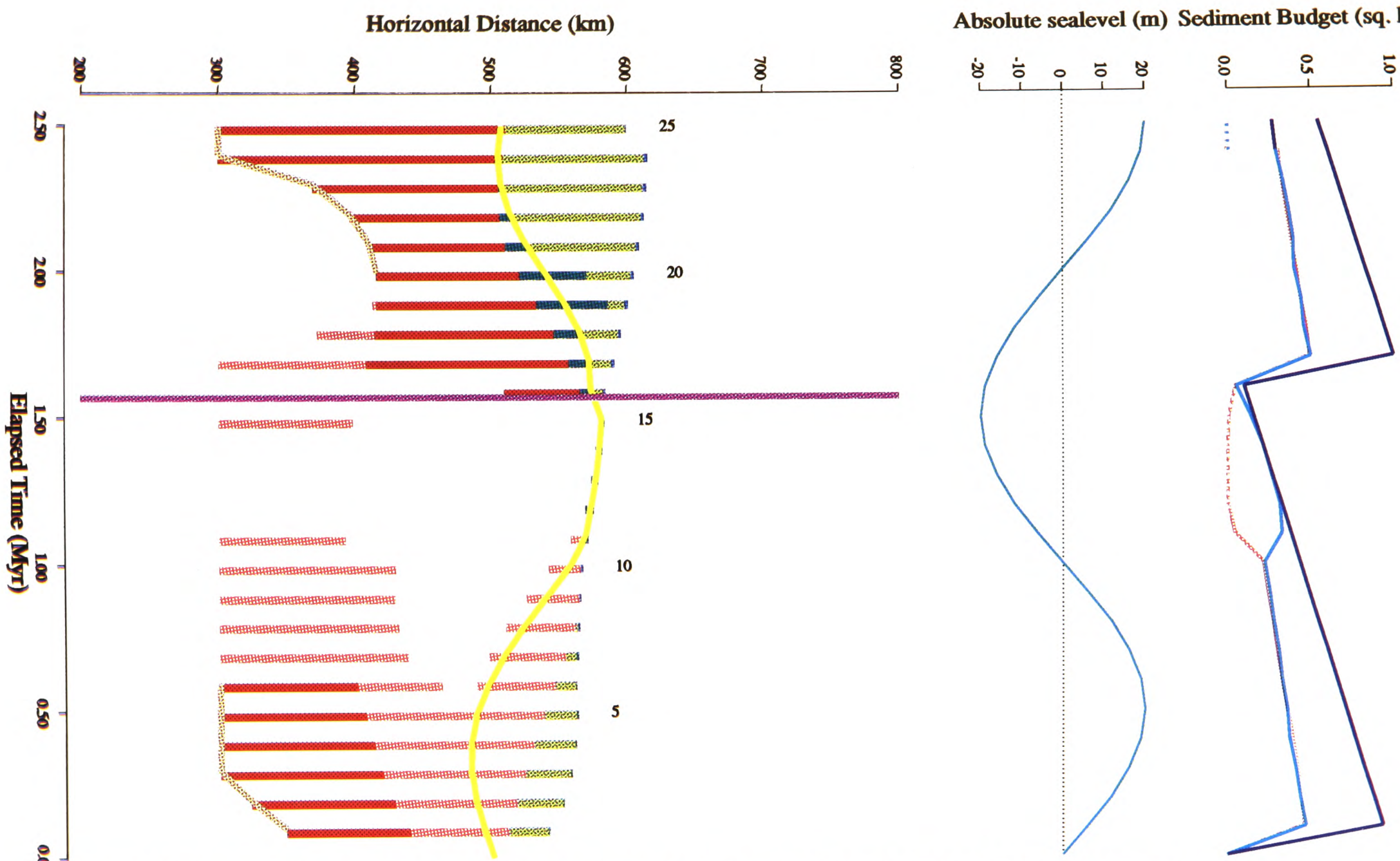

Figure 3.37. A chronostratigraphic diagram, an absolute sealevel curve, and a sediment supply curve from the model run with a saw-tooth external sediment supply curve ranging from 1.0 to 0.1 square kilometres per timestep with a period of 1.6Myrs. Sediment supply decreases steadily until chron 17 when it rises sharply. All other model parameters are the same as those used in the standard reference model. In this example the effects of the saw tooth sediment supply curve are less pronounced since the gradual fall in sediment supply occurs during a time of falling absolute sealevel, and the rise in sediment supply at an E.M.T. of 1.7Myrs reduces the erosive effect of the transgression.

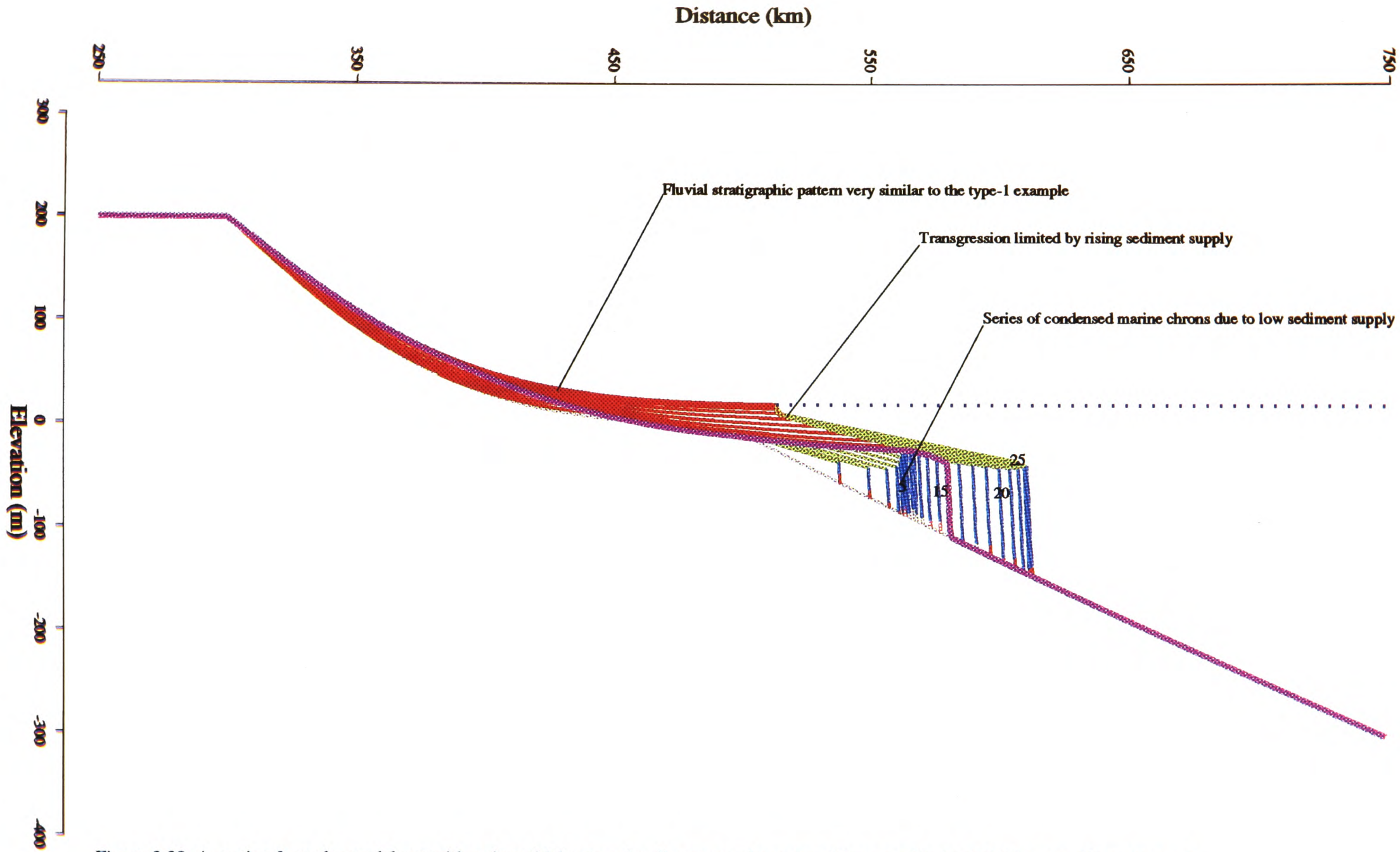

Figure 3.38. A section from the model run with a sinusoidal external sediment supply curve with an amplitude of 0.45 square kilometres and a period of 1.6Myrs (see figure 3.39). All the other model parameters are the same as those used in the standard reference model run. The impact of the variable sediment supply in this run is less pronounced than in some previous examples (e.g. figure 3.34) because the low point on the sediment supply curve occurs during a low point on the absolute sealevel curve. Consequently the period of low supply is expressed as a series of condensed chrons on the marine slope.

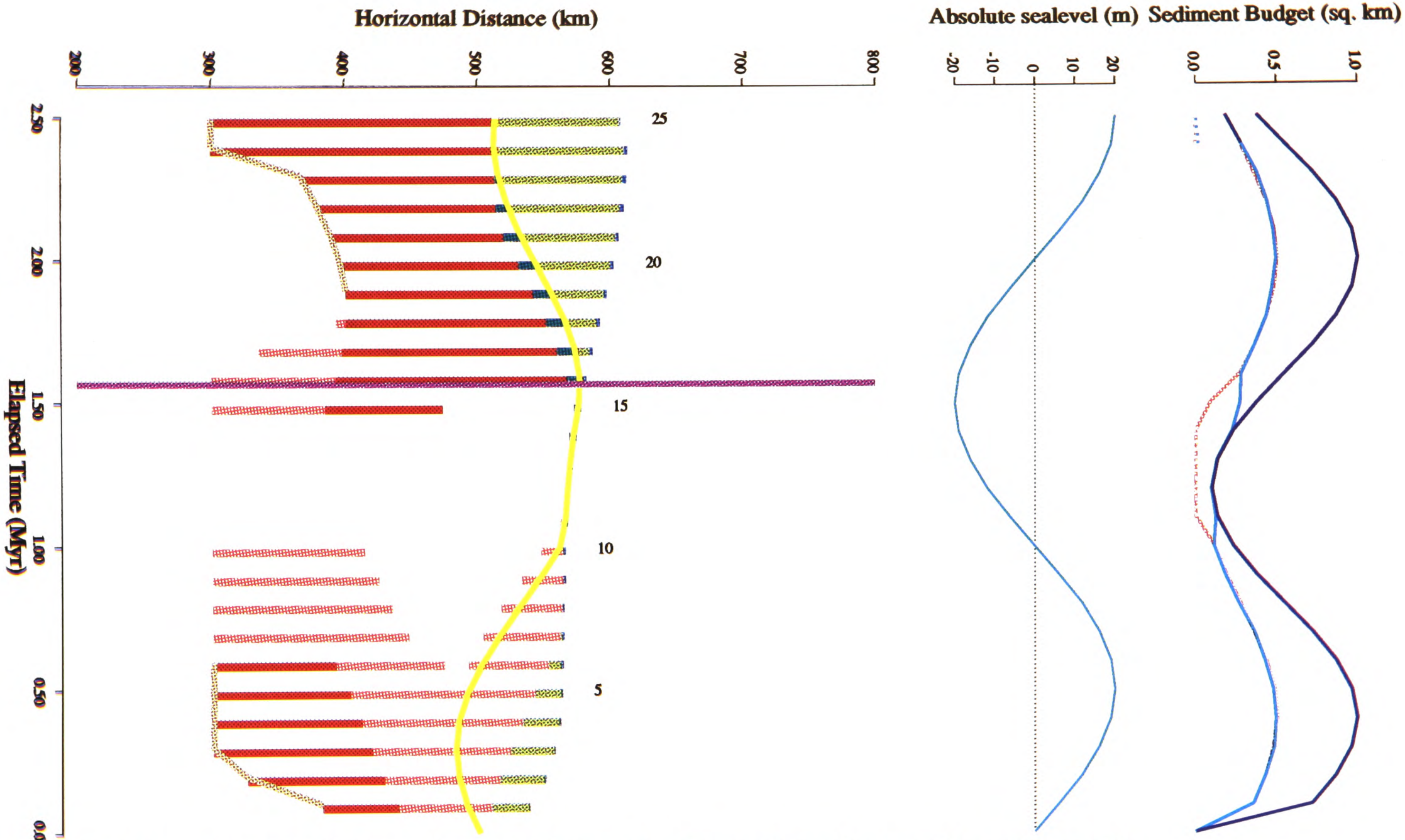

Figure 3.39. A chronostratigraphic diagram, absolute sealevel curve, and a sediment supply curve from the model run with a sinusoidal external sediment supply curve with an amplitude of 0.45 square kilometres and a period of 1.6Myrs. All the other model parameters are the same as those used in the standard reference model run. The impact of the variable sediment supply in this run is less pronounced than in some previous examples (e.g. figure 3.35) because the low point on the sediment supply curve occurs during a low point on the absolute sealevel curve. However, an increase in the lateral extent of fluvial erosion, and a reduction in the deposition of marine stratigraphy during the period of low sediment supply (E.M.T. 0.75 - 1.5Myrs) are clearly visible.

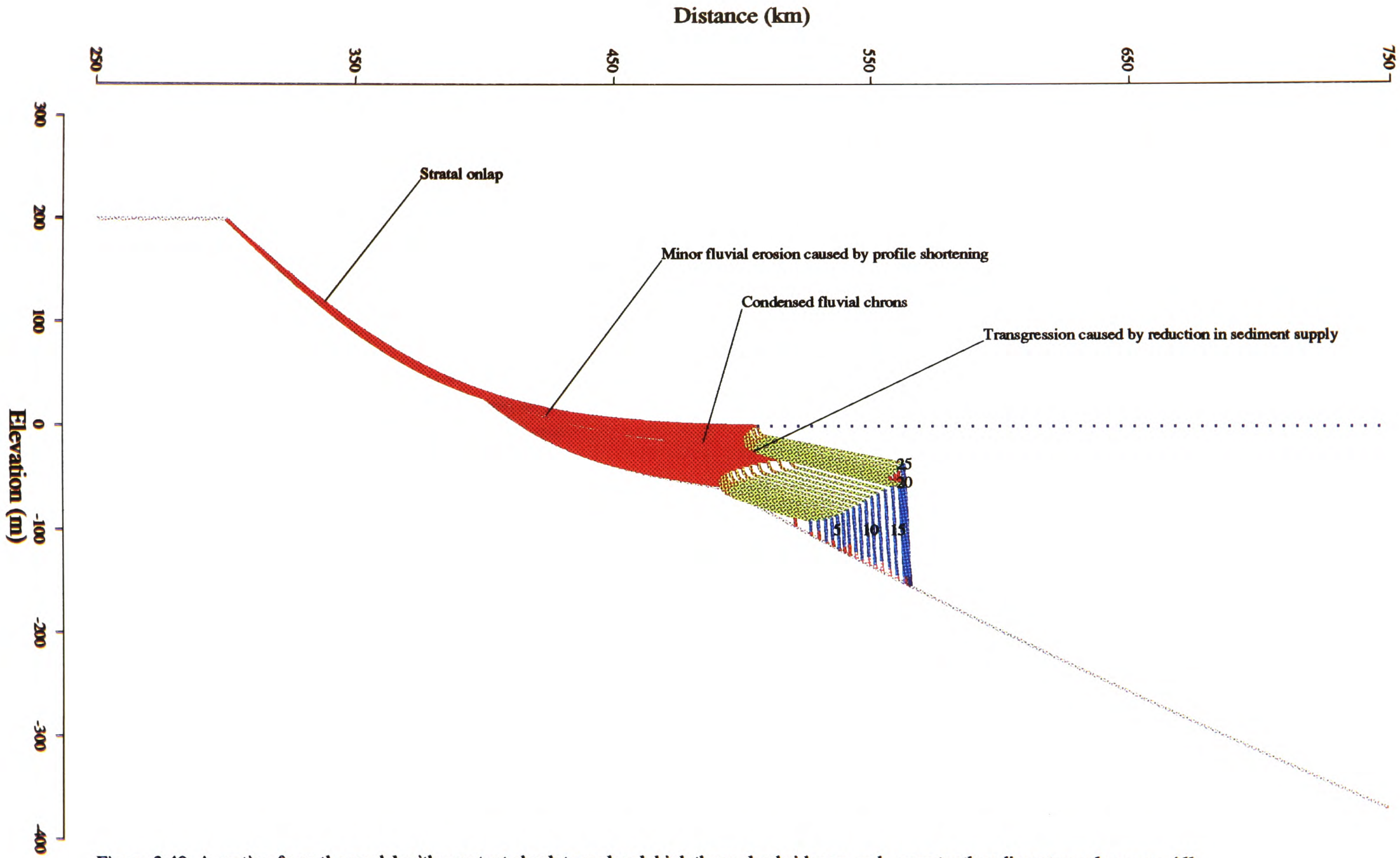

Figure 3.40. A section from the model with constant absolute sealevel, high thermal subsidence, and a saw-tooth sediment supply curve. All other model parameters are the same as those in the standard reference model. This example shows that some of the features of a type-1 sequence such as the stratal onlap and a transgressive ravinement surface can be produced in the model by variable sediment supply without absolute sealevel variations. However, it also demonstrates that one of the prime features of a type-1 sequence boundary, the vertical juxtaposition of fluvial stratigraphy against marine stratigraphy with a surface of erosion in between cannot be generated in this way.

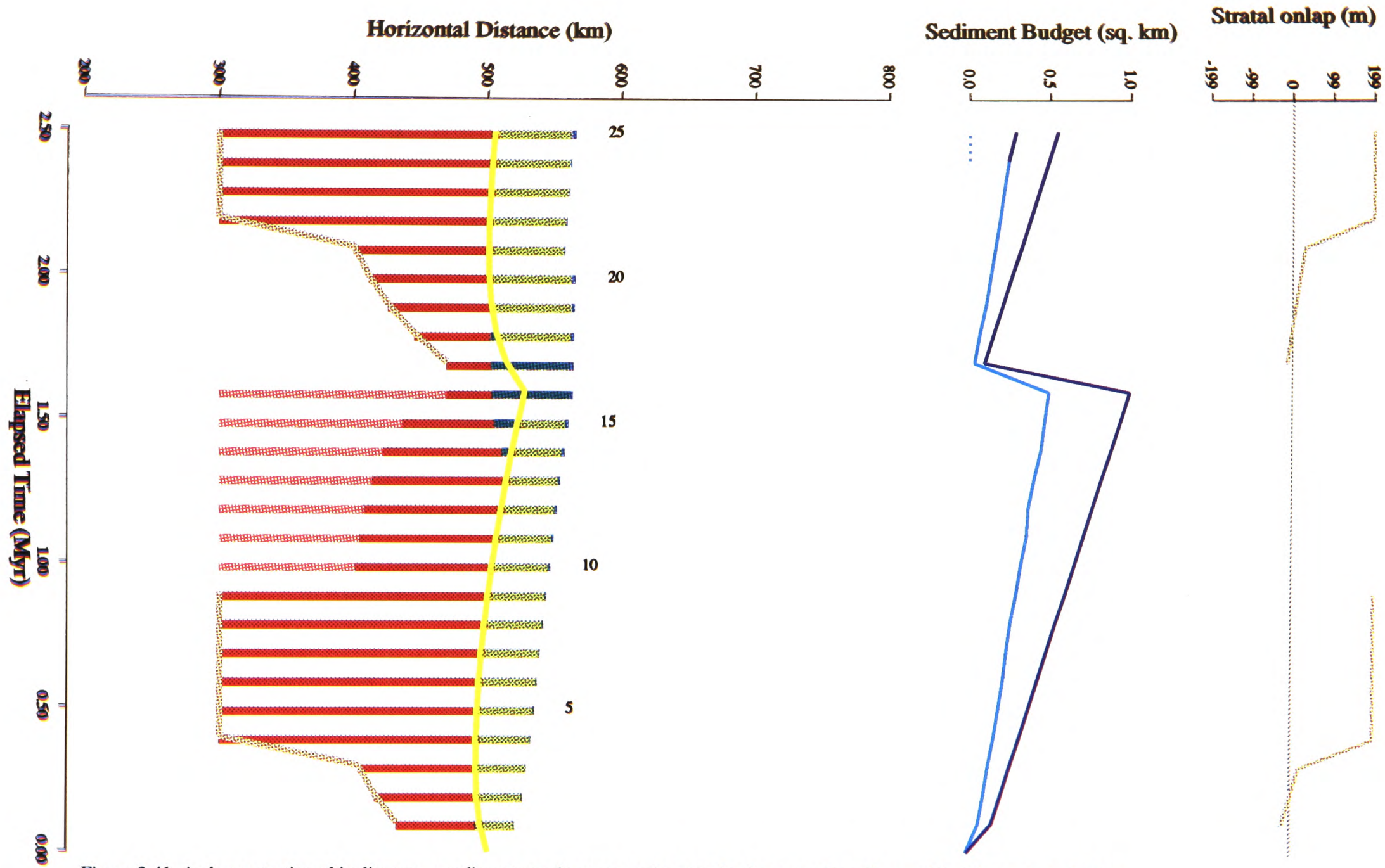

Figure 3.41. A chronostratigraphic diagram, a sediment supply curve, and a stratal onlap curve from the model with constant absolute sealevel, high thermal subsidence, and a saw-tooth sediment supply curve. All other model parameters are the same as those in the standard reference model. This example shows that some of the features of a type 1 sequence such as the stratal onlap and a transgressive ravinement surface can be produced in the model by variable sediment supply without absolute sealevel variations. However, it also demonstrates that one of the prime features of a type-1 sequence boundary, the juxtaposition of fluvial stratigraphy against marine stratigraphy with a surface of erosion or non-deposition in between cannot be generated in this way.

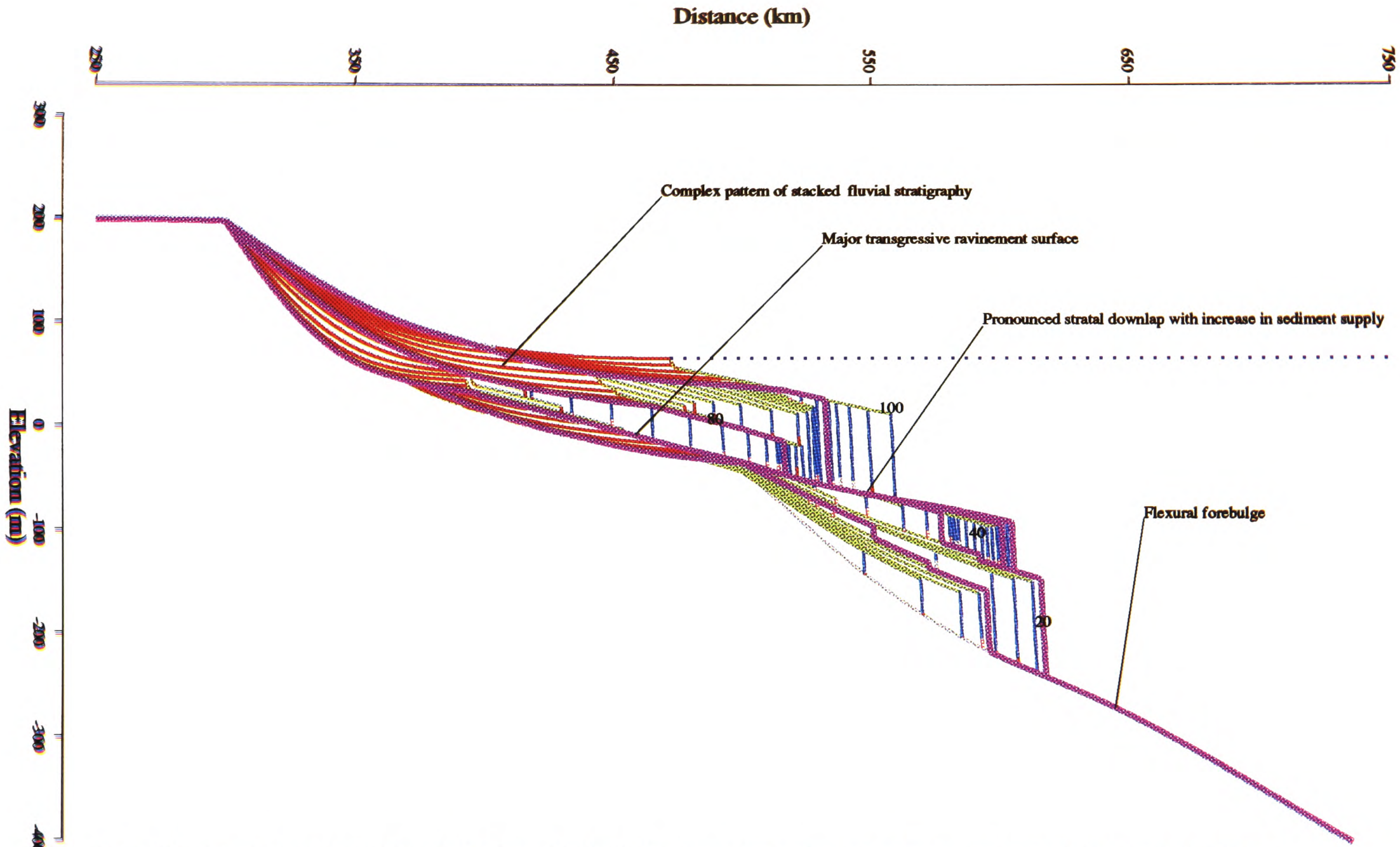

Figure 3.42. A section from the model run for 100 chrons (10Myrs) with a composite absolute sealevel curve made up from a 20m amplitude 2.0Myr sinusoidal curve superimposed upon a 15Myr 100m linear rise, a sinusoidal sediment supply curve with an amplitude of 0.45 square kilometres and a period of 1.6Myrs, a sinusoidally varying partitioning coefficient with an amplitude of 0.3 and a period of 1.4Myrs, and flexural isostasy with an elastic thickness value of 10km. All the remaining parameters are the same as those used in the standard reference model run. See the main text for a discussion of this model output.

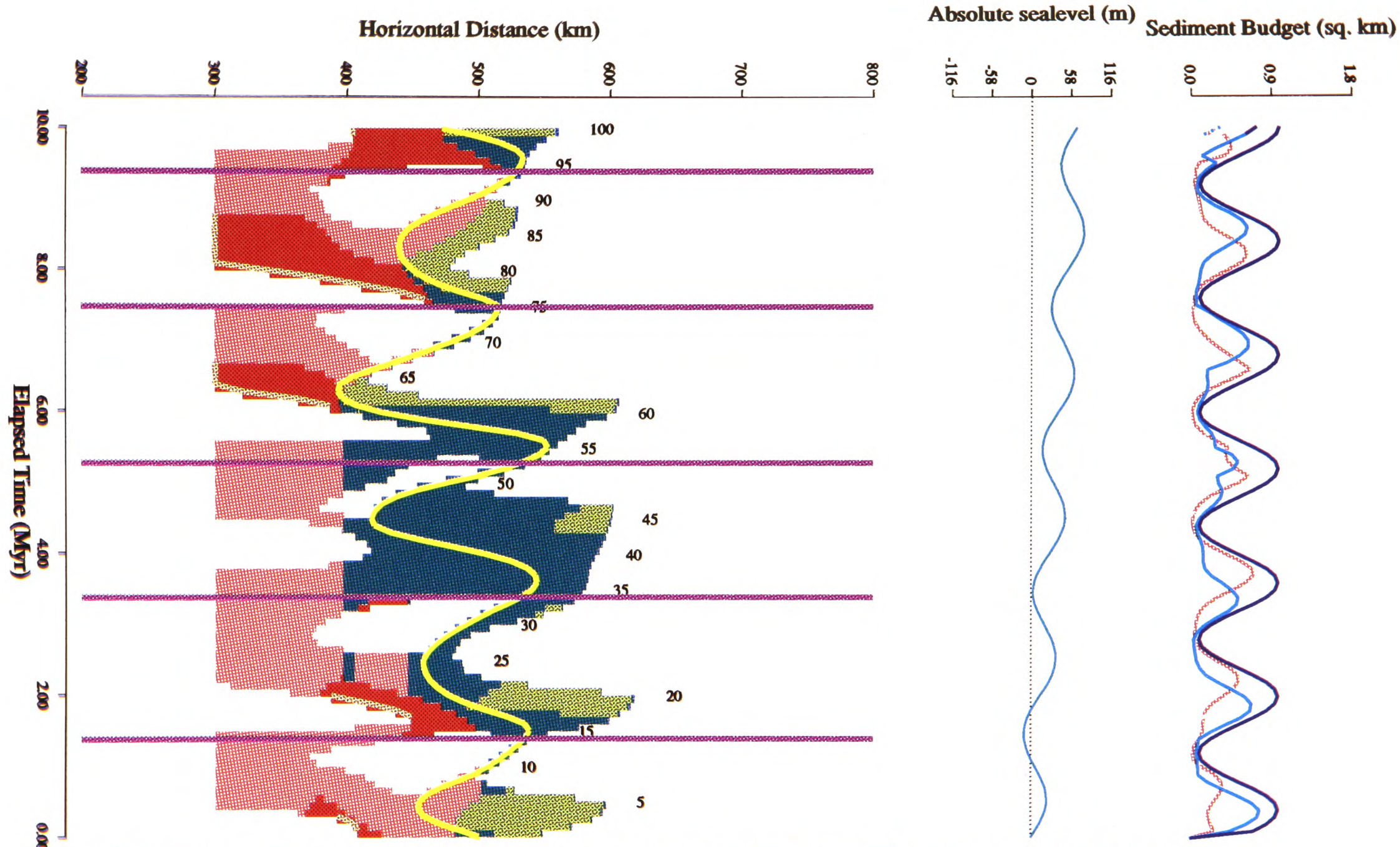

Figure 3.43. A chronostratigraphic diagram, an absolute sealevel curve, and a sediment supply curve from the model run for 100 chrons (10Myrs) with a composite sealevel curve made up from a 20m amplitude 2.0Myr sinsusoidal curve superimposed upon a 15Myr 100m constant gradient rise, a sinusoidal sediment supply curve with an amplitude of 0.45 square kilometres and a period of 1.6Myrs, a sinusoidally varying partitioning coefficient with an amplitude of 0.3 and a period of 1.4Myrs, and flexural isostasy with an elastic thickness value of 10km. All the remaining parameters are the same as those used in the standard reference model run. See the main text for a discussion of this model output.

Chapter 4

Chapter 4 - Complex interactions, cyclicity and numerical instabilities

"I'll keep a vigil in a wilderness of mirrors,

where nothing here is exactly as it seems.

We stand so close, but never understand it,

for all that we see is not all that it seems.

Am I blind?"

(Derek Dick, Vigil)

4.1 Introduction

The purpose of this chapter is to use the quantitative stratigraphic model to illustrate some of the problems that can occur in attempting to use a discretised model to investigate cyclical stratigraphic systems. Simple numerical experiments demonstrate the existence within the model of a complex feedback effect between thermal subsidence, deposition, erosion, and flexure. The feedback effect in the model produces cyclical stratigraphic patterns without external cyclical forcing. It is shown that the effect occurs in the model with a variety of initial conditions. However, the feedback effect is due to a numerical instability in the model. Consequently no conclusions can be drawn from the model behaviour regarding the possible existence of such feedbacks in natural stratigraphic systems.

4.2 Previous work

It is a common assumption in stratigraphic studies that periodic cyclicity in stratigraphy must be the result of external periodic forcing mechanisms (e.g. Steiner, 1973; Hays *et al.* 1976; Posamentier *et al.* 1988;Van Wagoner *et al.* 1990; Fischer, 1991; Vail *et al.* 1991; Quinn, 1991). Such assumptions are often based on tenuous evidence. For example, Van

Wagoner *et al.* (1990) attributed observed parasequence geometries to fourth or fifth order cycles in eustatic sealevel. No attempt was made to provide a mechanism for such high-order eustatic cycles, and this is particularly problematical since such parasequences are found throughout the stratigraphic column. Even if glacioeustasy is invoked as a causal mechanism, many periods of earth history show little or no evidence of the extensive ice sheets necessary to drive such glacioeustatic cycles.

More recently, attention has started to focus on possible alternative explanations. Shaw (1987) and Slingerland (1989) showed how even simple non-linear dynamic systems can produce periodic results through non-linear coupling between components in the system. This raises the possibility of such behaviour in natural stratigraphic systems, which often seem to be non-linear systems (Slingerland, 1989) and hence prone to such behaviour. Swift *et al.* (1991) discussed briefly the possibility that periodic stratigraphy at the parasequence level may be produced by non-linear interaction between components of stratigraphic systems such as sediment input rate, sediment character, sediment transport rate, and relative sea level change.

Gaffin and Maasch (1991) and Gaffin (1992) took the idea of non-linear interactions in stratigraphic systems a step further, and developed a simple stratigraphic model derived from a mass-conservation model for palaeo-ice sheet cyclicity. The stratigraphic model showed how base level instability resulting from positive feedbacks within the system can lead to non-linear behaviour, including free oscillations, which produce periodicity without external forcing.

Although Gaffin (1992) presented some very interesting ideas, the model is very simplistic, being heavily dependent upon the idea of a diffusion front beyond which sediment is not transported to provide a non linearity and hence a feedback effect in the model. In order to investigate the concepts of unforced oscillations in stratigraphy further, it is necessary to use a more detailed stratigraphic model. The model results presented

below give an example of how complex interaction between non-periodic model components can produce periodic patterns in modelled stratigraphy, and illustrate some of the potential problems in using discretised models to investigate non-linear oscillating systems.

4.3 Initial conditions

Figure 4.1 summarises in diagrammatic form some of the initial conditions for the standard reference model. The values selected are generally arbitrary values, but are constrained by observations of passive rift margins (e.g. Watts, 1988; Klitgord *et al.* 1988). The model run consists of fifty chrons generated with an interval of 100Kyrs, giving a total elapsed model time of 5Myrs. Thermal subsidence is produced by the one-layer stretching model of McKenzie (1978) with arbitrary stretching values from 1.0 at 400km, to 1.1 at 500km, to 4.0 at 1024km (figure 4.1). The lithosphere is given an arbitrary initial thermal age, or age since the onset of thermal subsidence, of 10Myrs. Absolute sealevel is held constant at 0.0m throughout the model run.

The flexural response of the lithosphere to deposition and erosion is calculated assuming an instantaneous response. The value of T_e is held constant at 10km over the period of the model run. The density of loading and unloading is taken as $1800kgm^{-3}$ to represent the density of uncompacted sediment.

The fluvial profile is modelled using a complementary error function with a length scale value of 3.0, which produces a steep upstream section, and a relatively flat coastal plain. The profile maintains a fixed geometry through the model run, as described in section 2.6.5.2. Portions of the profile which are uplifted due to flexure are eroded such that the original profile geometry is maintained. However, the lower portion of the profile is allowed to subside and be inundated in a relative sealevel rise without responding by aggradation (figure 2.8). This behaviour is analogous to a fluvial system with very low

sediment supply that is unable to aggrade following the relative sealevel rise. The length of the profile is held constant at 200km. The submarine profile consists of a 10m high, 2km wide shoreface, which passes into a shelf profile of gradient $0.001 mkm^{-1}$. This is in turn passes into a marine slope with a gradient of $0.04 mkm^{-1}$. Sediment supply is calculated for each time step from the area of sediment eroded on the fluvial and marine profiles. There is no external sediment input.

4.4 Model results

Results from the model run with the initial conditions described in section 4.3 show a complex interaction between four model components, namely thermal subsidence, erosion, flexure, and deposition.

4.4.1. The feedback mechanism

Figure 4.2 shows a simplified diagrammatic explanation of the feedback mechanism.

- 4.2.A shows the initial conditions, with thermal subsidence on the lower portion of the fluvial profile about to cause a relative sealevel rise, allowing a marine transgression.
- Figure 4.2.B shows the shoreface has jumped landward in response to the thermal subsidence, and erosion on the shoreface has caused flexural uplift in response to the unloading.
- Figure 4.2.C shows how this uplift on the lower portion of the fluvial profile is then removed by subsequent fluvial erosion, which in turn creates more uplift, of lower amplitude.
- This uplift is then removed by further fluvial erosion (figure 4.2.D), and thermal subsidence is on the point of outpacing the uplift, which will lead to a further transgression.

This cycle is repeated until the shoreface approaches the hinge point, where the stretching values are so low that thermal subsidence can no longer drive the shoreface landward, and the feedback effect ceases.

4.4.2. The standard reference model

Figure 4.3 shows a section from the model run with the standard parameters described in section 4.3. The main features to note in the section are the pulses of greater deposition visible in the distal portion of the stratigraphy. These are interspersed with chrons which do not extend so far into the basin, and represent periods of lower sediment supply. The distance of progradation of progressively younger chrons into the basin gradually decreases, until by the time of chron 30, deposition is minimal.

The chronostratigraphic diagram, and the sediment supply curve (figure 4.4) show more clearly the pattern of stratigraphy produced by the feedback effect. The spikes of erosion and deposition produced by the landward migration of the shoreface can be clearly seen. Each spike on the sediment supply curve matches a pulse of deposition on the Wheeler diagram (e.g. chron 5 at 0.5Myrs E.M.T.), and a jump landward in the position of the beach. The periods in between spikes show more restricted deposition, much of which has been removed by subsequent marine erosion. The Wheeler diagram also shows that the position of the beach stabilises after chron 15 at approximately 430km. After this time the beach continues to move landward very slowly, and there are no more jumps in the beach position. The position on the profile of the transition is determined by the distribution of thermal subsidence on the model profile. Landward of the 420km position the magnitude of the thermal subsidence is insufficient to cause further landward jumps, but the beach continues to move gradually landward, towards the hinge zone at 400km, driven by the small amounts of thermal subsidence still occurring (see the initial conditions shown in figure 4.1 and the discussion in section 4.3).

4.4.3. Sensitivity tests

Systematically changing some of the key parameters from the values used in the standard reference model run should identify the critical parameters, and the initial conditions, necessary for the feedback effect to operate. This will lead to a better understanding of the sensitivity of the effect to the model parameter values. Such understanding is important in order to correctly interpret the significance of the effect, and to determine under which conditions, if any, such a feedback effect may operate in natural stratigraphic systems.

Thermal subsidence and elastic thickness of the lithosphere

Thermal subsidence and flexure appear to play a key role in the feedback mechanism. Figure 4.5 shows chronostratigraphic diagrams and sediment supply curves from the model run with high and low values for the stretching factors, and high and low values for the lithospheric elastic thickness. The model runs show that the presence of the oscillatory behaviour is unaffected by the changed parameters, although in each case the exact detail of deposition and erosion is changed. The most significant change the shortening of the duration of the feedback effect shown in the example with higher magnitudes of thermal subsidence (figure 4.5.B). This reduced duration is due simply to the higher magnitudes of thermal subsidence moving the shoreline towards the hinge point more rapidly.

Fluvial and marine profile geometry

These profile geometries are the other two model parameters likely to be of significance to the feedback effect. To test this possibility, figure 4.6 shows another set of four chronostratigraphic diagrams and sediment supply curves from the model run with more and less concave fluvial profile geometries, and two different shoreface geometries. The shoreface geometry does not significantly alter the basic pattern of oscillations and

deposition and erosion of stratigraphy. The geometry of the fluvial profile, however, plays a more important role in the feedback.

The example in figure 4.6.A shows the effect of using a less concave profile. The reduction in profile concavity leads to higher slopes on the lower fluvial profile, and this inhibits the landward movement of the beach, forcing it to move landward in smaller jumps. Consequently the amplitude of the flexural uplift is reduced to such an extent that it no longer acts to block landward beach movement, and the oscillations no longer occur. The example in figure 4.6.B shows that increasing the concavity of the profile has the opposite effect, the lower slopes accentuating the jumps in beach position, leading to increased amplitude sediment supply peaks, and a reduced duration for the feedback.

These sensitivity tests demonstrate that the feedback effect is relatively insensitive to shoreface geometry, but very sensitive to the geometry of the fluvial profile.

Duration of the model time steps

Since the model is a discretised representation of continuous processes, it is important to test, as far as possible, the impact of the discrete model time steps on the feedback effect. The model includes several elements that are not time dependent such as the fluvial and marine profiles, and it is these elements that have the potential to introduce unstable behaviour to the model.

Figure 4.7 shows output from the model run with a time step of 50Kyrs, which is half the value used in the standard reference model. Looking at the sediment supply curve it is apparent that the oscillations in sediment supply are still present with the reduced time step. Most significantly, the oscillations in this model run have a period of two or three time steps, as they do in the standard reference model. However, since the model time step in figure 4.7 has been halved, the periodicity of the oscillations has also been halved, from

200 - 300Kyrs, to 100 - 150Kyrs. This suggests that the periodicity is directly dependent upon the magnitude of the time step used. The total duration of the oscillations in figure 4.7 is thirty five time steps, or 1.75Myrs. This is slightly more than half the total duration of 2.95Myrs of the oscillations in the standard reference model. Thus halving the model time step halves the periodicity of the sediment supply oscillations, and reduces by a factor of 0.59 the total duration of the oscillations.

Halving the model time step once more to a value of 25Kyrs shows a similar result. The period of the oscillations in figure 4.8 is again two to three model steps, or 50 to 75Kyrs. The duration of the oscillations has been reduced to thirty six model time steps, or 0.9Myrs, which is close to half the duration of 1.75Myrs seen in figure 4.7.

These two model runs strongly suggest that the oscillatory behaviour produced by the model with the specified initial conditions and parameter values is a numerical instability created by the discretised nature of the model. The fact that the period of the oscillation is halved when the model time step is halved suggests that the period would approach zero as the model time step approached zero. Figure 4.9 shows a contour plot of sediment supply values produced from one thousand model runs each with twenty five time steps ranging in magnitude from 0.1Kyrs to 0.1Myrs. The contours pick out the peaks of sediment supply produced by the feedback effect in the model. The first two peaks in each model run occur consistently at model steps one and four for each of the one thousand model runs. Thus the period of the oscillations ranges from 0.3Myrs to 0.3Kyrs, demonstrating irrevocably that the periodicity is dependent only upon the model time step. Note that the magnitude of the sediment supply peaks decrease as the time step decreases. This is due to the reduced distance of movement of the beach with smaller time steps, and is a further indication of numerical instability.

Figure 4.10 is a plot showing how the timing of the second sediment supply peak varies with model time step duration. The plot demonstrates the well-defined linear trend

between timing of the peak and the model time step for the first twenty model runs shown in figure 4.9. The intercept value on the best fit line is zero which demonstrates that as the time step duration is reduced to zero, the periodicity of the sediment supply is also reduced to zero. Thus the oscillations in the model described can be said with confidence to be the result of a numerical instability resulting from the time-independent discretisation represented by several of the model components.

Flexural response time

Thermal subsidence is the only time dependent component of the model used in the model runs in figures 4.4 to 4.8. This section investigates the effects on model output of introducing a simple time dependency to the flexural component of the model.

Studies of the response of the lithosphere and the asthenosphere to post-glacial unloading (Walcott, 1970a; Walcott, 1970b; Peltier, 1986; Bills and May, 1987; Sigmundson, 1991) suggest that both require a finite period of time in order to return to compensated equilibrium after a loading or unloading event. Walcott (1970b) suggests a response time for the asthenosphere in the order of 10 to 20Kyrs on the basis of the continued up-warping of the region of Canada previously covered by the Laurentide Ice Sheet. Sigmundson (1991) suggests a much shorter time period, in the order of 1000 years, from studies of postglacial rebound in Iceland.

The response of the lithosphere to loading and unloading is still poorly understood. There are few data or model information regarding the response of the lithosphere in the period between the very short term, (i.e. 10^3 yrs) when the response is controlled by the seismic thickness of the lithosphere, and the long term (i.e. 10^6 yrs) when the response is controlled by the elastic thickness (Bodine *et al.* 1981). The interval between is controlled by a process of stress relaxation, the understanding of which is crucial to understanding the lithospheric flexural response. Although work has been done regarding stress relaxation

using the concept of the yield strength envelope (e.g. Watts *et al.* 1980; Bodine, 1981; Bodine *et al.* 1981), understanding of the processes involved is still poor.

The response time of the lithosphere to loading and unloading events of various magnitudes and wavelengths may well be important in the behaviour of the feedback effect, and yet as discussed, it is not well understood. In order to test this possibility, the following model runs use a very simple method to spread the flexural response over several model time steps. The methodology is described in detail in section 2.6. Although it is very simplistic, it should be adequate to test the importance of flexural response time to the feedback effect.

Linear flexural response

Figure 4.11 shows a chronostratigraphic diagram and a sediment supply curve from the model run with a time step of 25Kyrs and a flexural response time of 0.1Myrs. This is significantly longer than the response time suggest by Walcott (1970b), but the purpose of this model run is simply to test the potential importance of a response time longer than the duration of the model time step. Figure 4.11 shows the effect of this response time on the behaviour of the feedback coupling. The pulses of deposition and erosion have been spread out such that the period between the three major pulses at chron 1, chron 7 and chron 13 has a mean value of 0.163Myrs. The fact that the inclusion of the linear flexural response in this model run changes the periodicity suggests that it contributes significantly to the model behaviour, and thus warrants further investigation.

Figure 4.12 is a contour plot of sediment supply of the same type as that shown in figure 4.9. Exactly the same methodology was used to generate both plots, but the model runs used to produce figure 4.12 included a linear flexural response with a response time of 0.1Myrs. Comparison of the two plots shows that the complexity of the model behaviour has been increased with the inclusion of the linear flexural response. Whereas in figure 4.9

the peaks in sediment supply occur consistently at particular model steps, in figure 4.12 this is no longer the case. For example, for a model time step duration of 40Kyrs, the second peak of sediment supply occurs at step five. However, for time step durations of 80Kyrs and 20Kyrs, the second peak occurs at step seven. The timing of the second peak for time step durations of 20Kyrs and less shows an interesting trend. As the time step duration decreases, the peak occurs at later step numbers, reduces in magnitude, and other peaks are introduced at earlier steps.

Converting the model step number to a value of elapsed model time shows that the peak is not occurring at the same E.M.T. This is demonstrated in figure 4.13 which plots the timing of the occurrence of the peak for different time steps. The plot shows that the relationship between the time of the peak occurrence and the model time step is non-linear. The non-linearity has been introduced by the inclusion of the flexural response time.

Thus although the inclusion of the finite flexural response time in the model has added an element of time dependency to the pattern of the oscillations of sediment supply, it has not removed the numerical instability.

4.5 Summary

1. There exists within the model, when run with the initial conditions described, a feedback effect between thermal subsidence, shoreface erosion, flexure and fluvial erosion, which is capable of producing cycles of synthetic stratigraphy without any external periodic forcing.

2. The effect occurs with a variety of initial conditions. Though variations in the initial conditions affect the details of the stratigraphic pattern, the basic pattern produced by the feedback effect is present in all the sensitivity tests which varied thermal subsidence, flexural and geomorphological model parameters.

3. Running the model with different time steps demonstrates that the period of the oscillations in sediment supply is entirely dependent upon the length of the time step used. Peaks in sediment supply always occur at the same chron regardless of the E.M.T. that the chron represents. As the model time step is reduced towards zero, so the period of the oscillation approaches zero. This demonstrates that the feedback effect in the model is a numerical instability resulting from the discretised nature of the model.

4. Running the model with a finite value for the flexural response time that is longer than the length of the time step shows that the inclusion of the response time complicates the unstable behaviour of the model, but does not surmount the fundamental problem of the instability. The timing and period of the oscillations are still dependent on the duration of the time step used, but no longer show a simple linear relationship with time step duration.

5. Although it seems intuitively possible that the feedback mechanism described may occur in natural stratigraphic systems, the stratigraphic model presented here can provide no indication either way of the existence of such a feedback. This is due to the numerical instability inherent in the model as a result of the discretised representation of continuous functions. Further investigation of potential feedback effects would thus require a model formulated with continuous time-dependent equations.

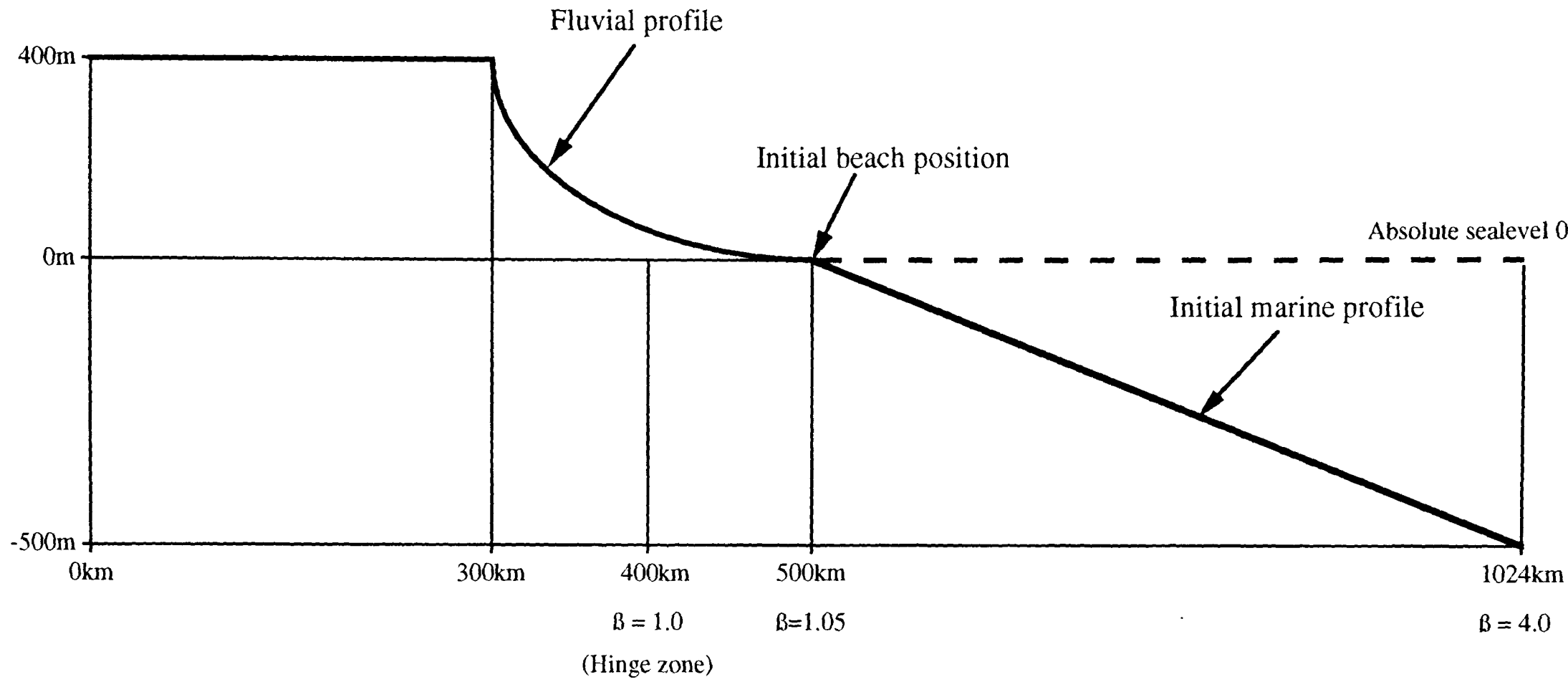

Figure 4.1 A diagrammatic summary of the initial conditions for the standard reference model. Note particularly the distribution of stretching values, the position of the hinge zone, and the starting position of the beach.

A) Initial conditions - thermal subsidence is set to cause a relative sealevel rise and force the shoreface landwards.

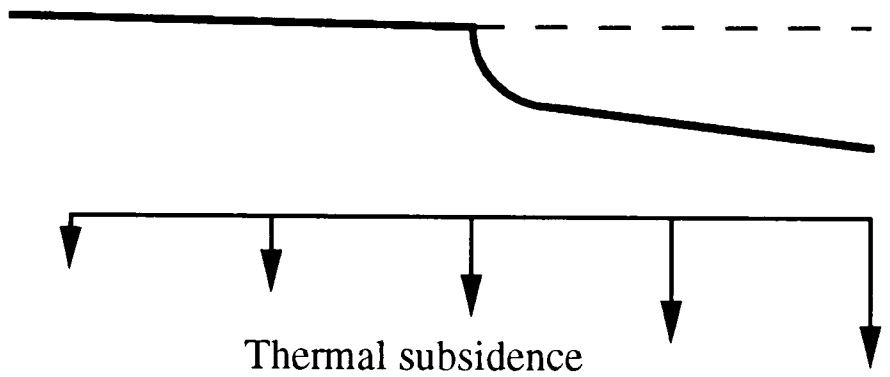

B) Shorface erosion causes flexural uplift.

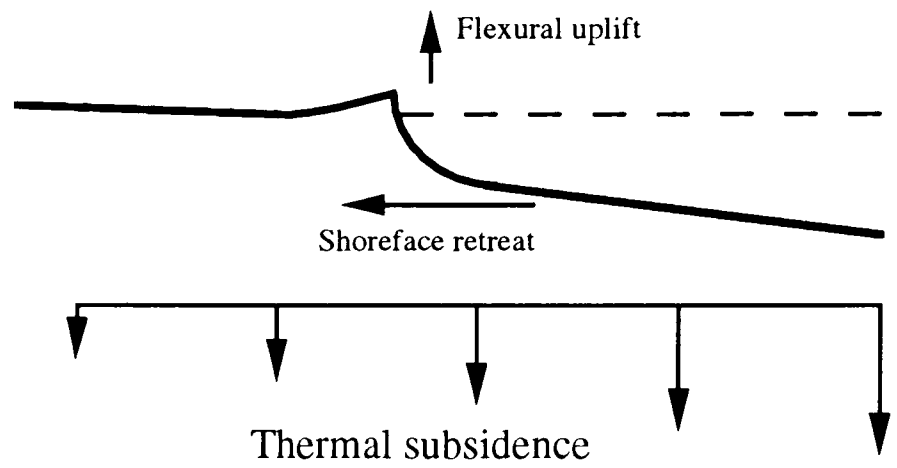

C) Fluvial erosion removes the uplift, causing further flexure of lower amplitude.

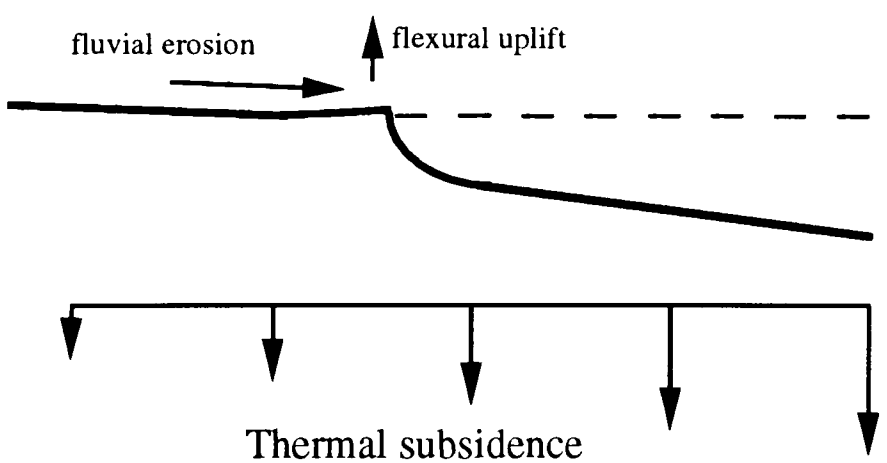

D) Fluvial erosion and thermal subsidence combine to lower the coastal plain ready for another transgression.

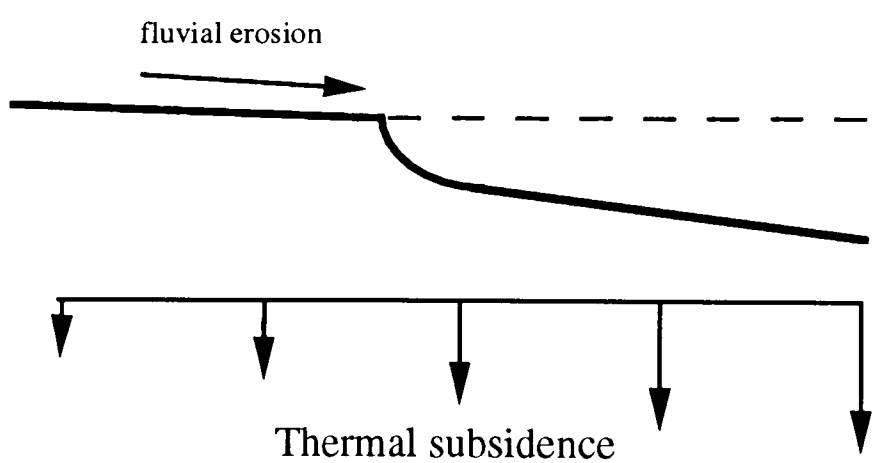

Figure 4.2

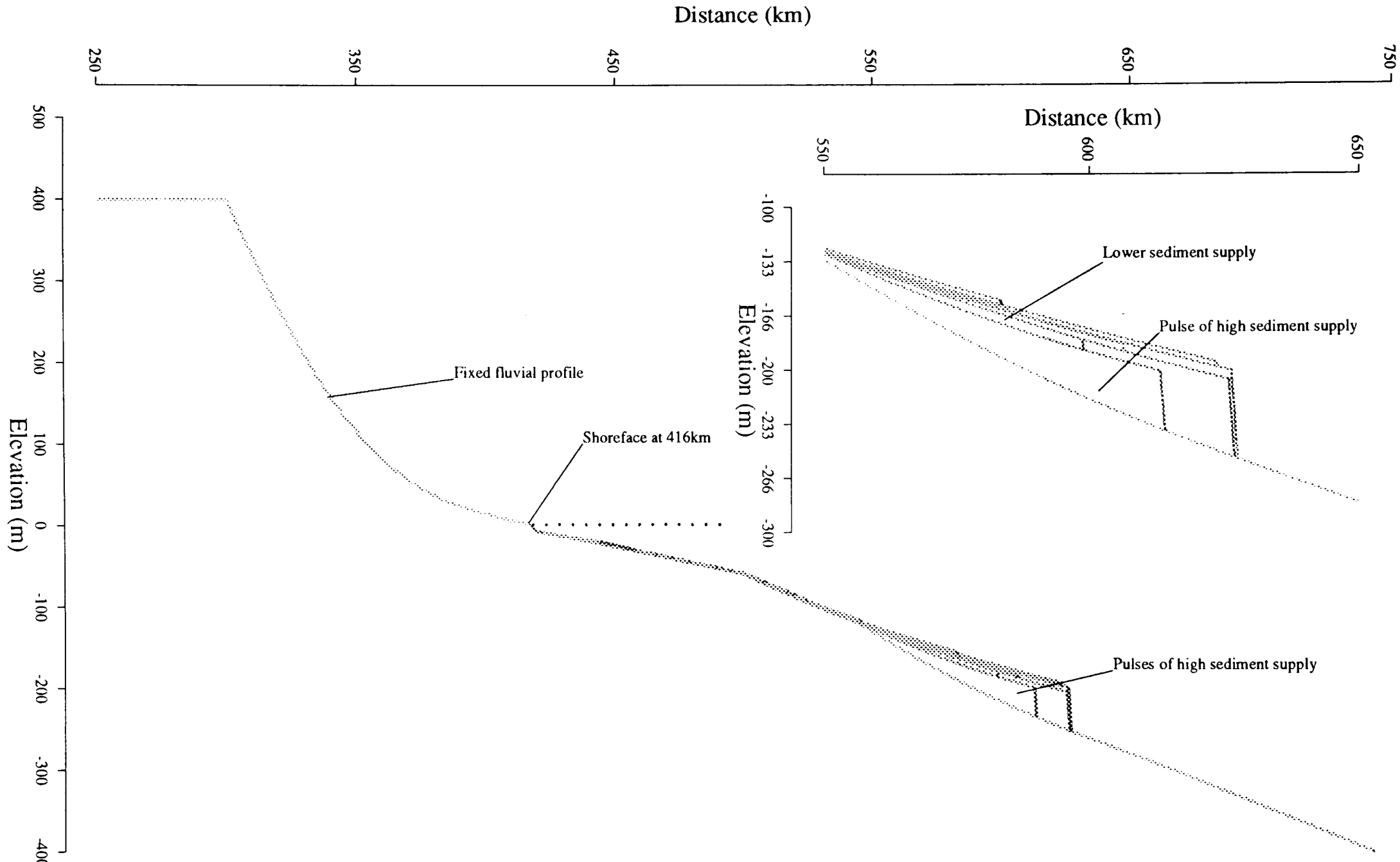

Figure 4.3. A section from the standard reference model run. The run is composed of 50 chrons with an interval of 0.1Myrs. Stretching factors range from 1.0 at 400km, to 1.1 at 500km, and 4.0 at 1000km. Elastic thickness is held constant at 10km. Absolute sealevel is constant at 0m. Sediment supply is calculated from the fluvial and marine profile erosion, with no external sediment input. Significant features of the model run such as the shortend fluvial profile, the erosion on the inner shelf, and the pulses of deposition on the more distal portions of the profile are clearly visible.

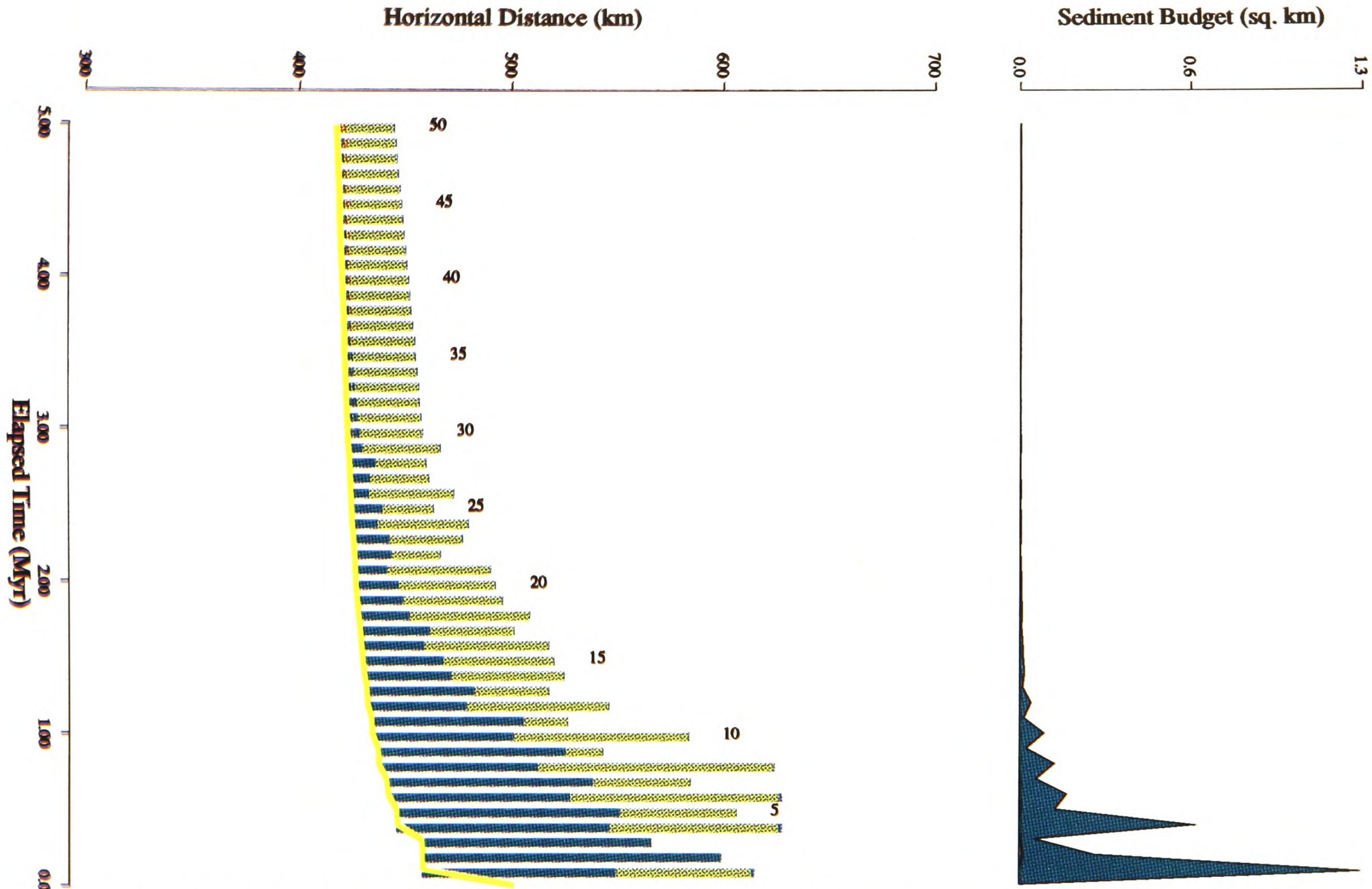

Figure 4.4. A chronostratigraphic diagram and a sediment supply curve from the standard reference model run. The model run is composed of 50 chrons, with an interval of 0.1Myrs. Stretching factors range from 1.0 at 400km, to 1.1 at 500km, and 4.0 at 1000km. Elastic thickness is held constant at 10km. Absolute sealevel is constant at 0m. Sediment supply is calculated from fluvial and marine profile erosion, with no external sediment input. Note the cyclicity in the pattern of marine downlap and sediment supply due to the landward jumps in the beach position.

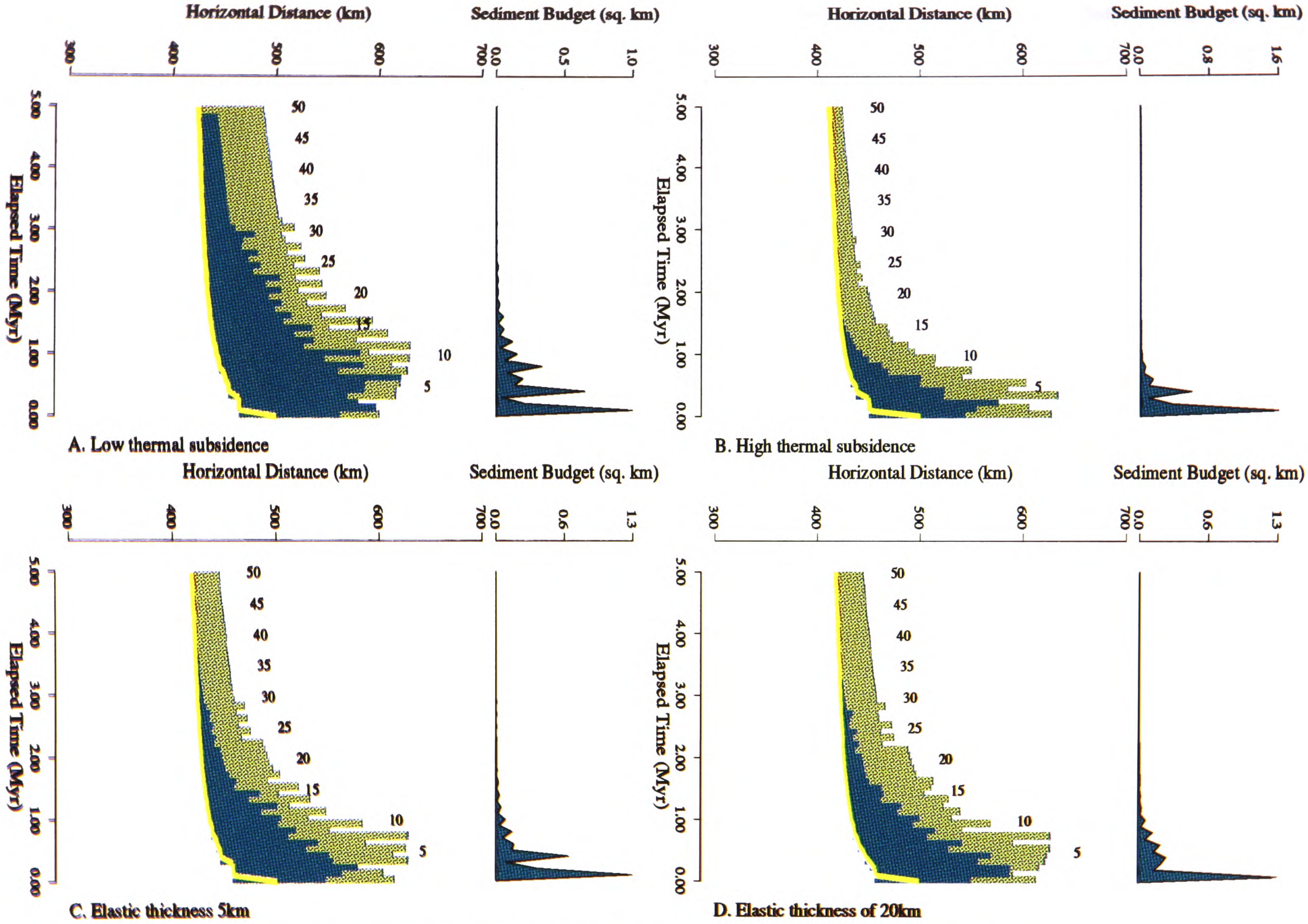

Figure 4.5. Chronostratigraphic diagrams and sediment supply curves from model runs with low and high thermal subsidence, and low and high elastic thickness values. The plots demonstrate that the feedback effect persists for these different model parameters.

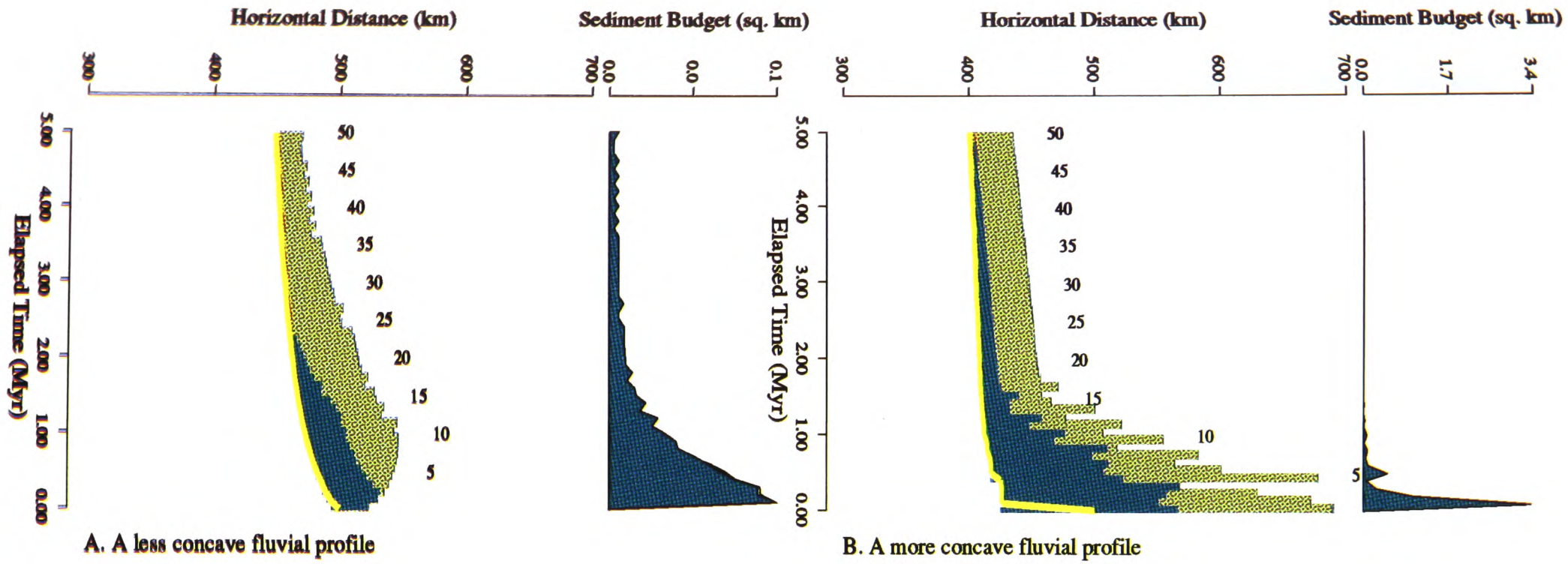

Figure 4.6. Chronostratigraphic diagrams and sediment supply curves from model runs with different fluvial and shoreface profile geometries. The diagram demonstrates the sensitivity of the feedback effect to decreasing the concavity of the fluvial profile, and its relative insensitivity to a more concave fluvial profile and different shoreface geometries.

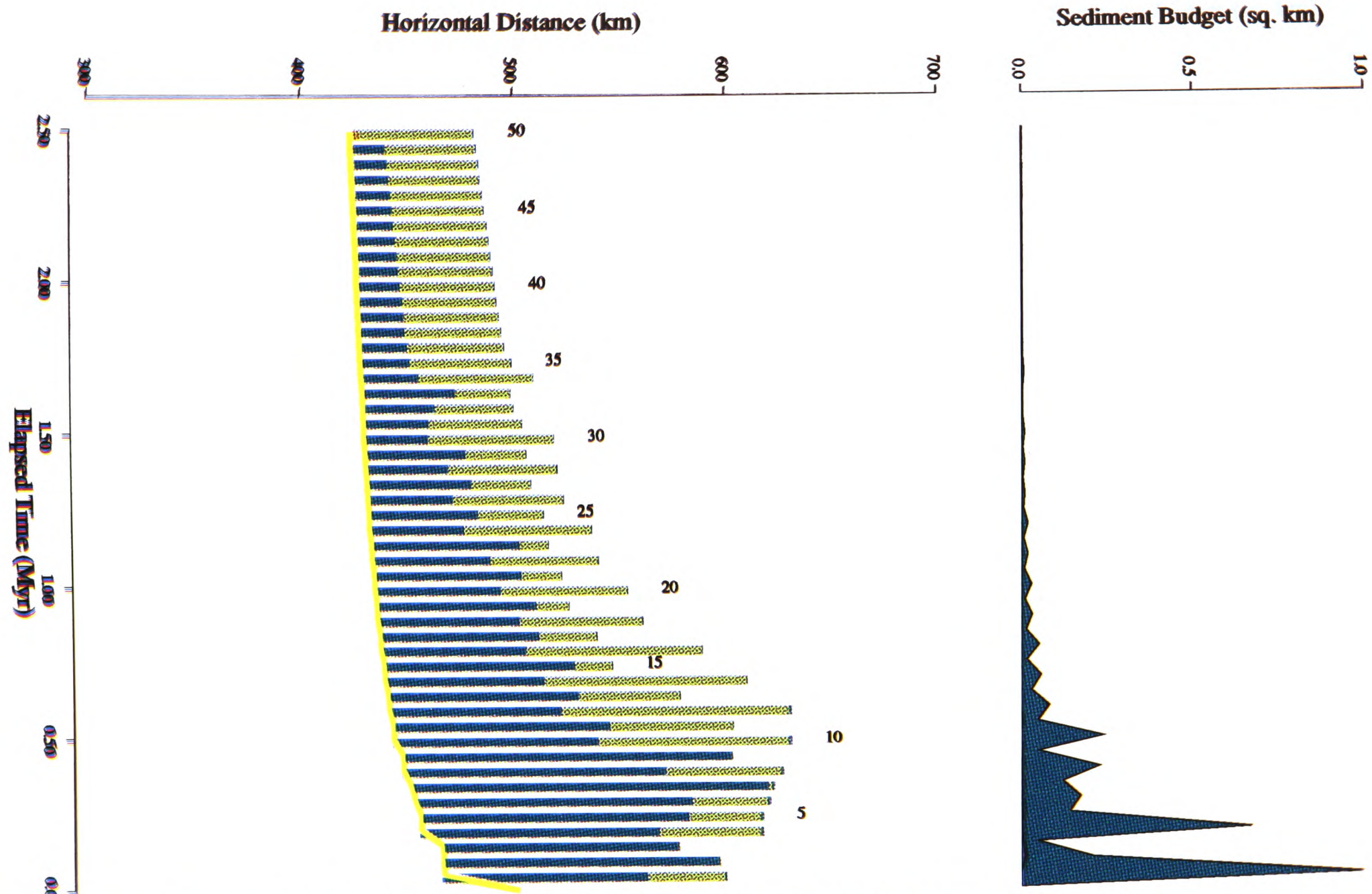

Figure 4.7. A chronostratigraphic diagram and a sediment supply curve from the model run with a timestep of 0.05Myrs. All other parameters are the same as those used in the standard reference model. The halving of the timestep duration has halved the period of the sediment supply oscillations. Note also that the magnitude of the sediment supply has been reduced due to the lower magnitude of thermal subsidence per time step.

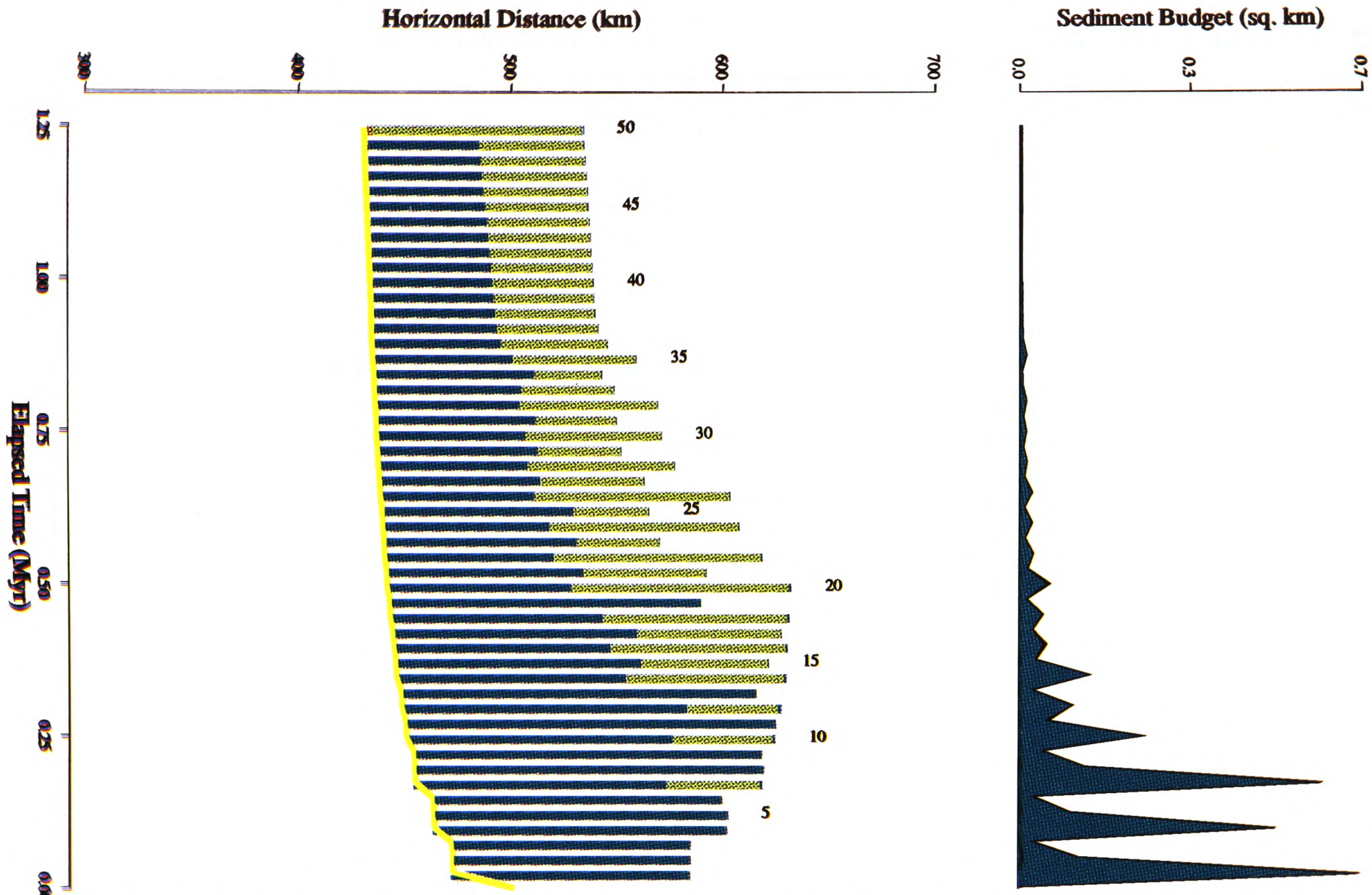

Figure 4.8. A chronostratigraphic diagram and a sediment supply curve from the model run with a timestep of 0.025Myrs. All other parameters are the same as those used in the standard reference model. The period of the oscillations in sediment supply show the same trend as in figure 4.7, i.e. halving the time step has halved the period of the oscillations.

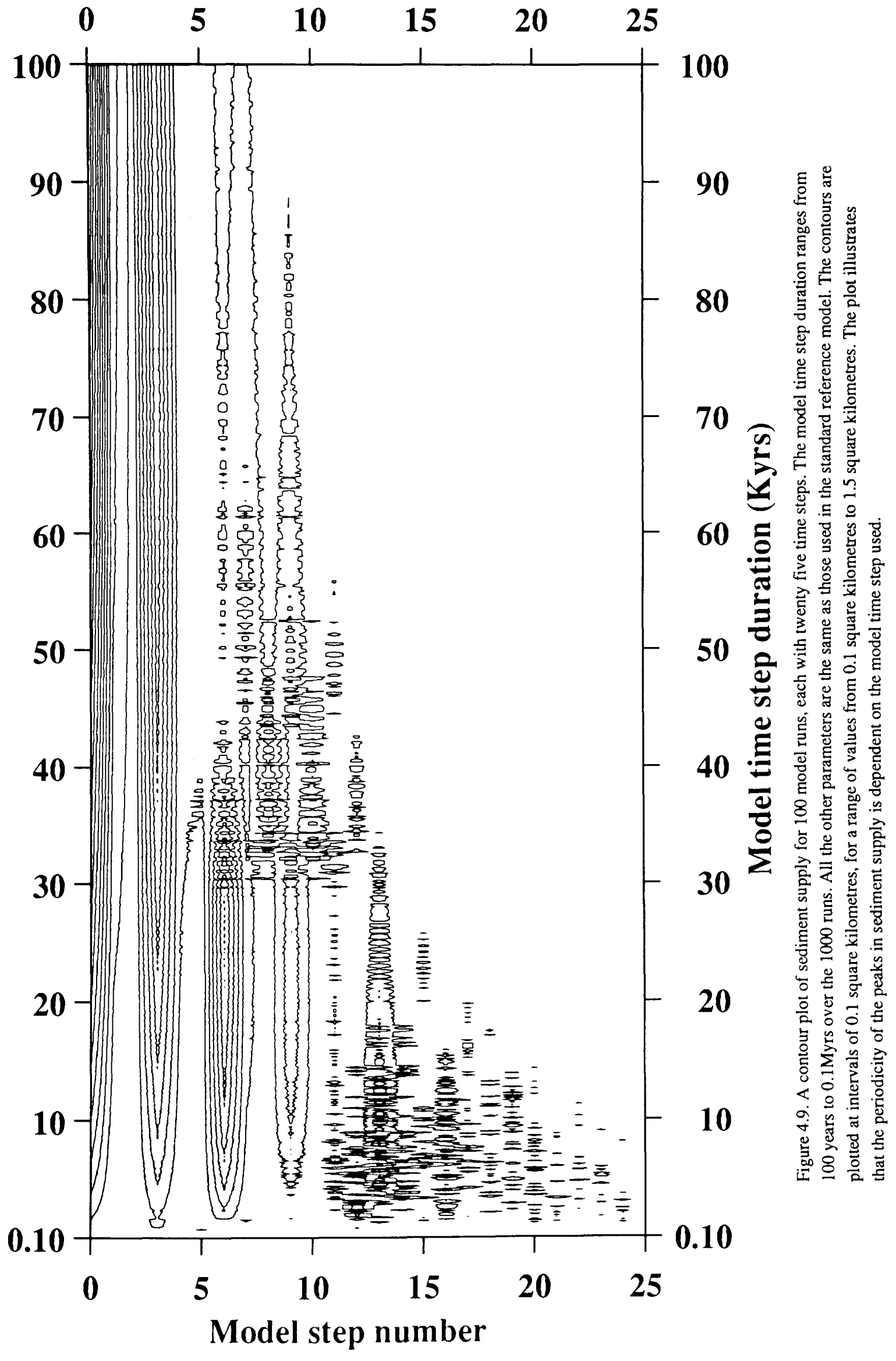

Figure 4.9. A contour plot of sediment supply for 100 model runs, each with twenty five time steps. The model time step duration ranges from 100 years to 0.1Myrs over the 1000 runs. All the other parameters are the same as those used in the standard reference model. The contours are plotted at intervals of 0.1 square kilometres, for a range of values from 0.1 square kilometres to 1.5 square kilometres. The plot illustrates that the periodicity of the peaks in sediment supply is dependent on the model time step used.

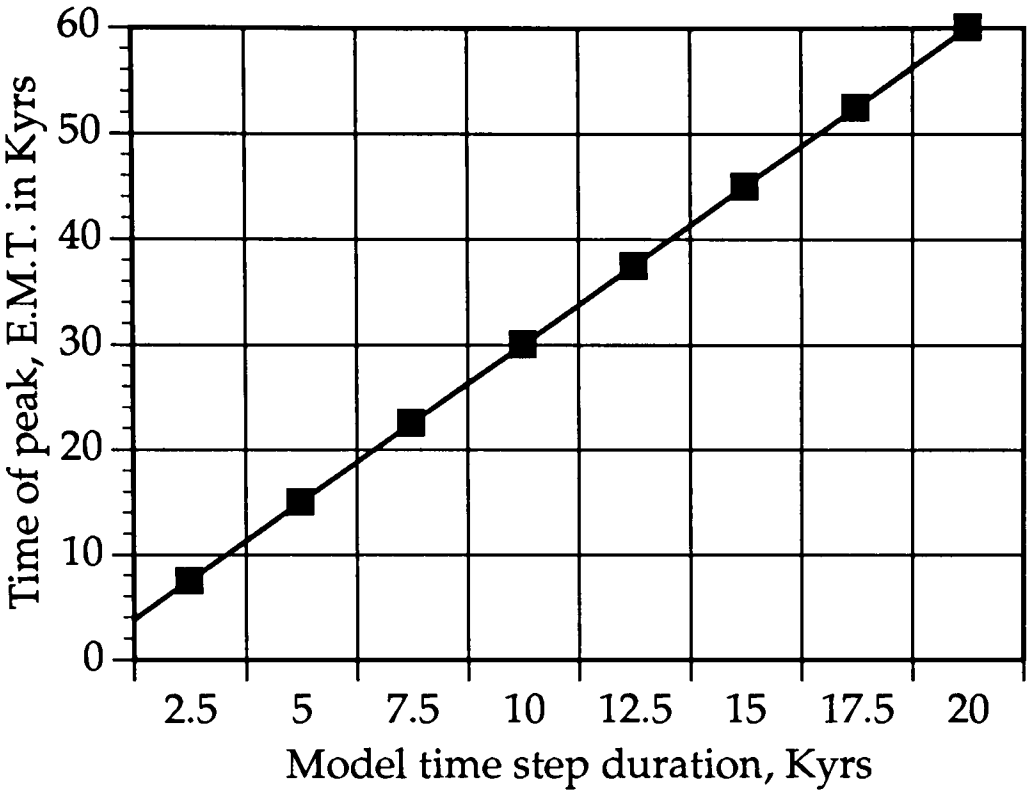

Figure 4.10. A plot to show the relationship between the timing of a sediment supply peak in E.M.T. and the model time step. The values are taken from figure 4.9. The plot shows that there is a simple linear relationship between the timing of the peak and the time step. The intercept on the best-fit line is zero, which shows that the timing of the peak goes to zero as the time step goes to zero.

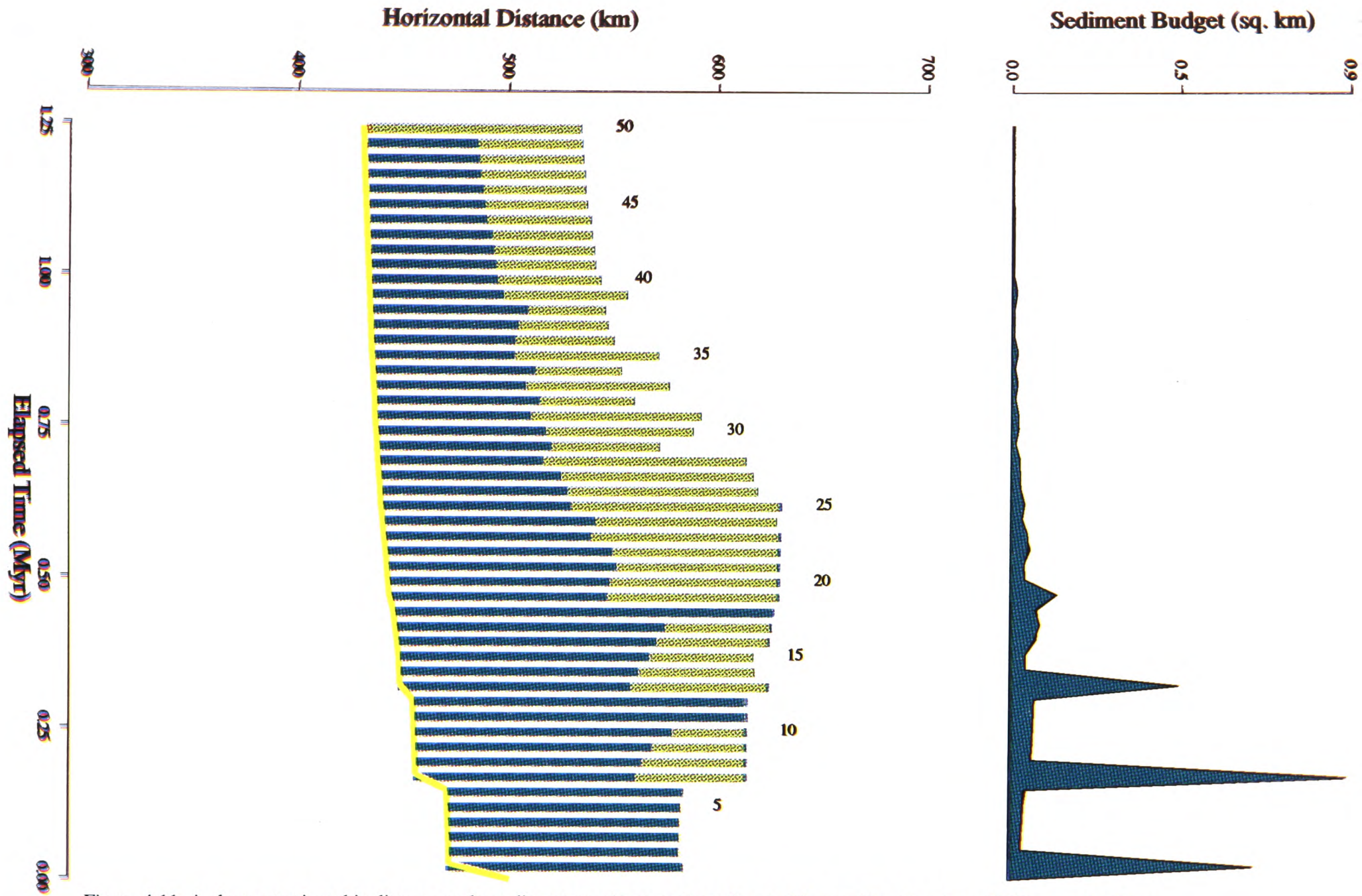

Figure 4.11. A chronostratigraphic diagram and a sediment supply curve from the model run with a timestep of 25Kyrs and a linear flexural response time of 0.1Myrs. All other parameters are the same as those used in the standard reference model. The inclusion of the linear flexural response time in the model has increased the number of model timesteps over which the oscillations in sediment supply occur.

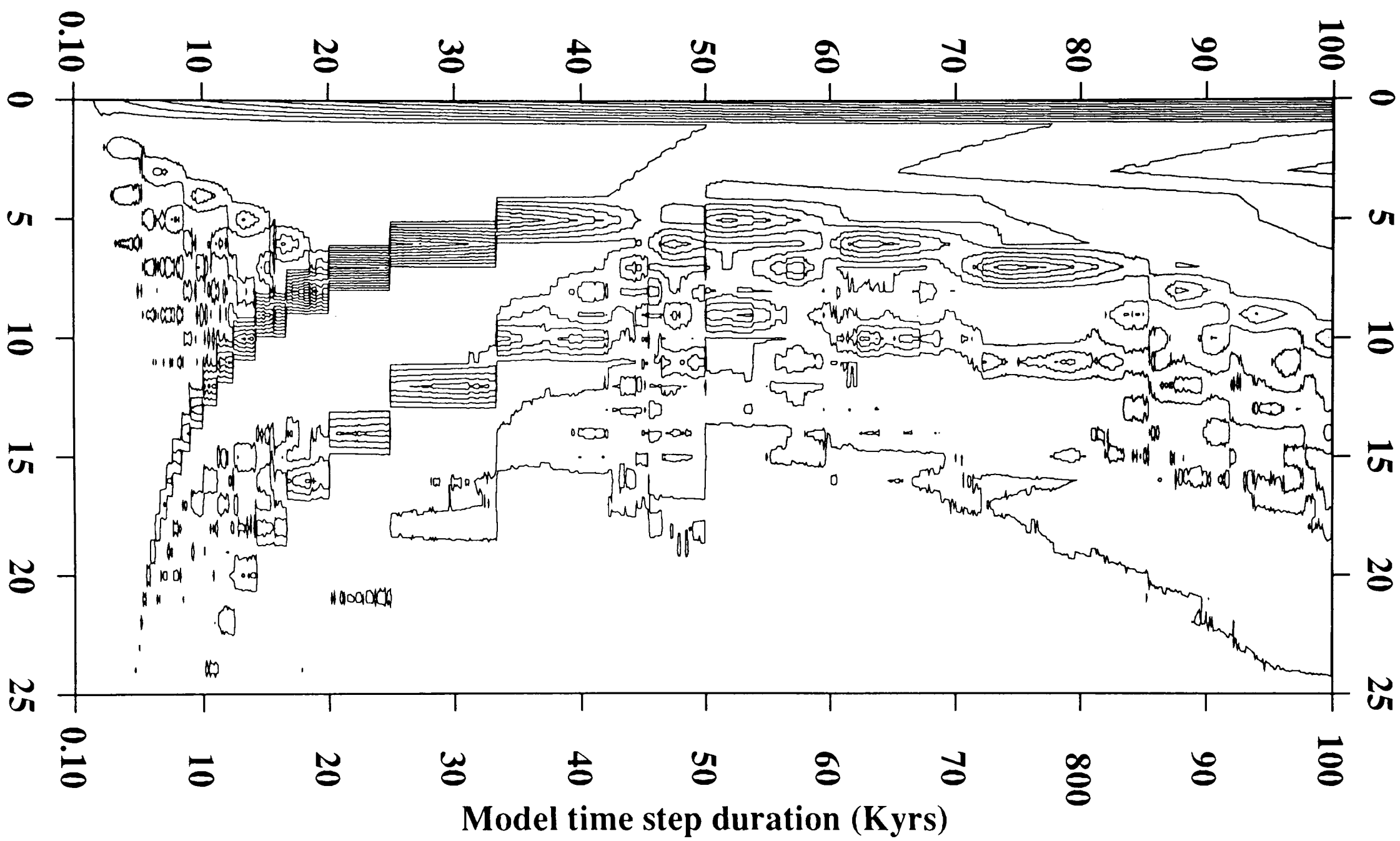

Figure 4.12. A contour plot of sediment supply for 1000 model runs, each with 25 time steps. The model time step duration ranges from 100 years to 0.1Myrs over the 1000 runs. The model run uses a linear flexural response time of 0.1Myrs. All the other parameters are the same as those used in the standard reference model. The contours intervals are the same as those in figure 4.9. The introduction of time dependence in the flexure has complicated the relationship between the signal period and the time step duration, particularly for the time step duration of 40Kyrs and less, but the period of the peaks is still not consistently independent of the time step duration.

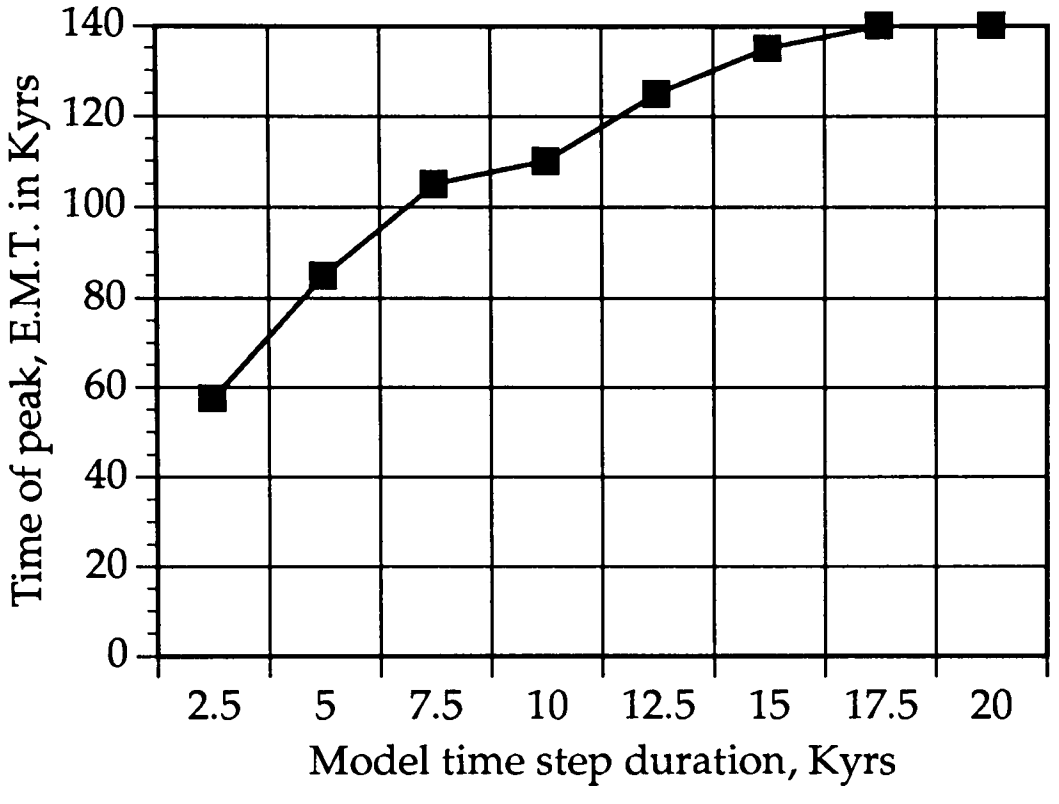

Figure 4.13. A plot to show the relationship between the timing of a sediment supply peak in E.M.T. and the model time step. The values are taken from the model runs with time dependent flexure shown in figure 4.12. The plot demonstrates that the timing of the peak still varies with the time step used, but it shows that the relationship is not a linear one, due to the influence of the flexural response time.

Chapter 5

Chapter 5 - Modelling the Neogene stratigraphy of the North American Atlantic passive rift margin

"My dog barks some. Mentally you picture

my dog, but in fact I have not told you

the type of dog which I have."

(David Lynch, Wild At Heart)

5.1 Introduction

The purpose of this chapter is to test the quantitative stratigraphic model developed here against an actual example of passive rift margin stratigraphy, namely the Neogene stratigraphy of the Atlantic margin of North America. In particular, the model will be used to investigate aspects of the Miocene progradation, such as the sediment supply, subsidence and sealevel history which may have been necessary to cause the progradation. This chapter will also demonstrate that this stratigraphic model is only capable of accurate fits with observed data on a very coarse scale, such as the overall sediment thickness, and the approximate distance of progradation. The model is not accurate enough to produce meaningful fits with observed stratigraphy at a more detailed level. For example, it cannot accurately reproduce details of onlap patterns.

5.2 Previous work on the North American Atlantic passive margin basins - constraints on model output

The stratigraphy on the North American Atlantic margin ranges in age from Triassic to Pleistocene and reaches a maximum thickness in excess of 15km in the Baltimore Canyon Trough (Grow and Sheridan, 1988). Rifting began in the Triassic, with the synrift phase of basin evolution lasting into the Jurassic when postrift thermal subsidence began (Klitgord *et al.* 1988). The tectonic and stratigraphic history of the margin has been deduced from a

mixture of interpretation of surface, subsurface and geophysical data (e.g. Klitgord *et al.* 1988,) and modelling studies (e.g. Watts, 1982; Steckler and Watts, 1982; Sawyer *et al.* 1983).

5.2.1 Chronostratigraphy

There exists a large and comprehensive database on the stratigraphy of the North American Atlantic margin (e.g. Poag and Valentine, 1988; Riggs and Belknap, 1988; Greenlee *et al.* 1992) based upon both surface and subsurface data. Greenlee *et al.* (1988) provides the most useful synthesis of stratigraphic data derived from seismic and borehole evidence which is displayed as both interpreted seismic sections and chronostratigraphic diagrams. Figure 5.1 shows the location of the seismic line and the surrounding boreholes. Figure 5.2 shows the seismic line, the interpreted seismic line, and the chronostratigraphic diagram from Greenlee *et al.* (1988). Throughout this chapter, the uninterpreted seismic data is referred to as observational data, while the interpreted seismic data, and the chronostratigraphic diagram are referred to as interpreted data. Figure 5.3 is modified from the chronostratigraphic chart from Greenlee *et al.* (1988). The interpreted data can be used to compare directly with model output. However, before doing this, it is important to examine the data and determine how it was derived, in order to appreciate possible biases of interpretation and other such weaknesses.

The chronostratigraphic diagram in plate 7 of Greenlee *et al.* (1988), shown in figure 5.2, and summarised in figure 5.3, shows the lateral extent through time of fluvial, coastal plain, nearshore marine, and slope basin sediments. However, little information is given regarding the exact methodology by which this information was derived. The age of the units shown on the chart was established on the basis of biostratigraphic age dating from available wells (figure 5.1), and correlation with the global cycles chart of Haq *et al.* (1988).

Greenlee *et al.* (1992) describe problems with the biostratigraphy relating to, for example, downhole sampling problems, and the limited environmental distribution of many of the diagnostic species of foraminifera used. As a result, the resolution of the dating of any particular surface is only plus or minus one or two million years. This limit on the resolution of the dating of the stratigraphy is of particular interest since the chronostratigraphic chart shows many breaks in deposition, which are presumably based on the biostratigraphic age data for the units and the correlation to the global cycles chart. With the limited resolution, such correlations may be particularly susceptible to the problems with correlation described by Mial (1992). If these data are prone to error, the interpretation of units separated by discreet breaks is suspect. Hence, in figure 5.3 no breaks are shown in the stratigraphy, except where there is observational evidence of erosion on an unconformity.

The distribution of the environments through time appears to have been based on observation of the seismic characteristics of the dated reflectors on the seismic line, i.e. the seismic facies. The methodology for this procedure for marine clastic sediments was described in Sangree and Widmier (1977) and Mitchum *et al.* (1977), but the procedure would appear to be very subjective and prone to interpretative error. For example, a fluvial mud will have the same acoustic impedance and other such physical characteristics as a marine mud, may well show the same type of reflector geometry (e.g. shingled, hummocky), and will have undergone similar post-depositional processes of diagenesis and compaction. Therefore, the suggested distribution of the environments from Greenlee *et al.* (1988), particularly the transition from fluvial to coastal plain and nearshore marine, should be treated with extreme caution. However, in the absence of better publicly available data (i.e. logged cores), this data must suffice for modelling comparisons.

Both the problems with the dating of reflector surfaces and the difficulty in accurately identifying the distribution of depositional environments from the seismic data must cast doubt upon the sequence stratigraphic interpretation being placed upon the observed

stratigraphy. For example, there appears to be no direct evidence on the seismic section for rapid landward or seaward movements of the beach, as suggested by Schroeder and Greenlee (1992). As already discussed, direct observational evidence for breaks in deposition as shown on the chronostratigraphic chart of Greenlee *et al.* (1988), are also lacking. These examples illustrate the potential pitfalls involved in the application of the sequence stratigraphic methodology beyond the limits of the data available.

5.2.2 Tectonics and subsidence history

Much previous work has concentrated on attempting to deduce the overall tectonic structure of the passive margin (e.g. Klitgord *et al.*, 1988; Sheridan *et al.*, 1988; Grow *et al.*, 1988; Watts, 1988) and in particular the subsidence history of the passive margin (e.g. Watts and Steckler, 1979; Steckler *et al.* 1988). Both areas of work provide essential data regarding attempts at quantitative forward modelling. In particular, Watts (1988) gives estimates for the crustal and subcrustal stretching factors on the passive margin, based upon subsidence studies. These are used as parameter values in the model (see section 5.3). Smith *et al.* (1976) gives values for palaeobathymetry in the COST-B2 well through the Miocene. These values are very useful, since they can be used to constrain the model output.

5.2.3. Eustatic curves

Figure 5.3 shows three eustatic sealevel curves derived from or used in, studies of North American Atlantic margin stratigraphy. The first of these curves is the Watts and Steckler (1979) curve. This was derived from backstripping studies by comparing a least squares fit exponential curve with the actual backstripped curve, and assuming that the difference is due to eustatic sealevel changes. The second curve is the Haq *et al.* (1988) curve. This was derived from studies of coastal onlap made within the framework of the sequence stratigraphic depositional model (Vail *et al.*, 1977a), and is thus based upon the

assumption that coastal onlap is controlled by fluctuations in eustatic sealevel, so that where global synchroneity can allegedly be established, the coastal onlap curve can be taken to represent eustatic fluctuations.

The third curve is the Greenlee and Moore (1988) curve. This was also calculated using coastal onlap and the sequence stratigraphic depositional model, but was based purely on interpretations of data from the Baltimore Canyon Trough, while the Haq *et al.* (1988) curve claims to be a more regional synthesis of stratigraphic interpretation. Despite this, the two curves share some common features i.e. the gross timing of most falls and rises. If the curves were derived from widely separated localities, this would strengthen the case for a global control on coastal onlap patterns, but this geographical diversity has yet to be demonstrated, and would still not be conclusive. The two curves also have quite different amplitudes. For example, the maximum amplitude of the Haq *et al.* curve is 144m above present sealevel, while the maximum amplitude of the Greenlee and Moore curve is 68m. This discrepancy must also cast doubt on the validity of one or both of the curves. The validity and use of the curves is discussed further in section 5.4.

5.2.4. Previous modelling work

Steckler and Watts (1982) studied the subsidence of the North American Atlantic margin via backstripping, and modelled the total stratigraphy using a thermo-mechanical model. The thermal element of the model was based on McKenzie (1978) and the mechanical element was derived from models of flexural isostasy with a time dependent elastic thickness. The model reproduces at a very coarse scale some of the elements of passive margin stratigraphy such as the approximate maximum thickness of the synrift and postrift sediment, and the gross pattern of stratal onlap on the Coastal Plain. Steckler and Watts (1982) suggested that this onlap was due to the increasing flexural rigidity of the lithosphere with age, rather than eustasy (Vail *et al.* 1977b) or two-layer lithospheric stretching (White and McKenzie, 1988).

Watts and Thorne (1984) developed this model further by adding two-layer stretching (e.g. Hellinger and Sclater, 1983), sediment compaction, a very simplistic model for subaerial erosion, based upon an average elevation algorithm acting upon the flexural forebulge, and changes in absolute sealevel. It was claimed that this model could reproduce the basic details of the observed stratigraphy on the North American Atlantic margin. However, there are several problems with this claim. Firstly, there is the problem of scale. Although the model does reproduce the overall pattern of stratal onlap, it does so at a time scale which is large enough to miss much of the finer detail, such as possible third order cycles. For example, the model groups the Aptian stage into one chron. Hence any detail during the Aptian is not reproduced by the model. Therefore, it is not viable to claim that the model negates the necessity for higher-order sealevel variations such as those proposed by Vail *et al.* (1977b).

The second problem with the Watts and Thorne (1984) model is related to the processes included in the model, and the way in which these processes are modelled. If the assumptions behind the model are weak, for example, constant palaeobathymetry over the duration of the model run, constant compaction, and a very simplistic model for erosion, then this weakens the conclusions which may be safely drawn from the model results.

The problem is also related to scale, since such assumptions probably do not significantly weaken the conclusion that thermal subsidence and flexural subsidence due to sediment loading are the most important controls on the overall development of the passive margin stratigraphy. However, they are important when looking, for example, at the details of the stratigraphy on the Coastal Plain. Thus it seems important to try and look at sections of the stratigraphy on the North American Atlantic margin using a model with a finer time resolution and a set of assumptions which are more suited to modelling stratigraphy at finer scale, both temporal and spatial.

Schroeder and Greenlee (1993) examined the stratigraphy of the North American Atlantic margin at a finer temporal scale with a quantitative model which attempted to reproduce the observed stratigraphy in the Neogene, over a period of approximately 18Myrs, and thus test the applicability of a variety of eustatic sealevel curves for this period. No details of the formulation of the model are given, except for some very crude flowcharts to indicate the sequence of events to generate each chron. Stratigraphy is modelled at each time step by taking the position on the eustatic curve, and then generating a geometric shape based on this position. For example, if the current portion of the eustatic curve was the lowstand limb, the model would generate a triangular wedge onlapping on the front of previous model stratigraphy. Thus, the model appears to be a model of a model, in that it is derived entirely from the conceptual sequence stratigraphic models of Vail *et al.* (1984), Jervey (1988), Posamentier *et al.* (1988) and Posamentier and Vail (1988). This approach has some very obvious drawbacks in terms of a lack of direct links with observed stratigraphic processes, and a large element of circular reasoning.

For example, Schroeder and Greenlee (1993) conclude that the sealevel curves of Haq *et al.* (1988) and Greenlee and Moore (1988), which include high-frequency eustatic oscillations, better fit the interpreted data than the curve of Watts and Steckler (1979), which lacks such high-frequency eustatic oscillations. However, the Haq *et al.* (1988) and Greenlee and Moore (1988) curves were calculated using the sequence stratigraphic model, the quantitative model of Schroeder and Greenlee (1993) was developed using the sequence stratigraphic model, with little or no reference to actual observed stratigraphic processes, and the data used for testing that model was interpreted using the sequence stratigraphic model (Greenlee *et al.* 1988). Central to the sequence stratigraphic model is the need for eustasy as a driving mechanism for variations in coastal onlap, and stratal geometry. Therefore, the conclusion of Schroeder and Greenlee (1993) regarding which eustatic curve best fits the interpreted data, is not surprising, and is probably not significant, being purely a function of a circular methodology.

Schroeder and Greenlee (1993) also concluded that the "Miocene progradation event", in which clinoforms prograded approximately 100km across the passive margin, was caused by higher than average sediment supply, combined with a low magnitude of thermal subsidence, and a second-order eustatic sealevel fall. Though this seems quite possible, it is important to test this interpretation further with more sensitivity tests using a more sophisticated model with some different basic assumptions.

The model used here has already been extensively described in chapter 2. The model has a strong link with those described in Steckler and Watts (1982) and Watts and Thorne (1984). All these stratigraphic models invoke a lithospheric stretching model, in the form of either the one layer model of McKenzie (1978) or a two-layer model (e.g. Hellinger and Sclater, 1983), and flexural isostasy, which together seem capable of accounting for the gross architecture of passive margin stratigraphy (Watts et al., 1982). The predominant difference between those previous models, and the model presented here is the higher time resolution of this model, which can be applied to periods of 20 - 30Myrs. Previous models such as Watts and Thorne (1984) are applicable for longer periods of up to 150Myrs. The higher time resolution, and the inherent different model assumptions and components, are essential in order to further investigate the details of passive margin stratigraphy, rather than the overall gross architecture, as has been done previously (Steckler and Watts, 1982; Watts and Thorne, 1984.

However, looking at stratigraphy at finer time scales (i.e. 10 -20Myr periods) raises the problem of the complexity of the sedimentary and geomorphological systems in comparison with the relatively simplistic nature of current stratigraphic models. This discrepancy in complexity means that any fits between model output and observed data are going to be generally low-resolution fits. In the case presented here, a broad fit between observed clinoform structure, sediment thickness, and distance of progradation is being aimed for. Details of onlap patterns and erosion patterns are very unlikely to match due to the discrepancy in complexity. A significant increase in model complexity and

sophistication, in terms of the processes included, and basic assumptions such as two-dimensionality, will be necessary to make more progress at this higher resolution time scale.

5.3 Initial standard model conditions

The total model run time is set to be 15Myrs. This model run time is split into 150 time steps, each of 0.1Myrs duration. This model duration represents the period from 18Ma, in the Early Miocene, to 3Ma in the Late Pliocene. This time interval was chosen because it spans the duration of the Miocene progradation being studied, but the exact timing was chosen on the basis of the chronostratigraphic chart of Greenlee *et al.* (1988) which covers this period of geological time.

As already discussed in section 5.2.1, the large-scale tectonic evolution of the North American Atlantic margin has been well studied (e.g. Watts and Steckler, 1979; Watts and Thorne, 1984; Klitgord *et al.* 1988; Watts, 1988; Watts, 1989) and seems to be well understood. Watts (1988) gave crustal and subcrustal stretching values across the Baltimore Canyon Trough estimated from backstripping, and gravity modelling across the basin. These values have been used as the initial conditions for crustal and subcrustal stretching in the model (figure 5.4) using the two-layer stretching model of Hellinger and Sclater (1983). The initial thermal age of the model is taken to be 180Myrs, which represents in the model the time elapsed since the end of the synrift phase of basin subsidence. This age is chosen on the basis of the age of the oldest sediments known to overlie the postrift unconformity which are thought to be Early or possibly Middle Jurassic in age (Klitgord *et al.* 1988; Poag and Valentine, 1988).

This value for the thermal age of the lithosphere is also used in the initial conditions for the modelled flexure. The standard reference model uses a time-dependent Te where Te is equal to approximately three times the square root of the thermal age of the lithosphere

(see section 2.6). This gives values in a range from 40.2km at 0Myrs E.M.T., to 41.89km at 15Myrs E.M.T. The value of Te does not vary with distance along the profile. The Te is high enough during the Miocene that such variations would make little difference to the final stratigraphy, since the amplitudes of flexure are so small.

The initial topography for the standard model run was selected on the basis of a combination of present day topographic data and estimates of shelf morphology and water depth at 18Ma. The maximum elevation of the profile at its landward end is set at 150m, which is based on the present elevation of the edge of the Coastal Plain (Klitgord, 1988). The submarine topography is derived from measurements of the clinoform height on the 18Ma chron on the interpreted seismic section of Greenlee *et al.* (1988), using the given value for vertical exaggeration with reference to the horizontal scale. These measurements suggest a probable initial water depth of, very approximately, 600m in front of the prograding clinoforms (e.g. the 17.5Ma clinoform at approximately 45km from the landward end of the profile), and increasing basinward. The initial topography, therefore, consists of a slope from 0m at the initial beach position at 400km, to -600m at 450km, -700m at 500km, and -2000m at 1024km.

A fluvial profile 200km in length is cut into this topography. The length of the profile is based on measurements of modern rivers on the Coastal Plain, and on the width of the present Coastal Plain (Klitgord, 1988). The profile is modelled using a complementary error function with an arbitrary length scale value of 2.0 (see section 2.6.5.2) The landward limit of the fluvial profile is fixed in position, since the Coastal Plain does not appear to have widened to any significant degree by headward movement of the limit of fluvial deposition during the Neogene (Judson, 1975).

A fluvial-marine partitioning coefficient of 0.11 is used (see section 2.5.7). This is a very difficult parameter to constrain, yet it is critical to the stratigraphic patterns produced. In this case, the value for the parameter was chosen to provide a fit with the interpreted data.

However, some very loose constraint on the value can be derived from studies of areas of deposition of modern deltas. Comparison of the subaerial and submarine planform areas of the Delaware river delta suggest a fluvial-marine partitioning coefficient value of 0.16 (Pers. comm., Hovius, 1993). This value is surprisingly close to the value chosen on the basis of the model fit.

The marine equilibrium profile consists of a shoreface 10km in width and 20m in height, a shelf with a gradient of $0.5mkm^{-1}$, and a continental slope with a gradient of $4.366mkm^{-1}$. These values are based on the present morphology of the North American Atlantic margin (Shor and McClennen, 1988). Three different eustatic curves (figure 5.4) are used in the model runs. The curves were taken from Schroeder and Greenlee (1993). Sediment supply was held steady for the standard run at $0.48km^2$ per 100Kyr time step. This value was chosen to produce a fit in the model with the observed distance of clinoform progradation, but it is in general agreement with Judson (1975) which suggests a rate of denudation of $0.03mkyr^{-1}$ between the Coastal Plain and the main divide, based on the volume of sediment observed offshore. Multiplying this figure by the distance across which the erosion occurred, approximately 200km, gives a figure of $0.6km^2$ per 100Kyrs.

The magnitude of post-Palaeozoic erosion, estimated on the basis of observed stratigraphic gaps along the East Coast, varies from approximately 0.25km to approximately 6km depending on structure. This gives an erosion rate of between $0.001mkyr^{-1}$ and $0.02mkyr^{-1}$, and demonstrates the potential variability of denudation rates along the passive margin. These figures give a much lower sediment supply value of between $0.0002km^2Kyr^{-1}$ and $0.004km^2Kyr^{-1}$. Although they are obviously gross average estimates, they do provide a guide line around which modelling can proceed. Thus, although the figure used of $0.48km^2$ per time step was chosen to facilitate a fit with observed data, it is only slightly higher than the maximum value calculated on the basis of the estimated erosion rates, and is only slightly lower than the value calculated on the basis of offshore sediment volumes.

5.4 Model Output

The following model runs have the parameter values described above in section 5.3, and include one of the three pre-defined absolute sealevel curves described in section 5.2.5. The model runs are not dependent upon the sequence stratigraphic depositional model, as were the modelling results of Schroeder and Greenlee (1993), but instead form a more independent, less inherently circular, test of the validity of the three curves. The results also provide an insight into the other stratigraphic controls which may have been responsible for the observed Neogene stratigraphy.

5.4.1 The Watts and Steckler curve results

Figure 5.5 shows a model section produced using the standard initial conditions and parameters described in section5.2 along with the Watts and Steckler sealevel curve. The section shows a steady progradation of submarine clinoforms into deep water, with approximately 700m thickness of marine slope sediment deposited in the clinoform foresets. The clinoform topsets are made up of shoreface sediment, possibly with a narrow shelf, topped by aggradational and progradational fluvial stratigraphy. The maximum thickness of fluvial sediment deposited is approximately 60m over the original position of the beach at 400km.

Figure 5.6 shows the chronostratigraphic diagrams from the model run. The Wheeler diagram shows the influence of the absolute sealevel curve on the pattern of beach and shelf-slope break progradation. Changes in the rate of sealevel fall at an E.M.T. of 4.4Myrs and 8.8Myrs (13.6Ma and 9.2Ma) clearly alter the rate of progradation of the beach. Changes in the rate of beach progradation in the interpreted data (figure 5.3) appear to occur at 15Ma, 13Ma and 5.5ma, though the exact position of the beach is not mapped, only the interpreted transition from fluvial to coastal plain and nearshore sediments, which

adds a margin of error in the beach position of between 25 and 50km. This in turn makes changes in rate of progradation difficult to establish exactly.

Comparing the timing of changes in model beach progradation rates and interpreted beach progradation shows poor correlation. However, what is very apparent is that the observed changes in the rate of beach progradation occur with a similar frequency to those in the model driven by the Steckler and Watts absolute sealevel curve. There is no evidence in the observed data for higher frequency variations in the rate of beach progradation which could be used to imply higher-order cycles of eustatic change.

Changes in the rate of progradation of the shelf-slope break in the interpreted data appear to occur at 16Ma and 10Ma. In the modelled stratigraphy, there is a steady decrease in the rate of shelf-slope progradation from 0.0Myrs E.M.T. to 4.0Myrs E.M.T. (18Ma to 14Ma) followed by steady progradation. This change in gradient is a function of the initial topography, so it can largely be dismissed as an artefact of the initial conditions, which as stated before, are poorly constrained.

Thus, comparing the model output with interpreted data from Greenlee *et al.* (1988) shows that the model output successfully reproduces some of the basic elements of the data:

- The overall uncompacted thickness of approximately 700m of the marine sediment in the model is in the same order of magnitude as the observed post-compaction thickness ranging from approximately 700m to 1250m.
- The 100km of beach progradation in the model matches well the interpreted distance of beach progradation of between 60km and 108km.
- The basic clinoform structure in the model produced by the progradation of the beach and the shelf-slope break matches the gross clinoform structure seen in the interpreted seismic section (figure 5.2).

- The decrease in water depth due to the progradation of the clinoforms matches the decrease in water depth through the Miocene shown in the palaeobathymetry curve of Smith *et al.* (1976).

These points of a basic match between the interpreted data and the model output suggest that, within the constraints imposed by uniqueness problems leading to multiple possible solutions, the processes represented in the model are probably essentially those responsible for the gross stratigraphic geometry. A combination of thermal subsidence, flexure, slowly varying absolute sealevel, and constant sediment supply can reproduce the interpreted gross stratigraphic geometry.

Looking at the results in slightly greater detail, however, shows that there are some discrepancies between the interpreted data and the model output :

- None of the stratal onlap onto the prograding clinoforms, or the stratal terminations beneath younger strata visible on interpreted seismic sections (figure 5.2) occur in the model.
- The model shows continuous deposition on the fluvial profile throughout the run, producing a maximum thickness of approximately 100m of fluvial sediment. There is no erosional truncation as observed on the Coastal Plain (e.g. Olsson *et al.* 1988), though on the basis of stratigraphic relationships, this truncation may have occurred in post-Miocene times, in which case it can be considered to be beyond the scope of the model run.

These discrepancies are most likely due to the difference between the relatively simplistic model and the much more complex stratigraphic systems. Many processes which are known, or suspected, to operate in the marine and terrestrial environments on the passive rift margins, are not adequately represented in the model. For example, several studies have shown that slope failure and mass wasting are very significant processes that strongly affect patterns of preserved stratigraphy (e.g. May et al., 1983; Miller et al., 1985; Shor

and McClennen, 1988; Pers. Comm., Hesselbo 1993). No such processes are included in the model, though it seems possible that they could be responsible for patterns of onlap observed at the base of some of the clinoforms. Also, as stated in chapter 2, the behaviour of the fluvial profile through time is very poorly understood, and is only grossly approximated in this model. Therefore, it is not surprising that the fit between the model and the observed data on the coastal plain area is poor.

The importance of circular reasoning with regards to the use of the Haq *et al.* (1988) and the Greenlee and Moore (1992) eustatic curves in the quantitative modelling study of Schroeder and Greenlee (1992) has been demonstrated. The possibility of circular reasoning in the use of the Watts and Steckler (1979) eustatic curve in this modelling study must also be investigated. As described in section 5.2.5, the Watts and Steckler curve was derived from a backstripping study. The study make assumptions regarding isostatic adjustment to sediment loading, compaction of sediment, and water depth at the time of sediment deposition. It does not make any assumptions regarding a stretching model, or any other components included in this model. Therefore, there is no element of circular reasoning involved. The basic fit between the interpreted data and the model output using the Watts and Steckler curve is not a result of circularity in the methodology of the modelling.

5.4.2 The Haq *et al.* curve results

Figure 5.7 shows a section generated using the standard model parameters with the addition of the Haq et. al. (1988) eustatic curve. Scrutiny of the section shows that the pattern of stratigraphy is very different to that shown in figure 5.5 and 5.6. The primary cause of this is the high-order cyclicity in the absolute sealevel curve which is absent in the Watts and Steckler curve.

The most notable features of the model stratigraphy shown in figure 5.7 are the 400m thick wedge of marine slope sediment, separated from approximately 100m of fluvial, shelf and slope stratigraphy by a marine erosion surface produces by the last major transgression at 12.5Myrs E.M.T. The 100m of shelf stratigraphy was all deposited in the last 2.5Myrs of model time. Older stratigraphy has been eroded by a combination of fluvial and shelf erosion driven by the rapid high-amplitude changes in absolute sealevel. The chronostratigraphic diagrams in figure 5.8 show the spatial and temporal extent of this erosion, some of which should be disregarded as an unrealistic artefact of the geometrical fluvial profile implementation. The position of the beach on the Wheeler diagram is clearly controlled by the absolute sealevel curve.

Comparison of the model output with the interpreted data shows a very poor fit. Even the basic details of the stratigraphy successfully reproduced using the Watts and Steckler curve are absent in this case. For example, the distance of the progradation of the clinoforms is approximately 50km which is outside the limits suggested by the chronostratigraphic diagram of Greenlee at al. (1988). The overall thickness of the stratigraphy also fits the observed data less accurately.

There are two end-member possibilities for the poorness of fit between the model results and the interpreted data. The first is that the Haq *et al.* eustatic sealevel curve is fundamentally flawed. There are a number of possible explanations for this. For example, the sequence stratigraphic methodology used to derive the curve may be flawed. Alternatively, the features of the stratigraphy used to derive the curve may be due to a process or processes other than eustasy, such as, for example, submarine mass wasting. The second possible explanation for the poorness of the fit is that the stratigraphic model is flawed. Such a fault with the model is most likely to be a result of the assumptions behind the model.

One such assumption which is obviously inaccurate is the assumption of two-dimensionality. This could well be a critical weakness in this particular case. The chronostratigraphic diagram from Greenlee *et al.* (1988) is derived from interpretation of a seismic section (figure 5.2), the location of which is shown in figure 5.1. However, the seismic line does not run parallel to or along the interpreted axis of Miocene fluvial sediment transport, also shown in figure 5.1. Therefore, the section imaged on the seismic line does not show features such as fluvial incisions if they are present, but rather shows the laterally equivalent surface which may not have been significantly incised. This is in direct contrast to the model section, which is exactly along the axis of fluvial transport, since the model is only operating in two-dimensions. Hence the model results show all the effects of fluvial incision and aggradation. This feature alone could be enough to explain the poorness of fit, and makes it impractical to draw other conclusions regarding the validity of the model results versus the validity of the interpreted data. The only solution to this is to extend the quantitative model into three dimensions.

5.4.3 The Greenlee and Moore curve results

Figure 5.9 shows a section from the model run with the standard parameters plus the addition of the Greenlee and Moore (1988) eustatic curve. The results are broadly similar to those obtained with the Haq *et al.* (1988) curve. The two curves are very similar with respect to the frequency and timing of eustatic falls and rises, and this similarity is responsible for the basic similarity of the two model runs. However, the curves do differ in magnitude, such that the Greenlee and Moore curve has only half the maximum amplitude (≈70m) of the Haq *et al.* (1988) curve (≈140m). These different amplitudes account for the differences in the two model sections.

For example, the 12.5Myr E.M.T. transgressive surface in the Haq *et al.* run was very well developed and remained largely unburied by subsequent deposition (figure 5.7). In the Greenlee and Moore model section shown in figure 5.9 this is not the case. The magnitude

of the eustatic rise at 12.5Myrs E.M.T. is less, and hence the transgressive surface is less well developed. The lower water depths on the shelf following the transgression (≈30m as opposed to ≈80m) mean that there is less accommodation space and so shallow water sediments can prograde further onto the shelf and bury the transgressive surface.

The quality of the fit of the model run using the Greenlee and Moore curve is no better than that of the model run using the Haq *et al.* curve. The same problems regarding the off-transport-axis nature of the data, and the two-dimensionality of the model apply equally in this case. As already stated, this makes it very difficult to draw conclusions regarding the validity of the curves from the model output. The only solution is to develop a three-dimensional stratigraphic model.

5.4.4 Variable sediment supply

The standard reference model run held sediment supply constant at 0.48km^2 per time step through the model run. One of the features of the section from the model run with the Watts and Steckler curve was the basic fit between the observed distance of beach and shelf-slope break progradation and the distance shown in the model section (figure 5.5). However, the rates of beach movement through time in the model did not match with the rates of beach movement implied from the Greenlee *et al.* (1988) chronostratigraphic diagram. To improve the fit, it is necessary to include variable sediment supply and variable fluvial-marine partitioning coefficient, since aside from the absolute sealevel curve, these are the major controls in the model on the gradient of the beach and shelf-slope break progradation.

Figures 5.11 and 5.12 show the section and the chronostratigraphic diagrams from the model run with the Watts and Steckler eustatic curve and time-variable sediment supply and fluvial-marine partitioning coefficient. The sediment supply curve is shown in figure 5.12. The partitioning coefficient changes with the same timing as the sediment supply

curve, from a value of 0.1, to 0.6, and then back to 0.1. The section in figure 5.11 shows two major differences from the section in figure 5.5.

- The thickness of the fluvial stratigraphy in the landward portion of the fluvial profile is slightly reduced, and topped by an erosive surface cause by the drop in sediment supply and the fluvial-marine partitioning coefficient at 9.0Myrs E.M.T. Again, this should be disregarded as an unrealistic model artefact.
- The shoreface and shelf are no longer as well developed. Instead, because of the different values of the fluvial-marine partitioning coefficient and the different values of sediment supply, the fluvial profile passes directly into the marine slope.

The chronostratigraphic diagrams in figure 5.12 shows the improved fit between the model result and the interpreted data more clearly. Comparison of the interpreted chronostratigraphic diagram with that shown in figure 5.12 shows that the match with the rate of interpreted beach progradation is now much better. For example, in the model, the beach changes its rate of progradation at 3Myrs E.M.T. from approximately 22kmMyr^{-1} to a higher value of approximately 59kmMyr^{-1}. A similar change of rate can be seen in the interpreted chronostratigraphic diagram at the equivalent time of 15Ma, though the actual values are quite different, from near zero to approximately 10kmMyr^{-1}. Much of this discrepancy can be explained by the broad bands of possible positions for the beach on the interpreted chronostratigraphic diagram.

The significance of this fit is limited by the simplistic nature of the model, and the problem of non-unique solutions. However, it is still significant in that it shows how a combination of control on stratigraphy by eustasy, thermal subsidence, palaeobathymetry, sediment supply and fluvial-marine partitioning can be used to reproduce and hence provide a possible explanation for the pattern of Miocene progradational stratigraphy observed on one section of the North American Atlantic margin.

5.5 Summary

The primary conclusion from this attempt to fit modelled stratigraphy with observed stratigraphy in the Miocene of the North American Atlantic margin is that there still exists a large discrepancy in terms of complexity between stratigraphic systems and stratigraphic models. While such complexity may not be apparent at longer time scales, it does become apparent when the temporal resolution of modelling is increased. The only solution to this is to continue to build more sophisticated models which account for more of this apparent complexity. Extending models into three dimensions, and including slope wasting processes seem like the most obvious steps forward in the case of modelling the stratigraphy of the North American Atlantic margin.

However, despite the problems with the simplistic nature of this stratigraphic model, it is possible to draw some conclusions on the basis of this modelling exercise :

1. The gross large-scale features of the Miocene stratigraphy such as the distance of clinoform migration, and the thickness of the succession, can be reproduced with the model using the parameter values outlined above. Even given the inevitable uniqueness problems, it seems safe to conclude from this that the basic processes of thermal subsidence, flexural isostasy, eustasy, and sediment progradation are those responsible for the basic features of the observed stratigraphy.

2. The higher-order eustatic curves of Haq *et al.* (1988) and Greenlee and Moore (1988) produce significantly worse fits in the model than the lower-order curve of Watts and Steckler (1979). There are large elements of circular reasoning in both the methodology used to define these higher-order curves, and in the methods previously used to test them (e.g. Schroeder and Greenlee, 1993). Even though the problem of the two-dimensionality of the model cannot be ruled out in explaining the poor fits, it still seems reasonable to

conclude that there are severe problems in using such high-order eustatic curves to explain the geometry of the observed stratigraphy.

3. Varying sediment supply and the fluvial-marine partitioning coefficient improves some of the details of the basic fit between the model and the interpreted data.

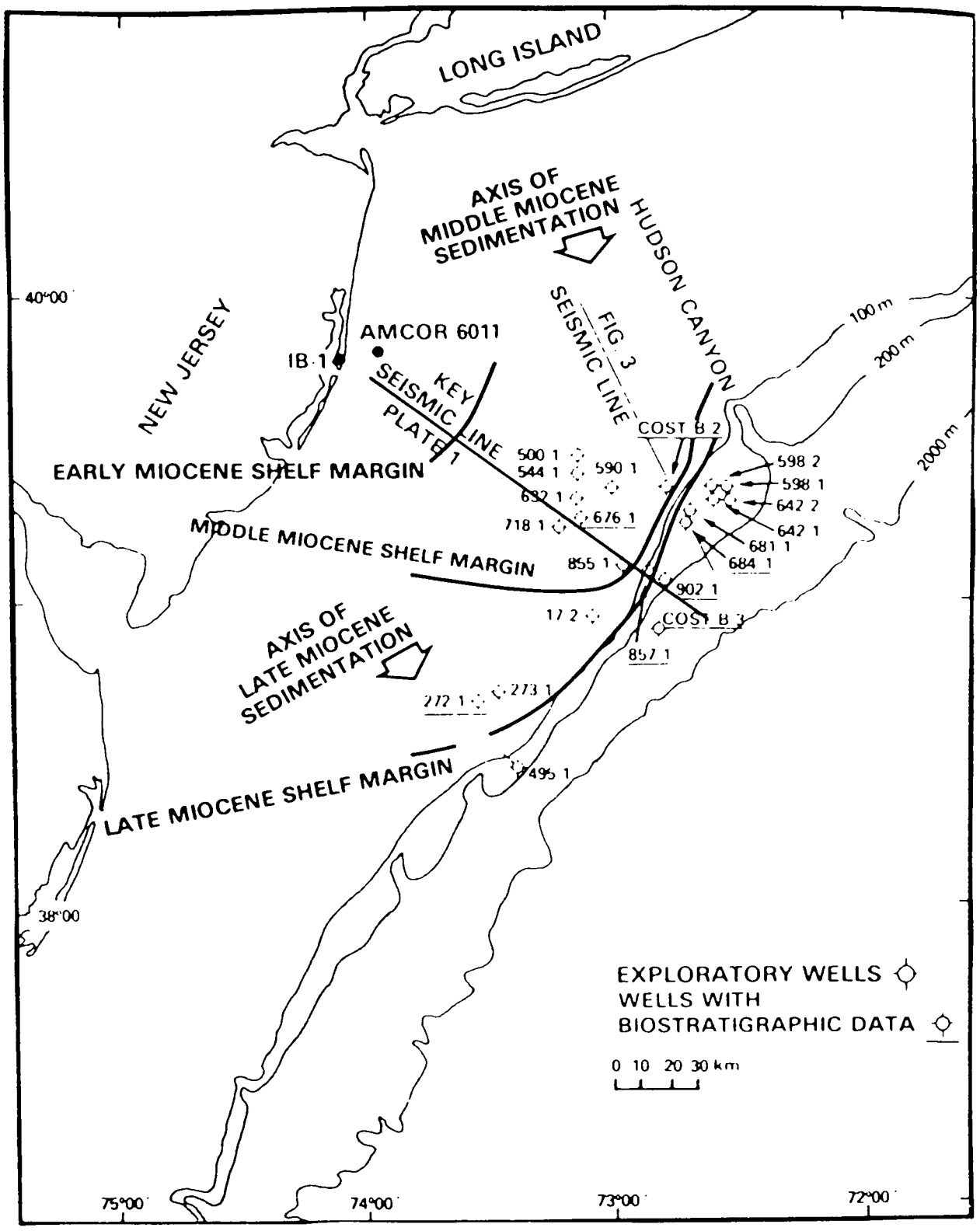

Figure 5.1 Location map from Greenlee et al. (1988) showing the location of the seismic line and boreholes providing the database which was used to compile the chronostratigraphic chart also given in Greenlee et al. (1988).

EQUENCES BALTIMORE CA

positional sequences, Baltimore Canyon trough.
ozoic global cycle chart
tinental Margin: U.S.
eology of North America (GNA-I2)

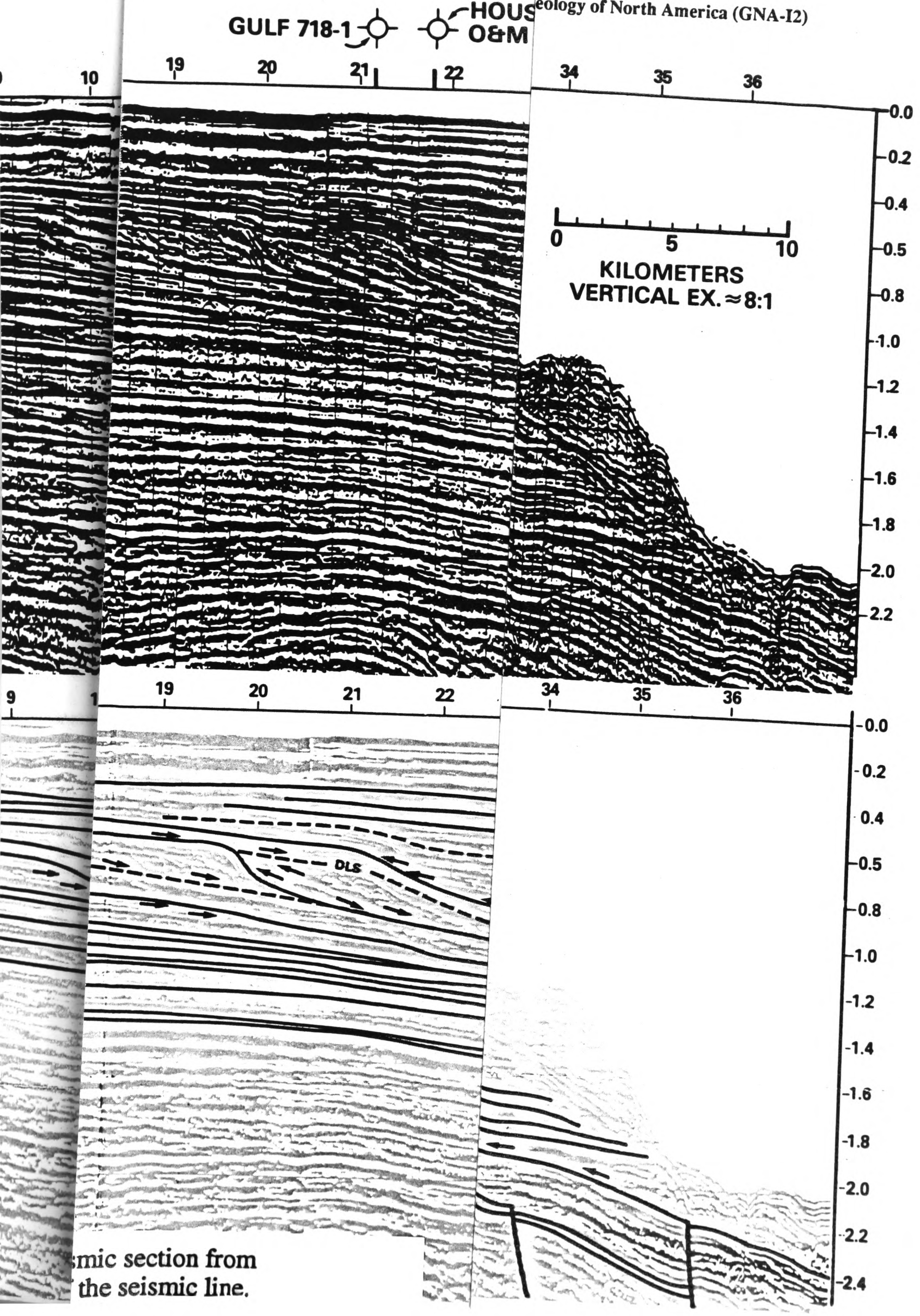

smic section from
the seismic line.

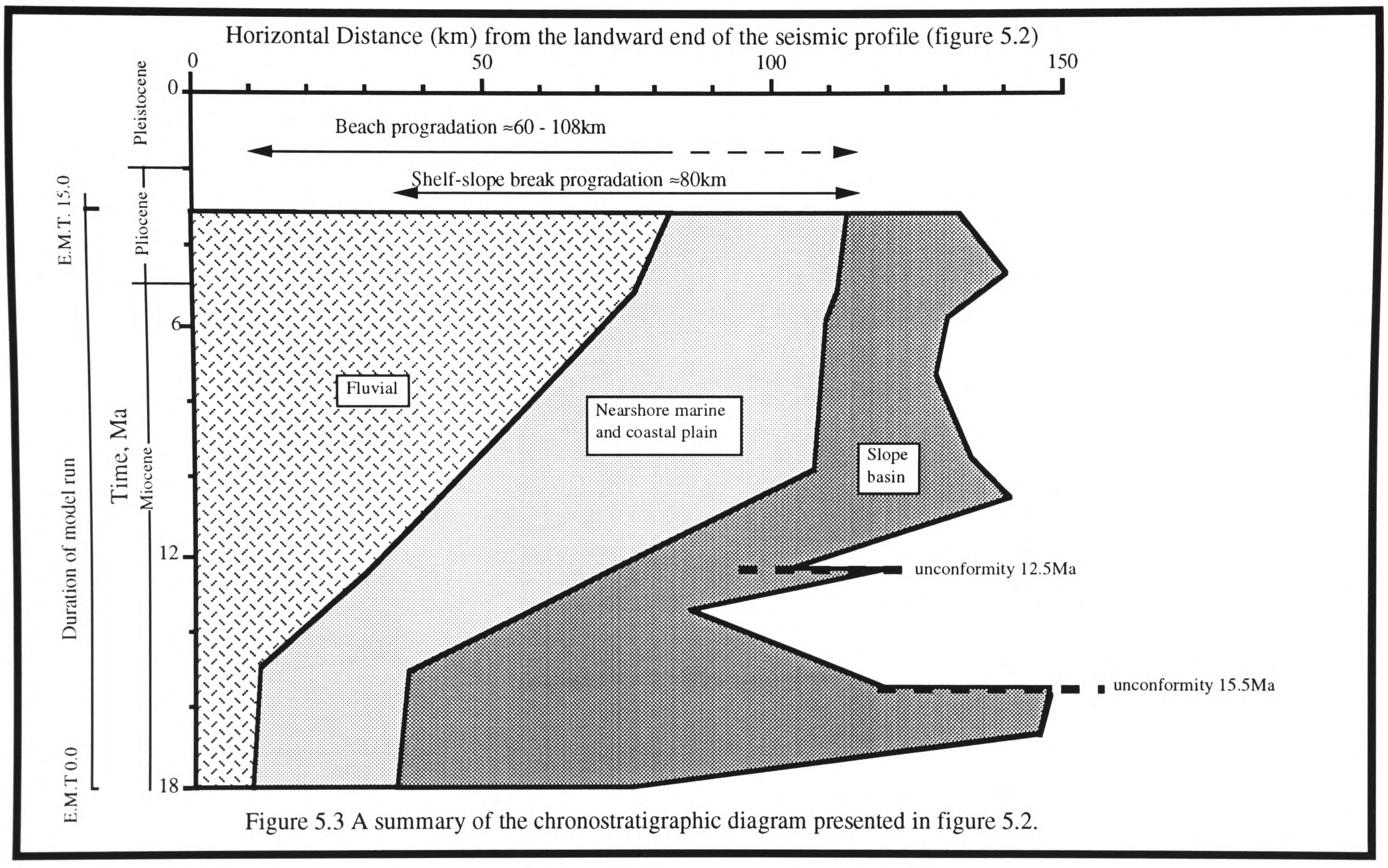

Figure 5.3 A summary of the chronostratigraphic diagram presented in figure 5.2.

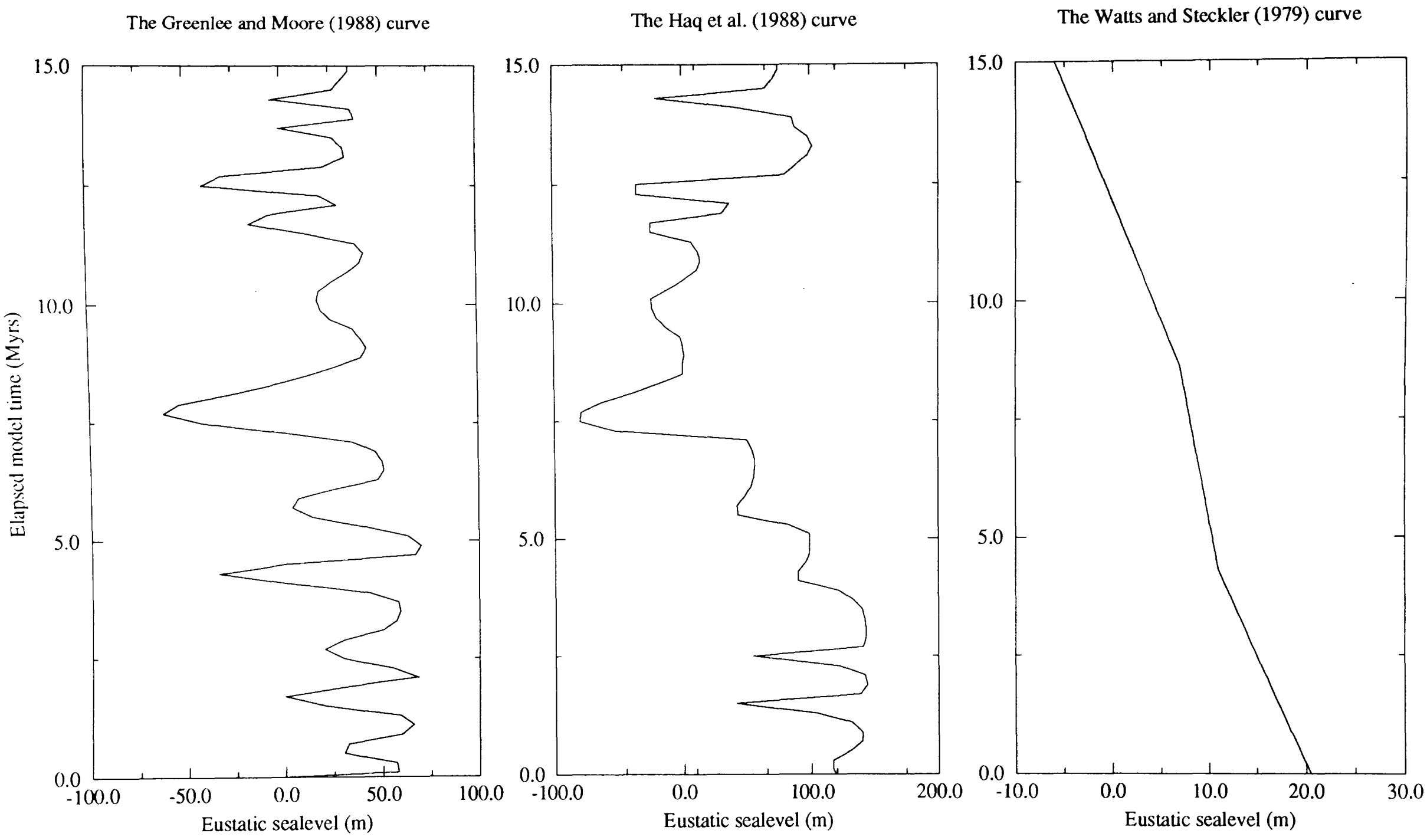

Figure 5.4 The three eustatic sealevel curves used in the model runs.

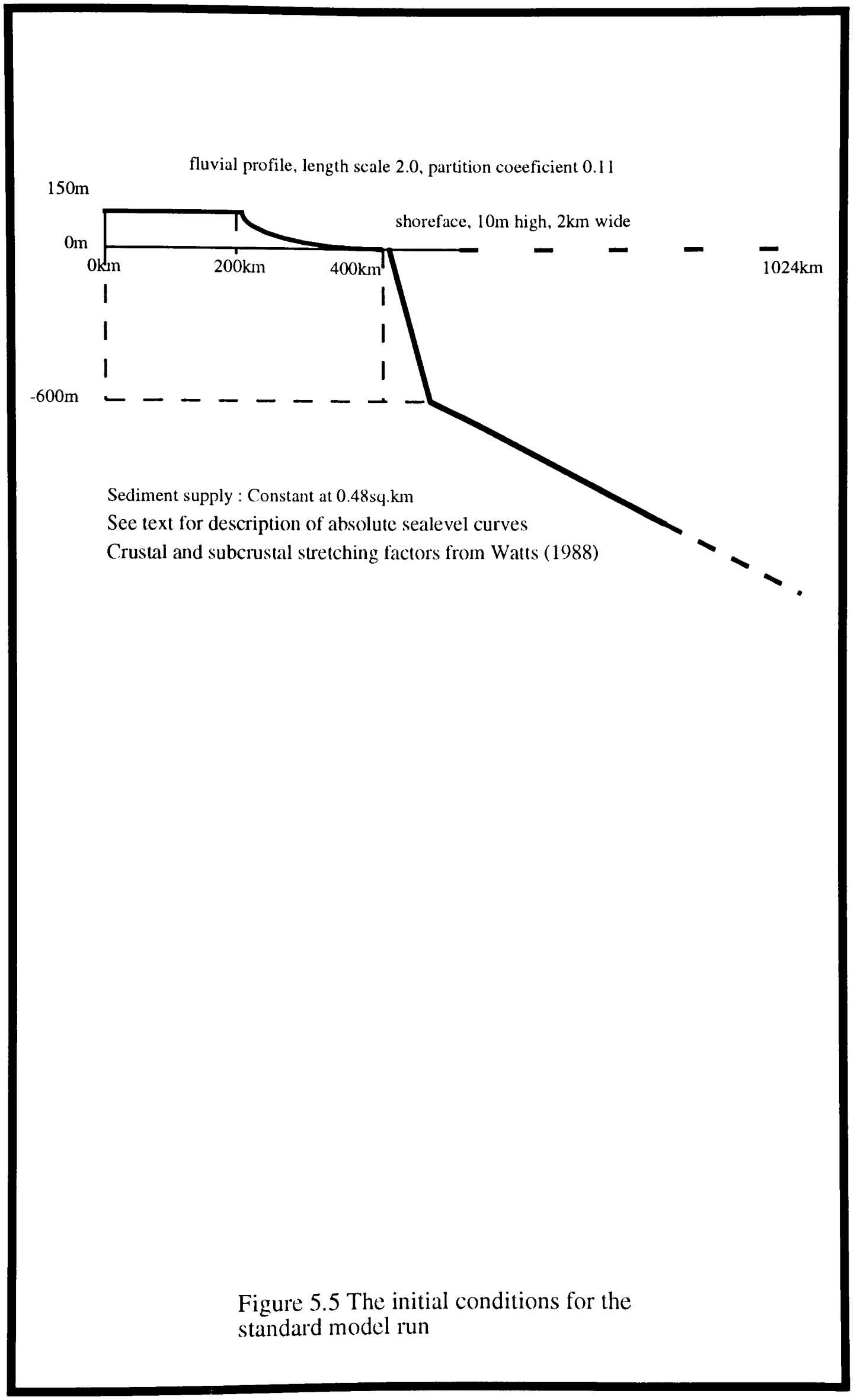

Figure 5.5 The initial conditions for the standard model run

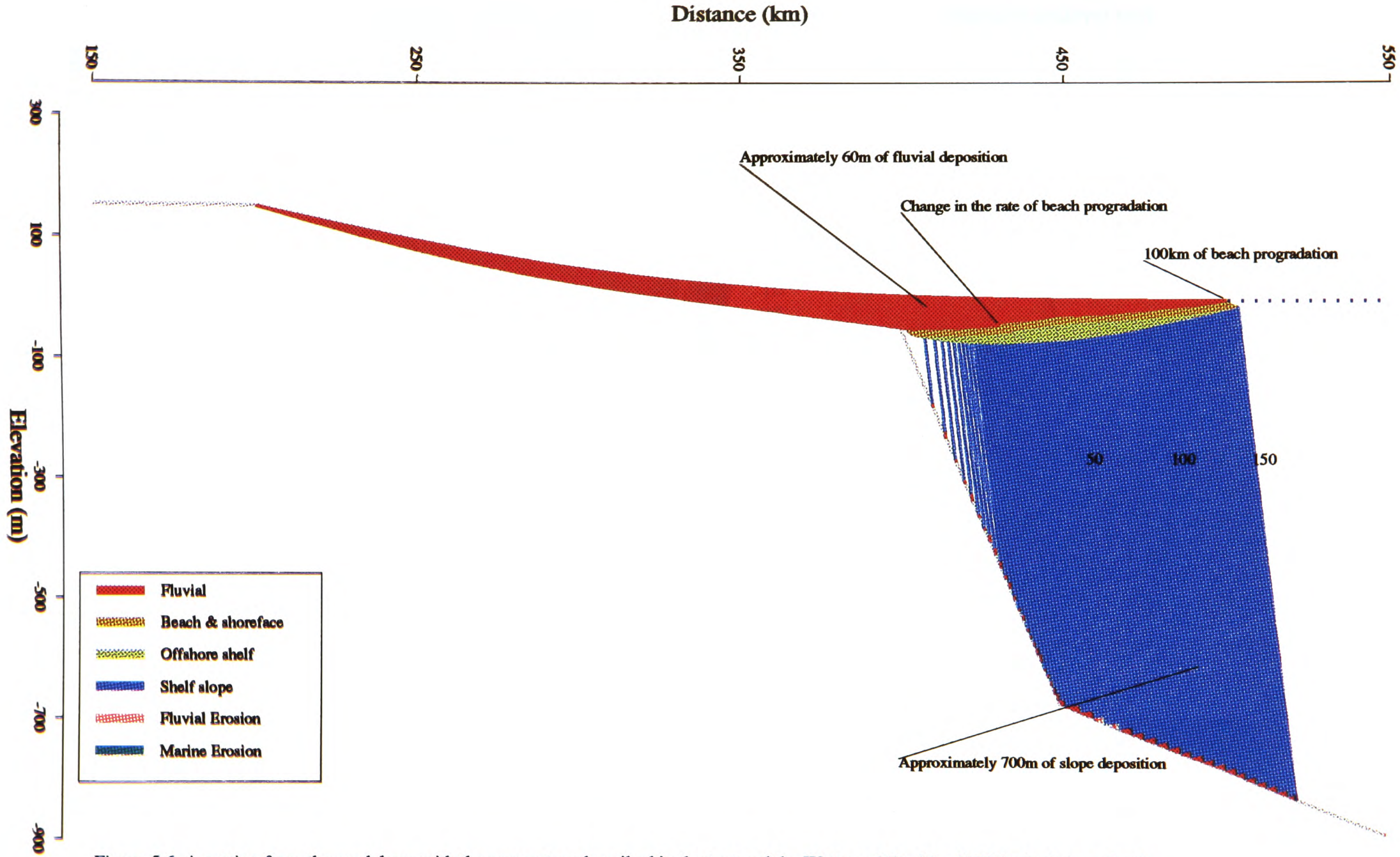

Figure 5.6. A section from the model run with the parameters described in the text and the Watts and Steckler (1979) absolute sealevel curve (figure 5.4.C). The model run successfully reproduces the basic 60-108km of beach progradation and the basic clinoform structures visible on the data and interpretations from Greenlee et al. (1988), but fails to reproduce many of the higher resolution interpreted features such as onlap and downlap patterns. The changes in the rate of beach progradation at, for example, chron 44, are due to changes in the rate of absolute sealevel change.

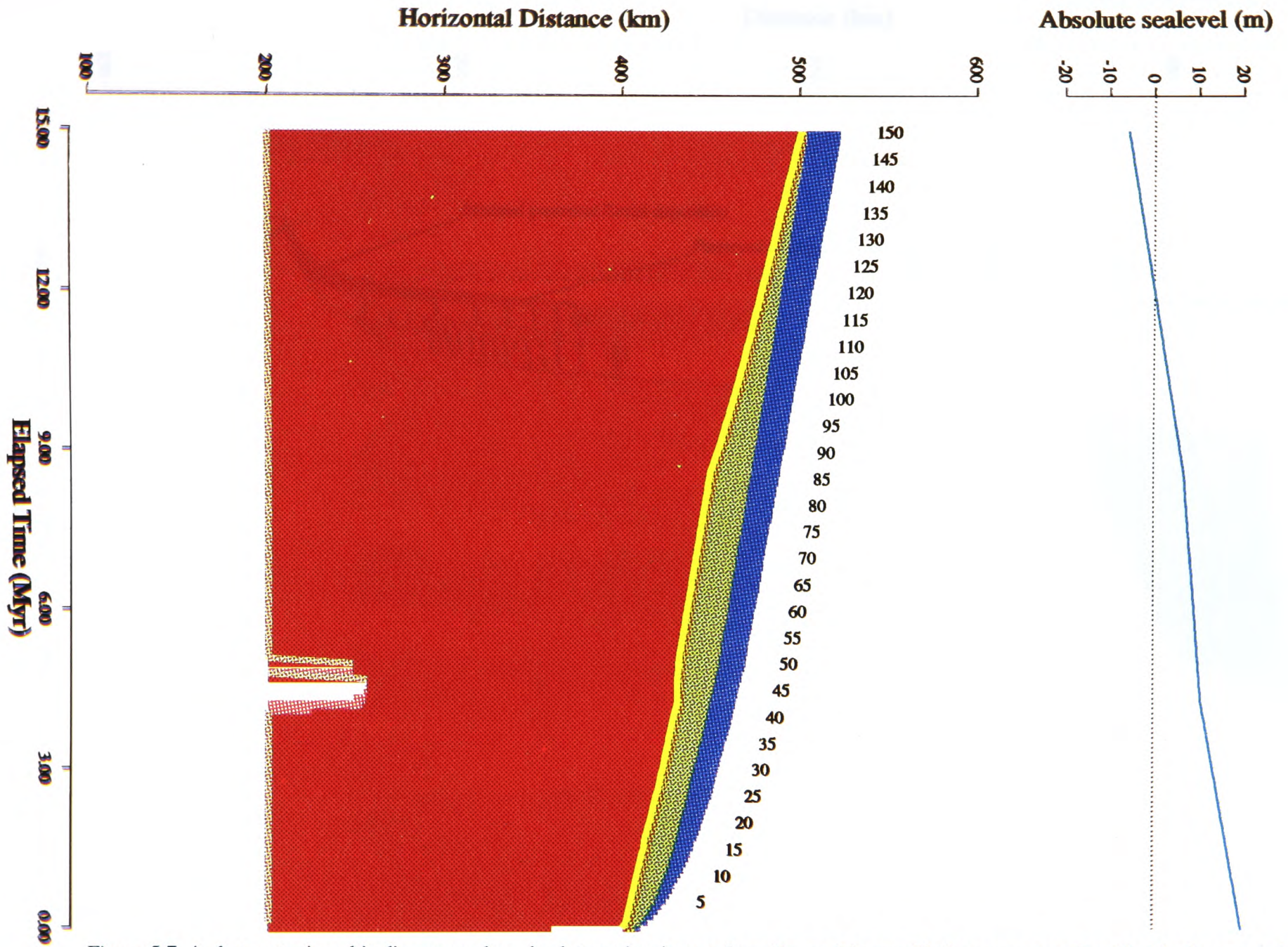

Figure 5.7. A chronostratigraphic diagram and an absolute sealevel curve from the model run with the parameters described in the text and the Watts and Steckler (1979) absolute sealevel curve. The figure shows that the model run successfully reproduces the basic 60-108km of beach progradation visible on the data and interpretations from Greenlee et al. (1988), but fails to reproduce many of the higher resolution interpreted features such as onlap and downlap patterns. The changes in the rate of beach progradation at, for example, chron 44 due to changes in the gradient of absolute sealevel curve, are clearly visible.

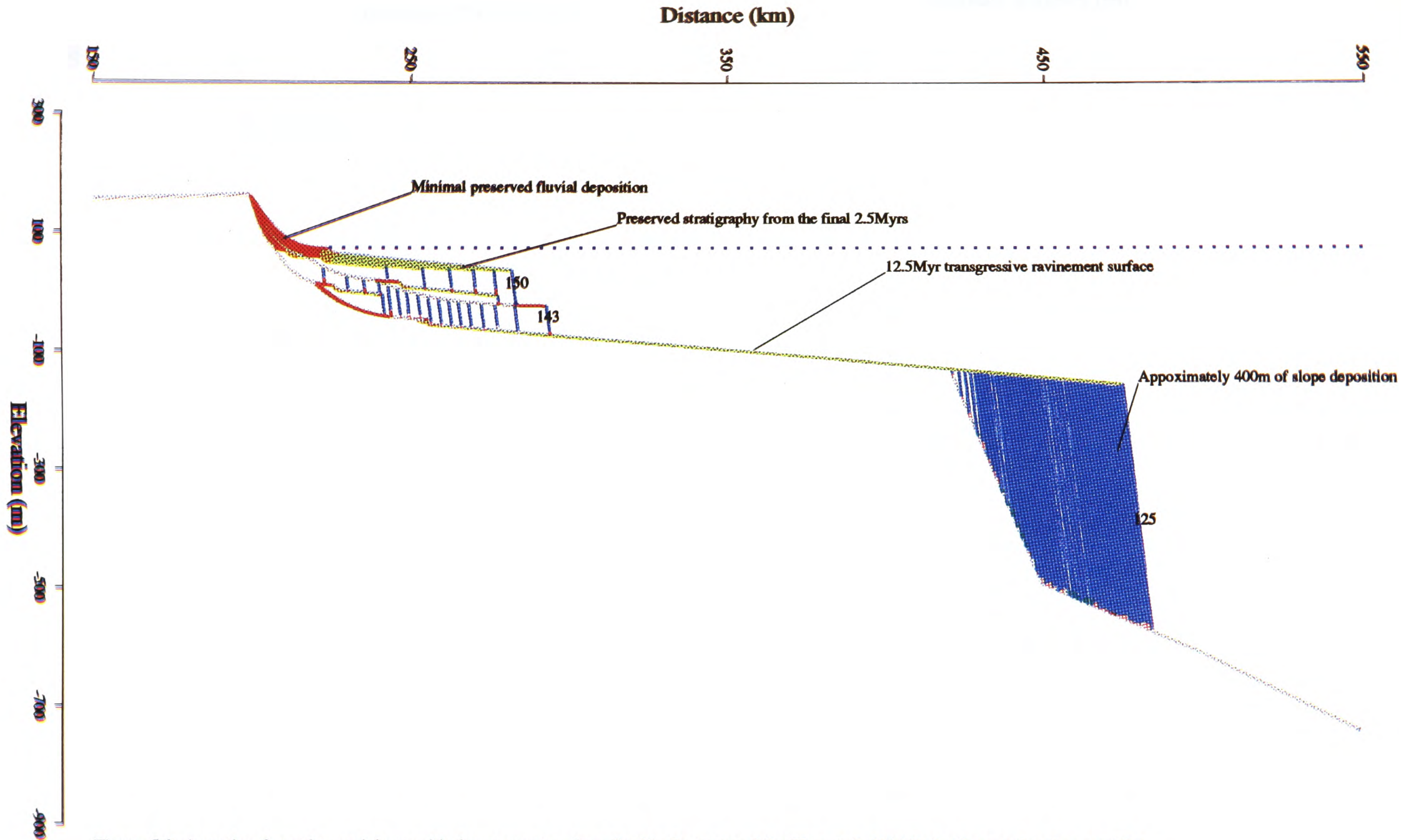

Figure 5.8. A section from the model run with the parameters described in the text and the Haq et al. (1988) absolute sealevel curve. The influence of the high-order fluctuations in absolute sealevel can be clearly seen. The stratigraphy is split spatially into two distinct parts. The stratigraphy on right of the section consists of distal slope deposits formed at various times during the model run, generally at low points on the absolute sealevel curve. The stratigraphy on the left is younger, representing deposition during the final 2.5Myrs of E.M.T., from 12.5 to 15Myrs E.M.T. Stratigraphy deposited in shallow water previously to this has been eroded by the 12.5Myr E.M.T. transgression.

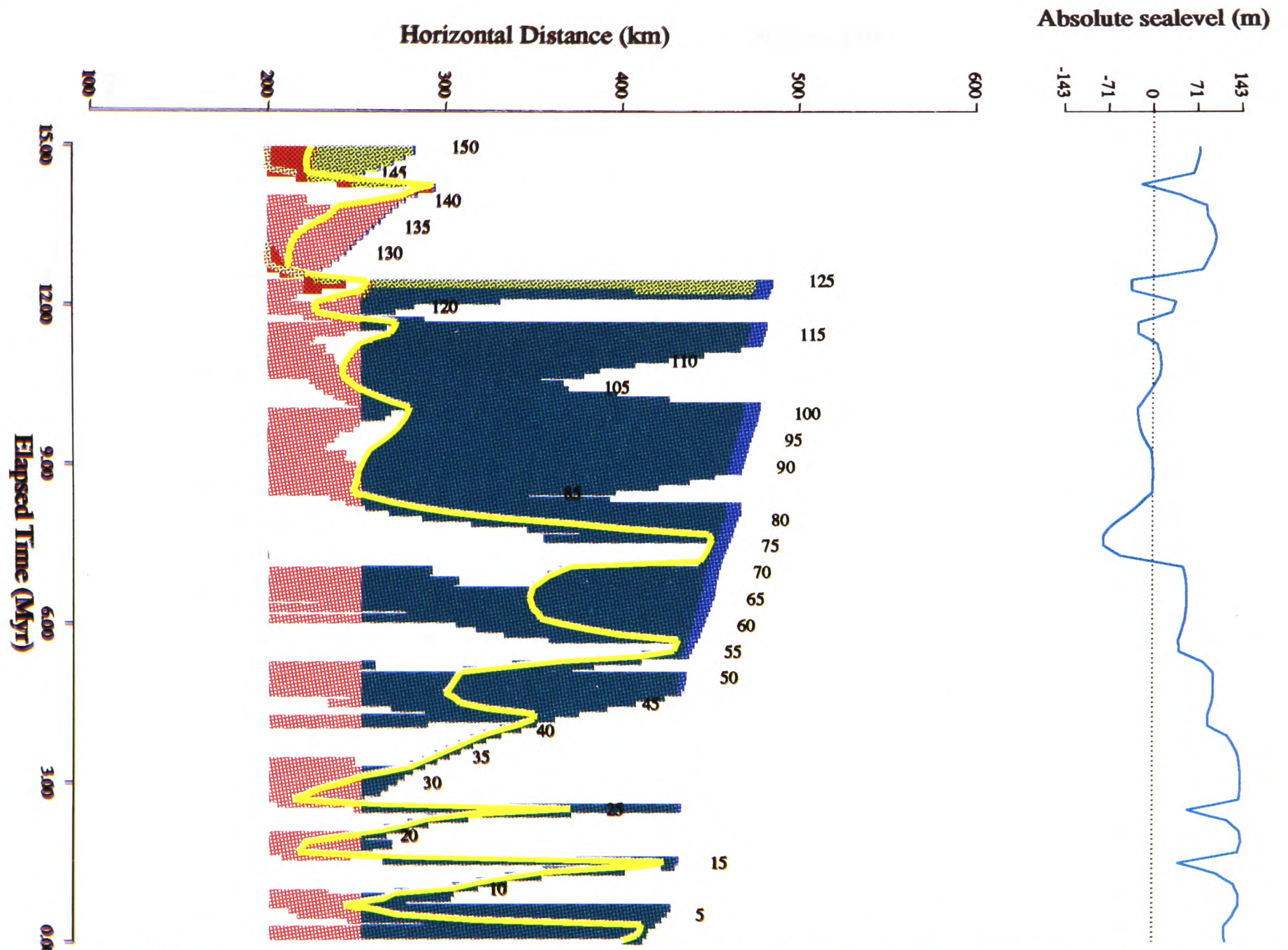

Figure 5.9. A chronostratigraphic diagram and an absolute sealevel curve from the model run with the parameters described in the text and the Haq et al. (1988) absolute sealevel curve. The influence of the high-order fluctuations in absolute sealevel on the distribution of stratigraphy is apparent. In particular, the absolute sealevel rise at 12.5Myrs E.M.T., and the subsequent fall at 14.3Myrs E.M.T. has removed much of the previous stratigraphy through both fluvial and marine erosion. The movement of the beach through time in response to the absolute sealevel fluctuations is also shown very clearly.

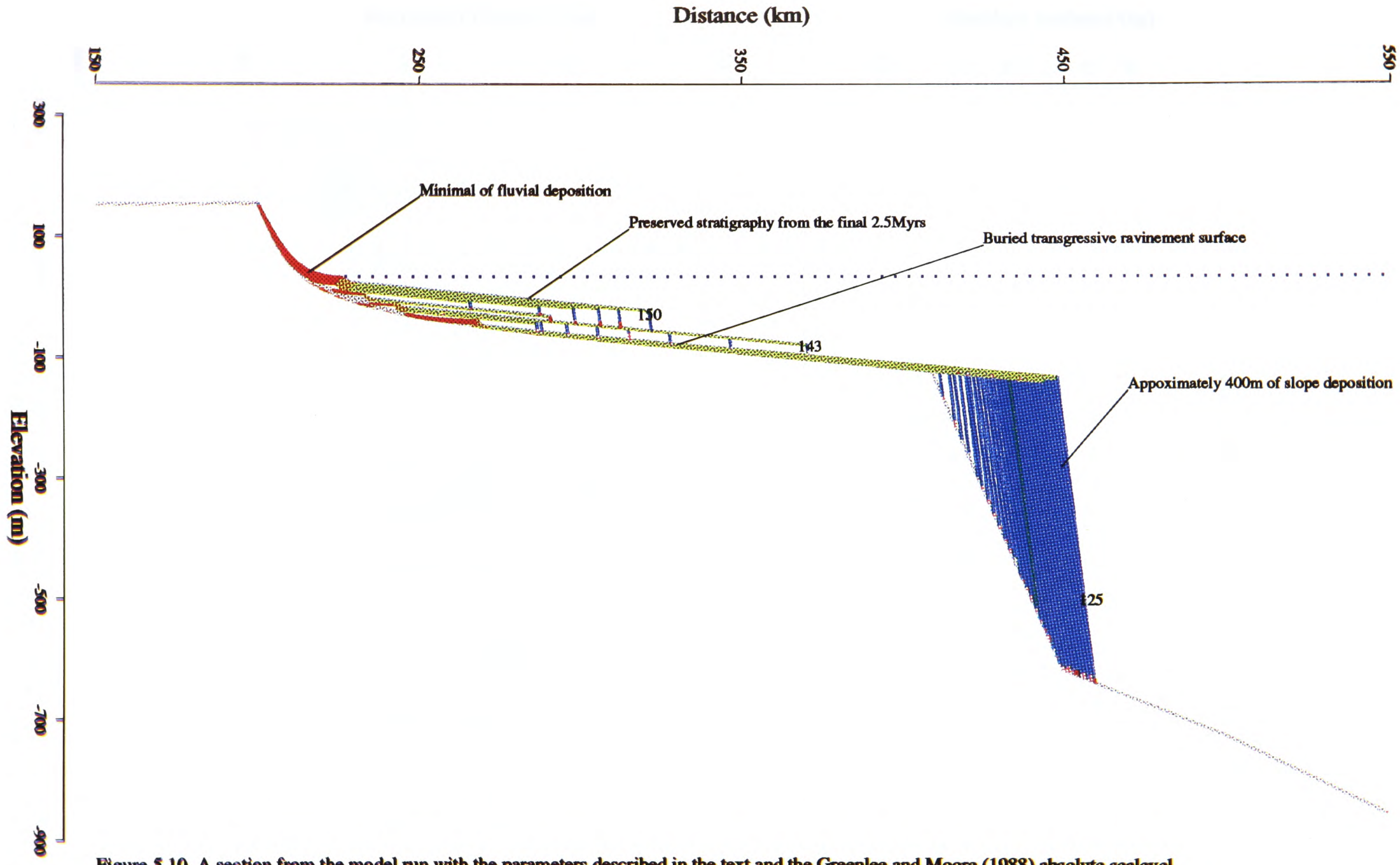

Figure 5.10. A section from the model run with the parameters described in the text and the Greenlee and Moore (1988) absolute sealevel curve. Though this curve has similar high-order fluctuations to the Haq curve, the amplitudes are less, and the detail different. The effect of these differences is to change details of the stratigraphic pattern produced. In particular the stratigraphy formed in the last 2.5Myrs of the model run progrades further, burying the 12.5Myr transgressive surface. This transgressive surface in this case eroded less of the older stratigraphy than in the surface produced at the same time by the Haq curve because of the lower amplitude of the Greenlee and Moore curve.

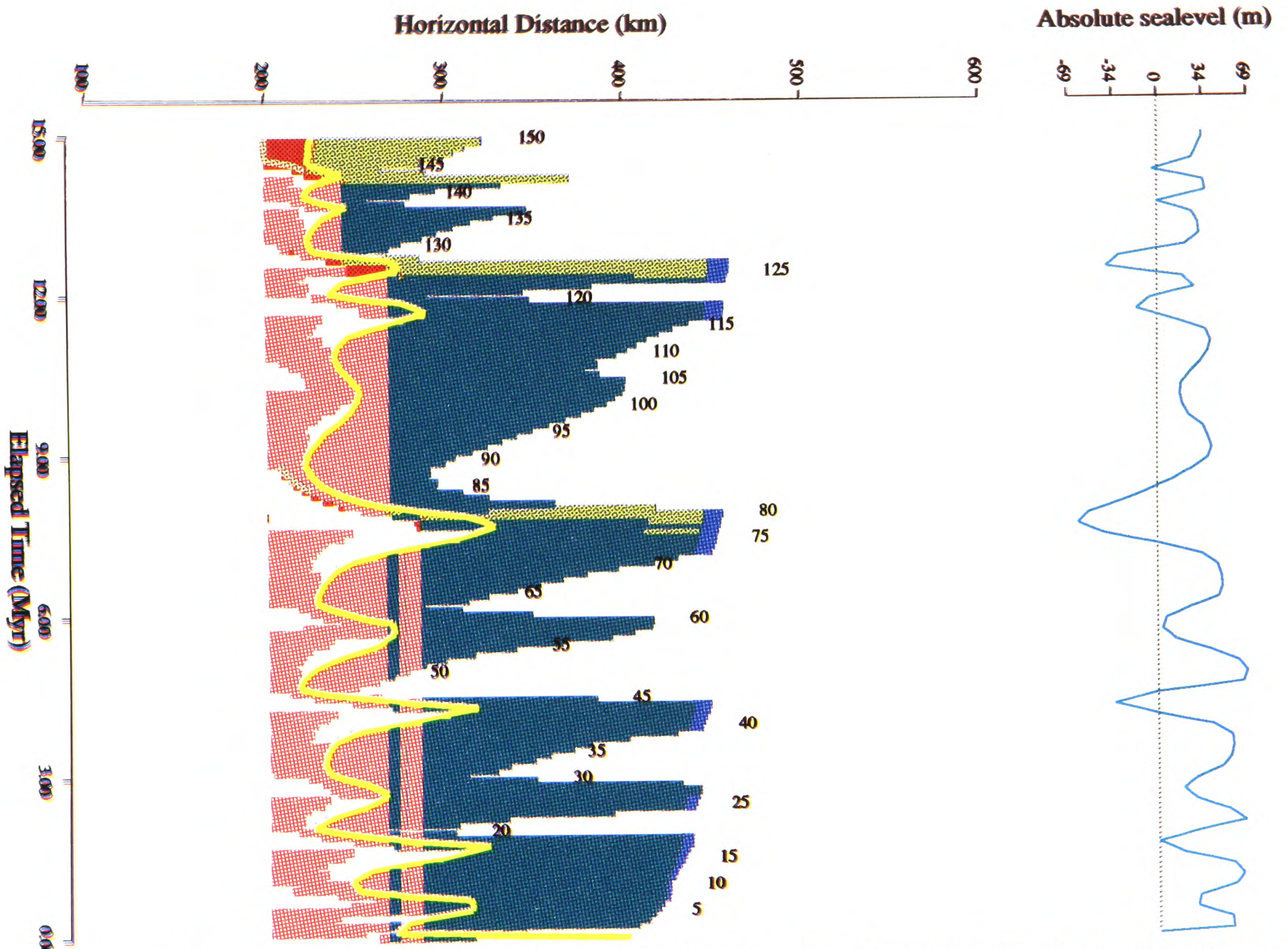

Figure 5.11. A chronostratigraphic diagram and an absolute sealevel curve from the model run with the parameters described in the text and the Greenlee and Moore (1988) absolute sealevel curve. Though this curve has similar high-order fluctuations to the Haq curve, the amplitudes are less, and the detail different. The effect of these differences is to change details of the stratigraphic pattern produced. For example, the exact pattern of beach movement is different in this example. Also the stratigraphy from the last 2.5Myrs has prograded further into the basin, burying the 12.5Myr transgressive surface which remains uncovered in the example generated with the Haq curve.

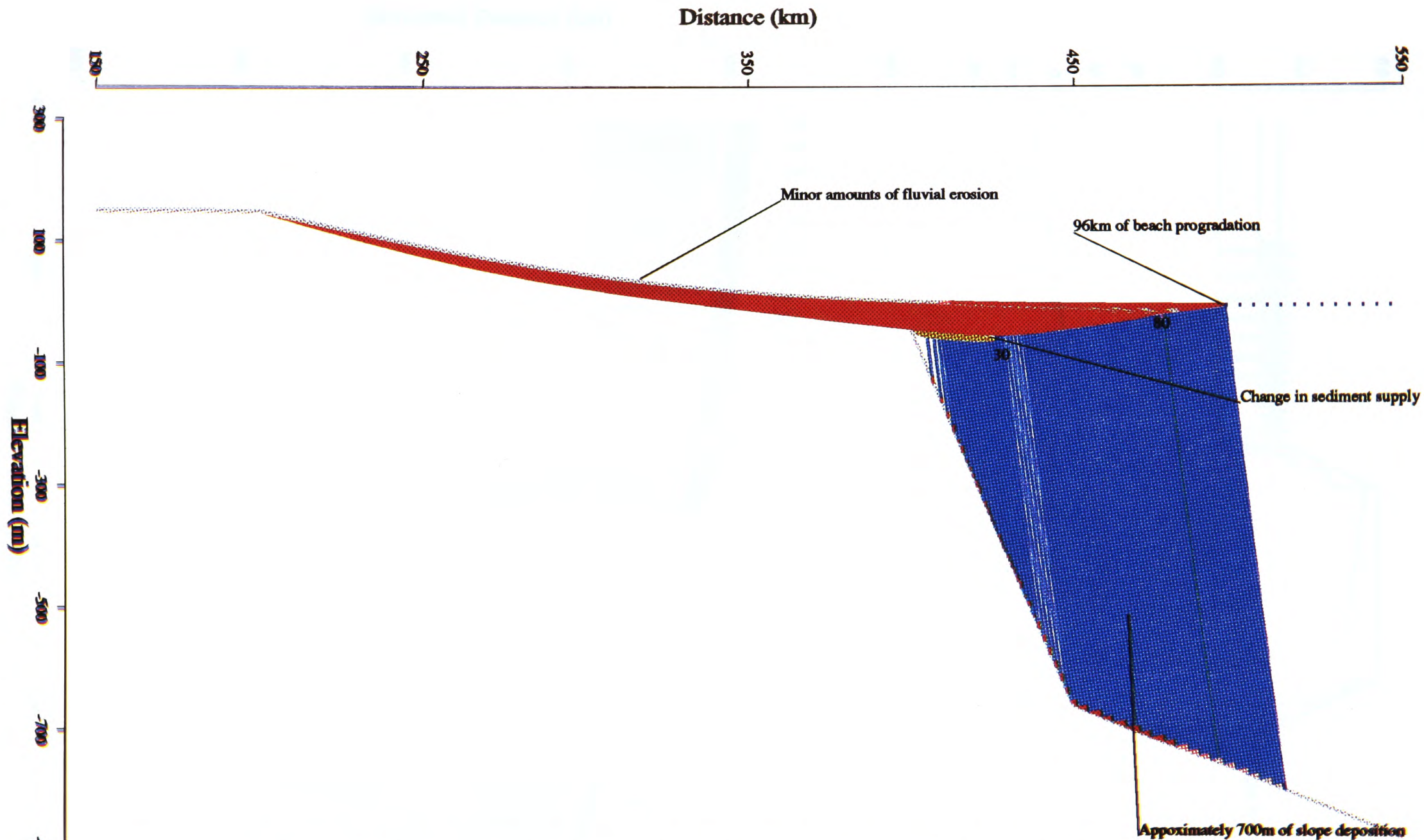

Figure 5.12. A section from the model run with variable sediment supply, variable partitioning coefficient values, and the Watts and Steckler (1979) absolute sealevel curve. All other parameters are as described for the initial model run in figure 5.6. Values for the partitioning coefficient vary from 0.1 to 0.6 in synchroneity with the changes in the sediment supply (figure 5.13). The visible effects of the changed sediment supply parameters are a change in the overall distance of progradation, and a distinct change in the pattern of shelf and shoreface deposition. The fluvial stratigraphy is topped by an erosion surface of minor vertical significance, and this should be ignored as an unrealistic artifact of the profile geometry.

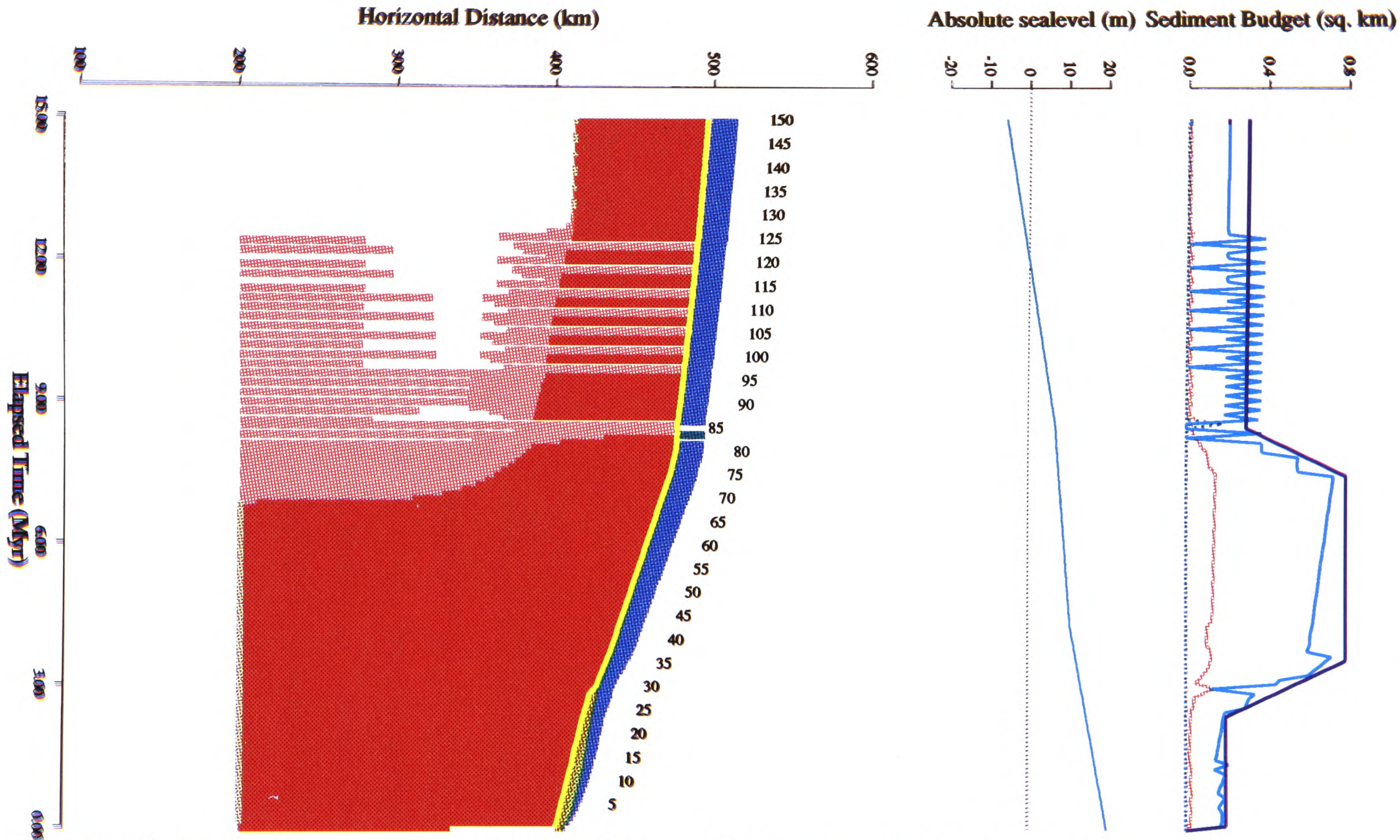

Figure 5.13. A chronostratigraphic diagram and an absolute sealevel curve from the model run with variable sediment supply, variable partitioning coefficient values, and the Watts and Steckler (1979) absolute sealevel curve. All other parameters are the as described for the initial model run in figure 5.6. Values for the partitiong coefficient vary from 0.1 to 0.6 in synchroncity with the changes in the sediment supply. The variable sediment supply and partitioning coefficient have the desired effect of changing the rate of progradation such that it is more similar to the rates shown in the chronostratigraphic diagram from Greenlee et al. (1988) (summarised in figure 5.3).

Chapter 6

Chapter 6 - The conclusions

"I have something to say.

It's better to burn out than to fade away.

There can be only one!"

(Gregory Widen Highlander)

6.1 Introduction

This chapter describes the conclusions that have been drawn from the modelling results presented in chapters three, four and five. It also attempts to indicate where future work in the study of passive rift-margin stratigraphy might focus to answer some of the specific points raised by this work

6.2 Controls on sequence geometry

In chapter three, the quantitative forward model was used to investigate the possible controls on sequence geometry using the depositional sequence stratigraphic model of, for example, Posamentier *et al.* (1988) and Van Wagoner *et al.* (1990) as a framework for comparison. This work lead to the following conclusions :

- The quantitative forward model is capable of reproducing the general geometry of type-1 and type-2 sequences in the sense of Posamentier *et al.* (1988), and Van Wagoner *et al.* (1990), but it cannot reproduce all of the parasequence stacking patterns shown in the depositional sequence stratigraphic model. This is because some of the patterns, such as the aggradational stacking pattern require a very specific distribution of accommodation space balanced with a very specific magnitude of sediment supply. The inability of the quantitative model to reproduce these patterns may be indicative of the rather unlikely pattern of accommodation space necessary to produce them.

- Calculation of the amplitude of absolute sealevel changes from coastal onlap patterns may be greatly complicated by the geometry of the fluvial profile. The model results show that the amplitude of the vertical component of the stratal onlap in the model is more dependent on the fluvial profile geometry than on the magnitude of the relative or absolute sealevel change. This result should be considered bearing in mind the weaknesses of the fluvial profile implementation in the model.
- The concepts of the hinge point and the equilibrium point used in the sequence stratigraphic model are flawed. The relative rates of thermal subsidence and absolute sealevel change mean that only during the points of lowest gradient on the absolute sealevel curve, can the rate of thermal subsidence or uplift on a passive rift margin equal the rate of absolute sealevel change.
- Flexural isostasy is not a first order control on the model stratigraphy when absolute sealevel is varied. Even with reasonably low values of T_e of, for example, 10km, the flexural subsidence simply adds small amounts of accommodation space, but does not significantly alter the basic pattern of stratigraphy preserved.
- The behaviour of the fluvial profile is a first order control on model stratigraphy. For example, a less concave profile produces a stratigraphic pattern very different from that produced by a more concave profile. Despite the unrealistic nature of aspects of the profile behaviour and the lack of direct link with physical process, the model results suggest that profile geometry may well be a very significant control on stratigraphic patterns.
- The sediment partitioning coefficient is also a first order control in the model, and the effects of sediment partitioning in natural systems could conceivably be misinterpreted to be due to eustasy. For example, a reduction in the amount of sediment being deposited subaerially, and an increase in bypassing of sediment into the sea, may produce a transgressive pattern of stratigraphy which would be difficult to distinguish from that due to an absolute sealevel rise.
- Variable sediment supply is a first order control on model stratigraphy. It has a particularly pronounced impact on the stratigraphic pattern when sediment supply is

low during a time of rising absolute sealevel. This has often been underestimated in other studies on stratigraphic controls. Accurately distinguishing in the ancient record between effects due to variable sediment supply, and effects due to variable absolute sealevel may prove very difficult.

- Variable sediment supply alone, without any contribution from variable absolute sealevel, is capable in the model of producing stratigraphic patterns with some similarities to those seen in type-2 sequences. This suggests that stratigraphy influenced by variable sediment supply due to factors such as point source switching, climatic changes, drainage basin morphology, or combinations of these, may be misinterpreted as being due to eustasy. However, a relative sealevel fall is still necessary in the model to cause the vertical juxtaposition of fluvial and marine stratigraphy across a subaerial erosion surface.
- Combined complex controls on stratigraphy should not be underestimated in terms of the difficulty in correctly interpreting the results. A model run with combined controls is difficult to interpret, even given the simplicity of the model, and the availability of the complete details of all the model parameters, such as the absolute sealevel curve, and the sediment supply curve. This highlights once more, the non-unique nature of most explanations of stratigraphic patterns.

Future work in this area should concentrate on the further investigation of the contribution of sediment supply and fluvial profile behaviour to stratigraphic patterns. Further work should also be carried out on processes which are as yet poorly understood in terms of their contribution to passive rift-margin stratigraphy. For example, the response of the fluvial profile to relative sealevel change, and the significance of submarine erosion, both on the shelf and on the slope, and its link with flexural uplift, all require further study.

6.3 Complex interactions, feedback effects and cyclicity

In chapter four, the quantitative forward model was used, via a series of sensitivity tests, to investigate the possibility of complex interactions within the model, and the generation by the model of patterns of cyclical sedimentation without the requirement for periodic external forcing. This work lead to the following conclusions :

- There exists within the model, when run with the initial conditions set to low fluvial sediment supply producing a transgressive beach, a feedback effect between thermal subsidence, shoreface erosion, flexure and fluvial erosion, which is capable of producing cycles of stratigraphy without any external periodic forcing.
- The effect occurs with a variety of initial conditions, including high and low magnitudes of thermal subsidence, a different shoreface geometry, and different fluvial profile geometries. Though variations in the initial conditions affect the details of the stratigraphic pattern, the basic pattern produced by the feedback effect is present in all these sensitivity tests.
- Running the model with different time steps demonstrates that the period of the oscillations in sediment supply is entirely dependent upon the length of the time step used. Peaks in sediment supply always occur at the same chron regardless of the E.M.T. that the chron represents. As the model time step is reduced towards zero, so the period of the oscillation approaches zero. This demonstrates that the feedback effect in the model is a numerical instability resulting from the discretised nature of the model.
- Running the model with a finite value for the flexural response time that is longer than the length of the time step shows that the inclusion of the response time complicates the unstable behaviour of the model, but does not surmount the fundamental problem of the instability. The timing and period of the oscillations are still dependent upon the duration of the time step used, but no longer show a simple linear relationship with the time step duration.

- Although it seems intuitively possible that the feedback mechanism described may occur in natural systems, the stratigraphic model presented here can provide no indication either way of the existence of such a feedback. This is due to the numerical instability inherent in the model as a result of the discretised representation of continuous functions. Further investigations of potential feedback effects would thus require a model formulated with continuous time-dependent equations.

6.4 Modelling the Neogene stratigraphy of the North American Atlantic passive rift margin

In chapter five, the quantitative forward model was used to investigate the contributory factors behind the pattern of stratigraphy preserved in the Neogene of the North American Atlantic margin. This investigation also served to test the ability of the model to reproduce the broad general patterns observed in an actual example of passive rift-margin stratigraphy. This work lead to the following conclusions :

- The gross large-scale features of the Miocene stratigraphy such as the distance of clinoform migration, and the thickness of the succession, can be reproduced with the model using the parameter values described in section 5.3. Even given the inevitable uniqueness problems, it seems safe to conclude from this that the basic processes of thermal subsidence, flexural isostasy, eustasy, and sediment progradation are those responsible for the basic features of the observed stratigraphy.
- The higher-order eustatic curves of Haq *et al.* (1988) and Greenlee and Moore (1988) produce significantly worse fits in the model than the lower-order curve of Watts and Steckler (1979). There are large elements of circular reasoning in both the methodology used to define the high-order curves, and in the methods previously used to test them (e.g. Schroeder and Greenlee, 1993). Even though the problem of the two-dimensionality of the model cannot be ruled out in explaining the poor fits, it still seems fair to conclude that there are severe problems in using such high-order eustatic curves to explain the geometry of the observed stratigraphy.

- Varying the magnitude of sediment supply and the value of the fluvial-marine partitioning coefficient improves some of the details of the basic fit between the model and the interpreted data. There is an element of circular reasoning in this, since the value of sediment supply was chosen on the basis of the requirement to reproduce the correct distance of progradation. However, despite this circularity, it still seems that variable sediment supply and sediment partitioning through time are necessary to reproduce the stratigraphic pattern if high-order eustatic changes are not occurring.

Future work in this area should concentrate on refining the model to include more processes, such as, for example, slope wasting and mass movement. It would also be desirable in the longer term to extend the model into three dimensions, so that the model output could be more readily and more accurately compared with observational data such as seismic lines and borehole cores. The addition of extra processes to the model may provide insights into the details of stratigraphic patterns, such as the fine scale onlap and downlap patterns, that the model cannot presently reproduce.

Appendix 1

Appendix 1 - Model Parameters

This appendix describes the model parameters in terms of there use in the model, and the range of values to which they can be set.

Chron Parameters

Total number of chrons : Integer, 1 - 200.

This specifies the total number of chrons that can be generated in any model run.

Number of chrons per execution step : Integer, 1 - 200.

This specifies the number of chrons generated by the model at each execution step before the output is displayed. For example, the total number of chrons may be 100, but the number of chrons generated before the model output is displayed could be 10.

Chron interval : Float, 0.01 - 10.0 Myrs.

This gives the length of each model time step in millions of years.

Frequency of chron storage : Float, 0.01 - 10.0 Myrs.

This defines the number of time steps between storage of chron surfaces. For example, the model time step may be 0.1Myrs, but the storage frequency may be 0.5Myrs, which would mean that only every fifth chron would be stored in the model data structure.

General Parameters

Profile length : Integer, 128 - 4196 km.

The length of the profile in kilometres. The values of the lengths used are powers of two in the range specified to allow the calculation of flexure using both a finite difference method and a FFT method.

Density of uncompacted sediment : Float, 1.0 - 3.0 kgm^{-3}.

The density of the sediment deposited and eroded on the profile. This is used in the flexure calculations.

Initial profile topography :

This is defined as a series of coordinate pairs, horizontal distance in kilometres and elevation in metres, which are used as the points for interpolation to define the topographic profile.

Fluvial Profile Parameters

Fluvial curve type :

A flag to indicate whether the model should use an exponential or a complementary error function curve for the fluvial profile.

Length of the fluvial profile : Integer, 0 - 2000km.

This determines the length of the fluvial profile from the beach to the landward end of the depositional profile.

Rate of lengthening of the profile : Float, 10.0 - 0.001km per time step.

This defines the landward movement per time step of the landward end of the fluvial profile.

Error function length scale : Float, 1.0 - 5.0.

This parameter determines the portion of the complementary error function to be used to determine the fluvial profile. For example, a length scale of 1.0 means that the portion of the curve from 0.0 to 1.0 is scaled to fit between the beach and the fall line position. This would produce a less concave profile than if, for example, a length scale of 3.0 was used.

Fluvial-marine partitioning coefficient : Float, 0.0 - 1.0.

This determines the areas of sediment deposited on the fluvial and marine portions of a chron. For example, a value of 0.4 means that 40% of the available area is deposited as fluvial stratigraphy, while the remaining 60% is deposited as marine stratigraphy.

Marine Profile Parameters

Shelf gradient : Float, 0.0 - 0.5 mkm^{-1}.

This parameter determines the gradient of the shelf profile.

Slope gradient : Float, 0.5 - 100.0mkm^{-1}.

This parameter defines the gradient of the marine slope.

Height of shoreface : Integer, 1.0 - 50.0m.

This is the height of the shoreface, which defines the depth at which the transition from shoreface to offshore shelf occurs.

Width of shoreface : Integer, 1.0 - 50km.

This is the width of the shoreface zone which marks the transition from the fluvial to the marine profile.

Tectonic Parameters

Beta stretching factors :

Values for the stretching factor used in the one and two-layer stretching models. Stretching values are given with a specified position on the profile, in kilometres. Linear interpolation between these points is used to define stretching values for the complete length of the profile.

Sigma stretching values :

Sub-crustal stretching factor used in the two-layer stretching model. These values are given in the same format as the beta stretching factors, and similarly defined across the complete profile by linear interpolation.

Depth to the two-layer boundary : 0 - 150km.

The depth to the boundary between the upper and lower layers in the two-layer stretching model.

Initial lithospheric thermal age : 0 - 200Myrs.

The age in millions of years, at the beginning of the model run, since the end of the rifting phase and the start of the postrift phase. This is used in both the stretching models and in the flexural model.

Elastic thickness of the lithosphere : Integer, 0, 5, 30, infinite or time-variable

This parameter defines the value of the elastic thickness of the lithosphere to be used in the flexure calculations.

T_e profile

Values for the elastic thickness of the lithosphere are defined at points on the profile, and linear interpolation is used to define values for the complete profile. These values are used in the calculation of flexure when the option for laterally varying T_e is selected.

Flexural response type :

This parameter defines the type of flexural response to loading and unloading to be used in the flexural model. It can be either instantaneous, a linear relaxation, or a exponential relaxation.

Flexural response time : Float, 0.1 to 100.0Myrs

This parameter defines the time taken by the modelled lithosphere to relax after a loading event when the linear relaxation option is used.

Absolute sealevel curve parameters

Type of absolute sealevel change:

Absolute sealevel in the model can be held constant at 0m, varied according to the curve parameters described below, or varied according to an external predefined file. If the latter is chosen, the file containing the values must have the same time-step values as chosen for the chrons in the model. For example, with a chron interval of 0.1Myrs, there must be a value in the absolute sealevel file at 0.1Myr intervals.

Short-term curve type :

The short-term curve can be either a simple linear curve, a minimum-to-maximum saw-tooth curve, a maximum-to-minimum saw-tooth curve, an initially increasing sinusoidal curve, or an initially decreasing sinusoidal curve.

Short-term curve minimum : Integer, -50 - 0m.

This parameter gives the lowest value for the short term curve.

Short-term curve maximum : Integer, 0 - 50m.

This parameter gives the highest value for the short term curve.

Short-term curve period : Float, 0 - 10Myrs.

This defines the period of the short-term absolute sealevel curve in millions of years.

Long-term curve type :

The long term absolute sealevel curve can be a linearly increasing curve, a linearly decreasing curve, an initially rising sinusoidal curve, or an initially falling sinusoidal curve.

Long-term curve minimum : Integer, -100 - 0m.

This parameter gives the lowest value for the long term curve.

Long-term curve maximum : Integer, 0 - 100m.

This parameter gives the highest value for the long term curve.

Long-term curve period : Integer, 1 - 100Myrs.

This defines the period of the long-term absolute sealevel curve in millions of years.

Sediment supply parameters

Sediment supply model type :

Sediment supply in the model can be calculated in one of four ways determined by this parameter; it can be held constant, or it can be calculated purely from erosion and deposition on the fluvial and marine profiles, or it can be calculated from profile erosion, with the addition of area from a pre-calculated curve, or it can be calculated purely from a pre-calculated curve.

Sediment supply curve type :

The sediment supply curve can have several forms; a simple linear increase, a simple linear decrease, an initially rising sinusoidal curve, an initially falling sinusoidal curve, a minimum-to-maximum saw tooth curve or a maximum-to-minimum saw tooth curve. The curve may also be defined from an external file.

Maximum sediment area : Float, 0 - 4km^2.

This parameter defines the maximum value for the sediment supply curves, or the value for the area available for deposition for each time step when the constant sediment supply option is used.

Minimum sediment area : Float, 0 - 4km^2.

This parameter defines the minimum value for the sediment supply curves.

Sediment supply curve period : Float, 0 - 10Myrs.

This parameter defines the period of the sediment supply curve in millions of years. If a saw tooth curve is selected, for example, it defines the period between sudden falls or rises.

Sediment release coefficient : Integer, 0 - 100.

This parameter specifies the percentage of the area of sediment eroded on the fluvial profile that is to be released for deposition on the model profile for each time step. For example, if a release coefficient of 50% were specified, then for each time step 50% of the eroded sediment area would be released, the remaining area would be added to the total area held for future release in subsequent time steps.

Appendix 2

Appendix 2 - Details of the computer system and the source code listings

This appendix describes the requirements of the model in terms of hardware, and software. A full listing of the model module and the include file are given.

Hardware requirements

The model system has been developed on a network of SUN Microsystems workstations, of various types and specifications ranging from Sun 3/80s acting as x-terminals, to a SPARC 2 colour workstation. File service is provided by a central fileserver. Output from the model was produced using a laser printer, and a QMS Colourscript 100 model 10 colour printer.

Software requirements

The software is written predominantly in C, though some routines such as the flexure calculations are written in FORTRAN. The C code has been compiled using the SUN cc compiler. The model uses the Openwindows graphical interface. The library files that have been used are shown in the model include file. Postscript output was produced from the model using the CAL2PS library routines.

The code listings

The program has been developed as five separate modules which fulfil individual functions. The main modules contains the majority of the actual model code. The other modules contain the code to define the model windows, canvases, and menus, to define the behaviour of the interface between the windows and the user, and to plot the model output, both directly onto the screen, and also into a postscript file. Many of the data structures

used throughout the modules are defined globally in the include file. For the sake of brevity, and because the details of the window definitions and the graphics output are not essential to the arguments in this thesis, only the header file and the main model module are listed here.

```
1     /* Program to forward model stratigraphy in a passive rift margin basin.
2      Written by Pete Burgess. Started January 1991.  Last Updated 1/3/94. */
3
4     /* Include basin header file to define functions, consts, global vars, and structures
       */
5     #include "includes/Xbasin_header.h"
6
7     struct File_params      files;
8     struct Params           params;
9     struct Options          options;
10    struct Zoombox          zoombox;
11    struct Eustasy          eustasy;
12    struct Sed_budget       sed_budget;
13    struct Strat            strat;
14    struct Tect             tect;
15    struct Post             post;
16    struct Exec             exec;
17    struct Exec_flags       exec_flags;
18    struct Chrono_plot      chrono_plot;
19
20    Xv_notice       notice;
21
22    FILE    *info, *sed_curve_file, *chrons, *beach;
23
24    void main(argc, argv)
25    /* Call the windows or the batch routine depending on command line arguments */
26    int argc;
27    char **argv;
28    {
29            /* Defined in include file set_windows.c */
30
31            if (argc == 1)
32            {
33                    files.batch = FALSE;
34                    setgraphics();
35                    window_main_loop(mainframe);
36            }
37            else
38            {
39                    files.batch = TRUE;
40                    batch_job(argc, argv);
41            }
42    }
43
44    void batch_job(argc, argv)
45    /* Control model execution if the program is being run as a batch job */
46    int argc;
47    char **argv;
48    {
49            char buffer[80], test_com[5];
50
51            info = fopen("info.txt","w");
52
53            if (argc < 4)
54                    fprintf(info,"\nIncorrect number of command line arguements!\nSyntax
      : basin -b <input file> <output file>\n");
55            else
56            {
57                    strcpy(test_com, "-b");
58                    strcpy(buffer, &argv[1][0]);
59
60                    if (strcmp(buffer,test_com) == 0)
61                    {
62                            /* NOTE - next lines commented out pending modification of th
      e load and save
63                                    routines.
64
65                            strcpy(files.directory, "/home/tigger_scratch/pete/");
66                            strcpy(files.fname, &argv[2][0] );
67                            strcpy(files.out_fname, &argv[3][0] );
68                            fprintf(info,"Reading from %s, writing to %s\n",files.fname,
```



```
69                                  fils.out_fname);
70
71                          fprintf(stderr,"Batch mode operation not currently supported\
      n")
72
73                          do_load();
74                          exec_flags.initialised = TRUE;
75                          fprintf(info,"Running model...");
76                          run_proc();
77                          fprintf(info,"Complete\n");
78                          do_save(); */
79                  }
80          }
81          fclose(info);
82    }
83
84    void special_case_run()
85    {
86          int     count = 1;
87          char    filename[80], number_tag[10];
88
89          do
90          {
91                  init_proc();
92                  params.chronfreq = params.chronint = (float) (count * 0.0001);
93
94                  fprintf(stderr,"Model run %d, chron interval %f\n", count, params.chr
      onint);
95                  run_proc();
96
97                  sprintf(number_tag,"%8.6f", params.chronint);
98                  strcpy(filename,"/home/tigger_scratch/pete/cint_sedcurve");
99                  strcat(filename,number_tag);
100
101                 dump_sedcurve(filename, count);
102                 fprintf(stderr,"Run %d complete\n", count);
103
104                 count++;
105         }
106         while (count < 1000);
107
108   }
109
110   void init_proc()
111   /* Initialise the execution variables, get profiles, set arrays, and start curves. */
112   {
113         FILE *outfile;
114         int loop;
115
116         XClearWindow(dpy, canvas_win);
117
118         get_params();
119
120         if (!check_params())
121         {
122                 exec.layer = 0;
123                 exec.chronelapsed = 0;
124                 exec.step_chrons_done = 0;
125                 exec.total_chrons_done = 0;
126                 exec.time_steps_done = 0;
127
128                 exec.elapsed = 0.0;
129                 exec.sea_cycle_elapsed = 0.0;
130                 exec.sed_cycle_elapsed = 0.0;
131
132                 /* Set all the curves elements to zero */
133                 zero_curve_data();
134
135                 if (eustasy.change_flag == 1) /* Curve defined from window */
136                         set_seastart();
137                 else
```

```
138                     if (eustasy.change_flag == 2) /* Curve defined in a file */
139                             exec.sealevel = read_user_seacurve();
140                     else
141                             exec.sealevel = 0; /* Constant sealevel */
142
143                     set_sedstart();
144                     set_pcstart();
145                     exec.Te = set_Te_start();
146                     set_strat(FALSE);
147
148                     setload_beta_Te_arrays();
149
150                     copy_chron(1);          /* Find the initial beach position */
151                     exec.beach_pos = strat.beach[0] = find_chron_sea_intersection();
152
153                     adjust_topog_to_sealevel(); /* Need to adjust topography if the initi
    al sealevel is not 0 */
154
155                     if (options.riv_prof)
156                             init_drainage();
157                     if (options.shelf_prof && options.init_shelf_prof)
158                             init_marine_prof();
159
160                     set_subsid_arrays();
161                     set_presev_data();
162
163                     exec_flags.box_drawing = FALSE;
164                     exec_flags.box_drawn = FALSE;
165                     exec_flags.zoomed = FALSE;
166                     exec_flags.diagpos = 0;
167                     exec_flags.execution_complete = FALSE;
168                     exec_flags.initialised = TRUE;
169
170                     full_screen_draw(); /* Draw the profile to show the initial condition
    s */
171
172             }
173     }
174
175     void get_params()
176     /* Retrieve the input parameters from the parameter windows,
177      and put these values into the appropriate parts of the various program structures */
178     {
179             char buffer[80];
180
181             /*xv_get retrieves the specified item to put into the struct.
182              The item is either retrieved as a string into buffer, which can then be
183              converted to a float value, or is retrieved directly as an integer.*/
184
185             options.prograde = (int) xv_get(gen_options_item, PANEL_TOGGLE_VALUE, 0);
186             options.riv_prof = (int) xv_get(gen_options_item, PANEL_TOGGLE_VALUE, 1);
187             options.shelf_prof = (int) xv_get(gen_options_item, PANEL_TOGGLE_VALUE, 2);
188             options.init_shelf_prof = (int) xv_get(gen_options_item, PANEL_TOGGLE_VALUE,
    3);
189             options.section_type = (int) xv_get(axis_option_item, PANEL_VALUE);
190
191             options.flex_type = (int) xv_get(flex_options_item, PANEL_VALUE);
192             options.Te_type = (int) xv_get(Te_options_item, PANEL_VALUE);
193             tect.response_type = (int) xv_get(response_type_item, PANEL_VALUE);
194             options.subside_type = (int) xv_get(subside_type_item, PANEL_VALUE);
195             options.profile_type = (int) xv_get(profile_type_item, PANEL_VALUE);
196             options.curve_type = (int) xv_get(curve_type_item, PANEL_VALUE);
197             options.fluvial_prog = (unsigned short int) xv_get(fluvial_prog_item, PANEL_V
    ALUE);
198             options.perm_fluv_prof = (unsigned short int) xv_get(perm_prof_item, PANEL_VA
    LUE);
199             options.onlap_type = (unsigned short int) xv_get(onlap_type_item, PANEL_VALUE
    );
200             options.water_loading = (unsigned short int) xv_get(water_loading_item, PANEL
    _VALUE);
201
```



```
202             params.proflen = pow(2.0, (double)xv_get(proflen_item, PANEL_VALUE) );
203
204             params.prof_gap = params.proflen / (float) USEDPTS;
205
206             params.marker_point = (int) (xv_get(marker_point_item, PANEL_VALUE) / params.
    prof_gap);
207
208             params.Psed =  atof((char *) xv_get(sed_density_item, PANEL_VALUE));
209
210             params.Pdisp = P_WATER;
211             params.Pmant = P_MANT;
212             params.Pinf = params.Pdisp; /* Water infill!! */
213
214             strcpy(params.loadfile, (char *) xv_get(loadfile_item, PANEL_VALUE));
215
216             strcpy(params.betafile, (char *) xv_get(betafile_item, PANEL_VALUE));
217
218             strcpy(params.sigmafile, (char *) xv_get(sigmafile_item, PANEL_VALUE));
219
220             strcpy(params.Tefile, (char *) xv_get(Tefile_item, PANEL_VALUE));
221
222             params.boundary_depth = (float) xv_get(boundary_depth_item, PANEL_VALUE);
223
224             params.crust_age = atof((char *) xv_get(crust_age_item, PANEL_VALUE));
225
226             tect.response_time = atof((char *) xv_get(response_time_item, PANEL_VALUE));
227
228             params.shelf_grad = atof((char *) xv_get(shelf_grad_item, PANEL_VALUE));
229
230             params.slope_grad = atof((char *) xv_get(slope_grad_item, PANEL_VALUE));
231
232             params.wave_base = atof((char *) xv_get(wave_base_item, PANEL_VALUE));
233
234             params.shore_width = atof((char *) xv_get(shore_width_item, PANEL_VALUE));
235
236             params.drainage_len = atof((char *) xv_get(drainage_item, PANEL_VALUE));
237
238             params.diff_coeff = atof((char *) xv_get(diffcoeff_item, PANEL_VALUE));
239
240             /*params.partition_coeff = atof((char *) xv_get(partition_item, PANEL_VALUE))
    ;*/
241
242             params.cutback_rate = atof((char *) xv_get(cutback_item, PANEL_VALUE));
243
244             params.length_scale = atof((char *) xv_get(length_scale_item, PANEL_VALUE));
245
246             params.fluv_depos_cutoff = atof((char *) xv_get(fluv_depos_cutoff_item, PANEL
    _VALUE));
247
248             params.chronint = atof((char *) xv_get(chronint_item, PANEL_VALUE));
249
250             params.chronfreq = atof((char *) xv_get(chronfreq_item, PANEL_VALUE));
251
252             params.chrons = (int) xv_get(chrons_item, PANEL_VALUE);
253
254             params.step_chrons = (int) xv_get(step_chrons_item, PANEL_VALUE);
255
256             eustasy.change_flag = (int) xv_get(sea_change_flag_item, PANEL_VALUE);
257
258             eustasy.max_level1 = (int) xv_get(seamax_item1, PANEL_VALUE);
259
260             eustasy.min_level1 = (int) xv_get(seamin_item1, PANEL_VALUE);
261
262             eustasy.freq1 = atof((char *) xv_get(seafreq_item1, PANEL_VALUE));
263
264             eustasy.curve_type1 = (int) xv_get(seacurve_item1, PANEL_VALUE);
265
266             strcpy(eustasy.curve_fname, (char *) xv_get(seafname_item, PANEL_VALUE));
267
268             eustasy.max_level2 = (int) xv_get(seamax_item2, PANEL_VALUE);
269
```

```
270             eustasy.min_level2 = (int) xv_get(seamin_item2, PANEL_VALUE);
271
272             eustasy.freq2 = (int) xv_get(seafreq_item2, PANEL_VALUE);
273
274             eustasy.curve_type2 = (int) xv_get(seacurve_item2, PANEL_VALUE);
275
276             sed_budget.supply_flag = (int) xv_get(supply_flag_item, PANEL_VALUE);
277
278             /* Needs to be converted to square metres */
279             /*sed_budget.external_budget = (int) xv_get(external_budget_item, PANEL_VALUE
        ) * 1.0E6;*/
280
281             sed_budget.maxsed = atof((char *) xv_get(sedmax_item, PANEL_VALUE)) * 1.0E6;
282
283             sed_budget.minsed = atof((char *) xv_get(sedmin_item, PANEL_VALUE)) * 1.0E6;
284
285             sed_budget.freq = atof((char *) xv_get(sedfreq_item, PANEL_VALUE));
286
287             sed_budget.drainage_ratio = (int) xv_get(drain_rat_item, PANEL_VALUE);
288
289             sed_budget.release_perc = (int) xv_get(release_item, PANEL_VALUE);
290
291             sed_budget.curve_type = (int) xv_get(sedcurve_item, PANEL_VALUE);
292
293             sed_budget.pc_type_flag = (unsigned short int) xv_get(pc_flag_item, PANEL_VAL
        UE);
294
295             sed_budget.pc_max = atof((char *) xv_get(pcmax_item, PANEL_VALUE));
296
297             sed_budget.pc_min = atof((char *) xv_get(pcmin_item, PANEL_VALUE));
298
299             sed_budget.pc_freq = atof((char *) xv_get(pcfreq_item, PANEL_VALUE));
300
301             /* Get the numbers for drawing the chrono strat
302             chrono_plot.show_chrono = (unsigned short int) xv_get(active_diags_item, PANE
        L_TOGGLE_VALUE, 0);
303             chrono_plot.show_eustasy = (unsigned short int) xv_get(active_diags_item, PAN
        EL_TOGGLE_VALUE, 1);
304             chrono_plot.show_sed_supply = (unsigned short int) xv_get(active_diags_item,
        PANEL_TOGGLE_VALUE, 2);
305
306             chrono_plot.wheeler_width = (unsigned short int)  xv_get(wheeler_width_item,
        PANEL_VALUE);
307             chrono_plot.sed_supply_width = (unsigned short int)  xv_get(sed_supply_width_
        item, PANEL_VALUE);
308             chrono_plot.eustasy_width = (unsigned short int)  xv_get(sed_supply_width_ite
        m, PANEL_VALUE);
309
310             chrono_plot.zoom_left = (int) xv_get(wheeler_zoom_left_item, PANEL_VALUE);
311             chrono_plot.zoom_right = (int) xv_get(wheeler_zoom_right_item, PANEL_VALUE);
        */
312     }
313
314     int check_params()
315     /* Check some of the major parameters are within proscribed limits. Returns TRUE if t
        here is a problem,
316     FALSE if everything checks out */
317     {
318             int             problem = FALSE;
319             FILE            *testfile;
320             Xv_notice       notice;
321
322             if (params.proflen < 100 || params.proflen > 5000)
323             {
324                     notice = xv_create( mainframe, NOTICE,
325                             NOTICE_MESSAGE_STRINGS, "Profile length too big or too small!
        ",
326                                                     "Range 100 - 5000 (km)", NULL,
327                             NOTICE_BUTTON,          "Continue", 1,
328                             XV_SHOW,                TRUE, NULL);
329                     problem = TRUE;
```



```
330             }
331
332             if ((testfile = fopen(params.loadfile, "r")) == NULL)
333             {
334                     notice = xv_create( mainframe, NOTICE,
335                             NOTICE_MESSAGE_STRINGS, "No such loadfile able to open in pre
        sent directory!",
336                                                     "Check filename and try again.", NULL
        ,
337                             NOTICE_BUTTON,          "Continue", 1,
338                             XV_SHOW,                TRUE, NULL);
339
340                     problem = TRUE;
341             }
342             fclose(testfile);
343
344             if ((testfile = fopen(params.betafile, "r")) == NULL)
345             {
346                     notice = xv_create( mainframe, NOTICE,
347                             NOTICE_MESSAGE_STRINGS, "No such betafile able to open in pre
        sent directory!",
348                                                     "Check filename and try again.", NULL
        ,
349                             NOTICE_BUTTON,          "Continue", 1,
350                             XV_SHOW,                TRUE, NULL);
351
352                     problem = TRUE;
353             }
354             fclose(testfile);
355
356             /*if (params.chronint < 0.009999 || params.chronint > 2.01)
357             {
358                     notice = xv_create( mainframe, NOTICE,
359                             NOTICE_MESSAGE_STRINGS, "Chron interval outside limits!",
360                                                     "0.01Myr to 2.00Myr.", NULL,
361                             NOTICE_BUTTON,          "Continue", 1,
362                             XV_SHOW,                TRUE, NULL);
363
364                     problem = TRUE;
365             }*/
366
367             if (params.chrons * params.chronint > 1000)
368             {
369                     notice = xv_create( mainframe, NOTICE,
370                             NOTICE_MESSAGE_STRINGS, "Total modal duration more than 100My
        r!",
371                                                     "Reduce number or duration of chrons.
        ", NULL,
372                             NOTICE_BUTTON,          "Continue", 1,
373                             XV_SHOW,                TRUE, NULL);
374
375                     problem = TRUE;
376             }
377
378
379             if (params.chronint > params.chronfreq)
380             {
381                     notice = xv_create( mainframe, NOTICE,
382                             NOTICE_MESSAGE_STRINGS, "Chron storage frequency less than ch
        ron interval!",
383                                                     "Reduce interval or increase storage
        frequency.", NULL,
384                             NOTICE_BUTTON,          "Continue", 1,
385                             XV_SHOW,                TRUE, NULL);
386
387                     problem = TRUE;
388             }
389
390             if (params.step_chrons > params.chrons)
391             {
392                     notice = xv_create( mainframe, NOTICE,
```

```
393                             NOTICE_MESSAGE_STRINGS, "Number of chrons per step greater th
    an total number of chrons!",
394                                                     "Reduce total or increase number of c
    hrons per step.", NULL,
395                             NOTICE_BUTTON,          "Continue", 1,
396                             XV_SHOW,                TRUE, NULL);
397
398                     problem = TRUE;
399             }
400
401             return(problem);
402     }
403
404     void set_seastart()
405     /* Initialise the sealevel curve, dependent on which curve type has been chosen. */
406     {
407             float temp;
408
409             temp = (float) (eustasy.max_level1 - eustasy.min_level1);
410             exec.sealevel = 0.0;
411
412             switch (eustasy.curve_type1)
413             {
414                     case 0 :        exec.sea_change1 = (fabs(temp * 2.0) / (float) (eusta
    sy.freq1 * 10.0));
415                                     break;
416
417                     case 1 :        exec.sea_change1 = fabs(temp) / (float) (eustasy.freq
    1 * 10.0);
418                                     break;
419
420                     case 2 :        exec.sea_change1 = -(fabs(temp) / (float) (eustasy.fr
    eq1 * 10.0));
421                                     break;
422
423                     case 3 :
424                     case 4 :        exec.sea_change1 = temp / 2.0; /* for sin function ch
    ange = amplitude */
425                                                     break;
426
427                     default :       exec.sea_change1 = 0;
428
429             }
430
431             temp = (float) (eustasy.max_level2 - eustasy.min_level2);
432
433             switch (eustasy.curve_type2)
434             {
435                     case 0 :        exec.sea_change2 = (fabs(temp) / (float) (eustasy.fre
    q2 * 10.0));
436                                     exec.sealevel = eustasy.min_level2;
437                                     break;
438
439                     case 1 :        exec.sea_change2 = (fabs(temp) / (float) (eustasy.fre
    q2 * 10.0));
440                                     exec.sealevel = eustasy.max_level2;
441                                     break;
442
443                     case 2 :        exec.sea_change2 = temp / 2.0;
444                                     /* for sin function change = amplitude */
445                                     /*exec.sealevel = eustasy.min_level2 + fabs(temp / 2.
    0);*/
446                                     break;
447
448                     case 3 :        exec.sea_change2 = temp / 2.0;
449                                     /* for sin function change = amplitude */
450                                     /*exec.sealevel = eustasy.min_level2 + fabs(temp / 2.
    0);*/
451                                     break;
452
453                     default :       exec.sea_change2 = 0;
```



```
454             }
455
456             exec.sea_marker1 = exec.sealevel;
457             exec.sea_marker2 = exec.sealevel;
458
459             init_sea_curve();
460     }
461
462     void init_sea_curve()
463     /* Set a value of absolute sealevel for each time step depending on which type of cur
    ve has been chosen */
464     {
465             int     loop;
466             float   sealevel1 = 0.0, sealevel2 = 0;
467
468             strat.curves_data[0][0] = 0.0;
469             strat.curves_data[0][SEALEVEL] = 0.0;
470
471             for (loop = 1; loop <= params.chrons; loop++)
472             {
473                     switch (eustasy.curve_type1)
474                     {
475                             case 0 :        sealevel1 += sea_smooth_linear();
476                                             break;
477
478                             case 1 :
479                             case 2 :        sea_saw_tooth(&sealevel1);
480                                             break;
481
482                             case 3 :        sea_sinusoidal_pos(&sealevel1, loop);
483                                             break;
484
485                             case 4 :        sea_sinusoidal_neg(&sealevel1, loop);
486                                             break;
487                     }
488
489                     switch (eustasy.curve_type2)
490                     {
491                             case 0 :        sealevel2 += sea_increase();
492                                             break;
493                             case 1 :        sealevel2 -= sea_decrease();
494                                             break;
495                             case 2 :        sea_sinusoidal2_pos(&sealevel2, loop);
496                                             break;
497
498                             case 3 :        sea_sinusoidal2_neg(&sealevel2, loop);
499                                             break;
500
501                             default :       break;
502                     }
503
504                     strat.curves_data[loop][SEALEVEL] = sealevel1 + sealevel2;
505             }
506     }
507
508     float sea_smooth_linear()
509     /* Change sea level with smooth linear curve */
510     {
511             /* If sealevel is at specified maximum or minimum reverse the sign of change
    */
512             if (exec.sealevel <= eustasy.min_level1 || exec.sealevel >= (eustasy.max_leve
    l1))
513                     exec.sea_change1 = -(exec.sea_change1);
514
515             return(exec.sea_change1);
516     }
517
518     void sea_saw_tooth(sealevel)
519     /* Change sea level with saw tooth curve */
520     float   *sealevel;
521     {
```

```
522             /* If min-max type and sealevel at max, change sealevel to minimum and output
        to
523             disc file to effect an instantaneous change */
524             if (eustasy.curve_type1 == 1 && exec.sealevel >= eustasy.max_level1)
525                     *sealevel = eustasy.min_level1;
526             else
527             /* Do the same but for a maximum to minimum curve */
528             if (eustasy.curve_type1 == 2 && exec.sealevel <= eustasy.min_level1)
529                     *sealevel = eustasy.max_level1;
530             else
531                     /* If not at max or min, just apply change amount */
532                     *sealevel += exec.sea_change1;
533     }
534
535     void sea_sinusoidal_pos(sealevel, loop)
536     /* Calculate sealevel after cycle-elapsed time as a sine function with
537      wavelength eustasy.freq, amplitude range and center point marker.  */
538     float   *sealevel;
539     int     loop;
540     {
541             float temp = (6.2831853 / (float)eustasy.freq1) * (loop * params.chronint);
542             *sealevel = exec.sea_marker1 + (exec.sea_change1 * sin(temp));
543
544     }
545
546     void sea_sinusoidal_neg(sealevel, loop)
547     /* As above, but the sine curve has the opposite polarity */
548     float   *sealevel;
549     int     loop;
550     {
551             float temp = (6.2831853 / (float)eustasy.freq1) * (loop * params.chronint);
552             *sealevel = exec.sea_marker1 - (exec.sea_change1 * sin(temp));
553     }
554
555
556     float sea_increase()
557     /* Change sea level with linear increase */
558     {
559             return(exec.sea_change2); /*exec.sea_marker1*/
560     }
561
562     float sea_decrease()
563     /* Change sea level with linear decrease */
564     {
565             return(exec.sea_change2);
566     }
567
568     void sea_sinusoidal2_pos(sealevel, loop)
569     /* Function to calculate sealevel after cycle-elapsed time as a sine function with
570      wavelength eustasy.freq, amplitude range and center point marker. Start curve increa
        sing...  */
571     float   *sealevel;
572     int     loop;
573     {
574             float temp = (6.2831853 / (float)eustasy.freq2) * (loop * params.chronint);
575             *sealevel = exec.sea_marker2 + (exec.sea_change2 * sin(temp));
576     }
577
578     void sea_sinusoidal2_neg(sealevel, loop)
579     /* Function to calculate sealevel after cycle-elapsed time as a sine function with
580      wavelength eustasy.freq, amplitude range and center point marker. Start curve decrea
        sing...  */
581     float   *sealevel;
582     int     loop;
583     {
584             float temp = (6.2831853 / (float)eustasy.freq2) * (loop * params.chronint);
585             *sealevel = exec.sea_marker2 - (exec.sea_change2 * sin(temp));
586     }
587
588     void set_sedstart()
589     /* Set the initial value of sediment supply depending on what type of supply curve ha
```



```
        s been chosen. */
590     {
591             float   temp = (float)(sed_budget.maxsed - sed_budget.minsed),
592                     freq_convert = sed_budget.freq / params.chronint;
593
594             if (sed_budget.supply_flag == 0)
595                     exec.external_budget = sed_budget.maxsed;
596             else
597             if (sed_budget.supply_flag == 2 || sed_budget.supply_flag == 3)
598                     switch (sed_budget.curve_type)
599                     {
600                             case 0 :
601                             case 4 :        exec.sed_change = fabs(temp) / (float) (freq_
        convert);
602                                             exec.external_budget = sed_budget.minsed;
603                                             break;
604
605                             case 1 :
606                             case 5 :        exec.sed_change = -(fabs(temp) / (float) ( fr
        eq_convert));
607                                             exec.external_budget = sed_budget.maxsed;
608                                             break;
609
610                             case 2 :        exec.sed_change = -(temp / 2.0);
611                                             /* for sin function change = amplitude */
612                                             exec.external_budget = sed_budget.minsed + fa
        bs(temp / 2);
613                                             break;
614
615                             case 3 :        exec.sed_change = (temp / 2.0);
616                                             /* for sin function change = amplitude */
617                                             exec.external_budget = sed_budget.minsed + fa
        bs(temp / 2);
618
619                             case 6 :        sed_curve_file = fopen(
620                                                     "/home/eeyore/pete/basincode/data/sed
        supply.dat","r");
621                                             break;
622                     }
623
624             exec.sed_marker = exec.external_budget;
625             exec.sed_stack_ptr = 0;
626     }
627
628     void set_pcstart()
629     {
630             float   two_amplitude = sed_budget.pc_max - sed_budget.pc_min,
631                     freq_var = sed_budget.pc_freq / params.chronint;
632
633             switch (sed_budget.pc_type_flag)
634             {
635                     case 0 : exec.sed_pc = sed_budget.pc_max;
636                              break;
637
638                             /* Negative sinusoidal */
639                     case 1 : exec.pc_change = -((two_amplitude) / 2.0);
640                              exec.sed_pc = exec.pc_marker =  sed_budget.pc_min - exec.pc_
        change;
641                              break;
642
643                             /* Positive sinusoidal */
644                     case 2 : exec.pc_change = (two_amplitude) / 2.0;
645                              exec.sed_pc = exec.pc_marker = sed_budget.pc_min + exec.pc_c
        hange;
646                              break;
647
648                             /* Decreasing sawtooth */
649                     case 3 : exec.pc_change = (fabs(two_amplitude)) / freq_var;
650                              exec.sed_pc = sed_budget.pc_max;
651                              break;
652
```

```
653                             /* Increasing sawtooth */
654                     case 4 : exec.pc_change = (fabs(two_amplitude)) / freq_var;
655                              exec.sed_pc = sed_budget.pc_min;
656                              break;
657
658                             /* External curve - see sed supply section */
659                     case 5 : break;
660             }
661     }
662
663     void adjust_topog_to_sealevel()
664     /* If the intial sealevel is greater than 0.0, add the value of the sealevel datum to
         the submarine
665     topography */
666     {
667             int     loop;
668
669             if (eustasy.change_flag == 2 && exec.sealevel > 0.0)
670                     for (loop = exec.beach_pos; loop < USEDPTS; loop++)
671                             strat.chrons[0][loop] += exec.sealevel;
672     }
673
674     float set_Te_start()
675     /* Set the starting value of Te */
676     {
677             float   temp;
678
679             if (options.Te_type == 0)
680                     temp = change_Te(params.crust_age); /* Te changes through time as oce
        anic crust */
681             else
682             if (options.Te_type == 1)
683                     temp = 30.0;    /* Te constant at 30km */
684             else
685             if (options.Te_type == 2)
686                     temp = 5.0;     /* Te constant at 5km */
687             else
688             if (options.Te_type == 3)
689                     temp = 0.0;     /* No flexural strength - Airy isostasy */
690             else
691             if (options.Te_type == 6)
692                     temp =  atof((char *) xv_get(Te_value_item, PANEL_VALUE));
693
694             return(temp);
695     }
696
697     void set_strat(absval)
698     /* absval = TRUE : Convert the negative values for elevation in the strat array
699      into positive values suitable for plotting in graphics routines.
700        absval = FALSE : Set all elements of strat and depos to zero ready to start.  */
701     int absval;
702     {
703             int loop1, loop2;
704
705             for (loop1 = 0; loop1 <= params.chrons; loop1++)
706                     for (loop2 = 0; loop2 <USEDPTS; loop2++)
707                             if (absval)
708                             {
709                                     if (strat.chrons[loop1][loop2] > 0)
710                                             strat.chrons[loop1][loop2] =
711                                                     -strat.chrons[loop1][loop2];
712                                     else
713                                             strat.chrons[loop1][loop2] =
714                                                     abs(strat.chrons[loop1][loop2]);
715                             }
716                             else
717                             {
718                                     strat.chrons[loop1][loop2] = 0.0;
719                                     strat.depos[loop1][loop2] = NO_DEPOS;
720                                     tect.flex_hist[loop1][loop2] = 0.0;
721                             }
```



```
722     }
723
724     void set_subsid_arrays()
725     /* Set the subsidence arrays to their sarting values. This is done by using the norma
        l tectonic subsidence
726     routines but sending zero as the elapsed time parameter */
727     {
728             int loop;
729
730             for (loop = 0; loop < USEDPTS; loop++)
731             {
732                     if (options.subside_type == 1)
733                     {
734                             exec.refsub[loop] = one_mckenzie_sub(exec.betaprof[loop], 0.0
        );
735
736                             if (exec.betaprof[loop] > 1.0)
737                                     exec.new_tect_sub[loop] = exec.refsub[loop] -
738                                             one_mckenzie_sub(exec.betaprof[loop], params.
        crust_age);
739                             else
740                                     exec.new_tect_sub[loop] = 0.0;
741                     }
742                     else
743                     if (options.subside_type == 2)
744                     {
745                             exec.refsub[loop] = one_two_layer_sub(exec.betaprof[loop], ex
        ec.sigmaprof[loop], 0.0);
746
747                             if (exec.betaprof[loop] > 1.0 || exec.sigmaprof[loop] > 1.0)
748                                     exec.new_tect_sub[loop] = exec.refsub[loop] -
749                                             one_two_layer_sub(exec.betaprof[loop], exec.s
        igmaprof[loop],
750                                             params.crust_age);
751                             else
752                                     exec.new_tect_sub[loop] = 0.0;
753                     }
754             }
755     }
756
757     void zero_curve_data()
758     /* Set all the strat curves to zero as an initial value */
759     {
760             int loop;
761
762             for (loop = 0; loop < MAX_STEPS; loop++)
763             {
764                     strat.curves_data[loop][0] = 0.0;
765                     strat.curves_data[loop][SEALEVEL] = 0.0;
766                     strat.curves_data[loop][FLUV_DEP] = 0.0;
767                     strat.curves_data[loop][FLUV_EROD] = 0.0;
768                     strat.curves_data[loop][MAR_DEP] = 0.0;
769                     strat.curves_data[loop][MAR_EROD] = 0.0;
770                     strat.curves_data[loop][EX_SED] = 0.0;
771                     strat.curves_data[loop][REL_SEA] = 0.0;
772                     strat.curves_data[loop][THERM_SUB] = 0.0;
773                     strat.curves_data[loop][V_ONLAP] = 0.0;
774             }
775
776             for (loop = 0; loop < MAXCHRONS; loop++)
777             {
778                     strat.equilib_point[loop] = 0; /* Set to zero so the drawing routine
        knows not to draw */
779                     strat.onlap[loop] = 0;
780                     strat.beach[loop] = 0;
781             }
782     }
783
784     void set_presev_data()
785     /* Set all the preservation array to zero. */
786     {
```

```
787             int loop;
788
789             for (loop = 0; loop < ENVIRONS; loop++)
790                     strat.presev_info[loop][0] = strat.presev_info[loop][1] = 0.0;
791     }
792
793     void init_drainage()
794     /* Define nick point positions and cut a river profile into basement (chrons[0][x]) *
        /
795     {
796             exec.drainage_divide = exec.nick_point = exec.beach_pos -
797                     (params.drainage_len / params.prof_gap);
798             exec.nick_count = 0;
799             exec.length_scale = params.length_scale;
800
801             exec.temp_elevation = strat.chrons[0][exec.drainage_divide];
802
803             switch (options.curve_type)
804             {
805                     case 0 : init_expo_curve();
806                              break;
807                     case 1 :
808                     case 2 : init_erfc_curve();
809                              exec.old_riv_prof_area = calc_prof_area(exec.drainage_divide
        , exec.beach_pos);
810             }
811
812             if (options.perm_fluv_prof)
813                     init_fixed_fluv_prof();
814     }
815
816     void init_expo_curve()
817     /* Initialise the exponential curve */
818     {
819             float   constant;
820             int     loop;
821
822             constant=( log(exec.base_chron[exec.drainage_divide] - exec.sealevel - 1.0) )
823                     / (double)(exec.drainage_divide - exec.beach_pos);
824
825             for (loop = exec.drainage_divide; loop < exec.beach_pos; loop++)
826                     strat.chrons[0][loop] = exec.base_chron[loop] = exec.work_chron[loop]
         =
827                             exp( (constant * (loop - exec.beach_pos))) + exec.sealevel -
        1.0;
828     }
829
830     void init_erfc_curve()
831     /* Initialise the complementary error function curve */
832     {
833             float   x_scale = params.length_scale / (exec.beach_pos - exec.drainage_divid
        e),
834                     end_value = erfc(params.length_scale),
835                     y_scale = (1.0 - end_value) /
836                             (exec.base_chron[exec.drainage_divide] - exec.sealevel);
837
838             int     loop;
839             FILE    *flux_out;
840
841             flux_out = fopen("init_prof_flux.dat","w");
842
843             /* See thesis, chapter 2, for details of the erfc curve formulation */
844             for (loop = exec.drainage_divide; loop <= exec.beach_pos; loop++)
845             {
846                     strat.chrons[0][loop] =  exec.base_chron[loop] =
847                     exec.work_chron[loop] = exec.new_eq_prof[loop] =
848                             ((erfc((float)(loop - exec.drainage_divide) * x_scale) - end_
        value) / y_scale)
849                             + exec.sealevel;
850                     fprintf(flux_out,"%f %f\n", (loop - exec.drainage_divide) * 0.25,
```



```
851                             -1000.0 * ((strat.chrons[0][loop] - strat.chrons[0][loop-1])
        / 250.0 ) );
852             }
853
854             fclose(flux_out);
855     }
856
857     void init_fixed_fluv_prof()
858     {
859             int     loop;
860
861             for (loop = exec.drainage_divide; loop <= exec.beach_pos; loop++)
862                     exec.fixed_fluv_prof[loop] = strat.chrons[0][loop];
863
864     }
865
866     void init_marine_prof()
867     /* Set up the intial marine profile with an expo shoreface and a fixed slope shelf cu
        t into
868     the initial topography */
869     {
870             int     loop,
871                     beach_bit_done = FALSE;
872             float   constant,
873                     vert_inc = params.shelf_grad * params.prof_gap * 2000.0, /* Double in
        itial slope */
874                     shore_width_points = params.shore_width / params.prof_gap,
875                     elevation;
876
877             constant = log( params.wave_base ) / (- shore_width_points);
878
879             for (loop = exec.beach_pos; loop < USEDPTS; loop++)
880                     if (!beach_bit_done )
881                     {
882                             /* Define a point on the expo shoreface */
883                             elevation =     exp( (constant * (loop - (exec.beach_pos + sh
        ore_width_points))))
884                                             + (exec.sealevel - params.wave_base);
885
886                             if (elevation < strat.chrons[0][loop])
887                             {
888                                     strat.chrons[0][loop]  = exec.new_eq_prof[loop] =
889                                     exec.base_chron[loop] = exec.work_chron[loop] = eleva
        tion;
890
891                                     beach_bit_done = check_equilib_grad(loop, exec.beach_
        pos);
892                             }
893                     }
894                     else
895                             /* Set const slope part by subtracting vert_inc from left pos
        ition, until
896                             the current point in the predefined topography is less than t
        he point just
897                             defined to the left. i.e. the shelf/slope break has been reac
        hed. */
898
899                             if (strat.chrons[0][loop] > strat.chrons[0][loop - 1] )
900                                     strat.chrons[0][loop] = exec.new_eq_prof[loop] =
901                                     exec.base_chron[loop] = exec.work_chron[loop] =
902                                             strat.chrons[0][loop - 1] - vert_inc;
903     }
904
905     void run_proc()
906     /* Run the initialised model. */
907     {
908             int chron_storage_freq = (int)(params.chronfreq / params.chronint);
909
910             int     loop1, loop2;
911
912             chrons = fopen("chron_dump.dat", "w");
```

```
913             beach = fopen("beach.dat","w");
914
915             if (!exec_flags.initialised || exec_flags.execution_complete)
916                     notice_prompt((Frame) mainframe, (Event*) NULL,
917                     NOTICE_MESSAGE_STRINGS,
918                     "Model has not been initialised, or run has been completed.",
919                     "Select the `Initialise` button then try again.", 0,
920                     NOTICE_BUTTON_YES,      "Continue", 0);
921
922             else
923             {
924                     do
925                     {
926                             /* Do first chron after elapsed time equal to
927                             the duration of a chron interval (0.1Ma units).
928                             N.B. This means time 0 will be basement only, no depos. */
929
930                             if (options.Te_type == 0) /* Time dependant Te */
931                                     exec.Te = change_Te();
932
933                             exec.elapsed += params.chronint; /* Increment elapsed time in
     Myr */
934                             exec.time_steps_done++; /* Has to be inc. before curves are c
    alced. */
935                             exec.chronelapsed += 1;
936
937                             if (eustasy.change_flag == 1 || eustasy.change_flag == 2)
938                             {
939                                     change_sealevel();
940                                     if (options.curve_type == 2)
941                                             calc_new_prof_area();
942                             }
943
944                             change_sed_budget();
945                             change_sedpc();
946                             change_drainage();
947
948                             fprintf(stderr,"\nPC %f ", exec.sed_pc );
949
950                             do_a_chron();
951
952                             /* Store the current chron if the number of chrons generated
    is appropriate */
953                             if (exec.chronelapsed == chron_storage_freq )
954                             {
955                                     copy_chron(2);
956
957                                     exec.chronelapsed = 0;
958                                     exec.total_chrons_done++;
959                                     exec.step_chrons_done++;
960                                     exec.layer++;
961                             }
962                     }
963                     while (exec.step_chrons_done != params.step_chrons &&
964                             exec.total_chrons_done <= params.chrons); /* Check to see if
    the model step is done*/
965
966                     exec.step_chrons_done = 0;
967                     calc_onlap();
968
969                     if (exec.total_chrons_done == params.chrons) /* The model run is comp
    lete */
970                     {
971                             exec_flags.execution_complete = TRUE;
972                             exec_flags.initialised = FALSE;
973                             strat.curves_data[exec.time_steps_done + 1][0] = -99.0;
974
975
976                             compile_presev_info();
977                     }
978
```



```
979                     if (!files.batch) /* Draw model output */
980                             if (!exec_flags.zoomed)
981                                     full_screen_draw();
982                             else
983                                     zoomed_screen_draw();
984
985                     for (loop1 = exec.drainage_divide; loop1 < 2400; loop1++)
986                     {
987                             fprintf(chrons,"%f ", loop1 * 0.250);
988
989                             for (loop2 = 0; loop2 < exec.layer+1; loop2++)
990                                     fprintf(chrons,"%f ", strat.chrons[loop2][loop1]);
991
992                             fprintf(chrons,"\n");
993                     }
994
995             }
996             fclose(chrons);
997             fclose(beach);
998     }
999
1000    void copy_chron(flag)
1001    /* If flag = 1, set work and base chrons to last layer created, and initialise equili
      b., flex and load profs
1002       if flag = 2, copy work chron, the just deposited chron, into the strat array for p
      erm. storage. */
1003    int flag;
1004    {
1005            int loop;
1006            unsigned short int enviro;
1007
1008            if (flag == 1)
1009            {
1010                    for (loop = 0; loop < USEDPTS; loop++)
1011                    {
1012                            /* Set base chron to last preserved strat layer. Set work chr
      on to same before
1013                                    equilib. profs are generated */
1014                            exec.base_chron[loop] = exec.work_chron[loop] = exec.last_chr
      on[loop]
1015                                    = strat.chrons[exec.layer][loop];
1016
1017                            /* Set eq prof. to current base chron to cover areas outside
      river profile */
1018                            exec.old_eq_prof[loop] = exec.new_eq_prof[loop];
1019                            exec.new_eq_prof[loop] = exec.base_chron[loop];
1020
1021                            exec.flexprof[loop] = 0.0;
1022                            exec.loadprof[loop] = 0.0;
1023                    }
1024            }
1025            else
1026            if (flag == 2)
1027            {
1028                    /* Chron is completed. Record work chron in strat array */
1029                    for (loop = 0; loop < USEDPTS; loop++)
1030                            strat.chrons[exec.layer+1][loop] = exec.work_chron[loop];
1031            }
1032    }
1033
1034    void do_a_chron()
1035    /* Call all the approriate routines to generate one chron. */
1036    {
1037            int     left, right, loop;
1038
1039            fprintf(stderr,"\nChron number %d ...",exec.layer + 1);
1040            layer_label(TRUE);
1041
1042            /* If subside_type is 0, no thermal subsidence */
1043            if (options.subside_type == 1)
1044                    mckenzie_subside();
```

```
1045          else
1046          if (options.subside_type == 2)
1047                  two_layer_subside();
1048
1049          find_equilib_point();
1050
1051          copy_chron(1);
1052
1053          exec.beach_pos = strat.beach[exec.layer + 1] = find_coast();
1054
1055          exec.ss_break_pos = generate_marine_profile();
1056          check_ss_break_pos();
1057
1058          if (options.prograde)
1059          {
1060                  if (options.riv_prof)
1061                          gen_riv_prof();
1062
1063                  prograde(&left, &right);
1064          }
1065
1066          record_chron_areas();
1067          compile_depos_info();
1068
1069          if (options.Te_type != 4) /* opt 4 is no flexure and rigid litho, so don't ex
      ecute any flex*/
1070          {
1071                  fprintf(stderr,"Flexure...");
1072                  calc_flex_disp_coeff();
1073
1074                  if (options.flex_type == 1 || options.flex_type == 2)
1075                          accurate_flex();
1076                  else
1077                          flex();
1078
1079                  switch (tect.response_type)
1080                  {
1081                          case 0 : inst_flex_subside();
1082                                   break;
1083                          case 1 : linear_flex_subside();
1084                                   break;
1085                          case 2 : expo_flex_subside();
1086                  }
1087          }
1088
1089          fprintf(beach,"%f %f\n", strat.beach[exec.layer] * 0.250,
1090                                   strat.chrons[exec.layer][strat.beach[exec.layer]] );
1091
1092
1093          layer_label(FALSE);
1094          fprintf(stderr,"Done...");
1095  }
1096
1097  void mckenzie_subside()
1098  /* Call the functions to calculate the thermal subsidence according to Mckenzie (1978
      ) */
1099  {
1100          fprintf(stderr,"Therm. Sub...");
1101          get_mckenzie_subs();
1102          tect_subside();
1103  }
1104
1105  void two_layer_subside()
1106  /* Call the functions to calculate the thermal subsidence according to Hellinger and
      Sclater (1983) */
1107  {
1108          fprintf(stderr,"Therm. Sub...");
1109          get_two_layer_subs();
1110          tect_subside();
1111  }
1112
```



```
1113  void tect_subside()
1114  /* Subside surfaces by magnitude of tectonic subsidence.*/
1115  {
1116          int loop, subloop;
1117
1118          for (loop = 0; loop < USEDPTS; loop++)
1119          {
1120                  for (subloop = 0; subloop <= exec.layer; subloop++)
1121
1122                          /* Subside by the difference between the value for therm sub
      at the last time
1123                          step, and the value for this time step */
1124                          strat.chrons[subloop][loop] -= exec.new_tect_sub[loop] -
1125                                  exec.old_tect_sub[loop];
1126
1127                  exec.fixed_fluv_prof[loop] -= exec.new_tect_sub[loop] - exec.old_tect
      _sub[loop];
1128          }
1129
1130  }
1131
1132  void get_mckenzie_subs()
1133  /* Loop to calculate the values for tectonic thermal subsidence across the profile */
1134  {
1135          int loop;
1136
1137          for (loop = 0; loop <USEDPTS; loop++)
1138          {
1139                  exec.old_tect_sub[loop] = exec.new_tect_sub[loop];
1140
1141                  if (exec.betaprof[loop] > 1.0)
1142                          exec.new_tect_sub[loop]  = strat.curves_data[exec.time_steps_
      done][THERM_SUB] =
1143                                  exec.refsub[loop] - one_mckenzie_sub(exec.betaprof[lo
      op], params.crust_age);
1144                  else
1145                          exec.new_tect_sub[loop] = 0.0;
1146          }
1147  }
1148
1149  float one_mckenzie_sub(beta, crust_age)
1150  /* Calculate the subsidence value at one point on the profile with a given beta value
       and age */
1151  float   beta,
1152          crust_age;
1153  {
1154          double  temp1, temp2, temp3, temp4, temp5,temp6, temp7,
1155                  sum = 0.0,
1156                  bigtime = (crust_age + exec.elapsed) * 60.0 * 60.0 * 24.0 * 365.0 * 1
      .0e6,
1157                  Pm = params.Pmant*10e2,
1158                  Pd = params.Pdisp*10e2,
1159                  TAU = 62.8 * 60.0 * 60.0 * 24.0 * 365.0 * 1.0e6,
1160                  A = 125000.0,
1161                  ALPHA = 3.28e-5,
1162                  TO = 1333.0;
1163
1164          int     loop;
1165
1166          for (loop = 0; loop< 5; loop++)
1167          {
1168                  temp1 =  2.0 * (double)loop + 1.0;
1169                  temp2 = 1.0 / (temp1 * temp1);
1170                  temp3 = beta / (temp1 * M_PI);
1171                  temp7 = (temp1 * M_PI) / beta;
1172                  temp4 = sin((double)temp7);
1173                  temp5 = (temp1 * temp1) * (bigtime / TAU);
1174                  temp6 = exp(-temp5);
1175                  sum += temp2 * (temp3 *temp4) * temp6;
1176          }
1177
```

```
1178            return(((A * Pm * ALPHA * TO) / (Pm - Pd)) * 0.4052847 * sum);
1179    }
1180
1181    void get_two_layer_subs()
1182    /* Calculate the thermal subsidence across the profile for the two-layer model */
1183    {
1184            int loop;
1185
1186            for (loop = 0; loop <USEDPTS; loop++)
1187            {
1188                    exec.old_tect_sub[loop] = exec.new_tect_sub[loop];
1189
1190                    if (exec.betaprof[loop] > 1.0 || exec.sigmaprof[loop] > 1.0)
1191                            exec.new_tect_sub[loop] = strat.curves_data[exec.time_steps_d
    one][THERM_SUB] =
1192                                    exec.refsub[loop] - one_two_layer_sub(exec.betaprof[l
    oop],
1193                                            exec.sigmaprof[loop], params.crust_age);
1194                    else
1195                            exec.new_tect_sub[loop] = 0.0;
1196            }
1197    }
1198
1199    float one_two_layer_sub(beta, sigma, crust_age)
1200    /* Calculate one two-layer subsidence value */
1201    float   beta,
1202            sigma,
1203            crust_age;
1204    {
1205            float   ratio, C, summation,
1206                    temp1, temp2, temp3,
1207                    Pmant = params.Pmant *10e2,
1208                    Pwater = params.Pdisp * 10e2,
1209                    tau =  62.8 * 60.0 * 60.0 * 24.0 * 365.0 * 1.0e6,
1210                    a = 125000.0,
1211                    crust_thick     = 35000.0,
1212                    alpha = 3.28e-5,
1213                    Tmant = 1333.0,
1214                    time =  (crust_age + exec.elapsed) * 60.0 * 60.0 * 24.0 * 365.0 * 1.0
    e6;
1215
1216            ratio = a / ((crust_thick / beta) + ((a - crust_thick) / sigma));
1217
1218            temp2 = (M_PI * crust_thick) /  (a * beta);
1219            C = (2.0 / (M_PI * M_PI)) * (((beta - sigma) * sin(temp2)) + (sigma * sin(M_P
    I / ratio)));
1220            summation = C * exp(-time / tau);
1221
1222            temp1 = 2.0 * a * alpha * Pmant * Tmant;
1223            temp2 = (Pmant - Pwater) * M_PI;
1224
1225            return((temp1 / temp2) * summation);
1226    }
1227
1228    int find_chron_sea_intersection()
1229    /* Find the point on the profile at which the chron surface and the sealevel datum in
    tersect.
1230    This is done by looping along the profile until the first point is encountered which
    is below sealevel */
1231    {
1232            int     loop = 0;
1233
1234            while (loop < USEDPTS && exec.base_chron[loop] > exec.sealevel)
1235                    loop++;
1236
1237            return(loop);
1238    }
1239
1240    int find_coast()
1241    /* Loop along the profile to find the coastline, i.e. the first point significantly a
    bove sealevel
```



```
1242            If no such point exists, return USEDPTS. If it does, set it's elevation to se
    alevel*/
1243    {
1244            int     loop = USEDPTS - 1;
1245
1246            fprintf(stderr,"Finding beach...");
1247
1248            /* Loop should terminate on the first point above sealevel */
1249            while (loop > 0 && exec.base_chron[loop--] < exec.sealevel);
1250
1251
1252            if (options.fluvial_prog && loop > 0)
1253                    adjust_beach_position(&loop);
1254            else
1255            if (!options.fluvial_prog && loop > 0)
1256                    generate_fluvial_profile(&loop);
1257            else
1258            if (loop == 0)
1259                    notice = xv_create( mainframe, NOTICE,
1260                            NOTICE_MESSAGE_STRINGS, "Cannot find the beach!",
1261                                                    "Things could well get messy...", NUL
    L,
1262                            NOTICE_BUTTON,          "Continue", 1,
1263                            XV_SHOW,                TRUE, NULL);
1264
1265            return(loop);
1266    }
1267
1268    void adjust_beach_position(temp_beach)
1269    /* Find the position of the beach which is closest to using all the available fluvial
     sediment */
1270    int *temp_beach;
1271    {
1272            int     pos_inc = 50,
1273                    too_much_used = FALSE,
1274                    too_little_used = FALSE,
1275                    rep_count1 = 0,
1276                    rep_count2 = 0;
1277            float   discrep, discrep1, discrep2, discrep3;
1278
1279            /* Loop adjusting the position of the beach by the amount pos_inc. When discr
    ep has been
1280            both positive and negative i.e. the beach has been both left and right of it'
    s ideal
1281            position, divide pos_inc by two and continue. Should get the beach pos at its
     optimum position */
1282
1283            do
1284            {
1285                    /* Discrep will be set to FALSE, i.e. 0.0 if there is a problem with
    the curve fitting
1286                    routine */
1287                    discrep = sufficient_sed_used(*temp_beach);
1288
1289                    if (discrep < 0.0)
1290                    {
1291                            (*temp_beach) += pos_inc;
1292                            too_much_used = TRUE;
1293                    }
1294                    else
1295                    {
1296                            (*temp_beach) -= pos_inc;
1297                            too_little_used = TRUE;
1298                    }
1299
1300                    if (too_much_used && too_little_used)
1301                    {
1302                            pos_inc /= 2;
1303                            too_much_used = FALSE;
1304                            too_little_used = FALSE;
1305                    }
```

```
1178            return(((A * Pm * ALPHA * TO) / (Pm - Pd)) * 0.4052847 * sum);
1179    }
1180
1181    void get_two_layer_subs()
1182    /* Calculate the thermal subsidence across the profile for the two-layer model */
1183    {
1184            int loop;
1185
1186            for (loop = 0; loop <USEDPTS; loop++)
1187            {
1188                    exec.old_tect_sub[loop] = exec.new_tect_sub[loop];
1189
1190                    if (exec.betaprof[loop] > 1.0 || exec.sigmaprof[loop] > 1.0)
1191                            exec.new_tect_sub[loop] = strat.curves_data[exec.time_steps_d
    one][THERM_SUB] =
1192                                    exec.refsub[loop] - one_two_layer_sub(exec.betaprof[l
    oop],
1193                                            exec.sigmaprof[loop], params.crust_age);
1194                    else
1195                            exec.new_tect_sub[loop] = 0.0;
1196            }
1197    }
1198
1199    float one_two_layer_sub(beta, sigma, crust_age)
1200    /* Calculate one two-layer subsidence value */
1201    float   beta,
1202            sigma,
1203            crust_age;
1204    {
1205            float   ratio, C, summation,
1206                    temp1, temp2, temp3,
1207                    Pmant = params.Pmant *10e2,
1208                    Pwater = params.Pdisp * 10e2,
1209                    tau =  62.8 * 60.0 * 60.0 * 24.0 * 365.0 * 1.0e6,
1210                    a = 125000.0,
1211                    crust_thick     = 35000.0,
1212                    alpha = 3.28e-5,
1213                    Tmant = 1333.0,
1214                    time =  (crust_age + exec.elapsed) * 60.0 * 60.0 * 24.0 * 365.0 * 1.0
    e6;
1215
1216            ratio = a / ((crust_thick / beta) + ((a - crust_thick) / sigma));
1217
1218            temp2 = (M_PI * crust_thick) /  (a * beta);
1219            C = (2.0 / (M_PI * M_PI)) * (((beta - sigma) * sin(temp2)) + (sigma * sin(M_P
    I / ratio)));
1220            summation = C * exp(-time / tau);
1221
1222            temp1 = 2.0 * a * alpha * Pmant * Tmant;
1223            temp2 = (Pmant - Pwater) * M_PI;
1224
1225            return((temp1 / temp2) * summation);
1226    }
1227
1228    int find_chron_sea_intersection()
1229    /* Find the point on the profile at which the chron surface and the sealevel datum in
    tersect.
1230    This is done by looping along the profile until the first point is encountered which
    is below sealevel */
1231    {
1232            int     loop = 0;
1233
1234            while (loop < USEDPTS && exec.base_chron[loop] > exec.sealevel)
1235                    loop++;
1236
1237            return(loop);
1238    }
1239
1240    int find_coast()
1241    /* Loop along the profile to find the coastline, i.e. the first point significantly a
    bove sealevel
```



```
1242            If no such point exists, return USEDPTS. If it does, set it's elevation to se
    alevel*/
1243    {
1244            int     loop = USEDPTS - 1;
1245
1246            fprintf(stderr,"Finding beach...");
1247
1248            /* Loop should terminate on the first point above sealevel */
1249            while (loop > 0 && exec.base_chron[loop--] < exec.sealevel);
1250
1251
1252            if (options.fluvial_prog && loop > 0)
1253                    adjust_beach_position(&loop);
1254            else
1255            if (!options.fluvial_prog && loop > 0)
1256                    generate_fluvial_profile(&loop);
1257            else
1258            if (loop == 0)
1259                    notice = xv_create( mainframe, NOTICE,
1260                            NOTICE_MESSAGE_STRINGS, "Cannot find the beach!",
1261                                                    "Things could well get messy...", NUL
    L,
1262                            NOTICE_BUTTON,          "Continue", 1,
1263                            XV_SHOW,                TRUE, NULL);
1264
1265            return(loop);
1266    }
1267
1268    void adjust_beach_position(temp_beach)
1269    /* Find the position of the beach which is closest to using all the available fluvial
     sediment */
1270    int *temp_beach;
1271    {
1272            int     pos_inc = 50,
1273                    too_much_used = FALSE,
1274                    too_little_used = FALSE,
1275                    rep_count1 = 0,
1276                    rep_count2 = 0;
1277            float   discrep, discrep1, discrep2, discrep3;
1278
1279            /* Loop adjusting the position of the beach by the amount pos_inc. When discr
    ep has been
1280            both positive and negative i.e. the beach has been both left and right of it'
    s ideal
1281            position, divide pos_inc by two and continue. Should get the beach pos at its
     optimum position */
1282
1283            do
1284            {
1285                    /* Discrep will be set to FALSE, i.e. 0.0 if there is a problem with
    the curve fitting
1286                    routine */
1287                    discrep = sufficient_sed_used(*temp_beach);
1288
1289                    if (discrep < 0.0)
1290                    {
1291                            (*temp_beach) += pos_inc;
1292                            too_much_used = TRUE;
1293                    }
1294                    else
1295                    {
1296                            (*temp_beach) -= pos_inc;
1297                            too_little_used = TRUE;
1298                    }
1299
1300                    if (too_much_used && too_little_used)
1301                    {
1302                            pos_inc /= 2;
1303                            too_much_used = FALSE;
1304                            too_little_used = FALSE;
1305                    }
```

```
1306            }
1307            while (pos_inc > 0 && (int)discrep != FALSE && ++rep_count1 < 500);
1308
1309            discrep2 = sufficient_sed_used(*temp_beach);
1310
1311            /* Move the beach until the discrepency is smaller than for points to the lef
    t and right */
1312            do
1313            {
1314                    discrep2 < 0.0 ? (*temp_beach)++ : (*temp_beach)--;
1315
1316                    discrep1 = sufficient_sed_used((*temp_beach) - 1);
1317                    discrep3 = sufficient_sed_used((*temp_beach) + 1);
1318                    discrep2 = sufficient_sed_used(*temp_beach); /* Has to be last of thr
    ee to ensure profile
1319                                                                    is left generated to
    the correct pos */
1320
1321            }
1322            while ((fabs(discrep2) > fabs(discrep1) || fabs(discrep2) > fabs(discrep3)) &
    & ++rep_count2 < 100);
1323    }
1324
1325    float sufficient_sed_used(temp_beach)
1326    /* Calculate the area of sediment required to fill the fluvial profile generated to t
    he
1327    temporary beach position passed. Return area deposited, or FALSE if curve fit was uns
    uccessfull. */
1328    int     temp_beach;
1329    {
1330            int     profile_endpoint,
1331                    old_beach_pos = strat.beach[exec.layer];
1332            float   sed_eroded,
1333                    sed_depos,
1334                    old_beach_elev = strat.chrons[exec.layer][old_beach_pos],
1335                    old_sealevel = strat.curves_data[exec.layer][SEALEVEL];
1336
1337            generate_fluvial_profile(&temp_beach);
1338
1339            calc_fluv_area_depos(exec.drainage_divide, old_beach_pos, temp_beach, exec.ne
    w_eq_prof,
1340                    &sed_eroded, &sed_depos);
1341
1342            /* Adjust sed budget calculations according to supply type.
1343            Note, this is just testing for the correct beach position, so don't alter glo
    bals!
1344            Type 0 and 3 are constant or external source only, so just set eroded to exte
    rnal budget.
1345            Tyep 2 is profile erosion plus external source, so just add external to measu
    red erosion.
1346            Type 1 is profile erosion only, so just leave as measured. */
1347            switch (sed_budget.supply_flag)
1348            {
1349                    case 0 :
1350                    case 3 : sed_eroded = exec.external_budget;
1351                             break;
1352                    case 2 : sed_eroded += (exec.external_budget - sed_depos);
1353            }
1354
1355            return(sed_depos - (sed_eroded * exec.sed_pc));
1356    }
1357
1358    void find_equilib_point()
1359    /* equilibrium point : the point on the profile at which rate of thermal subsidence i
    s equal to
1360    the rate of eustatic change. Find it by looping along the profile comparing the two u
    ntil therm sub
1361    is greater. NOTE - such a point rarely exists on the profile. See discussion in chapt
    er 3. */
1362    {
1363            float   eustasy_change = fabs(exec.sealevel - strat.curves_data[exec.layer][S
```



```
    EALEVEL]);
1364            int     loop = 0;
1365
1366            if (exec.time_steps_done < 3)
1367                    strat.equilib_point[exec.layer + 1] = 0.0;
1368            else
1369            {
1370                    while (exec.new_tect_sub[++loop] - exec.old_tect_sub[loop] < eustasy_
    change &&
1371                            loop < USEDPTS);
1372
1373                    strat.equilib_point[exec.layer + 1] = (loop == USEDPTS) ?       0.0 :
    loop;
1374            }
1375    }
1376
1377    void generate_fluvial_profile(beach_pos)
1378    /* Generate the fluvial equilibrium profile between the the nickpoint and the beach.
1379    Put the results into exec.new_eq_prof. */
1380    int     *beach_pos;
1381    {
1382            int     loop, profile_endpoint;
1383
1384            if (options.profile_type == 0 || options.profile_type == 1)
1385                    profile_endpoint = exec.drainage_divide; /* Set to drainage divide fo
    r full length profile */
1386            else
1387                    profile_endpoint = exec.nick_point; /* Set to nickpoint for advancing
     profile */
1388
1389            if (!options.perm_fluv_prof)
1390                    switch (options.curve_type)
1391                    {
1392                            case 0  : expo_fluvial_profile(profile_endpoint, *beach_pos);
1393                                      break;
1394                            case 1  : errfunc_fluvial_profile(profile_endpoint, *beach_po
    s, params.length_scale);
1395                                      break;
1396
1397                            case 2  : diffusion_fluvial_profile(profile_endpoint, beach_p
    os);
1398                                      break;
1399                    }
1400            else
1401                    perm_fluv_prof(profile_endpoint, *beach_pos);
1402    }
1403
1404
1405    void expo_fluvial_profile(profile_endpoint, beach_pos)
1406    /* Calculate the elevations on an exponential river profile */
1407    int     profile_endpoint,
1408            beach_pos;
1409    {
1410            float   constant = ( log(exec.base_chron[profile_endpoint] - exec.sealevel +
    1.0))
1411                    / (float)(profile_endpoint - beach_pos);
1412            int     loop;
1413
1414            for (loop = profile_endpoint; loop <= beach_pos; loop++)
1415                    exec.new_eq_prof[loop] = exp( (constant * (float)(loop - beach_pos)))
1416                            + exec.sealevel - 1.0;
1417
1418    }
1419
1420    void errfunc_fluvial_profile(profile_endpoint, beach_pos, length_scale)
1421    /* Same again, but using a complementary error function this time */
1422    int     profile_endpoint,
1423            beach_pos;
1424    float   length_scale;
1425    {
```

```
1426          float   x_scale = length_scale / (beach_pos - profile_endpoint),
1427                  end_value = erfc(length_scale),
1428                  y_scale = (1.0 - end_value) / (exec.base_chron[profile_endpoint] - ex
      ec.sealevel);
1429
1430          int     loop;
1431
1432          for (loop = profile_endpoint; loop <= beach_pos; loop++)
1433                  exec.new_eq_prof[loop] = ((erfc((float)(loop - profile_endpoint)
1434                          * x_scale) - end_value) / y_scale) + exec.sealevel;
1435  }
1436
1437  void diffusion_fluvial_profile(profile_endpoint, beach_pos)
1438  /* Use a finite difference solution of the diffusion equation applied to topography t
      o generate a new fluvial profile */
1439  int     profile_endpoint,
1440          *beach_pos;
1441  {
1442          float   time_step = 100.0,
1443                  temp1, temp2,
1444                  new_temp_prof[USEDPTS],
1445                  old_temp_prof[USEDPTS],
1446                  x_step = params.prof_gap * 1000.0,
1447                  temp_sealevel;
1448          int     time_loop,
1449                  dist_loop,
1450                  increments = params.chronint / (100.0 / 1000000.0),
1451                  count = 0;
1452          char    message[80];
1453
1454          fprintf(stderr,"Calculating diffusion profile");
1455
1456          if ((params.diff_coeff * time_step) / (x_step * x_step) >= 0.5)
1457          {
1458                  sprintf(message,"Value of r greater than 0.5 (%f).\n", (params.diff_c
      oeff * time_step) /
1459                          (x_step * x_step) );
1460                  notice = xv_create( mainframe, NOTICE,
1461                          NOTICE_MESSAGE_STRINGS, message,
1462                                                  "Will lead to unstable finite differe
      nce solution.",
1463                                                  "Reduce time step or diffusion coeffi
      cient,",
1464                                                  "or increase point spacing on horizon
      tal profile.", NULL,
1465                          NOTICE_BUTTON,          "Continue", 1,
1466                          XV_SHOW,                TRUE, NULL);
1467          }
1468
1469
1470          for (dist_loop = 0; dist_loop < USEDPTS; dist_loop++)
1471                  old_temp_prof[dist_loop] = exec.new_eq_prof[dist_loop] = exec.base_ch
      ron[dist_loop];
1472
1473          for (time_loop = 0; time_loop < increments; time_loop++)
1474          {
1475                  temp_sealevel = strat.curves_data[exec.time_steps_done - 1][SEALEVEL]
       +
1476                          ((( strat.curves_data[exec.time_steps_done][SEALEVEL] -
1477                          strat.curves_data[exec.time_steps_done - 1][SEALEVEL] ) / 100
      0.0) * time_loop);
1478
1479                  dist_loop = exec.drainage_divide + 1;
1480
1481                  do
1482                  {
1483                          temp1 = old_temp_prof[dist_loop+1] - (2 * old_temp_prof[dist_
      loop]) +
1484                                  old_temp_prof[dist_loop-1];
1485                          temp2 = params.diff_coeff * (time_step / (x_step * x_step)) *
       temp1;
```



```
1486                          exec.new_eq_prof[dist_loop] = old_temp_prof[dist_loop] + temp
      2;
1487                  }
1488                  while (exec.new_eq_prof[dist_loop++] > temp_sealevel);
1489
1490                  exec.beach_pos = dist_loop - 1;
1491                  generate_shelf_profile(USEDPTS);
1492
1493                  for (dist_loop = exec.drainage_divide; dist_loop < USEDPTS; dist_loop
      ++)
1494                          old_temp_prof[dist_loop] = exec.new_eq_prof[dist_loop];
1495
1496                  count++;
1497                  if (count == 100)
1498                  {
1499                          fprintf(stderr,".");
1500                          count = 0;
1501                  }
1502
1503          }
1504
1505          *beach_pos = exec.beach_pos;
1506
1507          fprintf(stderr,"Beach at %d with new profile elevation of %f\n", exec.beach_p
      os,
1508                  exec.new_eq_prof[exec.beach_pos]);
1509  }
1510
1511  void perm_fluv_prof(profile_endpoint, beach_pos)
1512  /* Same again, but using a complementary error function this time */
1513  int     profile_endpoint,
1514          beach_pos;
1515  {
1516          int     loop;
1517
1518          for (loop = profile_endpoint; loop <= beach_pos; loop++)
1519                  exec.new_eq_prof[loop] = exec.fixed_fluv_prof[loop];
1520  }
1521
1522  int generate_marine_profile()
1523  /* Generate the geometry for the marine profile */
1524  {
1525          float   dummy,
1526                  fluv_depos,
1527                  fluv_eroded,
1528                  marine_budget;
1529          int     ss_break_pos,
1530                  loop;
1531
1532          calc_fluv_area_depos(exec.drainage_divide, strat.beach[exec.layer], exec.beac
      h_pos, exec.new_eq_prof,
1533                          &fluv_eroded, &fluv_depos);
1534
1535          /* Adjust sed budget calculations according to supply type.
1536          Note, this is just testing for the correct slope position, so don't alter glo
      bals!
1537          Type 0 and 3 are constant or external source only.
1538          Tyep 2 is profile erosion plus external source.
1539          Type 1 is profile erosion only. */
1540          switch (sed_budget.supply_flag)
1541          {
1542                  case 0 :
1543                  case 3 : marine_budget = exec.external_budget - fluv_depos;
1544                           break;
1545                  case 1 : marine_budget = fluv_eroded * (float)sed_budget.drainage_rat
      io;
1546                           break;
1547                  case 2 : marine_budget = exec.external_budget - fluv_depos +
1548                                           (fluv_eroded * (float)sed_budget.drainage_rat
      io);
1549                           break;
```

```
1550            }
1551
1552            ss_break_pos = find_shelf_slope_break(marine_budget);
1553            return(ss_break_pos);
1554    }
1555
1556    int find_shelf_slope_break(external_budget)
1557    /* Find the position of the marine break-of-slope which most nearly uses the correct
        area of sediment */
1558    float   external_budget;
1559    {
1560            int     pos_inc = 50,
1561                    too_much_used = FALSE,
1562                    too_little_used = FALSE,
1563                    rep_count1 = 0,
1564                    rep_count2 = 0,
1565                    temp_ss_break = exec.beach_pos + 60,
1566                    slope_met_beach = FALSE;
1567            float   discrep, discrep1, discrep2, discrep3,
1568                    budget;
1569            Xv_notice       notice;
1570
1571            /* Loop adjusting the position of the beach by the amount pos_inc. When discr
        ep has been
1572            both positive and negative i.e. the beach has been both left and right of it'
        s ideal
1573            position, divide pos_inc by two and continue. Should get the beach pos at its
         optimum position.
1574
1575            NOTE - discrep < 0 when too LITTLE sediment has been used, positive when too
        much */
1576
1577            fprintf(stderr,"Finding the shelf slope break...");
1578
1579            do
1580            {
1581                    /* Mustn't allow the ss-break to be moved landward of the beach here,
         so if it is just
1582                            set discrep to -1.0 to indicate area of depos less than that
        required */
1583                    if (temp_ss_break < exec.beach_pos)
1584                            discrep = 1.0;
1585                    else
1586                            discrep = test_slope_pos(temp_ss_break, external_budget);
1587
1588                    /* If discrep > 0.0, sediment is left over, so move ss_break seaward
        by increment */
1589                    if (discrep > 0.0)
1590                    {
1591                            temp_ss_break += pos_inc;
1592                            too_little_used = TRUE;
1593                    }
1594                    /* If discrep < 0.0, no sediment is left over, move ss_break landward
         by increment */
1595                    else
1596                    {
1597                            temp_ss_break -= pos_inc;
1598                            too_much_used = TRUE;
1599                    }
1600
1601                    /* ss-break has been both left and right of the ideal position, so ha
        lve the
1602                    increment value, and reset the marker flags */
1603                    if (too_much_used && too_little_used)
1604                    {
1605                            pos_inc /= 2;
1606                            too_much_used = FALSE;
1607                            too_little_used = FALSE;
1608                    }
1609            }
1610            while (pos_inc > 0 && temp_ss_break > exec.beach_pos && temp_ss_break > 0 &&
```



```
1611                    temp_ss_break < USEDPTS && rep_count1++ < 100);
1612
1613            if (temp_ss_break >= exec.beach_pos)
1614            {
1615                    discrep2 = test_slope_pos(temp_ss_break, external_budget);
1616
1617                    /* Move the beach until the discrepency is smaller than for points to
        the left and right */
1618                    do
1619                    {
1620                            discrep2 < 0.0 ? temp_ss_break-- : temp_ss_break++;
1621
1622                            if (temp_ss_break <= exec.beach_pos) /* Cannot allow ss_break
        to be at or < beach */
1623                                    slope_met_beach = TRUE;
1624                            else
1625                            {
1626                                    discrep1 = test_slope_pos(temp_ss_break - 1, external
        _budget);
1627                                    discrep3 = test_slope_pos(temp_ss_break + 1, external
        _budget);
1628                                    discrep2 = test_slope_pos(temp_ss_break, external_bud
        get);
1629                                    /* Discrep 2 has to be last of three to ensure profil
        e is left
1630                                            generated to the correct pos */
1631                            }
1632                    }
1633                    while ((fabs(discrep2) > fabs(discrep1) || fabs(discrep2) > fabs(disc
        rep3)) &&
1634                            temp_ss_break > 0 && temp_ss_break < USEDPTS && rep_count2++
        < 100
1635                            && !slope_met_beach);
1636
1637                    if (rep_count1 == 100 || rep_count2 == 100 || temp_ss_break > USEDPTS
         || temp_ss_break < 0)
1638                            notice = xv_create( mainframe, NOTICE,
1639                            NOTICE_MESSAGE_STRINGS, "Cannot find a suitable position for
        the shelf slope break.",
1640                                                    "Model integrity may fail...", NULL,
1641                            NOTICE_BUTTON,          "Continue", 1,
1642                            XV_SHOW,                TRUE, NULL);
1643
1644                    return(temp_ss_break);
1645            }
1646            else
1647                    return(exec.beach_pos);
1648    }
1649
1650    float test_slope_pos(pos, external_budget)
1651    /* Calls the function to generate the shelf and shoreface profile, drops the slope fr
        om the shelf-slope
1652    break position, sets the basinward eq. prof. to base chron and returns the total area
         deposited -
1653    the external input and the area eroded, which should be the amount of sed left over f
        rom the total */
1654    int     pos;
1655    float   external_budget;
1656    {
1657            float   slope_inc = params.slope_grad * params.prof_gap * 1000.0,
1658                    eroded,
1659                    depos;
1660            int     loop = pos;
1661
1662            generate_shelf_profile(pos);
1663
1664            /* Do the slope bit until the new chron intersects the old */
1665            while (exec.new_eq_prof[loop++]  - slope_inc  > exec.base_chron[loop + 1] &&
        loop < USEDPTS)
1666                    exec.new_eq_prof[loop] = exec.new_eq_prof[loop - 1] - slope_inc;
1667
```

```
1668            while (loop < USEDPTS)
1669                    exec.new_eq_prof[loop] = exec.base_chron[loop++];
1670
1671            calc_marine_area_depos(strat.beach[exec.layer], exec.beach_pos, &eroded, &dep
    os, exec.new_eq_prof);
1672
1673            if (sed_budget.supply_flag == 0 || sed_budget.supply_flag == 3)
1674                    return(external_budget - depos);
1675            else
1676                    return((eroded + external_budget) - depos);
1677    }
1678
1679    void generate_shelf_profile(ss_break)
1680    /* Generate the marine equilibrium profile with an expo shoreface and a fixed slope s
    helf */
1681    int     ss_break;
1682    {
1683            int     loop,
1684                    beach_bit_done = FALSE;
1685            float   constant,
1686                    vert_inc = params.shelf_grad * params.prof_gap * 1000.0,
1687                    shore_width_points = params.shore_width / params.prof_gap, erosion =
    0.0;
1688
1689            constant = log( params.wave_base ) / (- shore_width_points);
1690
1691            for (loop = exec.beach_pos + 1; loop <= ss_break; loop++)
1692                    if (!beach_bit_done && options.shelf_prof)
1693                    {
1694                            exec.new_eq_prof[loop] = exp( (constant *
1695                                    (loop - (exec.beach_pos + shore_width_points))))
1696                                    + (exec.new_eq_prof[exec.beach_pos] - params.wave_bas
    e);
1697
1698                            beach_bit_done = check_equilib_grad(loop);
1699                    }
1700                    else
1701                            exec.new_eq_prof[loop] = exec.new_eq_prof[loop - 1] - vert_in
    c;
1702    }
1703
1704    void check_ss_break_pos()
1705    /* Check the position of the shelf slope break. If it is at the beach, need to calc t
    he slope meets beach
1706    function */
1707    {
1708            if (exec.ss_break_pos <= exec.beach_pos)
1709            {
1710                    exec.beach_pos = exec.ss_break_pos;
1711                    slope_meets_beach();
1712            }
1713    }
1714
1715    void slope_meets_beach()
1716    /* If there is insufficient marine sediment available to build the slope from the bea
    ch position,
1717    the beach must be moved landward until sufficient sediment is available to build the
    slope. This
1718    means that when this function is called the partition between marine and fluvial brea
    ks down */
1719    {
1720            float   tot_eroded,
1721                    old_tot_depos,
1722                    new_tot_depos,
1723                    fluv_eroded, fluv_depos,
1724                    total_sed_available;
1725
1726            calc_total_area_depos(&new_tot_depos, &tot_eroded, exec.new_eq_prof);
1727
1728            do
1729            {
```



```
1730                    /* Move the beach and the ss-break left one space, redefine the fluvi
    al profile and
1731                    the marine slope, and calculate the new total area */
1732
1733                    old_tot_depos = new_tot_depos;
1734                    exec.beach_pos--;
1735                    exec.ss_break_pos--;
1736
1737                    generate_fluvial_profile(&exec.beach_pos);
1738
1739                    calc_fluv_area_depos(exec.drainage_divide, strat.beach[exec.layer], e
    xec.beach_pos,
1740                            exec.new_eq_prof, &fluv_eroded, &fluv_depos);
1741
1742                    if (sed_budget.supply_flag == 1 || sed_budget.supply_flag == 2)
1743                            total_sed_available = exec.external_budget + fluv_eroded;
1744                    else
1745                            total_sed_available = exec.external_budget;
1746
1747                    test_slope_pos(exec.ss_break_pos, 0.0);
1748
1749                    calc_total_area_depos(&new_tot_depos, &tot_eroded, exec.new_eq_prof);
1750            }
1751            while (new_tot_depos > total_sed_available); /* Keep looping while insuff. to
    t. sed. used */
1752
1753            /* If the discrep. between the total deposited and the budget was less for th
    e previous beach pos
1754            use that oen instead. Need to redefine profiles
1755            if (fabs(new_tot_depos - exec.external_budget) > fabs(old_tot_depos - exec.ex
    ternal_budget) )*/
1756
1757            if (fabs(new_tot_depos - total_sed_available) > fabs(old_tot_depos - total_se
    d_available) )
1758            {
1759                    exec.beach_pos++;
1760                    exec.ss_break_pos++;
1761                    generate_fluvial_profile(&exec.beach_pos);
1762                    test_slope_pos(exec.ss_break_pos, 0.0);
1763            }
1764
1765            strat.beach[exec.layer + 1] = exec.beach_pos;
1766    }
1767
1768    int check_equilib_grad(loop)
1769    /* Calculates the gradient between two points on the profile and returns TRUE if it's
     less than the
1770    proscribed shelf gradient or FALSE if it is greater. This is used to control the tran
    sition from
1771    the exponential beach profile to the fixed slope shelf. */
1772    int loop;
1773    {
1774            float grad;
1775
1776            grad = fabs(exec.new_eq_prof[loop - 2] - exec.new_eq_prof[loop - 1]) / (param
    s.prof_gap * 1000.0 );
1777
1778            if (grad <= params.shelf_grad && loop > exec.beach_pos + 2)
1779                    return(TRUE);
1780            else
1781                    return(FALSE);
1782    }
1783
1784    float get_total_water_depth(profile_point)
1785    /* Return the thickness of the accomodation space at for the given elevation of chron
     surface.
1786     Calculated by taking magnitude of space between upper surface of latest strat
1787    and current sea level.
1788    Need to account for three possibilities and calc slightly differently :
1789    1) Positive sealevel, negative strat.
1790    2) Positive sealevel, positive strat.
```

```
1791  3) Negative sealevel, negative strat.
1792  (Strat must always be negative to be below neg. sealevel) */
1793  float   profile_point;
1794  {
1795          float   temp;
1796
1797          if (exec.sealevel > 0)
1798                  if (profile_point < 0)
1799                          temp = fabs(profile_point) + exec.sealevel;
1800                  else
1801                          temp = exec.sealevel - profile_point;
1802          else
1803                  temp = fabs(profile_point - exec.sealevel);
1804
1805          return(temp);
1806  }
1807
1808  void prograde(left, right )
1809  /* Call the routines to create a sed wedge of given area */
1810  int *left, *right;
1811  {
1812          float   temp,
1813                  left_over;
1814          int     temp_beach = exec.beach_pos;
1815
1816          fprintf(stderr,"Marine prog...");
1817
1818          if (options.shelf_prof)
1819                  gen_mar_prof();
1820  }
1821
1822  float calc_marine_prog_area(new_beach_pos)
1823  /* Calculate and return the area of sediment that has been used up below sealevel by
      the progradation
1824  of the fluvial system. This sediment is part of the marine deposition budget */
1825  int     new_beach_pos;
1826  {
1827          int     loop,
1828                  old_beach_pos = strat.beach[exec.layer],
1829                  testing;
1830          float   old_beach_elev = strat.chrons[exec.layer][old_beach_pos],
1831                  new_beach_elev = exec.work_chron[new_beach_pos],
1832                  area_used = 0.0;
1833
1834          /* Zero marine sediment used if beach has moved landward since last chron,
1835          or if the new beach is below the old beach, in which case the old beach has p
      rob. been eroded */
1836          if (old_beach_pos > exec.beach_pos)
1837                  return(0);
1838          else
1839          {
1840                  beach_interpolation(old_beach_pos, exec.beach_pos);
1841
1842                  for (loop = old_beach_pos + 1; loop <= new_beach_pos; loop++)
1843
1844                          if (new_beach_elev > old_beach_elev)
1845                                  area_used += calc_one_trap(exec.beach_array[loop],
1846                                                  exec.base_chron[loop - 1], exec.beach_array[l
      oop],
1847                                                  exec.base_chron[loop]);
1848                          else
1849                                  area_used +=  calc_one_trap(exec.new_eq_prof[loop - 1
      ],
1850                                                          exec.base_chron[loop - 1], exec.new_e
      q_prof[loop],
1851                                                          exec.base_chron[loop]);
1852          }
1853
1854          return(fabs(area_used));
1855  }
1856
```



```
1857  void beach_interpolation(old_beach, new_beach)
1858  /* Interpolate between the old beach postion and the new beach position, calculating
      an
1859  elevation for each point */
1860  int     old_beach,
1861          new_beach;
1862  {
1863          int     loop;
1864          float   old_elev = exec.base_chron[old_beach], /*strat.chrons[exec.layer][old
      _beach],*/
1865                  new_elev = exec.new_eq_prof[new_beach], /*exec.work_chron[new_beach],
      */
1866                  gradient = (new_elev - old_elev) / (float)(new_beach - old_beach);
1867
1868          exec.beach_array[old_beach] = old_elev;
1869
1870          for (loop = old_beach + 1; loop <= new_beach; loop++)
1871                  exec.beach_array[loop] = exec.beach_array[loop - 1] + gradient;
1872  }
1873
1874  void gen_mar_prof()
1875  /* This function actually stores the new shelf and slope geometry in the working chro
      n, and records
1876  the distribution of the marine envirnments */
1877  {
1878          int     loop,
1879                  loop1;
1880          float   water_depth;
1881
1882          for (loop = exec.beach_pos; loop < USEDPTS; loop++)
1883          {
1884                  exec.work_chron[loop] = exec.new_eq_prof[loop];
1885                  water_depth = get_total_water_depth(exec.new_eq_prof[loop]);
1886                  record_shelf_depos(loop, water_depth);
1887                  exec.loadprof[loop] = exec.work_chron[loop] - exec.base_chron[loop];
1888
1889                  for (loop1 = 0; loop1 <= exec.layer; loop1++)
1890                          if (exec.work_chron[loop] < strat.chrons[loop1][loop] && opti
      ons.section_type == 0)
1891                          {
1892                                  strat.chrons[loop1][loop] = exec.work_chron[loop];
1893                                  if (strat.depos[loop1][loop] != NO_DEPOS)
1894                                          strat.depos[loop1][loop] = MARINE_EROSION;
1895                          }
1896          }
1897  }
1898
1899  void record_shelf_depos(loop, water_depth)
1900  /* Record the environment at the current point */
1901  int loop;
1902  float water_depth;
1903  {
1904          if (loop < exec.ss_break_pos)
1905                  if (water_depth > params.wave_base)
1906                          strat.depos[exec.layer + 1][loop] = OFFSHORE_SHELF;
1907                  else
1908                          strat.depos[exec.layer + 1][loop] = SHOREFACE;
1909          else
1910          if (exec.new_eq_prof[loop] > exec.base_chron[loop])
1911                  strat.depos[exec.layer + 1][loop] = SLOPE;
1912  }
1913
1914  void inst_flex_subside()
1915  /* Subside layers  by amount of flexure generated by the new load (current layer).
1916   Also subside work_chron. */
1917  {
1918          int loop, subloop;
1919
1920          /* Subside current chron also - water infill */
1921
1922          /* Do the subsidence for the proscribed layers.  */
```

```
1     #define TRUE              1
2     #define FALSE             0
3     #define MAXPTS            4097    /* No. of pts. defined in arrays */
4     #define USEDPTS           4096    /* Actual number of points on profile */
5     #define MAXCHRONS         201     /* Maximum nuber of chrons */
6     #define MAX_STEPS         1002    /* Maximum number of 0.01Ma time steps allowable + st
      art and end */
7     #define SCALE             5       /* Scaling factor for vertical scale of profile */
8     #define X_OFFSET          50      /* X offset for profile from left of canvas */
9     #define Y_OFFSET          100     /* Y offset for profile from top of canvas */
10    #define MAXLEN            5000    /* Maximum profile length */
11    #define MAXHEIGHT         500
12    #define MAXDEPTH          3000    /* Max. basin width and depth as def. on canvas */
13    #define PI                3.1415927
14    #define TWOPI             6.2831853
15    #define RAD_CONV          180.0 / 3.1415927 /* Const to mult by rads to get degs. */
16    #define ENVIRONS          8       /* Number of different environments supported */
17    #define FLUVIAL           1
18    #define SHOREFACE         2
19    #define OFFSHORE_SHELF    3
20    #define SLOPE             4
21    #define AERIAL_EROSION    5
22    #define MARINE_EROSION    6
23    #define NO_DEPOS          7
24    #define COAST_ONLAP       8       /* Array ref for the colour used for coast onlap curv
      e */
25    #define MARKER            9
26    #define P_MANT            3.3     /* Density of mantle material */
27    #define P_WATER           1.03    /* Density of seawater */
28    #define P_AIR             0.0013  /* Density of air */
29    #define P_SED             1.8     /* Density of uncompacted sediment */
30    #define EMT               0       /* Elapsed time, Ma */
31    #define SEALEVEL          1       /* Sealevel */
32    #define FLUV_DEP          2       /* Fluvial deposition */
33    #define FLUV_EROD         3       /* Fluvial erosion */
34    #define MAR_DEP           4       /* Marine deposition */
35    #define MAR_EROD          5       /* Marine erosion */
36    #define EX_SED            6       /* External budget */
37    #define REL_SEA           7       /* Relative sealevel */
38    #define THERM_SUB         8       /* Thermal subsidence */
39    #define V_ONLAP           9       /* Coastal onlap - vertical element */
40    #define PART_COEFF        10      /* Sediment partitioning coefficient */
41
42    /* Definitions for use in flex include file */
43    #define PI2               6.283185307
44    #define Vconst            12.0 * (1.0 - 0.0625)
45    #define Econst            1.0e12
46    #define abs(i) (i)<0 ? -(i) : (i) /* Macro to convert to +sign */
47
48    /* Constants used in tectonic subsidence equations
49    #define A                 125000.0
50    #define ALPHA             3.28E-4
51    #define TO                1333.0
52    #define CRUST             31200.0
53    #define TAU               62.8 * 60.0 * 60.0 * 24.0 * 365.0 * 1.0e6 */
54
55    #define min(a,b)          (((a) < (b)) ? (a) : (b))
56    #define max(a,b)          (((a) > (b)) ? (a) : (b))
57
58    #include <stdio.h>
59    #include <math.h>
60    #include <string.h>
61    #include <malloc.h>
62
63    /* Include files for the windows and graphics routines */
64    #include <xview/xview.h>
65    #include <xview/canvas.h>
66    #include <xview/panel.h>
67    #include <xview/icon.h>
68    #include <xview/notice.h>
69    #include <xview/scrollbar.h>
```



```
70    #include <xview/font.h>
71    #include <xview/cursor.h>
72    #include <xview/cms.h>
73    #include <X11/X.h>
74    #include <X11/Xlib.h>
75
76    /* Defined functions within the main program */
77    void set_disp_flags();
78    void batch_job();
79    void special_case_run();
80    void init_proc();
81    void get_params();
82    int check_params();
83    void set_seastart();
84    void init_sea_curve();
85    void set_sedstart();
86    void set_pcstart();
87    float set_Te_start();
88    void set_strat();
89    void set_subsid_arrays();
90    void zero_curve_data();
91    void set_presev_data();
92    void adjust_topog_to_sealevel();
93    void init_drainage();
94    void init_expo_curve();
95    void init_erfc_curve();
96    void init_fixed_fluv_prof();
97    void init_marine_prof();
98    void run_proc();
99    void update_params();
100   void do_a_chron();
101   void copy_chron();
102   int find_sea_chron_intersection();
103   int find_coast();
104   void adjust_beach_position();
105   float sufficient_sed_used();
106   void accurate_beach_position();
107   void find_equilib_point();
108   void zeroflex();
109   void inst_flex_subside();
110   void linear_flex_subside();
111   void expo_flex_subside();
112   void mckenzie_subside();
113   void two_layer_subside();
114   void tect_subside();
115   void set_work_chrons();
116   void gen_equilib_prof();
117   void generate_fluvial_profile();
118   void expo_fluvial_profile();
119   void errfunc_fluvial_profile();
120   void diffusion_fluvial_profile();
121   void perm_fluv_prof();
122   int generate_marine_profile();
123   float test_slope_pos();
124   void generate_shelf_profile();
125   void slope_meets_beach();
126   int check_equilib_grad();
127   void prograde();
128   void gen_mar_prof();
129   float calc_marine_prog_area();
130   void beach_interpolation();
131   void prog_wedge();
132   void expo_slope_prog();
133   void set_slope();
134   float do_slope_strat();
135   void fixed_slope_prog();
136   void record_shelf_depos();
137   void check_ss_break_pos();
138   float check_slope_steep();
139   float change_Te();
140   void get_mckenzie_subs();
```

```
141   float one_mckenzie_sub();
142   void get_two_layer_subs();
143   float one_two_layer_sub();
144   void change_sealevel();
145   float sea_smooth_linear();
146   void sea_saw_tooth();
147   void sea_sinusoidal_pos();
148   void sea_sinusoidal_neg();
149   float sea_increase();
150   float sea_decrease();
151   void sea_sinusoidal2_pos();
152   void sea_sinusoidal2_neg();
153   void calc_new_prof_area();
154   void calc_new_water_prof();
155   void change_sed_budget();
156   void sed_linear_inc_dec();
157   void sed_saw_tooth();
158   void sed_sinusoidal();
159   void change_sedpc();
160   float scan_sed_stack();
161   void change_drainage();
162   void gen_riv_prof();
163   void normal_fluvial();
164   float fluvial_erosion();
165   float get_rel_sealevel();
166   void calc_onlap();
167   int precise_onlap_calculation();
168   void compile_depos_info();
169   void compile_presev_info();
170   float calc_area();
171   float calc_one_trap();
172   void calc_fluv_area_depos();
173   void calc_marine_area_depos();
174   void calc_total_area_depos();
175   void record_chron_areas();
176   float calc_prof_area();
177
178
179   /* Defined functions within set_windows.h */
180   void setgraphics();
181   void main_panel_setup();
182   void main_canvas_setup();
183   void set_cursor_and_icons();
184   void chrono_panel_setup();
185   void chrono_canvas_setup();
186   void presev_panel_setup();
187   void presev_canvas_setup();
188   void display_panel_setup();
189   void general_panel_setup();
190   void fluvial_panel_setup();
191   void marine_panel_setup();
192   void chrons_panel_setup();
193   void tect_panel_setup();
194   void sea_panel_setup();
195   void sed_panel_setup();
196   void post_panel_setup();
197   void labels_panel_setup();
198   void chron_labels_panel_setup();
199   void file_panel_setup();
200   void zoom_panel_setup();
201   void wheeler_zoom_panel_setup();
202   void wheeler_opt_panel_setup();
203   void point_info_panel_setup();
204   void set_up_colour_map();
205
206   /* Defined functions within graphics.h */
207   void full_screen_draw();
208   void dump();
209   float v_real2screen();
210   float v_screen2real();
211   float v_real2zoom();
```



```
212   float v_zoom2real();
213   float h_zoom2real();
214   float h_real2post();
215   float v_real2post();
216   void layer_label();
217   void chrons_done_label();
218   void draw_scales();
219   void show_load();
220   void show_flex();
221   void zoomed_screen_draw();
222   void draw_zoomed_axis();
223   void draw_zoomed_last_chron();
224   void draw_zoomed_load();
225   void draw_zoomed_flex();
226   void draw_zoomed_sealevel();
227   void draw_zoomed_equilib();
228   void draw_marker_chrons();
229   void do_unzoom();
230   void zoomer_show();
231   void draw_wheeler();
232   void connect_beach();
233   void connect_equilib_point();
234   void draw_wheeler_marked_chrons();
235   void wheeler_scales();
236   void timescale();
237   void draw_zoomed_wheeler();
238   void zoomed_wheeler_scales();
239   void draw_seacurve();
240   void seacurve_scales();
241   void draw_relsea_curve();
242   void relsea_curve_scales();
243   void draw_subsid_curve();
244   void subsid_curve_scales();
245   void draw_sedcurve();
246   void sedcurve_scales();
247   void find_curve_limits();
248   void do_crossplot();
249   void cross_plot_scales();
250   void do_presev_diag();
251   float get_max_pres();
252   void draw_presev_scales();
253   void draw_presev_data();
254   void gen_main_postscript();
255   void gen_chrono_postscript();
256   void wheeler_post();
257   void connect_beach_post();
258   void connect_onlap_post();
259   void draw_marker_chrons_post();
260   void sea_curve_post();
261   void relsea_curve_post();
262   void subsid_curve_post();
263   void onlap_curve_post();
264   void crossplot_post();
265   void sed_curve_post();
266   void post_plot_sed_area_line();
267   void post_plot_sed_area_solid();
268   void gen_zoomed_postscript();
269   void do_post_zoom();
270   void draw_chron_labels();
271   void get_chron_label_info();
272   void do_slope_label();
273   void do_fluvial_label();
274   void print_post_comments();
275   void post_zoomed_sealevel();
276   void post_zoomed_marker_chrons();
277   void draw_post_key();
278   void draw_labels();
279   void get_label_info();
280   void get_label_offsets();
281
282   /* Defined functions within interface.h */
```

```
283   float read_user_seacurve();
284   void mouse_cont();
285   void box_draw();
286   void norm_coords_and_chron();
287   void zoomed_coords_and_chron();
288   void params_pressed();
289   void apply_general();
290   void general_done();
291   void proflen_slider_label();
292   void apply_display();
293   void display_done();
294   void apply_fluvial();
295   void fluvial_done();
296   void apply_marine();
297   void marine_done();
298   void apply_chrons();
299   void chrons_done();
300   void apply_tect();
301   void tect_done();
302   void apply_sea();
303   void quit_sea();
304   void apply_sed();
305   void quit_sed();
306   void prepare_zoom();
307   void do_box_zoom();
308   void do_window_zoom();
309   void hide_zoom_frame();
310   void quit_proc();
311   void display_point_info();
312   void point_info_hide();
313   void do_chrono();
314   void chrono_init();
315   void chrono_refresh();
316   void wheeler_zoom_show();
317   void wheeler_zoom_hide();
318   int set_wheeler_zoom();
319   void wheeler_options_show();
320   void wheeler_options_hide();
321   void set_wheeler_options();
322   void diags_pressed();
323   void wheeler_pressed();
324   void do_wheeler();
325   void presev_refresh();
326   void do_seacurve();
327   void do_relseacurve();
328   void find_curve_minmax();
329   void do_subsidcurve();
330   void do_onlap_curve();
331   void do_sedcurve();
332   void quit_chrono();
333   void quit_presev();
334   void dump_sedcurve();
335   void var_plot_pressed();
336   void do_preserv();
337   void do_postscript();
338   void quit_postscript();
339   void get_postscript_params();
340   void postscript_use_options();
341   void postscript_zoom_defaults();
342   void postscript_chrono_defaults();
343   int  check_postscript_file();
344   void show_post_labels_panel();
345   void hide_post_labels_panel();
346   void show_chron_labels_panel();
347   void hide_chron_labels_panel();
348   void do_load_save();
349   void quit_load_save();
350   void do_load();
351   int  get_structures();
352   int  read_strat();
353   void do_save();
```



```
354   void save_structures();
355   int  write_strat();
356
357   void flex();
358   void accurate_flex();
359   void water_flex();
360   void calc_flex_disp_coeff();
361
362   /* Define all the windows environment variables */
363
364   extern Frame            mainframe, displayframe, generalframe, chronsframe, fluvialfr
      ame, marineframe,
365                           tectframe, seaframe,
366                           sedframe, postframe, fileframe,  chrono_frame, presev_frame,
      zoomframe,
367                           wheeler_zoom_frame, wheeler_opt_frame, point_info_frame, post
      _labels_frame,
368                           chron_labels_frame;
369
370   extern Panel            mainpanel, displaypanel, generalpanel, chronspanel, fluvialpa
      nel, marinepanel,
371                           tectpanel, seapanel, sedpanel, postpanel, filepanel,  chrono_
      panel, presev_panel,
372                           zoompanel, wheeler_zoom_panel, wheeler_opt_panel, point_info_
      panel,
373                           post_labels_panel, chron_labels_panel;
374
375   extern Canvas           canvas, chrono_canvas, presev_canvas;
376
377   extern Display          *dpy, *chrono_dpy, *presev_dpy;
378   extern GC               gc, chrono_gc, presev_gc;
379   extern XGCValues        gcvalues;
380   extern unsigned long    *main_cols, *chrono_cols, *presev_cols;
381   extern Window           canvas_win, chrono_win, presev_win;
382
383   extern Scrollbar        main_vbar, main_hbar, chrono_hbar, presev_hbar;
384   extern Pixwin           *pw, *chronopw;                 /* Graphics canvas & pointer
      */
385   extern Xv_font          norm;
386   extern Xv_font          bold;                   /* Window fonts */
387   extern Server_image     main_closed_image, chrono_closed_image, presev_closed_image,
      postscript_closed_image,
388                           zoom_closed_image, sealevel_closed_image, chrons_closed_image
      , tect_closed_image,
389                           sed_closed_image, cursor_image;
390   extern Icon             main_icon, chrono_icon, presev_icon, postscript_icon, zoom_ic
      on, sealevel_icon,
391                           chrons_icon, tect_icon, sed_icon;
392                           /* Icons for closed windows */
393
394   extern Pixmap           smile_tile, sad_tile;
395
396   extern Xv_notice        notice;
397
398   extern Panel_item       proflen_item, proflen_message, sed_density_item, loadfile_ite
      m, gen_options_item,
399                           axis_option_item, disp_options_item, marker_point_item, marke
      r_chron_item;
400
401   extern Panel_item       shelf_grad_item, slope_grad_item, wave_base_item, shore_width
      _item;
402
403   extern Panel_item       drainage_item, fluvial_prog_item, perm_prof_item, cutback_ite
      m, diffcoeff_item,
404                           length_scale_item, profile_type_item, curve_type_item, partit
      ion_item,
405                           onlap_type_item, fluv_depos_cutoff_item;
406
407   extern Panel_item       chronint_item, chronfreq_item, chrons_item, step_chrons_item;
408
409   extern Panel_item       message1, message2, message3, message4, message5;
```

```
410
411   extern Panel_item       betafile_item, sigmafile_item, Tefile_item,Te_value_item, bou
      ndary_depth_item,
412                           crust_age_item, Te_options_item, flex_options_item, synrift_t
      ype_item,
413                           subside_type_item, response_time_item, response_type_item, wa
      ter_loading_item;
414
415   extern Panel_item       sea_change_flag_item, seamax_item1, seamin_item1, seafreq_ite
      m1, seacurve_item1,
416                           seamax_item2, seamin_item2, seafreq_item2, seacurve_item2,
417                           seafname_item;
418
419   extern Panel_item       supply_flag_item, external_budget_item, release_item, drain_r
      at_item,
420                           sedmax_item, sedmin_item, sedfreq_item, sedcurve_item, testin
      g,
421                           pc_flag_item, pcmax_item, pcmin_item, pcfreq_item;
422
423   extern Panel_item       fname_item,  params_item, format_item, pen_width_item,  backg
      round_item, colour_item,
424                           key_flag_item, print_sealevel_item, axis_ticks_item, depth_ti
      ck_num_item,
425                           length_tick_num_item, ax_label_height_item, image_width_item,
       image_height_item,
426                           x_offset_item, y_offset_item, mult_time_axis_item, x_gap_item
      , key_X_pos_item,
427                           key_Y_pos_item, commentX_item, comment_size_item, multi_comme
      nt_item;
428
429   extern Panel_item       label1_item, label2_item, label3_item, label4_item, label5_it
      em,
430                           Xpos1_item, Ypos1_item, pointX1_item, pointY1_item,
431                           Xpos2_item, Ypos2_item, pointX2_item, pointY2_item,
432                           Xpos3_item, Ypos3_item, pointX3_item, pointY3_item,
433                           Xpos4_item, Ypos4_item, pointX4_item, pointY4_item,
434                           Xpos5_item, Ypos5_item, pointX5_item, pointY5_item;
435
436   extern Panel_item       chron1_item, noX1_item, noY1_item, chron2_item, noX2_item, no
      Y2_item,
437                           chron3_item, noX3_item, noY3_item, chron4_item, noX4_item, no
      Y4_item,
438                           chron5_item, noX5_item, noY5_item, chron6_item, noX6_item, no
      Y6_item,
439                           chron7_item, noX7_item, noY7_item, chron8_item, noX8_item, no
      Y8_item,
440                           chron9_item, noX9_item, noY9_item, chron10_item, noX10_item,
      noY10_item,
441                           chron_label_number_item, chron_label_size_item;
442
443   extern Panel_item       directory_item, filename_item;
444
445   extern Panel_item       run_status_item;
446
447   extern Panel_item       zoom_left_item, zoom_right_item, zoom_top_item, zoom_bott_ite
      m;
448
449   extern Panel_item       wheeler_zoom_left_item, wheeler_zoom_right_item, wheeler_firs
      t_chron_item,
450                           wheeler_last_chron_item;
451
452   extern Panel_item       active_diags_item, wheeler_width_item, sed_supply_width_item,
       eustasy_width_item,
453                           relsea_width_item, subsid_width_item, onlap_width_item, cross
      plot_width_item,
454                           crossplot_X_item, crossplot_Y_item;
455
456   extern Panel_item       profile_point_item, beta_message_item, sigma_message_item,
457                           last_therm_sub_message_item, tot_therm_sub_message_item,
458                           Te_message_item, flexure_message_item, elevation_message_item
      ;
```



```
459
460   extern Menu             wheeler_menu, params_menu, zoom_menu, diagrams_menu, var_plot
      _menu;
461
462   extern Xv_Cursor        cursor; /*Canvas cursor */
463
464   extern Cms              cms;
465
466   extern char             curve_labels[8][30];
467
468   extern Xv_singlecolor   colors[255];
469
470   /* Data structure which contains flags to control graphical display and model options
       */
471   struct Options  {
472           unsigned short int prograde;
473           unsigned short int section_type;
474           unsigned short int riv_prof;
475           unsigned short int curve_type;
476           unsigned short int shelf_prof;
477           unsigned short int init_shelf_prof;
478           unsigned short int show_enviros;
479           unsigned short int show_last_chron;
480           unsigned short int show_equilib;
481           unsigned short int show_load;
482           unsigned short int show_flex;
483           unsigned short int show_sealevel;
484           unsigned short int flex_type;
485           unsigned short int Te_type;
486           unsigned short int synrift_type;
487           unsigned short int subside_type;
488           unsigned short int fluvial_prog;
489           unsigned short int perm_fluv_prof;
490           unsigned short int profile_type;
491           unsigned short int water_loading;
492           unsigned short int onlap_type;
493           unsigned short int fluv_response_type;
494           unsigned short int show_marker_chrons;
495   };
496
497   /* data structure which contains parameters to model */
498   struct Params   {
499           float proflen;                  /* Length of profile (km) */
500           float prof_gap;                 /* Gap between prof sample points (Calc. not
      input) */
501           int marker_point;               /* Position to take relative sea level and su
      bsid curves */
502           int marker_chrons[20];          /* Ages in e.m.t. to draw marker chrons */
503           float Pdisp;                    /* Density of sea water */
504           float Psed;                     /* Density of load material i.e. sediment */
505           float Pinf;                     /* Density of infill */
506           float Pmant;                    /* Density of mantle */
507           float crust_age;                /* Starting age of crust */
508           char Tefile[80];                /* Filename for the Te values */
509           char loadfile[80];              /* Filename containing load coords */
510           char betafile[80];              /* Filename for the beta values */
511           char sigmafile[80];             /* Filename for the sigma values */
512           float boundary_depth;           /* Depth to boundary for two layer stretching
       */
513           float shelf_grad;               /* Gradient of the marine shelf */
514           float slope_grad;               /* Gradient of the marine slope */
515           float wave_base;                /* Height of the shoreface */
516           float shore_width;              /* Width of the shoreface */
517           float drainage_len;             /* Length of the fluvial profile */
518           float diff_coeff;               /* Fluvial diffusion coefficient */
519           float cutback_rate;             /* Rate of fluvial profile landward migration
       */
520           float length_scale;             /* ERFC length scale */
521           float fluv_depos_cutoff;        /* Minimum thickness of fluvial deposition to
       be recorded */
522           float chronint;                 /* Interval between chrons in Ma */
```

```
523             float chronfreq;                /* Frequency of chron stroage */
524             int chrons;                     /* Total Number of chrons */
525             int step_chrons;                /* Number of chrons per execution step */
526     };
527
528     struct Exec     {
529             int layer;                      /* The last chron generated */
530             int chronelapsed;
531             int total_chrons_done;          /* The total number of chrons generated */
532             int step_chrons_done;           /* The number of chrons generated this model
        step */
533             int time_steps_done;            /* Time steps done for the current execution
        step */
534             int drainage_divide;            /* Position of the end of the fluvial profile
         */
535             int nick_point;                 /* Position of a nickpoint on the profile */
536             int beach_pos;                  /* The position on the profile of the beach *
        /
537             int ss_break_pos;               /* The position on the profile of the marine
        break of slope */
538             float beach_array[MAXPTS];      /* The interpolated points between beach posi
        tions */
539             float nick_count;               /* Counter for headward movement of the river
         profile */
540             float betaprof[MAXPTS];         /* The beta profile */
541             float sigmaprof[MAXPTS];        /* The sigma profile */
542             float loadprof[MAXPTS];         /* The initial topography */
543             float flexprof[MAXPTS];         /* The flexural profile */
544             float TeArray[MAXPTS];          /* The Te profile */
545             float ak[MAXPTS];               /* The restoring force profile */
546             float oldflex[MAXPTS];          /* The flexural profile for the previous chro
        n */
547             float old_water_prof[MAXPTS];   /* Not used */
548             float new_water_prof[MAXPTS];   /* Not used */
549             float new_tect_sub[MAXPTS];     /* Tectonic subsidence for the current time s
        tep */
550             float old_tect_sub[MAXPTS];     /* Tectonic subsidence for the previous time
        step */
551             float refsub[MAXPTS];           /* Reference profile for subsidence calculati
        ons */
552             double elapsed;                 /* Elapsed model time */
553             float Te;                       /* Single value of Te for laterally constant
        model */
554             float area;                     /* Not used */
555             float sea_cycle_elapsed;        /* How much of sealevel cycle elapsed - for s
        in curve etc*/
556             float sed_cycle_elapsed;        /* How much of sediment cycle elapsed - for s
        in curve etc*/
557             float sed_budget;               /* Sed budget calculate from profile erosion
        and deposition */
558             float external_budget;          /* External supply from curves etc */
559             float sed_change;               /* Rate of change on sediment supply curve */
560             float sed_marker;               /* Midpoint on the sediment supply curve */
561             float sed_pc;
562             float pc_change;
563             float pc_marker;
564             int sed_stack_ptr;              /* Not used */
565             float fluvial_depos;            /* Area of fluvial sediment deposited for one
         chron */
566             float fluvial_erod;             /* Area of fluvial sediment eroded for one ch
        ron */
567             float marine_depos;             /* Area of marine sediment deposited for one
        chron */
568             float marine_erod;              /* Area of marine sediment eroded for one chr
        on */
569             float sealevel;                 /* Elevation of the absolute sealevel datum *
        /
570             float sea_change1;              /* Rate of change for short-term sealevel cur
        ve */
571             float sea_marker1;              /* Mid point on short-term curve */
572             float sea_change2;              /* Rate of change for long-term sealevel curv
```



```
        e */
573             float sea_marker2;              /* Mid point on long-term curve */
574             float new_eq_prof[MAXPTS];      /* Equilibrium profiles for current chron */
575             float old_eq_prof[MAXPTS];      /* Equilibrium profiles for the previous chro
        n */
576             float fixed_fluv_prof[MAXPTS];  /* Static fluvial equilibrium profile */
577             float work_chron[MAXPTS];       /* Working chron - used for area fits etc */
578             float base_chron[MAXPTS];       /* Previous chron being built on to */
579             float fluv_change[MAXCHRONS][MAXPTS];
580             float old_fluv_prof[MAXCHRONS][MAXPTS];
581             float fluv_disp_coeff[MAXCHRONS];
582             float last_chron[MAXPTS];       /* Not used */
583             float old_riv_prof_area;        /* Not used */
584             float length_scale;             /* Not used */
585
586             float temp_elevation;           /* Definitely not used */
587     };
588
589     struct Exec_flags {
590             unsigned short int box_drawing;
591             unsigned short int box_drawn;
592             unsigned short int zoomed;
593             unsigned short int diagpos;
594             unsigned short int execution_complete;
595             unsigned short int initialised;
596     };
597
598
599     struct Strat    {
600             float chrons[MAXCHRONS][MAXPTS]; /* 2d array to contain X Y coords of each
601                                                 layer of strat generated in the basin */
602
603             float curves_data[MAX_STEPS + 2][11];   /* 2d array to hold sealevel and sedi
        ment budget info
604                                                     (total depos. and input) for each  ti
        mestep :
605                                 0 : Elapsed time, Ma
606                                 1 : Absolute sealevel
607                                 2 : Fluvial deposition
608                                 3 : Fluvial erosion
609                                 4 : Marine deposition
610                                 5 : Marine erosion
611                                 6 : External budget
612                                 7 : Relative sealevel
613                                 8 : Thermal subsidence
614                                 9 : Vertical element of Coastal onlap
615                                 10 : Sediment partitioning coefficient */
616
617             float sed_stack[MAX_STEPS + 2]; /* array to hold the drainage basin sediment
        budget stack. */
618
619             unsigned short int depos[MAXCHRONS][MAXPTS];    /* 2d array to contain flags
        to indicate depos
620                                                             environment. See #define sect
        ion at beginning
621                                                             for code info. Used to draw W
        heeler diagram */
622             unsigned short int beach[MAXCHRONS];            /* Array to store the lateral
         position of the
623                                                             beach for each chron */
624             unsigned short int equilib_point[MAXCHRONS];    /* Array to store the lateral
         position of the
625                                                             equilibrium point (Posser, Je
        rvey & Vail, 1988) */
626             unsigned short int onlap[MAXCHRONS];            /* Used to store the horizont
        al postion of the
627                                                             stratal onlap */
628
629             float presev_info[ENVIRONS][2]; /* 2d array to hold the total deposited and
630                                                the total preserved for each environment */
631     };
```

```
523             float chronfreq;                /* Frequency of chron stroage */
524             int chrons;                     /* Total Number of chrons */
525             int step_chrons;                /* Number of chrons per execution step */
526     };
527
528     struct Exec     {
529             int layer;                      /* The last chron generated */
530             int chronelapsed;
531             int total_chrons_done;          /* The total number of chrons generated */
532             int step_chrons_done;           /* The number of chrons generated this model
        step */
533             int time_steps_done;            /* Time steps done for the current execution
        step */
534             int drainage_divide;            /* Position of the end of the fluvial profile
         */
535             int nick_point;                 /* Position of a nickpoint on the profile */
536             int beach_pos;                  /* The position on the profile of the beach *
        /
537             int ss_break_pos;               /* The position on the profile of the marine
        break of slope */
538             float beach_array[MAXPTS];      /* The interpolated points between beach posi
        tions */
539             float nick_count;               /* Counter for headward movement of the river
         profile */
540             float betaprof[MAXPTS];         /* The beta profile */
541             float sigmaprof[MAXPTS];        /* The sigma profile */
542             float loadprof[MAXPTS];         /* The initial topography */
543             float flexprof[MAXPTS];         /* The flexural profile */
544             float TeArray[MAXPTS];          /* The Te profile */
545             float ak[MAXPTS];               /* The restoring force profile */
546             float oldflex[MAXPTS];          /* The flexural profile for the previous chro
        n */
547             float old_water_prof[MAXPTS];   /* Not used */
548             float new_water_prof[MAXPTS];   /* Not used */
549             float new_tect_sub[MAXPTS];     /* Tectonic subsidence for the current time s
        tep */
550             float old_tect_sub[MAXPTS];     /* Tectonic subsidence for the previous time
        step */
551             float refsub[MAXPTS];           /* Reference profile for subsidence calculati
        ons */
552             double elapsed;                 /* Elapsed model time */
553             float Te;                       /* Single value of Te for laterally constant
        model */
554             float area;                     /* Not used */
555             float sea_cycle_elapsed;        /* How much of sealevel cycle elapsed - for s
        in curve etc*/
556             float sed_cycle_elapsed;        /* How much of sediment cycle elapsed - for s
        in curve etc*/
557             float sed_budget;               /* Sed budget calculate from profile erosion
        and deposition */
558             float external_budget;          /* External supply from curves etc */
559             float sed_change;               /* Rate of change on sediment supply curve */
560             float sed_marker;               /* Midpoint on the sediment supply curve */
561             float sed_pc;
562             float pc_change;
563             float pc_marker;
564             int sed_stack_ptr;              /* Not used */
565             float fluvial_depos;            /* Area of fluvial sediment deposited for one
         chron */
566             float fluvial_erod;             /* Area of fluvial sediment eroded for one ch
        ron */
567             float marine_depos;             /* Area of marine sediment deposited for one
        chron */
568             float marine_erod;              /* Area of marine sediment eroded for one chr
        on */
569             float sealevel;                 /* Elevation of the absolute sealevel datum *
        /
570             float sea_change1;              /* Rate of change for short-term sealevel cur
        ve */
571             float sea_marker1;              /* Mid point on short-term curve */
572             float sea_change2;              /* Rate of change for long-term sealevel curv
```



```
        e */
573             float sea_marker2;              /* Mid point on long-term curve */
574             float new_eq_prof[MAXPTS];      /* Equilibrium profiles for current chron */
575             float old_eq_prof[MAXPTS];      /* Equilibrium profiles for the previous chro
        n */
576             float fixed_fluv_prof[MAXPTS];  /* Static fluvial equilibrium profile */
577             float work_chron[MAXPTS];       /* Working chron - used for area fits etc */
578             float base_chron[MAXPTS];       /* Previous chron being built on to */
579             float fluv_change[MAXCHRONS][MAXPTS];
580             float old_fluv_prof[MAXCHRONS][MAXPTS];
581             float fluv_disp_coeff[MAXCHRONS];
582             float last_chron[MAXPTS];       /* Not used */
583             float old_riv_prof_area;        /* Not used */
584             float length_scale;             /* Not used */
585
586             float temp_elevation;           /* Definitely not used */
587     };
588
589     struct Exec_flags {
590             unsigned short int box_drawing;
591             unsigned short int box_drawn;
592             unsigned short int zoomed;
593             unsigned short int diagpos;
594             unsigned short int execution_complete;
595             unsigned short int initialised;
596     };
597
598
599     struct Strat    {
600             float chrons[MAXCHRONS][MAXPTS]; /* 2d array to contain X Y coords of each
601                                                 layer of strat generated in the basin */
602
603             float curves_data[MAX_STEPS + 2][11];   /* 2d array to hold sealevel and sedi
        ment budget info
604                                                 (total depos. and input) for each  ti
        mestep :
605                             0 : Elapsed time, Ma
606                             1 : Absolute sealevel
607                             2 : Fluvial deposition
608                             3 : Fluvial erosion
609                             4 : Marine deposition
610                             5 : Marine erosion
611                             6 : External budget
612                             7 : Relative sealevel
613                             8 : Thermal subsidence
614                             9 : Vertical element of Coastal onlap
615                             10 : Sediment partitioning coefficient */
616
617             float sed_stack[MAX_STEPS + 2]; /* array to hold the drainage basin sediment
        budget stack. */
618
619             unsigned short int depos[MAXCHRONS][MAXPTS];    /* 2d array to contain flags
        to indicate depos
620                                                             environment. See #define sect
        ion at beginning
621                                                             for code info. Used to draw W
        heeler diagram */
622             unsigned short int beach[MAXCHRONS];            /* Array to store the lateral
         position of the
623                                                             beach for each chron */
624             unsigned short int equilib_point[MAXCHRONS];    /* Array to store the lateral
         position of the
625                                                             equilibrium point (Posser, Je
        rvey & Vail, 1988) */
626             unsigned short int onlap[MAXCHRONS];            /* Used to store the horizont
        al postion of the
627                                                             stratal onlap */
628
629             float presev_info[ENVIRONS][2]; /* 2d array to hold the total deposited and
630                                                the total preserved for each environment */
631     };
```

```
632
633
634   struct Tect     {
635           float flex_hist[MAXCHRONS][MAXPTS];
636           float disp_coeff[MAXCHRONS];
637           float response_time;
638           unsigned short int      response_type;
639   };
640
641   struct Eustasy  {
642           unsigned short int change_flag;
643           int max_level1;
644           int min_level1;
645           float freq1;
646           int curve_type1;
647           int max_level2;
648           int min_level2;
649           int freq2;
650           int curve_type2;
651           char curve_fname[80];
652   };
653
654   struct Sed_budget       {
655           unsigned short int supply_flag;
656           int drainage_ratio;
657           int release_perc;
658           float maxsed, minsed, freq;
659           unsigned short int curve_type;
660           unsigned short int pc_type_flag;
661           float pc_max, pc_min, pc_freq;
662   };
663
664   struct File_params      {
665           char directory[80];
666           char fname[80];
667           char out_fname[80];
668           unsigned short int batch; /* Must not be overwritten by file read so
669                                                                   needs to go in this structure
       */
670   };
671
672   /* Data structure which contains coords of two corners of mouse defined box */
673   struct Zoombox  {
674           int xco1;
675           int yco1;
676           int xco2;
677           int yco2;
678           int point_x;
679           int point_y;
680   };
681
682   struct Chrono_plot      {
683           unsigned short int show_chrono;
684           unsigned short int show_eustasy;
685           unsigned short int show_sed_supply;
686           unsigned short int show_relsea;
687           unsigned short int show_subsid;
688           unsigned short int show_onlap;
689           unsigned short int show_crossplot;
690           int zoom_left;
691           int zoom_right;
692           float first_chron;
693           float last_chron;
694           unsigned short int wheeler_width;
695           unsigned short int sed_supply_width;
696           unsigned short int eustasy_width;
697           unsigned short int relsea_width;
698           unsigned short int subsid_width;
699           unsigned short int onlap_width;
700           unsigned short int crossplot_width;
701           unsigned short int crossplot_X_var;
```



```
702           unsigned short int crossplot_Y_var;
703   };
704
705
706   struct Post     {
707           char    fname[80];
708           short int       param_type;
709           short int       format;
710           int     pen_width;
711           char    multi_comment[1400];
712           int     background;
713           int     colour;
714           int     key_flag;
715           int     print_sealevel;
716           int     axis_ticks;
717           int     depth_tick_num;
718           int     horiz_tick_num;
719           double  ax_label_height;
720           float   comment_size;
721           int     mult_time_axis;
722           float   x_gap;
723           float   key_Y_pos;
724           float   key_X_pos;
725           double  image_width, image_height, x_offset, y_offset;
726           char    label1[80], label2[80], label3[80], label4[80], label5[80];
727           float   xpos1, ypos1, xpoint1, ypoint1;
728           float   xpos2, ypos2, xpoint2, ypoint2;
729           float   xpos3, ypos3, xpoint3, ypoint3;
730           float   xpos4, ypos4, xpoint4, ypoint4;
731           float   xpos5, ypos5, xpoint5, ypoint5;
732           char    chron_labels[10][5];
733           float   chron_label_X[10], chron_label_Y[10];
734           int     chron_label_number;
735           float   chron_label_size;
736           float   frame_width;
737           float   frame_height;
738   };
739
740   extern struct File_params       files;
741   extern struct Params            params;
742   extern struct Options           options;
743   extern struct Zoombox           zoombox;
744   extern struct Eustasy           eustasy;
745   extern struct Sed_budget        sed_budget;
746   extern struct Strat             strat;
747   extern struct Tect              tect;
748   extern struct Post              post;
749   extern struct Exec              exec;
750   extern struct Exec_flags        exec_flags;
751   extern struct Chrono_plot       chrono_plot;
```

References

References

BAUM, G. R., & VAIL, P.R., (1988). Sequence stratigraphic concepts applied to Paleogene outcrops, Gulf and Atlantic basins, in : C. K. Wilgus, Hastings, C.G., Kendall, St. C., Posamentier, H.W., Ross, C.A., and Van Wagoner, J.C., *Sea level changes : An integrated approach*, Spec. Publ. Soc. Econ. Paeont. Mineral, **42**, 309 - 327.

BEGIN, Z. B., MEYER, D.F. & SCHUMM, S.A., (1981). Development of longitudinal profiles of alluvial channels in response to base-level lowering, *Earth Surface Processes and Landforms*, **6**, 49-68.

BILLS, B. G., & MAY, G.M., (1987). Lake Bonneville: constraints on lithosphere thickness and upper mantle viscosity from isostatic warpings of Bonneville, Provo and Gilbert stage shorelines, *Journal of Geophysical Research*, **92**, B11, 11493 - 11508.

BODINE, J. H., (1981). Numerical computation of plate flexure in marine geophysics, *Lamont-Doherty Geol. Obs.*, tech. Rep. no. 1, CU 1-80, 36 pp.

BODINE, J. H., STECKLER, M.S., & WATTS, A.B., (1981). Observations of flexure and the rheology of the oceanic lithosphere, *Journal of Geophysical Research*, **86**, 3695 - 3707.

BULL, W. B., (1991). Geomorphic responses to climatic change, *Oxford University Press*, Oxford, pp.326.

CANT, D. J., (1991). Geometric modelling of facies migration : theoretical development of facies successions and local unconformities, *Basin Research*, **3**, 51-62.

CHRISTIE-BLICK, N., (1991). Onlap, offlap, and the origin of unconformity bounded depositional sequences, *Marine Geology*, **97**, 35 - 56.

COCHRAN, J. R., (1983). Effects of finite extension times on the development of sedimentary basins, *Earth and Planet Science Letters*, **66**, 289 - 302.

CRANK, J., (1975). The mathematics of diffusion, 2nd edition, Oxford University Press, 414.

CROSS, T. A., & HARBAUGH, J.W., (1989). Quantitative dynamic stratigraphy: A workshop, a philosophy, a methodology, in : T. A. Cross, *Quantitative Dynamic Stratigraphy*, Prentice Hall, 3 - 20.

CURRAY, J. R., (1965). Late Quaternary history, continental shelves of the United States, in : H. E. Wright Jr., *The quaternary of the United States*, Princeton University Press, 723 - 735.

DAVIS, W. M., (1899). The geographical cycle, *The Geographical Journal,* **14**, 481 - 504.

DAVIS, W. M., (1902). Base-level, grade, and peneplain, *Journal of Geology*, **10**, 77 - 111.

EVERTS, C. H., (1987). Continental shelf evolution in response to a rise in sea level, in : D. Nummedal, Pilkey, O.H., and Howard, J.D., *Sea level fluctuation and coastal evolution*, Soc. Econ. Palaeo. Min. Spec. Publ., **41,** 49 - 57.

FISCHER, A. G., (1991). Orbital cyclicity in Mesozoic strata, in : Einsele, G., Ricken, W., and Seilacher, A., *Cycles and events in stratigraphy*, Springer-Verlag, 48 - 62.

FLEMINGS, P.B. & JORDAN, T.E., (1989). A synthetic stratigraphic model of foreland basin development, *Journal of Geophysical Research*, **94**, 3851 - 3866.

GAFFIN, S. R. &. MAASCH, K.A., (1991). Anomalous cyclicity in climate and stratigraphy and modelling non-linear oscillations, *Journal of Geophysical Research*, **96**, B4, 6701 - 6711.

GAFFIN, S., (1992). Unforced oscillations in a freeboard and basin model: analogue to glacial/climate oscillators, *The Journal of Geology,* **100**, 717 - 729.

GALLOWAY, W. E., (1989). Genetic stratigraphic sequences in basin analysis I : Architecture and genesis of flooding-surface bounded depositional units, *American Association of Petroleum Geologists Bulletin.* **73**, 125 - 142.

GREENLEE, S. W., SCHROEDER, F.W. & VAIL, P.R., (1988). Seismic stratigraphic and geohistory analysis of Tertiary strata from the continental shelf off New Jersey; Calculation of eustatic fluctuations from stratigraphic data, in : Sheridan, R. E. and Grow, J.A., *The Atlantic Continental Margin: U.S.*, Geological Society America, **I-2**, 437 - 444.

GREENLEE, S. M., & MOORE, T.C., (1988). Recognition and interpretation of depositional sequences and calculation of sea-level changes from stratigraphic data - offshore New Jersey and Alabama Tertiary, in : C. K. Wilgus Hastings, C.G., Kendall, St. C., Posamentier, H.W., Ross, C.A., and Van Wagoner, J.C., *Sea level changes : An integrated approach,* Spec. Publ. Soc. Econ. Paeont. Mineral, **42**, 329 - 356.

GREENLEE, S. M., DEVLIN, W.J., MILLER, K.G., MOUNTAIN, G.S. & FLEMINGS, P., (1992). Integrated sequence stratigraphy of Neogene deposits, New Jersey continental shelf and slope: Comparison with the Exxon model, *Geological Society of America Bulletin*, **104,** 1403 - 1411.

GROW, J. A. & SHERIDAN, R.E., (1988). U.S. Atlantic continental margin; A typical Atlantic-type or passive continental margin, in : Sheridan, R. E. and Grow, J.A., *The Atlantic Continental Margin, U.S.*, Geological Society of America, **I-2**, 1 - 7.

HACK, J. T., (1957). Studies of longitudinal stream profiles in Virginia and Maryland, *U.S. Geological Survey Professional Paper*, **294**, B, 97.

HACK, J. T., (1960). Interpretation of erosional topography in humid temperate regions, *American Journal Science*, **258-A**, 89 - 97.

HAQ, B. U., HARDENBOL, J., & VAIL, P.R., (1987). Chronology of fluctuating sealevels since the Triassic, *Science*, **235**, 1156 - 1167.

HAQ, B. U., HARDENBOL, J. & VAIL, P.R., (1988). Mesozoic and Cenozoic chronostratigraphy and cycles of sea-level change, in : C. K. Wilgus Hastings, C.G., Kendall, St. C., Posamentier, H.W., Ross, C.A., and Van Wagoner, J.C., *Sea level changes : An integrated approach*, Spec. Publ. Soc. Econ. Paeont. Mineral, **42**, 71 - 108.

HAYS, J. D., IMBRIE, J. & SHACKLETON, N.J., (1976). Variations in the Earth's orbit : pacemaker of the ice ages, *Science*, **194**, 1121 - 1132.

HELLER, P. L., BURNS, B.A. & MARZO, M., (1993). Stratigraphic solution sets for determining the roles of sediment supply, subsidence, and sealevel on transgressions and regressions, *Geology,* **21**, 747 - 750.

HELLINGER, S. J. & SCLATER, J.G., (1983). Some comments on two-layer extensional models for the evolution of sedimentary basins, *Journal Geophysical Research*, **88**, B10, 8251 - 8269.

HOWARD, A. D., (1982). Equilibrium and time scales in geomorphology: Application to sand-bed alluvial channels, *Earth Surface Processes*, **7**, 303 - 325.

HOWARD, A. D., DIETRICH.W.E., & SEIDL, M.A., (in press). Modelling fluvial erosion on regional or continental scales.

HUBBARD, R. J., PAPE, J., & ROBERTS, D.G., (1985). Depositional sequence mapping as a technique to establish tectonic and stratigraphic framework and evaluate hydrocarbon potential on a passive continental margin, in : Berg, O.R. and Woolverton, D., *Seismic stratigraphy II : An Integrated Approach*, American Association of Petroleum Geologists Memoir, **39**, 79-91.

IMBRIE, J., (1985). A theoretical framework for the Pleistocene ice ages, *Journal of the Geological Society of America* **142**, 417 - 432.

JARVIS, G. T. &. MCKENZIE., D.P., (1980). The development of sedimentary basins with finite extension rates, *Earth Planetary Science Letters*, **48**, 42 - 52.

JERVEY, M. T., (1988). Quantitative geologic modelling of siliclastic rock sequences and their seismic expression, in : C. K. Wilgus Hastings, C.G., Kendall, St. C., Posamentier, H.W., Ross, C.A., and Van Wagoner, J.C., *Sea level changes : An integrated approach*, Spec. Publ. Soc. Econ. Paeont. Mineral, **42**, 47 - 69.

JORDAN, T. E., & FLEMINGS, P.B., (1991). Large scale stratigraphic architecture, eustatic variation, and unsteady tectonism : A theoretical evaluation, *Journal Geophysical Research*, **96**, 6681 - 6699.

JUDSON, S., (1975). Evolution of the Appalachian topography, in : Melhorn, W. N. and Flemal, R.C., *Theories of landform development*, 29 - 44.

KAUFMAN, P., GROTZINGER, J.P., & McCORMICK, D.S., (1991). Depth-dependent diffusion algorithm for simulation of sedimentation in shallow marine depositional systems, in : E. K. Franseen Watney, L.W., Kendall, C.G.St.C., and Ross, W., *Sedimentary*

modelling : Computer simulations and methods for improved parameter definition, Kansas Geological Survey Bulletin, **233**, 498 - 508.

KENDALL, C. G. S. C., STROBEL, J., CANNON, R., BEZDEK, J., & BISWAS,G., (1991). The simulation of the sedimentary fill of basins, *Journal of Geophysical Research*, **96**, B4, 6911 - 6929.

KENDALL, C. G. S. C., MOORE, P., WHITTLE, G. & CANNON, R., (1992). A challenge : Is it possible to determine eustasy and does it matter?, in : R. H. J. Dott, *Eustasy : The ups and downs of a major geological concept*, Geological Society of America Memoir, **180**, 93 - 107.

KENYON, P. M. & TURCOTTE, D.L., (1985). Morphology of a prograding delta by bulk sediment transport, *Geological Society of America Bulletin*, **96**, 1457 - 1465.

KLITGORD, K. D., HUTCHINSON, D.R. & SCHOUTEN, H., (1988). U.S. Atlantic continental margin; Structural and tectonic framework, in : Sheridan, R. E. and Grow, J.A., *The Atlantic Continental Margin: U.S.*, Geological Society America, **I-2**, 19 - 56.

KNOX, J. C., (1975). Concept of the graded stream, in : Melhorn, W. N. a. Flemal, R.C., Theories of landform development, 169 - 198.

LASE GROUP, (1986). Deep structure of the US East Coast passive margin from large aperture seismic experiments, *Marine Petroleum Geology,* **3**, 234 - 242.

LAWRENCE, D. T., DOYLE, M., & AIGNER, T., (1990). Stratigraphic simulation of sedimentary basins: Concepts and calibration, *American Association of. Petroleum Geologists Bulletin*, **74**, 273 - 295.

LEEDER, M.R., (1992). Denudation, vertical crustal movements and sedimentary basin infill, *Geologische Rundschau*, **80**, 2, 441-458.

LEOPOLD, L. B., & BULL, W.B., (1979). Base level, aggradation, and grade, *American Philosophical Society, Proceedings*, **123**, 3, 168 - 202.

LERCHE, I., (1989). Philosophies and strategies of model building, in : T. A. Cross, *Quantitative dynamic stratigraphy*, Prentice Hall, 21 - 44.

MACKIN, J. H., (1948). Concept of the graded river, *Bulletin of the Geological Survey of America*, **59**, 463 - 512.

MATTHEWS, R. K. & FROHLICH, R.C., (1991). Orbital forcing of low-frequency glacioeustasy, *Journal of Geophysical Research,* **96**, B4, 6797 - 6803.

MAY, J. A., WARME, J.E., & SLATER, R.A., (1983). Role of submarine canyons on shelfbreak erosion and sedimentation : modern and ancient examples, in : Stanley, D,J., Moore, G.T., *The shelfbreak: Critical interface on continental margins*, Society of Economic Palaeontologists and Mineralogists Special Publication, **33**, 315 - 332.

McGINNIS, J. P., DRISCOLL, N.W., KARNER, G.D., BRUMBAUGH, W.D. & CAMERON, N., (1993). Flexural response of passive margins to deep-sea erosion and slope retreat: Implications for relative sea-level change, *Geology,* **21**, 893 - 896.

MCKENZIE, D. P., (1978). Some remarks on the development of sedimentary basins, *Earth and Planetary Science Letters*, **40**, 25 - 32.

MIALL, A. D., (1989). Stratigraphic sequences and their chronostratigraphic correlation, *Journal of Sedimentary Petrology*, **61**, 497 - 505.

MIALL, A. D., (1992). The Exxon global cycle chart: An event for every occasion, *Geology*, **20,** 787 - 790.

MILLER, K. G., MOUNTAIN, G.S., & TUCHOLKE, B.E., (1985). Oligocene glacio-eustasy and erosion on the margins of the North Atlantic, *Geology*, **13**, 10 - 13.

MITCHUM, R. M., VAIL, P.R., & THOMPSON, S., (1977). Seismic stratigraphy and global changes of sea level, Part 2 : The depositional sequence as a basic unit for stratigraphic analysis, in : C.E.Payton, *Seismic stratigraphy - applications to hydrocarbon exploration.*, American Association of Petroleum Geologists Memoir, **26**, 53 - 62.

MITCHUM, R. M., (1977). Seismic stratigraphy and global changes of sea level, part 11: Glossary of terms used in seismic stratigraphy, in : C.E.Payton, *Seismic stratigraphy - applications to hydrocarbon exploration.*, American Association of Petroleum Geologists Memoir, **26**, 205 - 212.

NICOLIS, G. & NICOLIS, C., (1991). Nonlinear dynamic systems in the geosciences, in : Franseen, E.K., Watney, W.L., Kendall, C.G.St.C., and Ross, W. *Sedimentary modeling: Computer simulations and methods for improved parameter definition*, Kansas Geological Survey Bulletin, **233**, 33 - 42.

NUMMEDAL, G., RILEY, G.W., & TEMPLET, P.L., (1993). High-resolution sequence architecture: a chronostratigraphic model based on equilibrium profile studies, in: Posamentier, H.W., Summerhayes, C.P., Haq, B.U., and Allen, G.P. *Sequence stratigraphy and facies associations*, Special Publication of the International Association of Sedimentologists, **18**, 55-68.

OLSSON, R. K., GIBSON, T.G., HANSEN, H.J., & OWENS, J.P., (1988). Geology of the northern Atlantic coastal plain : Long Island to Virginia, in : Sheridan, R.E., and Grow, J.A., *The Atlantic Continental Margin, U.S.*, Geological Society of America, **I-2**, 87 - 105.

PAOLA, C., (1989). A simple basin-filling model for coarse grained alluvial systems, in : T. A. Cross, *Quantitative dynamic stratigraphy*, Prentice Hall, 363 - 374.

PELTIER, W. R., (1986). Deglaciation-induced vertical motion of the North American continent and transient lower mantle rheology, *Journal of Geophysical Research,* **91**, 9099 - 9123.

PITMAN, W. C., III, (1978). Relationship between eustasy and stratigraphic sequences of passive margins, *Geological Society of America Bulletin*, **89**, 1389 - 1403.

PITMAN, W. C. &. ANDREWS, J.A., (1985). Subsidence and thermal history of small pull-apart basins, in : Biddle, K. T. and Christie-Blick, N., *Strike slip deformation, basin formation and sedimentation,* Special Publication of the Society of economic Palaeontologists Mineralogists, **37**, 45 - 49.

PITMAN, W. C., & GOLOVCHENKO, X., (1988). Sea-level changes and their effect on the stratigraphy of Atlantic-type margins, in : Sheridan, R.E. and Grow, J.A., *The Atlantic Continental Margin, U.S.*, Geological Society of America, **I-2**, 429 - 426.

POAG, C. W. & VALENTINE, P.C., (1988). Mesozoic and Cenozoic stratigraphy of the United States Atlantic continental shelf and slope, in : Sheridan, R. E. and Grow, J.A., *The Atlantic continental margin, U.S.*, Geological Society of America, **I-2**, 67 - 85.

POSAMENTIER, H. W., JERVEY, M.T. & VAIL, P.R., (1988). Eustatic controls on clastic deposition I - conceptual framework, in : C. K. Wilgus Hastings, C.G., Kendall, St. C., Posamentier, H.W., Ross, C.A., and Van Wagoner, J.C., *Sea level changes : An integrated approach,* Soc. Econ. .Paleon. Mineral., **42**, 109 - 124.

POSAMENTIER, H. W., JERVEY, M.T., & VAIL, P.R., (1988). Eustatic controls on clastic deposition II - sequence and systems tract models, in : Wilgus, C.K., Hastings, C.G., Kendall, St. C., Posamentier, H.W., Ross, C.A., and Van Wagoner, J.C., *Sea level changes : An integrated approach*, .Soc. Econ. .Paleon. Mineral., **42**, 125 - 154.

POSAMENTIER, H. W., ALLEN, G.P., JAMES, D.P. & TESSON, M., (1992). Forced regressions in a sequence stratigraphic framework : concepts, examples, and exploration significance, *American Association of Petroleum Geologists Bulletin*, **76**, 11, 1687 - 1709.

POSAMENTIER, H. W. &. ALLEN, G.P., (1993a). Siliclastic sequence stratigraphic patterns in foreland ramp-type basins, *Geology*, **21**, 455 - 458.

POSAMENTIER, H. W. & ALLEN, G.P., (1993b). Variability of the sequence stratigraphic model : effects of local basin factors, *Sedimentary Geology*, **86**, 91 - 109.

PRESS, W. H., FLANNERY, B.P., TEULOLSKY, S.A. & VETTERLING, W.T., (1986). Numerical recipes in C, the art of scientific computing, Cambridge University Press, Cambridge, pp.735.

QUINLAN, G. M. & BEAUMONT, C., (1984). Appalachian thrusting, lithospheric flexure and the Palaeozoic stratigraphy of the eastern interior of North America, *Canadian Journal of Earth. Science.*, **21**, 973 - 996.

QUINN, T. M., (1991). The history of Post-Miocene sea level change: Inferences from stratigraphic modelling of Enewatok atoll, *Journal of Geophysical Research,* **96**, B4, 6713 - 6725.

REYNOLDS, D. J., STECKLER, M.S. & COAKLEY, B.J., (1991). The role of the sediment load in sequence stratigraphy : the influence of flexural isostasy and compaction, *Journal of Geophysical. Research*, **96**, 6931 - 6949.

RIGGS, S. R. & BELKNAP, D.F., (1988). Upper Cenozoic processes and environments of continental margin sedimentation: eastern United States, in : Sheridan, R. E. and Grow, J.A., *The Atlantic continental margin, U.S.*, Geological society of America, **I-2**, 131 - 176.

RIVENAES, J. C., (1992). Application of a dual lithology, depth-dependent diffusion equation in stratigraphic simulation, *Basin Research*, **4**, 133 - 146.

ROSS, C. A., & ROSS, J.R.P., (1988). Late Palaeozoic transgressive-regressive deposition, in : Wilgus, C.K., Hastings, C.G., Kendall, St. C., Posamentier, H.W., Ross, C.A., and Van Wagoner, J.C., *Sea level changes : An integrated approach*, Spec. Publ. Soc. Econ. Paeont. Mineral., **42**, 227 - 247.

ROWLEY, D. B. &. MARKWICK, P.J., (1992). Haq *et al.* eustatic sea level curve: Implication for sequestered water volumes, *Journal of Geology*, **100**, 703 - 715.

ROYDEN, L. & KEEN, C.E., (1980). Rifting processes and thermal evolution of the continental margin of eastern Canada determined from subsidence curves, *Earth and Planetary Science Letters,* **51**, 343 - 361.

SANGREE, J. B. & WIDMIER, J.M., (1977). Seismic stratigraphy and global changes of sea level, part 9 : seismic interpretation of clastic depositional facies, in : Payton, C.E. *Seismic stratigraphy - applications to hydrocarbon exploration*, American Associations of Petroleum Geologists, **26**, 165 - 184.

SAWYER, D. S., TOKSOZ, M.N., SCLATER, J.G., & SWIFT, B.A., (1983). Thermal evolution of the Baltimore Canyon Trough and Georges Bank Basin, *American Association of Petroleum Geologists Memoir*, **34**, 743 - 762.

SCHROEDER, F. W. & GREENLEE, S.M., (1993). Testing eustatic curves based on Baltimore canyon Neogene stratigraphy: An example application of basin-fill simulation, *American Association of Petroleum Geologists Bulletin*, **77**, 4, 638 - 656.

SCHUMM, S. A., (1993). River response to baselevel change : implications for sequence stratigraphy, *Journal of Geology,* **101**, 279 - 294.

SCLATER, J. G., & CHRISTIE, P.A.F., (1980). Continental stretching : an explanation of the post Mid-Cretaceous subsidence of the central North Sea basin, *Journal of Geophysical Research*, **85,** 3711 - 3739.

SHAW, H. R., (1987). The periodic structure of the natural record and non-linear dynamics, *EOS*, **68**, 1651 - 1665.

Sheridan, R. E., Grow, J.A., and Klitgord, K.D., (1988). Geophysical data, in : Sheridan, R. E. and Grow, J.A., *The Atlantic Continental Margin: U.S.*, The Geological Society of America, **I - 2**, 177 - 196.

SHOR, A. N. & MCCLENNAN, C.E., (1988). Marine physiography of the U.S. Atlantic margin, in : Sheridan, R. E. and Grow, J.A., *The Atlantic Continental Margin: U.S.*, Geological Society of America, **I - 2**, 9 - 18.

SIGMUNDSON, F., (1991). Post-glacial rebound and asthenosphere viscosity in Iceland, *Geophysical Research Letters*, **18**, 1131 - 1134.

SLINGERLAND, R., (1989). Predictability and chaos in quantitative dynamic stratigraphy, in : T. A. Cross, *Quantitative Dynamic Stratigraphy*, Prentice Hall, 45 - 53.

SLOSS, L. L., (1988). Forty years of sequence stratigraphy, *Bulletin of the Geological Society of America*, **100**, 1661 - 1665.

SLOSS, L. L., (1991). The tectonic factor in sea level change: A countervailing view, *Journal of Geophysical Research.*, **96**, B4, 6609 - 6617.

SMITH, G.D., (1985). The numerical solution of partial differential equations : finite difference methods, 3rd edition, Oxford University Press, pp. 151.

SMITH, M. A., AMATO, R.V., FURBUSH, M.A., PERT, D.M., NELSON, M.E., HENDRIX, J., TAMM, L.C., WOOD, JR. G. & SHAW, D.R., (1976). Geological and operational summary, COST No. B-2 well, Baltimore Canyon trough area, Mid-Atlantic OCS : *U.S. Geological Survey, Open file report*, **76**- 774, 79.

SNOW, R. S. & SLINGERLAND, R.L., (1987). Mathematical modelling of graded river profiles, *Journal of Geology*, **95**, 15 - 33.

SNOW, R. S. & SLINGERLAND, R.L., (1990). Stream profile adjustment to crustal warping: nonlinear results from a simple model, *Journal of Geology*, **98**, 699 - 708.

STECKLER, M. S. & WATTS, A.B., (1982). Subsidence history and tectonic evolution of Atlantic-type continental margins, *American Geophysical Union, Geodynamics Series*, **8**, 184 - 196.

STECKLER, M. S., WATTS, A.B., & THORNE, J.A., (1988). Subsidence and basin modelling at the U.S. Atlantic passive margin, in : Sheridan, R. E. and Grow, J.A., *The Atlantic Continental Margin: U.S.*, Geological Society of America, **I - 2**, 399 - 416.

STEINER, J., (1973). Possible galactic causes for synchronous sedimentation sequences of the North American and Eastern European cratons, *Geology*, **1**, 2, 89 - 92.

STROBEL, J., SOEWITO,F., KENDALL, C.G.ST.C., BISWAS, G., BEZDEK, J., & CANNON, R., (1989). Interactive simulation (SED-pak) of clastic and carbonate sedimentation in shelf to basin settings, in : T. A. Cross, *Quantitative dynamic stratigraphy*, Prentice Hall, 433 - 444.

SWIFT, D. J. P., (1970). Quaternary shelves and the return to grade, *Marine Geology* **8**, 5 - 30.

SWIFT, D. J. P., PHILIPS, S. & THORNE, J.A., (1991). Sedimentation on continental margins, V: parasequences, in : Swift, D. J. P., Oertel, G.F., Tilman, R.W. and Thorne, J.A., *Shelf sand and sandstone bodies, geometry, facies and sequence stratigraphy*, Special Publication International Association Sedimentologists, **14**, 153 - 187.

THORNE, J. A. & SWIFT, D.J.P, (1991). Sedimentation on continental margins, VI: a regime model for depositional sequences, their component system tracts, and bounding surfaces, in : Swift, D. J. P., Oertel, G.F., Tillman, R.W. and Thorne, J.A., *Shelf sand and sandstone bodies, geometry, facies and sequence stratigraphy*, Special Publication International Association Sedimentologists, **14**, 189 - 258.

TURCOTTE, D. L. & SCHUBERT, G., (1982). Geodynamics, applications of continuum physics to geological problems, John Wiley and Sons, New York, pp.450.

UNDERHILL, J. R., (1991). Controls on Late Jurassic seismic sequences, Inner Moray Firth, UK North Sea : A critical test of a key segment of Exxon's original global cycle chart, *Basin Research*, **3**, 51 - 62.

UNDERHILL, J. A., & PARTINGTON, M.A., (1993). Jurassic thermal doming and deflation in the North Sea: Implications of the sequence stratigraphic evidence, in press.

VAIL, P. R., MITCHUM, R.M., & THOMPSON, S., (1977a). Seismic stratigraphy and global changes of sea level, part 3: Relative changes of sea level from coastal onlap, in : Payton, C.E., *Seismic stratigraphy - applications to hyrdrocarbon exploration*, American Association of Petroleum Geologists. Memoir, **26**, 63 - 81.

VAIL, P. R., MITCHUM, R.M., & THOMPSON, S., (1977b). Seismic stratigraphy and global changes of sea level, part 4: Global cycles of relative changes of sea level, in :

Payton, C.E.,*Seismic stratigraphy - applications to hyrdrocarbon exploration*, American Association of.Petroleum.Geologists. Memoir, **26**, 83 - 97.

VAIL, P. R., HARDENBOL, J., & TODD, R.G., (1984). Jurassic unconformities, chronostratigraphy, and sea-level changes from seismic stratigraphy and biostratigraphy, in : Schlee, J.S., *Inter-regional unconformities and hydrocarbon accumulation*, American Association of Petroleum Geologists Memoir, **36**, 129 - 144.

VAIL, P. R., AUDEMARD, F., BOWMAN, S.A., EISNER, P.N., & PEREZ-CRUZ, C., (1991). The stratigraphic signatures of tectonics, eustasy and sedimentology - an overview, in : Einsele, G., Ricken, W., and Seilacher, A., *Cycles and events in stratigraphy*, Springer Verlag, 617 - 681.

VAN WAGONER, J. C., POSAMENTIER, H.W., MITCHUM, R.M., VAIL, P.R., SARG, J.F., LOUTIT, T.S., & HARDENBOL, J., (1988). An overview of the fundamentals of sequence stratigraphy and key definitions, in : Wilgus, C.K., Hastings, C.G., Kendall, St. C., Posamentier, H.W., Ross, C.A., and Van Wagoner, J.C., *Sea level changes : An integrated approach*, Soc. Econ. Paleon. Mineral., **42**, 39 - 45.

VAN WAGONER, J. C., MITCHUM, R.M., CAMPION, K.M., & RAHMANIAN, V.D., (1990). Siliclastic sequence stratigraphy in well logs, cores, and outcrops, American Association of Petroleum Geologists, methods in exploration series, **7**, pp. 55.

WALCOTT, R. I., (1970a). Flexural rigidity, thickness and viscosity of the lithosphere, *Journal of Geophysical Research*, **75**, 20, 3941 - 3954.

WALCOTT, R. I., (1970b). Isostatic response to loading of the crust in Canada, *Canadian Journal of Earth Sciences*, **7**, 716 - 727.

WATTS, A. B. & STECKLER, M.S., (1979). Subsidence and eustasy at the continental margin of eastern North America, in : Talawani Hay, M.A., and Ryan, W.B.F., *Deep drilling results in the Atlantic ocean:* Continental Margins and Palaeoenvironments, **3**, 218 - 234.

WATTS, A. B., BODINE, J.H., & STECKLER, M.S., (1980). Observations of flexure and the state of stress in the oceanic lithosphere, *Journal of Geophysical Research*, **85**, B11, 6369 - 6376.

WATTS, A. B., (1982). Tectonic subsidence, flexure and global changes in sealevel, *Nature*, **297**, 469 - 474.

WATTS, A. B., KARNER, G.D., & STECKLER, M.S., (1982). Lithospheric flexure and the evolution of sedimentary basins, *Philosophical Transactions of the Royal Society of London*, **A305**, 249 - 281.

WATTS, A. B. & THORNE, J., (1984). Tectonics, global changes in sealevel and their relationship to stratigraphical sequences at the US Atlantic continental margin, *Marine Petroleum Geology*, **1**, 319 - 339.

WATTS, A. B., (1988). Gravity anomalies, crustal structure and flexure of the lithosphere at the Baltimore Canyon trough, *Earth and Planetary Science Letters*, **89**, 221 - 238.

WATTS, A. B., (1989). Lithospheric flexure due to prograding sediment loads: implications for the origin of offlap/onlap patterns in sedimentary basins, *Basin Research*, **2**, 133 - 144.

WEISSEL, J. K., (1990). Long-term erosional development of rifted continental margins: Towards a quantitative understanding, *Australasian Institute Mining Metallurgy*, 63 - 70.

WHITE, N., & MCKENZIE, D., (1988). Formation of the "steer's head" geometry of sedimentary basins by differential stretching of the crust and mantle, *Geology*, **16**, 250 - 253.

WOOD, L.J., ETHRIDGE, F.G., & SCHUMM, S.A., (1993). The effects of base-level fluctuations on coastal-plain, shelf and slope depositional systems: an experimental approach, in: Posamentier, H.W., Summerhayes, C.P., Haq, B.U., and Allen, G.P. *Sequence stratigraphy and facies associations*, Special Publication of the International Association of Sedimentologists, **18**, 45-53.